USGS
science for a changing world

Contractor Report
USGS/BRD/CR-1998-0002
OCS Study MMS 98-0044

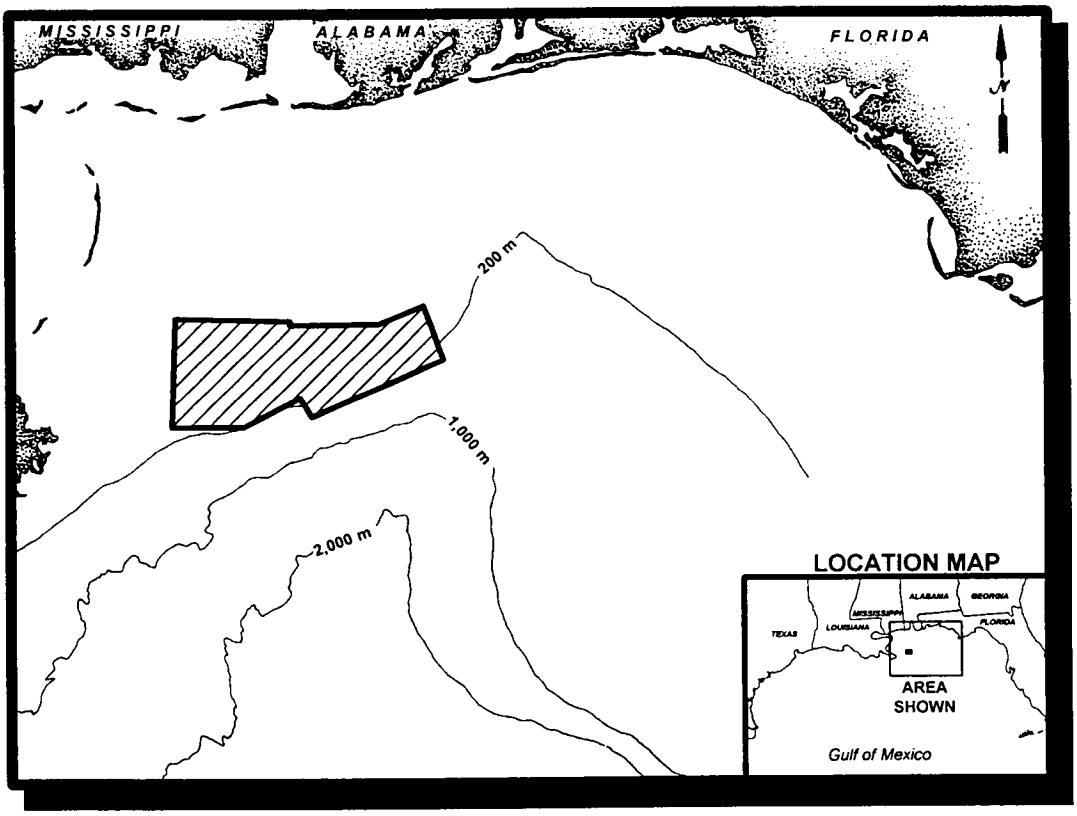

Northeastern Gulf of Mexico Coastal and Marine Ecosystem Program: Ecosystem Monitoring, Mississippi/Alabama Shelf; Second Annual Interim Report

U.S. Department of the Interior
U.S. Geological Survey
Biological Resources Division

MMS
U.S. Department of the Interior
Minerals Management Service
Gulf of Mexico OCS Region

Contractor Report
USGS/BRD/CR-1998-0002
OCS Study MMS 98-0044

Northeastern Gulf of Mexico Coastal and Marine Ecosystem Program: Ecosystem Monitoring, Mississippi/Alabama Shelf; Second Annual Interim Report

December 1998

Prepared under BRD contract
1445-CT09-96-0006
by
Continental Shelf Associates, Inc.
759 Parkway Street
Jupiter, Florida 33477
and
Texas A&M University, Geochemical and
Environmental Research Group
833 Graham Road
College Station, Texas 77845

in cooperation with the

U.S. Department of the Interior
Minerals Management Service
Gulf of Mexico OCS Region

PROJECT COOPERATION

This study was procured to meet information needs identified by the Minerals Management Service (MMS) in concert with the U.S. Geological Survey, Biological Resources Division (BRD).

DISCLAIMER

REPORT AVAILABILITY

Extra copies of this report may be obtained from:

U.S. Department of the Interior
U.S. Geological Survey
Biological Resources Division
Eastern Regional Office
1700 Leetown Road
Kearneysville, WV 25430

Telephone: (304) 725-8461 (ext. 675)

U.S. Department of the Interior
Minerals Management Service
Gulf of Mexico OCS Region
Public Information Unit (MS 5034)
1201 Elmwood Park Boulevard
New Orleans, LA 70123-2394

Telephone: (504) 736-2519 or
1-800-200-GULF

SUGGESTED CITATION

Continental Shelf Associates, Inc. and Texas A&M University, Geochemical and Environmental Research Group. 1998. Northeastern Gulf of Mexico Coastal and Marine Ecosystem Program: Ecosystem Monitoring, Mississippi/Alabama Shelf; Second Annual Interim Report. U.S. Department of the Interior, U.S. Geological Survey, Biological Resources Division, USGS/BRD/CR-1998-0002 and Minerals Management Service, Gulf of Mexico OCS Region, New Orleans, LA, OCS Study MMS 98-0044. 198 pp.

Contributors

Program Management

Program Manager	David A. Gettleson[1]
Deputy Program Manager	Mahlon C. Kennicutt II[2]
Field Logistics Coordinator	Frederick B. Ayer II[1]
Data Manager	Alan D. Hart[1]
Deputy Data Manager	Gary A. Wolff[2]

Report Editor and Authors

Editor	Neal W. Phillips[1]
Geological Characterization	William W. Sager[2] William W. Schroeder[6]
Sediment Dynamics	Ian D. Walsh[5]
Geochemistry	Mahlon C. Kennicutt II[2]
Physical Oceanography/Hydrography	Frank J. Kelly[2] Norman L. Guinasso, Jr.[2]
Hard Bottom Communities	Dane D. Hardin[3] Keith D. Spring[1] Bruce D. Graham[1] Stephen T. Viada[1]
Fish Communities	David B. Snyder[1]
Companion Study: Micro-Habitat Studies	Ian R. MacDonald[2]
Companion Study: Epibiont Recruitment	Paul A. Montagna[4]

Report Production

Technical Editor	Melody B. Powell[1]
Administrative Assistant	Debbie Paul[2]
Word Processing	Deborah V. Raffel[1]
Graphics	Suzanne R. Short[1]
Clerical	Deborah M. Cannon[1] Caroline M. Simpson[1]

---

[1]Continental Shelf Associates, Inc.
[2]Texas A&M University
[3]Applied Marine Sciences
[4]University of Texas at Austin
[5]Oregon State University
[6]Independent consultant

Contents

Contents
(continued)

Page

Contents
(continued)

Page

Figures

Figures
(continued)

Page

Figures
(continued)

Figures
(continued)

Page

Figures
(continued)

Page

Tables

Tables
(continued)

Page

Acronyms and Abbreviations

ADCP	Acoustic Doppler Current Profiler
AVHRR	Advanced Very High Resolution Radiometer
BLM	Bureau of Land Management
BP	before present
COTR	Contracting Officer's Technical Representative
CTD	conductivity/temperature/depth
CVAAS	cold vapor atomic absorption spectrophotometry
DO	dissolved oxygen
EOM	extractable organic matter
EPA	Environmental Protection Agency
FAAS	flame atomic absorption spectrophotometry
GC/FID	gas chromatography/flame ionization detection
GC/MS	gas chromatography/mass spectrometry
GFAAS	graphite furnace or flameless atomic absorption spectrophotometry
GIS	geographic information system
GPS	Global Positioning System
INAA	instrumental neutron activation analysis
LATEX	Texas-Louisiana Shelf Circulation and Transport Process Program
LSS	light scattering sensor
mab	meters above bottom
MAFLA	Mississippi-Alabama-Florida
MAMES	Mississippi-Alabama Marine Ecosystems Study
MASPTHMS	Mississippi-Alabama Shelf Pinnacle Trend Habitat Mapping Study
MDL	method detection limit
MMS	Minerals Management Service
NOAA	National Oceanic and Atmospheric Administration
NODC	National Oceanographic Data Center
NTU	nephelometric turbidity unit
OBS	optical backscatter
OCS	outer continental shelf
PAH	polycyclic aromatic hydrocarbon
PAR	photosynthetically active radiation
QA/QC	quality assurance/quality control
RLM	reef-like mound
ROV	remotely operated vehicle
SIM	selected ion monitoring
SOP	standard operating procedure
TAMU	Texas A&M University
TIC	total inorganic carbon
TOC	total organic carbon
TPH	total petroleum hydrocarbons
UCM	uresolved complex mixture
USGS	U.S. Geological Survey
UTC	Coordinated Universal Time

Chapter 1
Executive Summary

This Annual Interim Report summarizes the second year of a four-year program to characterize and monitor hard bottom features on the Mississippi/Alabama outer continental shelf (OCS). The "Northeastern Gulf of Mexico Coastal and Marine Ecosystems Program: Ecosystem Monitoring, Mississippi/Alabama Shelf" is being conducted by Continental Shelf Associates, Inc. and the Geochemical and Environmental Research Group of Texas A&M University, for the U.S. Geological Survey (USGS), Biological Resources Division.

The program consists of an integrated suite of reconnaissance, baseline characterization, monitoring, and process-oriented "companion studies." Based on previous studies and new geophysical reconnaissance, nine hard bottom sites in the Mississippi-Alabama pinnacle trend area have been selected for study (Fig. 1.1). The central focus of the program is monitoring of hard bottom community structure and dynamics. The potential sensitivity of these communities to OCS oil and gas industry activities is of interest to the Minerals Management Service (MMS), the client agency for whom the USGS is administering this program. Other monitoring components (geological and oceanographic processes) are needed to provide an understanding of the dominant environmental processes that control or influence hard bottom community distributional patterns, establishment, and development. These may include substrate characteristics such as relief, microtopography, sedimentology, and contaminant levels, as well as water column characteristics such as temperature, salinity, dissolved oxygen, near-bottom current patterns, and the presence and extent of bottom nepheloid layers. In addition, two companion studies have been designed to complement monitoring by providing information on benthic recruitment and micro-habitat environmental influences on community structure and dynamics.

Objectives

The overall goal of this program is to characterize and monitor biological communities and environmental conditions at carbonate mounds along the Mississippi-Alabama OCS. Specific objectives are as follows:

- To describe and monitor seasonal and interannual changes in community structure and zonation and relate these to changes in environmental conditions (i.e., dissolved oxygen, turbidity, temperature, salinity, etc.); and

- To characterize the geological, chemical, and physical environment of the mounds as an aid in understanding their origin, evolution, present-day dynamics, and long-term fate.

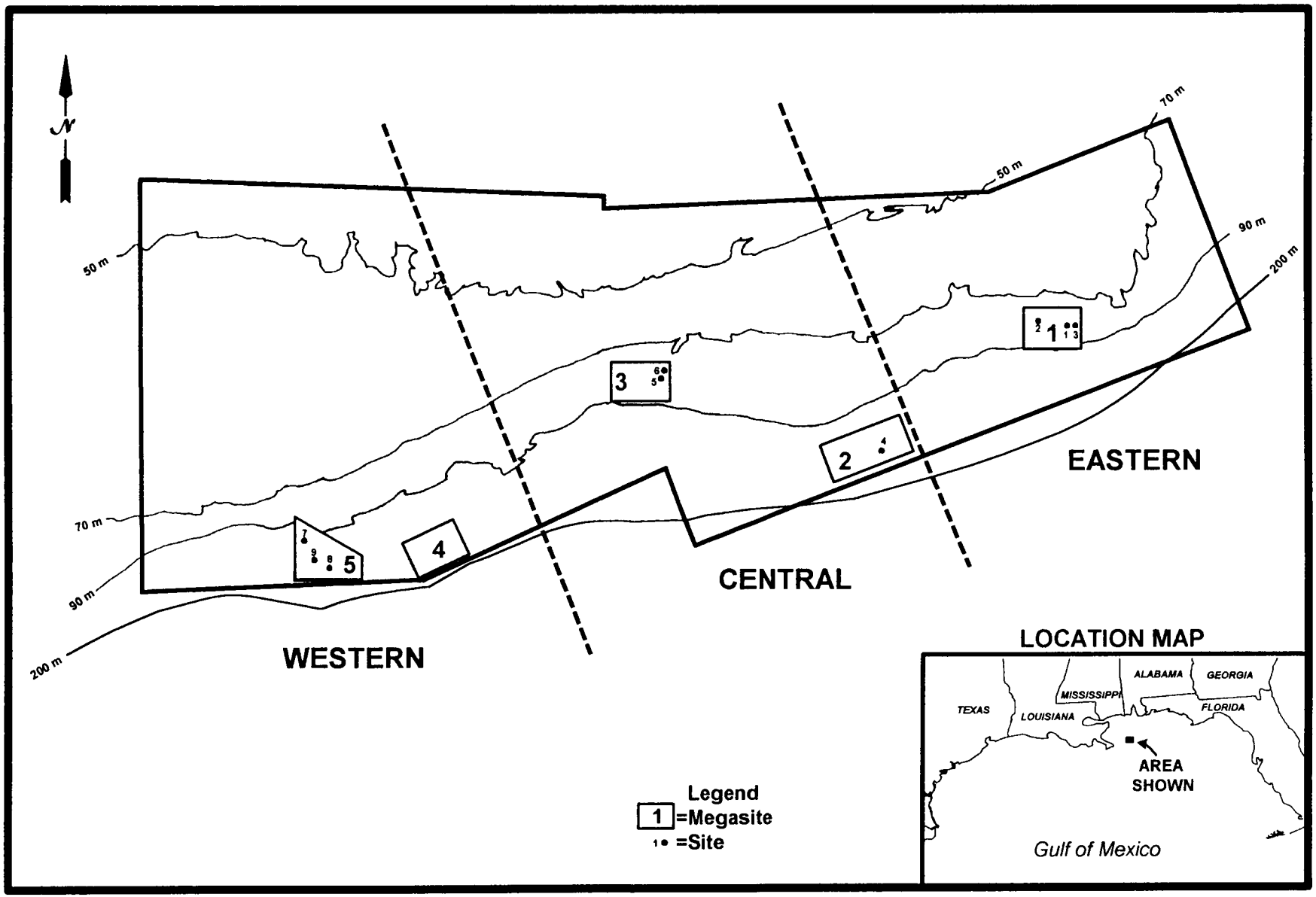

Fig. 1.1. Locations of final monitoring sites.

Phases and Cruise Scheduling

The program consists of four phases, each lasting approximately 12 months:

- Phase 1: Reconnaissance, Site Selection, Baseline Characterization, Monitoring, and Companion Studies;
- Phase 2: Monitoring and Companion Studies;
- Phase 3: Monitoring and Companion Studies; and
- Phase 4: Final Synthesis.

Phase 1 included three cruises. Cruise 1A (November 1996) was a geophysical reconnaissance of five megasites containing potential monitoring sites. Cruise 1B (March 1997) was a visual reconnaissance to provide further data on a few candidate sites that had little or no previous video or photographic data. The cruise also field tested the remotely operated vehicle (ROV) and monitoring techniques. Cruise 1C (May 1997), which was conducted after nine final study sites had been selected and approved, was the first of four cruises during which monitoring and companion studies are to be conducted. Activities during this first monitoring cruise included establishing fixed stations, collecting samples and data, and deploying oceanographic and biological moorings.

Phase 2, the subject of this report, included two monitoring cruises that revisited the stations established during Cruise 1C. These were Cruise M2 (October 1997) and Cruise M3 (April-May 1998). (Cruise M3 began in April but operations were suspended due to weather delays; it was completed in August 1998.) In addition, mooring service cruises were conducted in July 1997 (S1), January 1998 (S2), and July 1998 (S3). Monitoring and companion studies will continue during Phase 3 with Monitoring Cruise M4 (currently scheduled for April-May 1999) and two additional mooring service cruises.

This report is the second of three Annual Interim Reports summarizing the methods and results of Phases 1-3. During Phase 4, a Final Synthesis Report will be produced in which all findings will be summarized, analyzed, synthesized, and discussed in relation to historical data from the region.

Site Selection

The contract specified that a total of nine sites be selected, including high (>10 m), medium (5 to 10 m), and low (<5 m) relief sites in the eastern, central, and western portions of the study area. Other factors considered in site selection were representativeness, availability of existing video and photographic data, and previous oil and gas industry activities. Site selection during Phase 1 involved the following steps:

- *Megasite Selection.* Prior to Cruise 1A, five large areas ("megasites") were selected for geophysical reconnaissance. The selection of the five megasites was based on geophysical data collected during the Mississippi-Alabama Marine Ecosystems Study (MAMES; Brooks 1991) and the Mississippi-Alabama Shelf Pinnacle Trend Habitat Mapping Study (MASPTHMS; Continental Shelf Associates, Inc. 1992). The megasites were selected because they were known to contain numerous features of varying relief (candidate sites) and could be surveyed within the time and financial constraints of the contract.

- *Geophysical Reconnaissance and Preliminary Site Selection.* During Cruise 1A, the five megasites were surveyed using swath bathymetry, high-resolution side-scan sonar, and subbottom profiler to produce detailed maps. After the initial survey of all five megasites, small subsets were chosen for higher resolution mapping. After the cruise, a list of candidate high, medium, and low relief features within the megasites was prepared and the historical video and photographic data were tabulated. At this point, three high relief and two medium relief sites were tentatively selected.

- *Visual Reconnaissance.* Three low relief sites and one medium relief site with little or no previous video or photographic data were identified as needing visual reconnaissance. During Cruise 1B, these features were briefly surveyed using an ROV to determine whether a hard bottom community was present. All of the sites visited during Cruise 1B were ultimately chosen as final sites.

- *Final Site Selection.* After the completion of Cruises 1A and 1B, the program managers and key principal investigators prepared a final site list. Site selection was discussed and approved during a teleconference with the USGS Contracting Officer's Technical Representative, the Scientific Review Board, and the program principal investigators.

Overview of Sampling Program

An overview of the sampling program, including mooring deployments and retrievals at the monitoring sites, is provided in Table 1.1. During Cruise 1C (May 1997), subbottom profiling was conducted to geophysically characterize each site in more detail than was possible with the broad-scale geophysical reconnaissance (Cruise 1A). Grab samples were collected for geological and geochemical analyses (see Chapters 4 and 6). Hydrographic profiling was also conducted at each station, including conductivity/temperature/depth (CTD), dissolved oxygen (DO), photosynthetically active radiation (PAR), transmissivity, and optical backscatter (OBS) (see Chapter 7). Hard bottom and fish community monitoring was conducted at each site using the ROV (see Chapters 8 and 9). Monitoring included random video/photographic transects and stations and establishment of fixed video/photoquadrats. Voucher specimens were also collected at some sites to aid in species identification.

Table 1.1. Summary of activities conducted on each monitoring cruise and mooring service cruise.

Site	Cruise and Date(s)						
	1C (May 1997)	S1 (Jul 1997)	M2 (Oct 1997)	S2 (Jan 1998)	M3 (Apr-May 1998)	M3 (Aug 1998)	S3 (Jul 1998)
1	P H G V D(3) d(1)	S(3)	H G V S(3)	S(3) d(1)	H G V S(1) R(2)	r(1)	S(1)
2	P H G V	--	H G V	--	H G	V	--
3	P H G V	--	H G V	--	H G	V	--
4	P H G V D(1) d(8)	S(1)	H G V S(1) r(1)	S(1) d(1)	H G S(1)	V r(3)	S(1)
5	P H G V D(1) d(1)	S(1)	H G V S(1)	S(1) d(1)	H S(1) D(2)	G	S(3)
6	P H G V	--	H G V	--	H	G	--
7	P H G V	--	H G V	--	H	G V	--
8	P H G V	--	H G V	--	H	G V	--
9	P H G V D(1) d(1)	S(1)	H G V S(1)	S(1) d(1)	H S(1)	G V r(1)	S(1)

Abbreviations:
P = subbottom profiling
H = hydrographic profiling
G = grab sampling
V = video and photography
D(#) = deploy oceanographic mooring(s)
S(#) = service oceanographic mooring(s)
R(#) = remove oceanographic mooring(s)
d(#) = deploy biomooring(s)
r(#) = retrieve biomooring(s)

The overall program consists of repeating the Cruise 1C sampling on three subsequent monitoring cruises (M2, M3, and M4). The only exception is the subbottom profiling at each site, which will not be repeated.

Six physical oceanographic/sediment dynamics moorings were installed during Cruise 1C (see Chapter 7). Three moorings were installed at Site 1, and one each at Sites 4, 5, and 9. Each site will have at least one oceanographic mooring in place throughout the study. Two of the three moorings at Site 1 are "re-locatable" and were subsequently redeployed at Site 5 on Cruise M3. Each mooring includes current meters at 4 and 16 meters above bottom (mab), sediment traps at 2, 7, and 15 mab, and an instrument at 2 mab that measures temperature, conductivity, DO, and turbidity.

Eleven "biomoorings" (moorings containing sets of settling plates) were also deployed during Cruise 1C as part of the companion study of epibiont recruitment (see Chapter 11). Eight were deployed at Site 4 and one each at Sites 1, 5, and 9. The biomoorings at Sites 1 and 9 were retrieved during the continuation of Cruise M3 (August 1998); turbidity prevented retrieval of the Site 5 biomooring. Another set of biomoorings was deployed at the same sites on Cruise S2 (January 1998) and will be recovered on Cruise M4 (April-May 1999). The eight biomoorings at Site 4 are a "time-series" experiment; the original plan was to retrieve one on each subsequent Service Cruise and Monitoring Cruise until all eight were retrieved. However, as explained below, this has been changed so that all biomoorings can be retrieved on monitoring cruises when the ROV is present to cut the anchor line. One Site 4 mooring was retrieved on Cruise M2 (October 1997) and redeployed on Cruise S2 (January 1998). Three of the original Site 4 moorings were recovered on the continuation of Cruise M3 (August 1998) and the remaining five will be recovered on Cruise M4 (April-May 1999).

Chapter Summaries

The main body of the Annual Interim Report consists of Chapters 2 to 11. Chapter 2 (Introduction) discusses the rationale and historical background for the program and summarizes program objectives, phases, components, and report contents and organization. Site selection, a sampling program overview, cruise summaries, and data management are described in Chapter 3. The remainder of the report consists of chapters describing the individual components of the program. One-page summaries for Chapters 4 through 11 are presented on the following pages.

Geologic Characterization (Chapter 4)

Investigators

W. Sager, W. Schroeder

Objectives

- Define seafloor topography at/around each site
- Determine how topographic highs affect sediment distribution
- Geologic characterization of sites, including composition, origin, probable fate, roughness, and friability
- Determine subtle differences of orientation, size, and morphology
- Characterize substrate
- Determine the distribution of sediment types

Methods

- Geophysical surveys (high-resolution side-scan sonar, swath bathymetry, subbottom profiler)
- Grain size analysis of grab samples
- Visual analysis of ROV photographs and videotapes
- Analysis of rock samples (thin section petrography, x-ray diffractometry, scanning electron microscopy, electron microprobe, stable isotopes, ^{14}C dating) (few samples have been collected to date, and none analyzed)

Data Sets Discussed in this Report

- Geophysical data from Cruises 1A (November 1996) and 1C (May 1997)
- Grain size data from grab samples from Cruise 1C (May 1997)
- Analysis of ROV photos and videotapes from Cruise 1C (May 1997)

Results and Discussion

Side-scan sonar mosaics of each megasite are presented, followed by summaries of megasite and monitoring site bathymetry and megasite subbottom profiles. Geological characterizations of monitoring sites are developed based on ROV photos and videotapes, as well as grain size data from grab samples.

From prior MMS-funded surveys, it was known that carbonate mounds were often clustered with sizes ranging from several meters on a side to hundreds of meters wide and 10 to 18 m high. It was also known that areas of high acoustic backscatter were associated with many mounds and that in some cases these areas were preferentially located to the southwest of the mounds. This new study has emphasized and broadened these findings. In addition, the study is beginning to produce a better understanding of the relationship of backscatter to the mounds and the sediment characteristics.

Although it was known previously that many of the carbonate mounds are subcircular in plan view, new side-scan sonar data show the details of mound flanks and co-occurrences with far greater resolution than previously documented. These relationships are still being investigated.

The morphologic differences among mounds suggest differences in development. The low, wide carbonate hard bottoms imply slow upward growth over a large area, perhaps indicating stable sea level or slow sea level rise. It was previously speculated that such mounds grew at the shelf-edge during the slow sea level rise after the last ice age, but now they are known to be even more widespread. The tall, steep-sided "pinnacle" mounds suggest rapid growth during faster sea level rise. The widely-dispersed, shallower mounds, which are highly variable in size and height, may represent a short period of sea level stabilization in the middle of the deglaciation.

The newly acquired data also give insights about the location of mound formation. Prior data implied the mounds formed atop erosional unconformities on the two mounds in the MAMES survey area. New data have strengthened this observation. The data also imply that in some places, larger mound groups formed on bathymetric scarps, as shown by depth offsets across these mounds. Both observations imply that the mounds formed where suitable substrates were available.

Sediments at the monitoring sites are mainly sand, with a small and variable amount of clay. The sand-silt-clay ternary diagram implies two end-members, sand and clay, that are intermixed. Since the sediments currently being deposited in the region are fine clays, this could occur due to resuspension events that mix clay with sand in sediments. A third component consists of gravel-sized fragments, usually shell fragments or other biogenic debris. Gravel content is usually highest near mounds, indicating them as a source or suggesting mound proximity is an important factor controlling the presence of organisms.

Sediment Dynamics (Chapter 5)

Investigator

I. Walsh

Objectives	Methods
• Provide quantitative and qualitative measurements of the extent and occurrence of the nepheloid layer • Determine sedimentation and resuspension rates • Determine how topographic highs affect present-day sedimentation • Determine temporal variations in sediment texture • Relate short-term sediment dynamics to long-term sediment accumulation	• Vertically separated sediment traps (2 m, 7 m, and 15 m above bottom) • CTD/transmissometer/OBS profiles on each cruise • OBS instruments on current meter arrays • Trace metal, grain size and TOC/TIC analysis of sediment trap samples • ROV observations

Data Sets Discussed in this Report

- Water column profiles: Cruise M2 (October 1997) and Cruise S2 (January 1998)
- Sediment trap data: First two intervals (May to July 1997 and July to October 1997)

Results and Discussion

While full analysis of the data remains to be completed, the data collected to date indicate that the study site is an area of high spatial and temporal variability. Some regional trends are apparent from the data set. The surface layer was characterized by low salinity and a local maximum in the particle concentration reflecting biological activity during both the October 1997 and January 1998 cruises, with lower salinity and higher particle concentrations towards the west. A benthic nepheloid layer (BNL) was present at all sites in all casts, though its intensity as measured by the beam attenuation and the vertical gradient in attenuation was variable. The BNL was found to be associated with lower bottom water temperatures during both cruises.

Sediment trap results from the first two mooring periods reflect the influence of resuspension at the study sites, with fluxes increasing to the bottom for all moorings and time periods. Total organic carbon (TOC) concentrations decreased towards the bottom, probably reflecting dilution of fresher water column material with resuspended sediment. However, sediment TOC data analyzed from these sites were higher than all but the 15 meters above bottom (mab) traps. At this point no obvious explanation for this conundrum has presented itself.

The bulk flux ranged from 2 to 20 g m^{-2} d^{-1}, with all of the fluxes in the 15 mab traps below 5 g m^{-2} d^{-1} while all of the 2.5 mab traps recorded fluxes greater than 5 g m^{-2} d^{-1}. The highest fluxes at all depths were found at Site 5, with decreasing fluxes from Sites 5 to 9 and the lowest fluxes at Sites 1 and 4.

Comparing the two periods, the fluxes recorded were similar in the traps 15 mab but generally higher in the deeper traps in the August to October period than in May to July. At Site 1 the three moorings recorded similar fluxes at the 7 and 15 mab traps during the May to July period, with increasing fluxes in the bottom traps. In the August to October period the 7 and 15 mab traps recorded higher fluxes than in the earlier period with a greater degree of variability in the 7 mab traps. The higher fluxes and higher variability between the two periods may reflect a higher average bed shear stress between the two periods.

Geochemistry (Chapter 6)

Investigator

M. C. Kennicutt II

Objectives	Methods
• Document the degree of hydrocarbon and trace metal contamination in the benthic environment at each site • Characterize the benthic abiotic environment at each site to aid in determining the origins of sediment and to define the relationship between sediment texture and biological patterns	• Analysis of hydrocarbons [total petroleum hydrocarbons (TPH), extractable organic matter (EOM), polycyclic aromatic hydrocarbons (PAH)], and trace metals (Al, Ba, Cd, Cr, Fe, Hg, Pb, and Zn) in grab samples (Cruise 1C only) • Analysis of total organic carbon (TOC) and total inorganic carbon (TIC) in grab samples • Trace metal and TOC/TIC analysis of sediment trap samples

Data Sets Discussed in this Report

- Grab samples from Cruise 1C (May 1997) analyzed for hydrocarbons, trace metals, and TOC/TIC
- Grab samples from Cruise M2 (October 1997) analyzed for TOC/TIC

Results and Discussion

Measures of sediment hydrocarbons at the sites were low and relatively uniform. Little or no evidence of petroleum related hydrocarbons was observed at any of the nine study sites. The slight increase in EOM and PAH towards the west most likely represents a general fining of sediments. Trace metals indicative of contamination were observed to be at or near background levels at all sites as well. In particular, barium, a tracer of drill mud discharges, was observed to be at background levels with only a very few samples that might be interpreted as slightly elevated. The slight increase in a few metals (Ba, Cr, Fe, Zn) towards the west also most likely represents a general fining of sediments. In conclusion, the sediments collected at the study sites exhibited little or no evidence of a significant history of contamination from drilling related or other activities and only a slight geographic trend in concentrations.

Heterogeneous distributions of organic and inorganic carbon in sediments were observed. The relationships between environmental conditions and sediment composition is unclear. Significant variability in sediment carbon content was apparent between cruises, most likely representing small scale heterogeneity in sediments at the sites.

Physical Oceanography/Hydrography (Chapter 7)

Investigators

F. Kelly, N. Guinasso, Jr.

Objectives

- Characterize the regional and local current dynamics in the study area
- Determine the dynamics of important environmental parameters including temperature, salinity, dissolved oxygen, and turbidity
- Define the relationship of the current dynamics and environmental parameters to the geological and biological processes of the pinnacle features

Methods

- Moored instrument arrays (currents, conductivity, temperature, dissolved oxygen, turbidity, sediment traps)
- CTD/DO/transmissivity/PAR/OBS profiles
- Collateral data (satellite imagery, meteorological observations, etc.)

Data Sets Discussed in this Report

- Hydrographic profiles from first four cruises: 1C (May 1997), S1 (July 1997), M2 (October 1997), and S2 (January 1998)
- Instrument mooring data from first three intervals: May to July 1997, July to October 1997, and October 1997 to January 1998

Results and Discussion

The current meters at 16 meters above bottom (mab) measure the mesoscale flow just above the pinnacles. Across the entire pinnacle study region there was substantial similarity in the observed flow fields. During the first deployment interval, the principal direction sectors were east and northeast. Maximum speeds were in the 30 to 40 cm/s range, but occurred briefly and infrequently. During the second deployment period (mainly August and September), flow at 16 mab was generally weaker and more directionally variable. The principal direction sectors of east and northeast were balanced to some degree by currents in the south and southwest sectors. Maximum speeds were in the 25 to 30 cm/s range. During the third deployment period (mainly October through January) currents were more energetic than during the previous two periods. Currents were greater than 20 cm/s more frequently, but maximum speeds were still in the 30 to 40 cm/s range. The principal direction sectors were still east and northeast, but vector means were low because flow was to the south and southwest a significant amount of the time.

Compared with the flow at 16 mab, the near-bottom flow at 4 mab was more site specific. Bottom friction and the local topography influenced flow. The most frequent direction octants were those with a southerly component. Average scalar speeds were comparable at times to those at 16 mab, and mean vector speeds sometimes exceeded the overlying flow because of greater directionality.

Time series of dissolved oxygen and turbidity were collected at each mooring. Dissolved oxygen values were generally near or above 4 mg/L, except at Site 5, the shallowest site, during the second deployment period. At this site, values were below 3.0 mg/L much of the time and fell below 2.0 mg/L during 18 to 28 August and 5 to 13 September. Turbidity values were generally quite low, i.e., 0 to 2 nephelometric turbidity units (NTU), with brief periods during which turbidity rose to the 2 to10 NTU range.

Temperature from the instrument moorings followed a seasonal trend with superimposed variability caused by advective changes from tidal and inertial currents and possible intrusions by mesoscale water mass motion. Salinity ranged from 34.0 to 36.8 but generally was in the 36.2 to 36.4 range. Values above 36.5 suggest possible intrusion of Loop Current related water.

Vertical profiles showed almost all the water sampled on the four cruises had a density less than 26.25 sigma-theta. During Cruise 1C, Sites 5 and 6 had surface salinities below 30. The other sites had surface salinities as low as 33.5 and bottom water salinities close to 36.4. During Cruise S1, the setting was very different; no salinities below 34.5 were observed. Bottom salinities were around 36.2 to 36.4 with a salinity maximum of around 36.6 at midwater depths. During Cruise M2, bottom salinities were between 36.4 and 36.5. Lowest salinities were at Site 1 where the surface mixed layer was around 34.6. During Cruise S2, bottom salinities varied between 35.8 to just above 36. Lowest salinities were at Site 9 where the surface layer, extending to 5 m depth, was about 33.

Hard Bottom Communities (Chapter 8)

Investigators

D. Hardin, K. Spring, B. Graham, S. Viada

Objectives

- Describe hard bottom community structure and seasonal dynamics at each site
- Identify differences in hard bottom community structure among sites differing in relief (high/med/low) and location (east/central/west)
- Understand relationships between community structure and environmental parameters such as small-scale habitat variability, rock type, sediment cover, turbidity, and other geologic and oceanographic variables

Methods

- Random video/photographic transects and stations (ROV)
- Fixed video/photoquadrats (ROV)
- Collection of voucher specimens (ROV)

Data Sets Discussed in this Report

- Videotapes and photographs from Cruise 1C (May 1997)

Results and Discussion

A total of 790 random photoquadrats was analyzed from Cruise 1C. Most sites had at least 98 photoquadrats for analysis, but all but six photographs at Site 9 were rejected due to turbidity. Compiling the 10 most abundant taxa at each site yielded a list of 43 numerically dominant taxa. Cnidaria was the most-represented phylum with 13 taxa of octocorals, 10 of ahermatypic corals, 4 of antipatharians, and single taxa of hermatypic corals and actinarians (anemones). Porifera was next with five taxa, followed by Ectoprocta with four taxa. Ahermatypic corals had the highest mean density of 327.97 organisms/m^2 over all sites, due to the numerical dominance of *Rhizopsammia manuelensis*. Octocorals were second with 9.43 organisms/m^2, followed by poriferans, ectoprocts, and antipatharians with 5.30, 3.17, and 2.75 organisms/m^2, respectively. Densities and numbers of taxa at each site were highly variable.

Little of the biological variation among sites is apparently due to water depth, vertical relief, distance from the Mississippi River, or suspended sediment flux. Only 8 of the 21 taxa recorded at six or more sites had statistically significant regression coefficients for any of these physical variables, and there was no consistent pattern to the results. However, density of the numerically dominant *R. manuelensis* increased with proximity to the Mississippi River.

Significant correlations occurred between 20 pairs of taxa. Highly significant correlations among *Antipathes ?furcata*, *Ellisella* sp., and the large white solitary scleractinian are probably the result of their common significant positive association with depth. The tan-purple solitary scleractinian, the white solitary scleractinian, *?Paracyathus pulchellus*, and *Madracis myriaster* were also significantly correlated, but with no apparent effect of the four physical variables.

Despite the preliminary nature of the results, several findings conflict with those reported by others. For example, Gittings et al. (1992b) reported abundances of *Rhizopsammia* and overall organism abundances were positively related to distance from the Mississippi River at a range of 27 to 70 km, but the new data indicate abundances of this species and the combined densities of the 43 dominant taxa are negatively related to distance from the river at a range of 70 to 145 km. It is not known whether this contradiction is enigmatic or whether it indicates abundance maxima at approximately 70 km from the Mississippi. Also, the results do not indicate increases in the density of epibiota or number of taxa with increasing vertical relief. However, this preliminary analysis focused on between-site variations, whereas the physical and biological variations within sites may be nearly as large as those between sites. The more detailed statistical analyses planned for future reports should help address these questions.

Fish Communities (Chapter 9)

Investigator

D. Snyder

Objectives	Methods
• Describe fish community composition and temporal dynamics at each site • Identify differences in fish community composition among sites differing in relief and location • Understand relationships between fish communities and environmental parameters such as small-scale habitat variability, rock type, sediment cover, etc. • Identify trophic relationships among fishes, as well as between fishes and the epibenthic community	• Analysis of video and photographs from hard bottom community monitoring (ROV) • Literature review of trophic relationships

Data Sets Discussed in this Report

- Videotapes and photographs from Cruises 1C (May 1997) and M2 (October 1997)

Results and Discussion

Videotapes and still photographs from the first two monitoring cruises revealed a total of 69 fish taxa from 28 families. The most speciose families were sea basses (Serranidae), squirrelfishes (Holocentridae), lizardfishes (Synodontidae), jacks (Carangidae), wrasses (Labridae), and butterflyfishes (Chaetodontidae). The most frequently occurring taxa in video transects for the combined cruises were roughtongue bass (*Pronotogrammus martinicensis*), short bigeye (*Pristigenys alta*), bank butterflyfish (*Chaetodon aya*), and red barbier (*Hemanthias vivanus*).

The most commonly occurring species represent the deep reef fish assemblage reported for water depths of 50 to 100 m in the western Atlantic. Similar species have been reported by previous investigations of the pinnacle features, off the southeastern U.S., within the lower portion of the Algal-Sponge Zone of the West Flower Garden Banks in the northwestern Gulf of Mexico, and near the head of De Soto Canyon. The total of 69 taxa represents about half of the fish fauna known from the hard banks and reefs of the northern Gulf of Mexico.

Streamer basses (e.g., roughtongue bass and red barbier) probably numerically dominate the pinnacle habitats. These species feed upon plankton and were commonly observed hovering above the substrate picking plankton from the water column. Streamer basses provide forage for a number of piscivorous species (e.g., amberjacks, groupers, sharks, and mackerels).

A cluster analysis did not resolve distinctive patterns with respect to location and relief. Ordination showed some weak differences related to location, with eastern samples separating from central and western samples. Also, western samples showed more variability than the eastern or central samples. Qualitative data on the scale of the study area as used here may be too coarse to resolve any differences or similarities that may exist among the sites with respect to location or relief. A closer examination, at the level of transects within sites, along with an analysis of substrate preference of the dominant species, will be undertaken for the final synthesis report. This approach should provide greater insight into the processes structuring these assemblages.

Companion Study: GIS and Micro-Habitat Studies (Chapter 10)

Investigator

I. MacDonald

Objectives	Methods
• To integrate physical measurements with biological observations • To combine descriptive statistics from the hard bottom community structure and dynamics effort with the micro-habitat categorizations in a cross-cutting design • To provide a control on the within-site variability of the sessile community that can be used to determine the influence of abiotic factors --particularly current direction and the effect of pinnacle slope on current intensity	• Geographic information system (GIS) techniques are being used to integrate available data into consistent map formats and standardized displays. • Subsets of all bathymetric data were compiled in 300 by 300 m areas centered on the pinnacle or pinnacles within each site. The data were fitted to a 1 m grid. The 300 by 300 m grids were then contoured to provide base maps of each site. • A simple flow model was derived as a preliminary step toward using regional current meter data in conjunction with a realistic hydrodynamic model to approximate current flow on a scale that is compatible with the spatial resolution of other data sets. The model provides a crude approximation of current intensity on a several meter scale across each site.

Data Sets Discussed in this Report

- The ARC View GIS completed for this report incorporated data from Cruise 1A (November 1996), Cruise 1B (March 1997), and Cruise 1C (May 1997) as well as limited information from Cruise M2 (October 1997) (sediment grabs). For this report, GIS was used to determine the average exposure to currents at random photo stations in Megasite 1 as a demonstration of the application.

Results and Discussion

Plots of relative current exposure were prepared for Sites 1, 2, and 3. Generally, the plots show a relatively uniform exposure in the middle range, with localized pockets of relatively higher or lower exposure. Overall, the values suggest that bathymetry exercises the greatest influence to create variable current exposure at Site 2, where the spread of random photo stations encompasses all sides of the pinnacle. At Site 1, the high relief site, much of the actual study area is the flat top of the pinnacle, which was toward the up-current side of the site. There were, however, areas of apparent shadowing on the northwest margin of the feature. As might be expected, the low relief site showed the least variability at spatial scales that could be detected in the bathymetric grid. It is likely that more pronounced differences in current exposures do occur--on the up-current and down-current sides of a boulder for example--but it is not possible to model these differences with the available bathymetric data.

This highly simplified model does not take into account differences due to turbulent flow across the pinnacles. Nor does it delineate topographic steering that evidently occurs in the near-bottom layer. Data presented in Chapter 7 show that the uniform current vector in Megasite 1 was consistently to the northeast throughout the first deployment period. A mean current vector would be less valid for determining exposure if there were frequent reversals in flow direction as occurred during subsequent intervals. The data do show which regions of the sites would be most prone to local turbulence.

Companion Study: Epibiont Recruitment (Chapter 11)

Investigator

P. Montagna

Objectives

- To document the process of larval settlement, growth, and community development of hard bottom epibiota
- To test hypotheses about the effects of location, height above bottom, duration of deployment, surface texture, predation, and water flow on recruitment

Methods

Settling plates are attached to "biomoorings." The major elements of the settling plate experiment studies are:

1. Spatial study with biomoorings deployed at four sites (1, 4, 5, and 9) for about 16 months (May 1997 to August 1998)
2. Replication of the spatial study for a second 16 month period (January 1998 to April 1999)
3. Two settling surface treatments: hard and soft
4. Three settling plate treatments: uncaged (U), caged (C), and partially caged (P)
5. Three heights above the bottom (0, 2, and 13 m)
6. Time series study at Site 4, with eight biomoorings deployed initially (May 1997), one retrieved after 6 months (October 1997) and redeployed in January 1998, three retrieved after 16 months (August 1998) and the remaining five retrieved after 24 months (April 1999)

Data Sets Discussed in this Report

- The first time-series biomoorings were deployed on Cruise 1C (May 1997), and a single biomooring from Site 4 was retrieved on Cruise M2 (October 1997). These are the only data available for this report.

Results and Discussion

The biomass of organisms was small, diversity was low, and total coverage of organic matter was extensive. The organic matter was primarily due to bryozoan colonies that comprised an average of 94% of total coverage on the settlement plates. While the sample size is too small to calculate statistical significance, it is worth noting that both total coverage and bryozoan colony coverage were less in the caged (C) treatments than in the uncaged (U) treatments. Total polychaete coverage, however, was greater in the caged (C) treatments.

Because coverage was comprised almost entirely of small, filamentous bryozoan colonies, it is interpreted as an early succession community. Generally, low diversity, opportunistic (or *r*-selected) species, high growth rates, and small animals characterize early succession. In contrast, late succession communities are characterized by high diversity, specialized slow-growing (or *k*-selected), and large species. Gross recruitment rates of organisms other than bryozoans in the pinnacle habitat were extremely low.

Several differences were noted between treatments. Polychaetes other than serpulids increased in the caged treatments. These polychaetes were larger than the serpulid worms, and their large size may make them more vulnerable to predation. In contrast, serpulid worms were not affected negatively by predation.

None of the organisms appeared to be affected by small-scale turbulence produced by the caging material because all had positive recruitment rates relative to water flow. This is surprising because small-scale turbulence has been shown to have an impact on vertical and horizontal distributions of organisms in deep-water environments.

Chapter 2
Introduction

This Annual Interim Report summarizes the second year of a four-year program to characterize and monitor hard bottom features on the Mississippi/Alabama outer continental shelf (OCS). The study area is shown in Fig. 2.1. The "Northeastern Gulf of Mexico Coastal and Marine Ecosystems Program: Ecosystem Monitoring, Mississippi/Alabama Shelf" is being conducted by Continental Shelf Associates, Inc. and the Geochemical and Environmental Research Group of Texas A&M University, for the U.S. Geological Survey (USGS), Biological Resources Division.

The program consists of an integrated suite of reconnaissance, baseline characterization, monitoring, and process-oriented "companion studies." Based on previous studies and new geophysical reconnaissance, nine hard bottom sites in the Mississippi-Alabama pinnacle trend area have been selected for study. The central focus of the program is monitoring of hard bottom community structure and dynamics. The potential sensitivity of these communities to OCS oil and gas industry activities is of interest to the Minerals Management Service (MMS), the client agency for whom the USGS is administering this program. Other monitoring components (geological and oceanographic processes) are needed to provide an understanding of the dominant environmental processes that control or influence hard bottom communities. These may include substrate characteristics such as relief, microtopography, sedimentology, and contaminant levels, as well as water column characteristics such as temperature, salinity, dissolved oxygen, near-bottom current patterns, and the presence and extent of the bottom nepheloid layer. In addition, two companion studies have been designed to complement monitoring by providing information on key ecological processes such as benthic recruitment, growth, and community dynamics.

Background

The Mississippi-Alabama pinnacle trend area has been described as an important multiple use area for human commerce, fisheries harvest, recreation, and other activities, including oil and gas exploration and development (Texas A&M University 1990). The area has historically been of importance to adjacent states because of heavy demands placed on its natural resources for marine transportation, dredge dumping, and commercial and recreational fishing. Because of the petroleum industry's interest in the area and the potential for environmental impacts, an understanding of hard bottom communities and the dominant environmental processes that influence the system is critical.

Fig. 2.2 shows locations of previous hard bottom surveys and studies in the region. The pinnacle trend area was first reported by Ludwick and Walton (1957), who documented a 1.6 km wide band of shelf-edge prominences in water depths ranging from 68 to 101 m. The pinnacles typically had a vertical relief of about 9 m, with some having over 15 m relief. Subsequent pinnacle observations were reported during oil and gas lease block

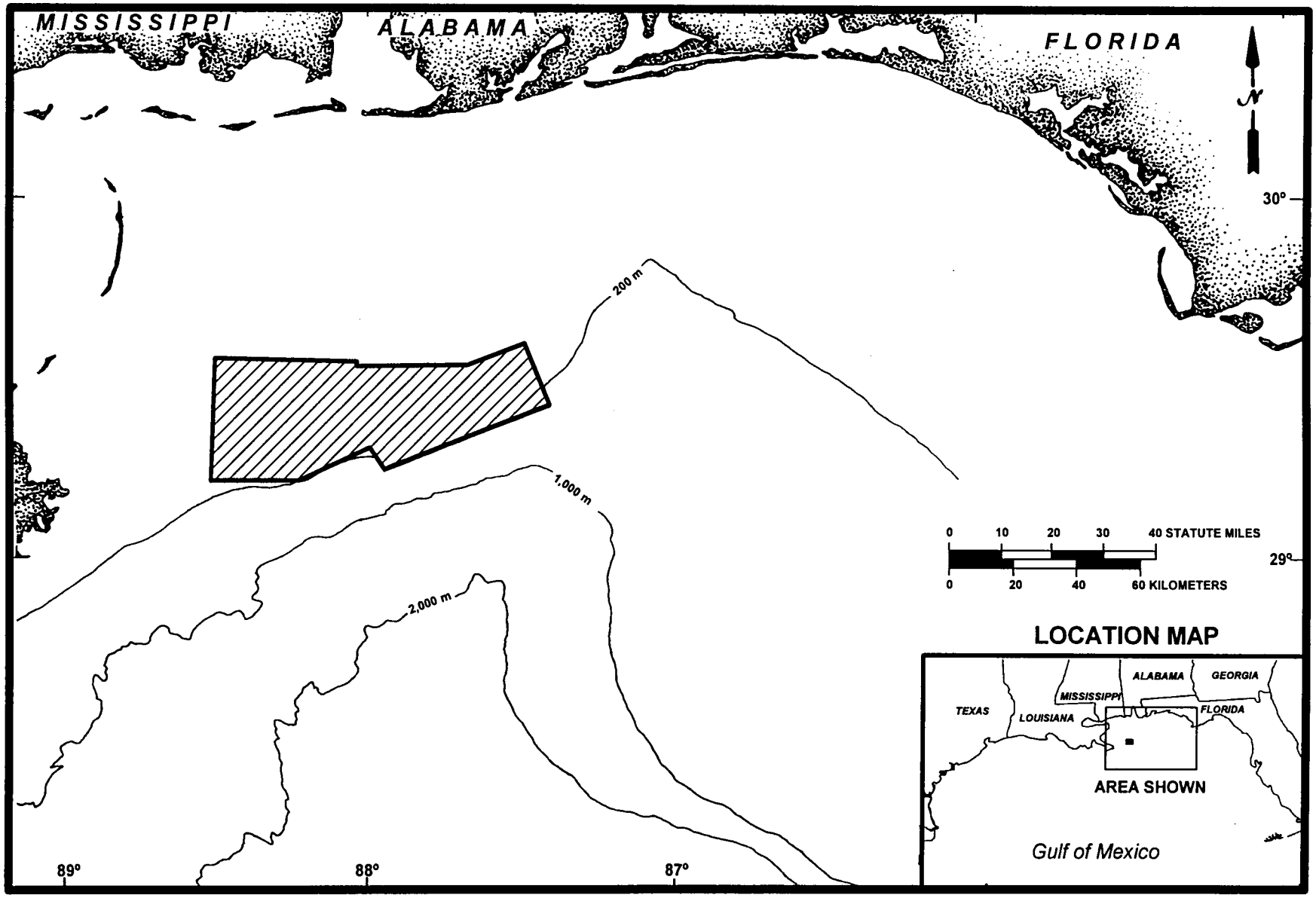

Fig. 2.1. Study area.

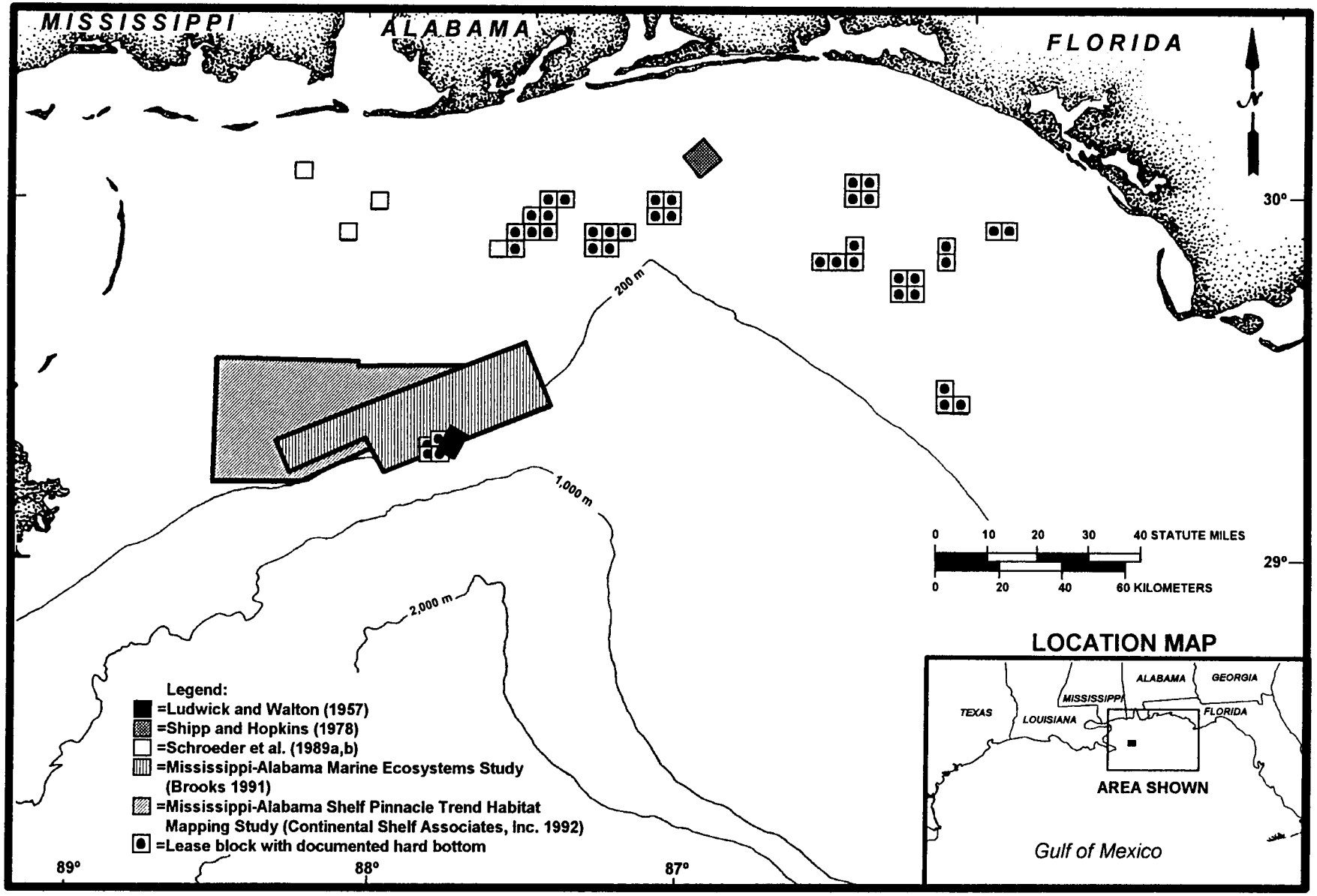

Fig. 2.2. Locations where hard bottom has been documented in the region of the study area.

surveys by Woodward-Clyde Consultants (1979) and Continental Shelf Associates, Inc. (1985a). Two major mapping/characterization studies in the pinnacle region were subsequently funded by the MMS: the Mississippi-Alabama Marine Ecosystems Study (MAMES) (Brooks 1991) and the Mississippi-Alabama Shelf Pinnacle Trend Habitat Mapping Study (MASPTHMS) (Continental Shelf Associates, Inc. 1992). MAMES included new field studies and provided a detailed synthesis of existing regional information about water masses and circulation, sediment characteristics and contaminants, water column biota, and soft bottom benthic communities including demersal fishes. However, information on pinnacle communities and related hard bottom features consisted mainly of descriptive observations from reconnaissance surveys.

At the conclusion of MASPTHMS, Continental Shelf Associates, Inc. (1992) identified several data needs. These included investigations to determine the origin, current state, and probable future of these structures, both biologically and geologically; investigations concerning the geographic and temporal distribution of turbidity/nepheloid layers that may occur throughout the Mississippi-Alabama shelf; and studies of species tolerance to various abiotic parameters such as turbidity.

The National Research Council (1992) has identified six objectives of obtaining information for assessing the environmental impacts of OCS oil and gas activities:

1. Characterization of major habitat types.
2. Identification of representative species (or major species groups) in the area of interest.
3. Description of seasonal patterns of distribution and abundance of representative species.
4. Acquisition of basic ecological information on key or representative species (e.g., trophic relationships, habitat requirements, and reproduction).
5. Determination of basic information on factors that determine the likelihood that various populations and communities would be affected by OCS activities, and the potential for recovery.
6. Determination of potential effects of various agents of impact (e.g., spilled oil, operational discharges, noise, and other disturbances).

Previous reconnaissance efforts in the pinnacle region have addressed the first two goals, by providing a characterization of major habitat types and identification of representative species. However, information is lacking on seasonal patterns of distribution and abundance, basic ecological information on key or representative species, and factors that determine the likelihood of impacts from OCS activities (e.g., tolerance to natural turbidity due to the presence of a nepheloid layer). The current program is intended to help address goals (3) through (5) above. Goal (6) would involve additional applied studies such as laboratory toxicity tests or monitoring around production platforms, and is beyond the scope of this program.

Commenting specifically on benthic processes, the National Research Council (1992) noted that "understanding of spatial and temporal variability in continental shelf habitats is limited, and there is little understanding of the relative vulnerability of the habitats to environmental impacts of OCS oil and gas activities." The report further noted that "the need for only broad-scale survey work has passed. Future research should focus on process-oriented programs designed to evaluate mechanisms that control the distribution of populations and communities, such as trophic links between benthic habitats and pelagic communities. The processes by which and the rates at which populations recover from disturbance must be understood in all habitats affected by OCS-related activities."

Multidisciplinary "ecosystem" studies of hard bottom communities have been conducted on the South Atlantic OCS (Marine Resources Research Institute 1984) and Southwest Florida shelf (Continental Shelf Associates, Inc. 1987a; Environmental Science and Engineering et al. 1987; Phillips et al. 1990). These studies provided broad-scale characterization of biological communities, information on seasonal dynamics and relationships to environmental variables, and some understanding of ecological interrelationships and processes. For example, the Southwest Florida Shelf Ecosystems Study included process-oriented studies involving sediment traps, time-lapse cameras, and colonization plates, as well as coordinated primary productivity studies. More recently, an integrated suite of monitoring and process-related studies of hard bottom communities has been conducted during the California OCS Monitoring Program (Steinhauer and Imamura 1990; Hardin et al. 1994; Science Applications International Corporation 1995). The current program similarly involves an integrated, interdisciplinary approach. The results will afford an opportunity to understand processes affecting the dynamics of pinnacle trend hard bottom communities and potentially determining their susceptibility to impacts from OCS activities.

Ultimately, the information from this program may be used to aid in OCS leasing decisions and to evaluate potential lease stipulations to protect pinnacle communities during petroleum exploration and development. A series of studies during the 1970's and 1980's resulted in a biological community-based classification scheme for the Flower Garden Banks and northern Gulf hard banks (Rezak et al. 1985). These studies also documented the extent and importance of the nepheloid layer in controlling the composition of hard bottom communities. Biological, geological, and oceanographic data from these studies were used to develop lease stipulations, including shunting requirements and no-discharge zones near certain banks, which have been used successfully for many years in the northern Gulf of Mexico.

Objectives

The overall goal of this program is to characterize and monitor biological communities and environmental conditions at carbonate mounds along the Mississippi-Alabama OCS. Specific objectives are as follows:

- To describe and monitor seasonal and interannual changes in community structure and zonation and relate these to changes in environmental conditions (i.e., dissolved oxygen, turbidity, temperature, salinity, etc.); and

- To characterize the geological, chemical, and physical environment of the mounds as an aid in understanding their origin, evolution, present-day dynamics, and long-term fate.

Phases

The program consists of four phases, each lasting approximately 12 months:

- Phase 1: Reconnaissance, Site Selection, Baseline Characterization, Monitoring, and Companion Studies;
- Phase 2: Monitoring and Companion Studies;
- Phase 3: Monitoring and Companion Studies; and
- Phase 4: Final Synthesis.

The flow of events is summarized in Fig. 2.3 and the schedule is given in Fig. 2.4. Phase 1 included two reconnaissance cruises (Cruise 1A, November 1996; and Cruise 1B, March 1997) followed by final site selection (April 1997) and the initiation of monitoring and companion studies on Baseline Characterization and Monitoring Cruise 1C (May 1997).

Phase 2 included two monitoring cruises, M2 (October 1997) and M3 (April 1998). (Cruise M3 began in April but was shut down due to weather delays; it was completed in August 1998.) In addition, mooring service cruises were conducted in July 1997 (S1), January 1998 (S2), and July 1998 (S3). Monitoring and companion studies will continue during Phase 3 with Cruise M4 (currently scheduled for April-May 1999) and two mooring service cruises.

At the end of each of the first three phases, Annual Interim Reports will be produced summarizing methods and results. Finally, during Phase 4, a Final Synthesis Report will be produced in which all data collected during Phases 1 through 3 will be summarized, analyzed, synthesized, and discussed in relation to historical data from the region.

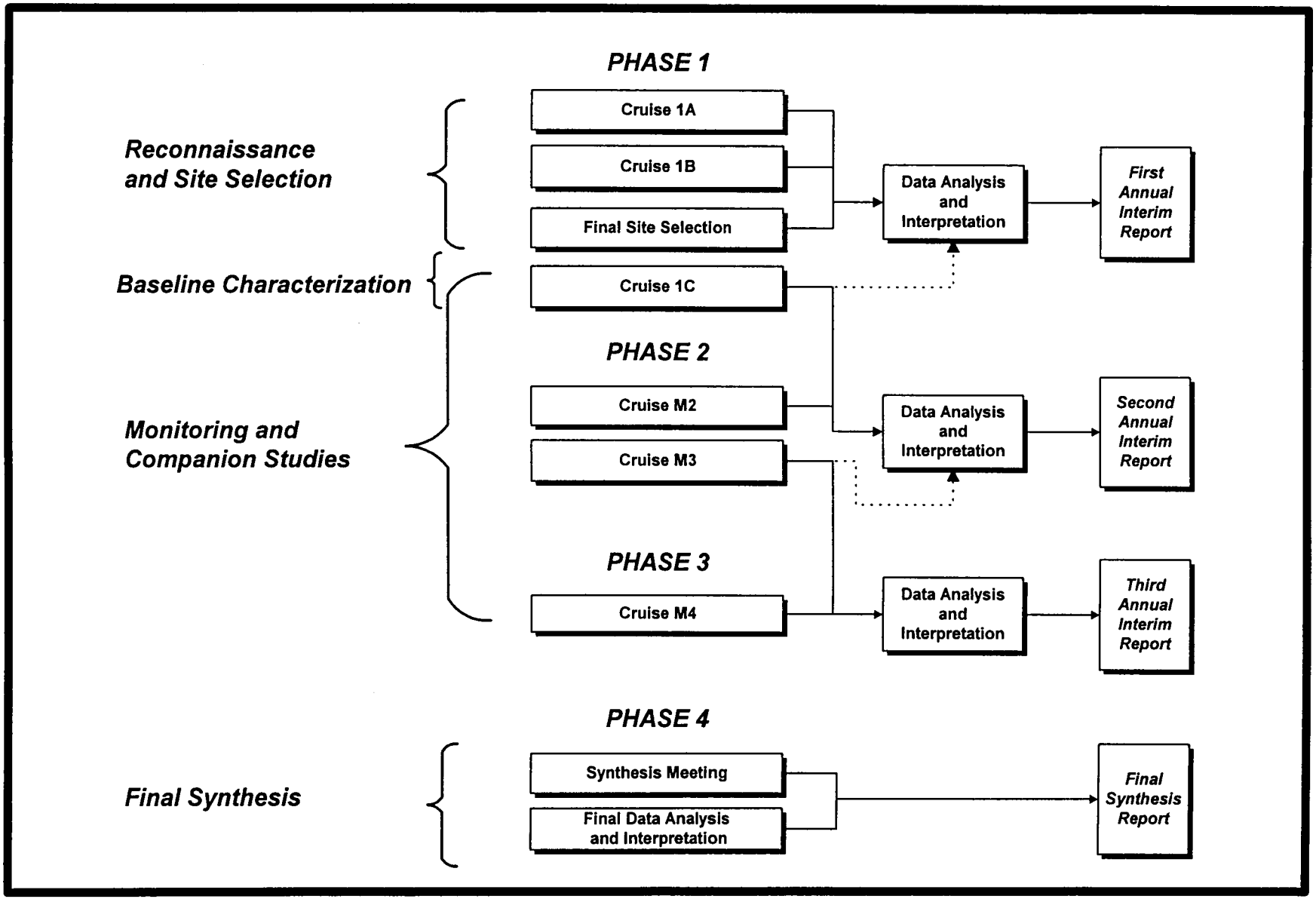

Fig. 2.3. Program flow chart.

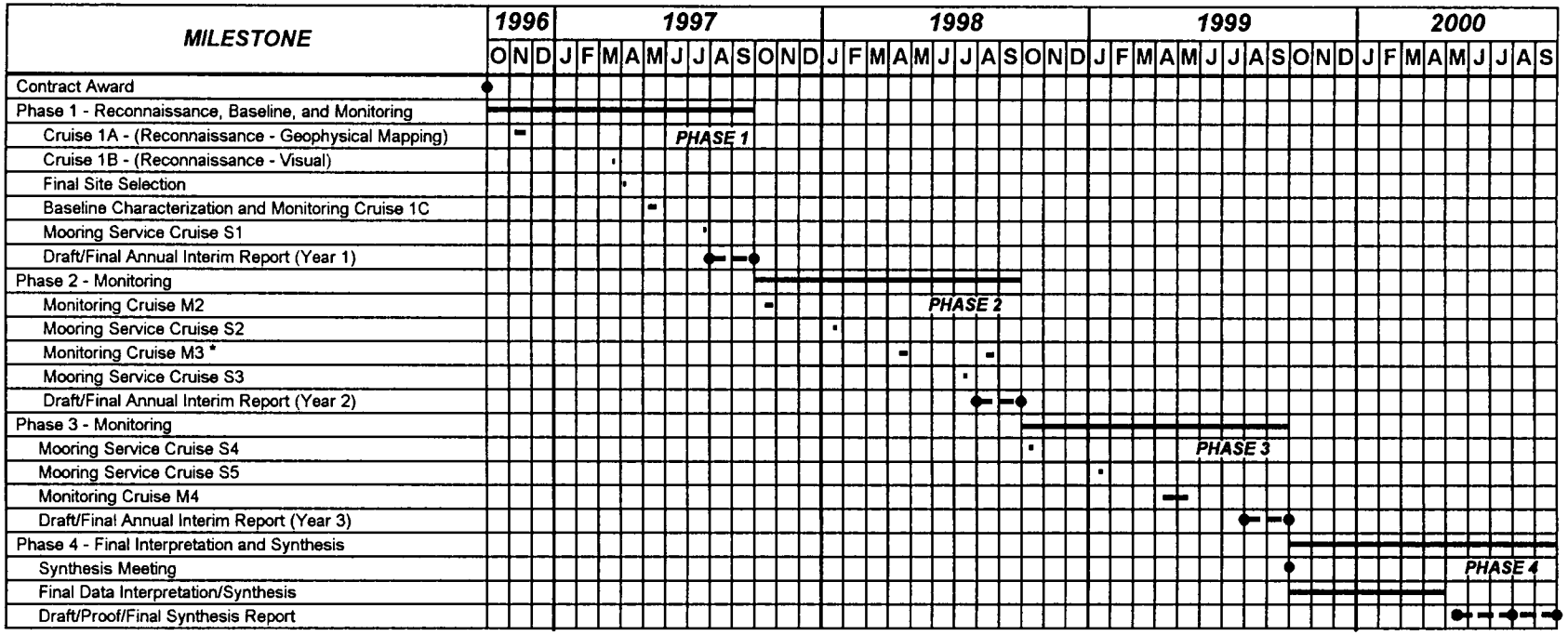

* Note: Cruise M3 began in April 1998
but was shut down due to weather delays.
It was completed in August 1998.

Fig. 2.4. Program schedule and milestones.

Components

The program consists of an integrated suite of monitoring and process-oriented companion studies to be conducted at the nine sites during Monitoring Cruise 1C, M2, M3, and M4. Table 2.1 summarizes the monitoring components and companion studies, including objectives, methods, and principal investigators.

Four monitoring components form the core of the program. These are hard bottom communities, fish communities, geology/sediment dynamics/geochemistry, and physical oceanography/hydrography. Hard bottom and fish community monitoring consists mainly of video and photographic sampling at each site. These data will help us to understand spatial and temporal variability within sites and will allow statistical comparisons among sites differing in relief, water depth, and proximity to the Mississippi River (among other factors). Geophysical surveys and data from laboratory analysis of grab samples and rock collections will be used to characterize the seafloor topography, sedimentology, and geochemistry (including contaminant levels) at each site and help to understand the origin, developmental history, and probable fate of the pinnacle features. The geological component also includes monitoring of nepheloid layer dynamics using sediment traps, transmissometer and optical backscatter profiles, and optical instruments on moored arrays. The data will be a critical factor in interpreting hard bottom biology, because the nepheloid layer is known to be a major influence on hard bottom community zonation in the northern Gulf of Mexico (Rezak et al. 1985). Physical oceanographic and hydrographic data are needed to understand both the geological and biological processes of the pinnacle features. Data from moored instrument arrays, hydrographic profiles, and collateral sources will allow a characterization of regional and local current dynamics and help understand the dynamics of important environmental parameters including temperature, salinity, dissolved oxygen, and turbidity. Currents and hydrographic variables are potentially important direct and indirect influences on hard bottom communities and could account for differences both within and between sites.

The two companion studies are designed to complement monitoring by providing information on key ecological processes such as benthic recruitment, growth, and community dynamics. The first, Micro-Habitat Studies, involves independent analysis of photographs and video collected during hard bottom community monitoring in relation to geological and oceanographic data. The analysis will focus on fine-scale factors such as microtopography, orientation, substrate characteristics, small-scale current patterns, and gradients in chemical contaminants. Techniques will include statistical analysis, modeling, and fine-scale mapping using geographic information systems (GIS). The second companion study focuses on Epibiont Recruitment. Through the use of settlement plates deployed on moored arrays, this study will document the process of larval settlement, growth, and community development of hard bottom epibiota. Experimental enclosures will be used to evaluate effects of predation and disturbance.

Table 2.1. Summary of program components.

Component	Objectives	Methods	Principal Investigators
Geology/Sediment Dynamics/Geochemistry			
Site Characterization	• Define seafloor topography at/around each site • Determine how topographic highs affect sediment distribution • Geologic characterization of sites, including composition, origin, probable fate, roughness, and friability • Determine subtle differences of orientation, size, and morphology • Characterize substrate • Determine the distribution of sediment types	• Geophysical surveys (high-resolution side-scan sonar, swath bathymetry, subbottom profiler) • Grain size analysis of grab samples • Visual and laboratory analysis of photographs and rock samples • Analysis of rock samples (thin section petrography, x-ray diffractometry, scanning electron microscopy, electron microprobe, stable isotopes, ^{14}C dating)	W. Sager W. Schroeder D. Benson
Mound History	• Determine the origin of calcareous mounds • Determine developmental history of the mounds • Predict the future fate of the mounds	• ROV rock collections • Analyze using thin section petrography, x-ray diffractometry, scanning electron microscopy, electron microprobe, stable isotopes, ^{14}C dating	W. Sager W. Schroeder
Sediment Dynamics	• Provide quantitative and qualitative measurements of the extent and occurrence of the nepheloid layer • Determine sedimentation and resuspension rates • Determine how topographic highs affect present-day sedimentation • Determine temporal variations in sediment texture • Relate short-term sediment dynamics to long-term sediment accumulation	• Vertically separated sediment traps • CTD/transmissometer/OBS profiles • Optical instruments on moored arrays • ROV observations • Trace metal and grain size analysis of sediment trap samples	I. Walsh
Sediment Geochemistry	• Degree of hydrocarbon and trace metal contamination in the benthic environment at each site	• Hydrocarbon and trace metal analysis of grab samples (Phase 1) • TOC/TIC analysis of grab samples and sediment trap samples	M. Kennicutt
Physical Oceanography/ Hydrography	• Characterize the regional and local current dynamics in the study area • Determine the dynamics of important environmental parameters including temperature, salinity, dissolved oxygen, and turbidity. • Define the relationship of the current dynamics and environmental parameters to the geological and biological processes of the pinnacle features.	• Moored instrument arrays (currents, suspended sediments, conductivity, temperature, and dissolved oxygen, sed. traps) • CTD/DO/transmissivity/OBS profiles • Meteorological observations • Collateral data (satellite imagery, etc.)	F. Kelly N. Guinasso

Table 2.1. (continued).

Component	Objectives	Methods	Principal Investigators
Hard Bottom Communities	• Describe hard bottom community structure and seasonal dynamics at each site • Describe differences in hard bottom community structure among sites differing in relief (high/med/low) and location (east/central/west) • Describe relationships between community structure and environmental parameters such as small-scale habitat variability, rock type, sediment cover, turbidity, and other geologic and oceanographic variables	• Random video/photographic transects and stations (ROV) • Fixed video/photoquadrats (ROV) • Collection of voucher specimens (ROV)	D. Hardin K. Spring B. Graham S. Viada
Fish Communities	• Describe fish community composition and temporal dynamics at each monitoring site • Identify differences in fish community composition among sites differing in relief and location • Identify relationships between fish communities and environmental parameters such as small-scale habitat variability, rock type, sediment cover, etc. • Identify trophic relationships among fishes, as well as between fishes and the epibenthic community	• Analysis of video and photographs from hard bottom community monitoring (ROV) • Literature review of trophic relationships	D. Snyder
Companion Study #1 Micro-Habitat Studies	• Improved understanding of relationships between hard bottom epibiota and microhabitat factors (e.g., microtopography, orientation, substrate characteristics, small-scale current patterns)	• Use of GIS to integrate and analyze biotic and abiotic data collected during hard bottom community monitoring	I. MacDonald
Companion Study #2 Epibiont Recruitment	• Document process of larval settlement, growth, and community development of hard bottom epibiota	• Settling plates on moored arrays; experimental enclosures to evaluate predation and disturbance	P. Montagna

Abbreviations: CTD = conductivity/temperature/depth; DO = dissolved oxygen; OBS = optical backscatter; ROV = remotely operated vehicle.

Report Contents and Organization

This report covers the approach, rationale, and methods for all work to date and includes data that have been analyzed and interpreted as of July 1998. This includes results from Monitoring Cruises 1C (May 1997) and M2 (October 1997), as well as mooring retrievals on Service Cruises S1 (July 1997) and S2 (January 1998). Some preliminary Cruise 1C data were previously presented in the Phase 1 report, but most of the data were not available at that time. Also, because Cruise M3 (April 1998) was shut down due to weather problems and completed in August 1998, none of the results are available for this report.

Following this introduction, Chapter 3 describes Site Selection and General Methods. Subsequent chapters present the rationale, field and laboratory methods, results, and discussion for each monitoring component and companion study.

Chapter 3
Site Selection and General Methods

Detailed methods for each program component are included in the individual chapters. As a general framework, this chapter first discusses site selection. An overview of the sampling program is then presented, followed by cruise summaries for Phase 2. Finally, data management is discussed.

Site Selection

The contract specified that a total of nine sites be selected, including one of each relief type (high, medium, and low) in the eastern, central, and western portions of the study area. The relief categories were defined as follows:

- high (>10 m)
- medium (5 to 10 m)
- low (<5 m)

Stratification of sites by relief and longitude is reasonable, based on previous studies. Studies of hard bottom communities in the Gulf of Mexico, South Atlantic Bight, and off Southern California have shown that community structure varies greatly with substrate relief (Marine Resources Research Institute 1984; Rezak et al. 1985; Continental Shelf Associates, Inc. 1987a; Phillips et al. 1990; Hardin et al. 1994). Observations with a remotely operated vehicle (ROV) during the MAMES surveys showed that pinnacle community composition varied with relief and proximity to the Mississippi River plume. It was hypothesized that the river plume influences long-term water quality, resulting in diminished community development on hard bottom features close to the Mississippi River delta (Gittings et al. 1992b).

Other factors considered in site selection were representativeness, availability of existing video and photographic data, and previous oil and gas industry activities. The site selection process is described in detail below.

Megasite Selection

Prior to Cruise 1A, five large areas ("megasites") were selected for geophysical reconnaissance (Fig. 3.1). The selection of the five megasites was based on geophysical data collected during the MAMES (Brooks 1991) and MASPTHMS (Continental Shelf Associates, Inc. 1992) surveys.

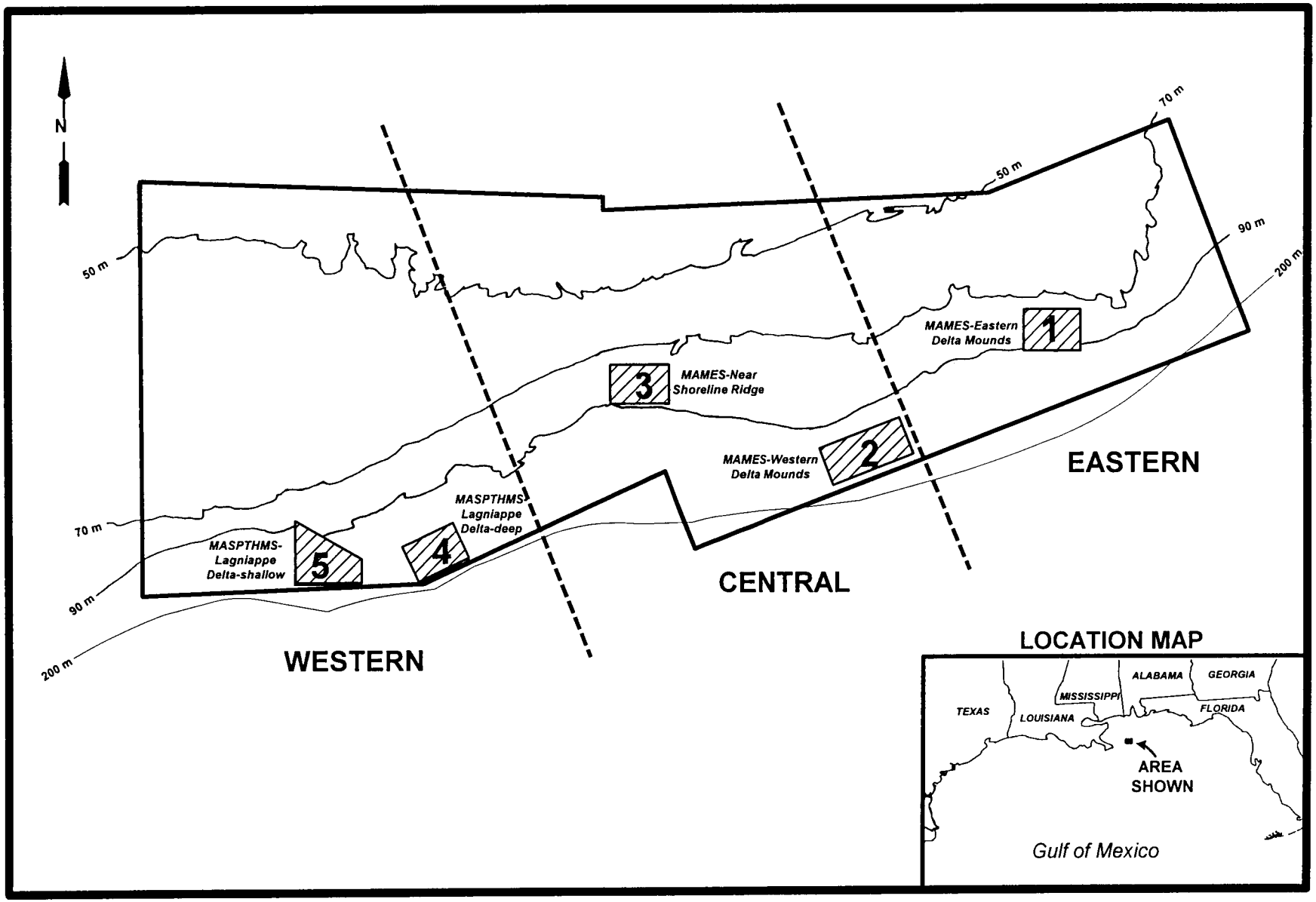

Fig. 3.1. Geographic locations of megasites surveyed during Cruise 1A.

- Megasite 1 - MAMES - Eastern Delta mounds
- Megasite 2 - MAMES - Western Delta mounds
- Megasite 3 - MAMES - Near-shoreline ridge
- Megasite 4 - MASPTHMS - Lagniappe Delta, deep
- Megasite 5 - MASPTHMS - Lagniappe Delta, shallow

The megasites were selected because they are known to contain numerous features of varying relief (candidate sites) and could be surveyed within the time and financial restrictions of the contract.

Geophysical Reconnaissance and Preliminary Site Selection

During Cruise 1A (November 1996), the five megasites were surveyed using swath bathymetry, high-resolution side-scan sonar, and subbottom profiler to produce detailed maps. After the initial survey of all five megasites, small subsets were chosen within Megasites 1, 2, 3, and 5 for higher resolution mapping. Most candidate sites ultimately selected were located in these high resolution mapping areas. Chapter 4 of the First Annual Interim Report describes the reconnaissance process in more detail.

After the cruise, we prepared a list of candidate high, medium, and low relief features within the megasites and tabulated the historical video and photographic data (Table 3.1). At this point, candidate high relief Sites 1, 5, and 7 were selected. The sites are located on flat-top mounds in Megasites 1, 3, and 5. The flat-top mounds seemed an obvious choice for the high relief category because these large, striking features were common in all three megasites and video coverage was available from the earlier MAMES and MASPTHMS surveys. Medium relief features were also selected within the high-resolution mapping areas in Megasites 1 and 2 (Sites 2 and 4, respectively). The candidate medium relief sites were located on steep-sided pinnacles, which are common in both megasites and provide a contrast to the flat-top mounds selected for the high relief category. Previous video and photographic data were available from the vicinity of Site 4.

Visual Reconnaissance

After the geophysical reconnaissance and review of historical data, we were able to select all three high relief sites and two of three medium relief sites. The main problem at this point was identifying low relief sites. A visual reconnaissance was necessary because there were no historical video or photographic data from low relief sites and because geophysical data alone cannot indicate whether a biological community is present on low relief hard bottom. For example, although geophysical data may indicate possible hard bottom, a thin sand veneer may be present which can prevent the attachment of hard bottom biota.

Table 3.1. Monitoring site selection in relation to types of hard bottom features and availability of previous video data. Bullets indicate the presence of each type of hard bottom feature within a megasite and whether previous video data were available (●) or not available (○). Candidate sites visited during Cruise 1B (visual reconnaissance) are shaded. Boxes indicate the final sites (with site numbers next to the bullets).

Type of Feature	Eastern	Central		Western	
	Megasite 1	Megasite 2	Megasite 3	Megasite 4	Megasite 5
High Relief (>10 m)					
Flat-top mounds	●1		●5		●7
Steep-sided pinnacles		●			●
Medium Relief (5-10 m)					
Steep-sided pinnacles	○2	●4[a]	○	○	○8
Low Relief (<5 m)					
Patch reefs/raised hard bottom		○	○6		
Pinnacles/mounds	○3	○	○	○	○9
Linear hard bottom	○				

[a] Previous video data were available for higher relief pinnacles in the area.

Four candidate sites lacking previous video or photographic data were identified as needing visual reconnaissance (Table 3.1). During Cruise 1B (March 1997), these features were surveyed briefly using an ROV to determine whether a hard bottom community was present. Candidate Sites 3, 6, and 9 were low relief sites within Megasites 1, 3, and 5. Candidate Site 8 was a medium relief site within Megasite 5. All of the candidate sites visited during Cruise 1B had hard bottom communities present and were ultimately chosen as final sites.

Final Site Selection

After the completion of Cruises 1A and 1B, the program managers and key principal investigators prepared a final site list. Site selection was discussed and approved in April 1997 during a teleconference with the USGS Contracting Officer's Technical Representative (COTR), the Scientific Review Board, and the program principal investigators. The final sites are shown in Fig. 3.2 and summarized in Table 3.2.

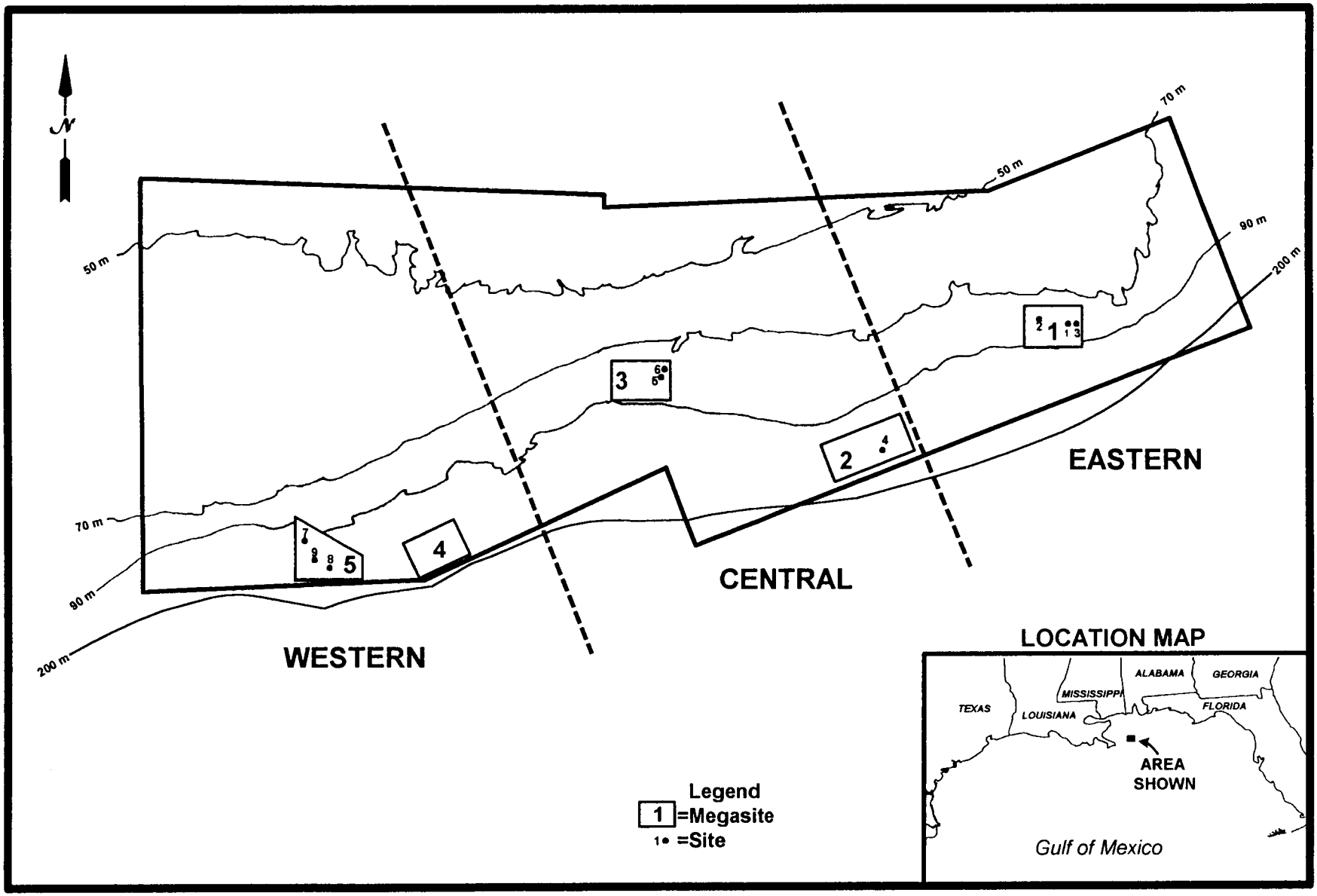

Fig. 3.2. Locations of final monitoring sites.

Table 3.2. Final monitoring sites.

Site	Area and Megasite	Relief Category	Water Depth and Lat/Long	Leasing Status	Previous Video and/or Photographic Data	Notes
1	Eastern (Megasite 1)	High	63-76.5 m 29°26'19.131"N 87°34'27.273"W	In Destin Dome Block 533 which is not leased	MAMES Video Stations 13 and 14	Site diameter 200 m. Flat top feature known as 40 Fathom fishing grounds in eastern high resolution survey area. Site extends across top of pinnacle and down the northeastern and eastern edges
2	Eastern (Megasite 1)	Medium	69.5-81.5 m 29°26'41.053"N 87°36'26.512"W	In Destin Dome Block 532 which is not leased	None	Site diameter 120 m. Steep sided pinnacle is largest within western high resolution survey area. Site includes numerous irregular outcrops with heights ranging from less than 1 m at the periphery up to 10 m toward the site center
3	Eastern (Megasite 1)	Low	76-80.3 m 29°26'15.901"N 87°34'15.266"W	In Destin Dome Block 533 which is not leased	None. First visited during Cruise 1B on 24 March 1997	Site diameter 150 m. Patchy low relief rock outcrops with diameters ranging from 1 to 10 m and relief ranging from <1 to 4.5 m
4	Central (Megasite 2)	Medium	95-107 m 29°19'39.041"N 87°46'7.849"W	In Destin Dome Block 661 which is not leased. May be within 900 m of a previous drillsite to the east-northeast in Destin Dome Block 617	MAMES Video Station 18 is in general area	Site diameter 140 m. Gradual sloping mound of hard bottom with thin sand veneer and low relief rock outcrops (0.5 to 2 m). Located in southern high resolution survey area
5	Central (Megasite 3)	High	62-78 m 29°23'35.930"N 87°58'51.055"W	In Main Pass Block 223 which has been leased and has a production platform	MAMES Video Station 8 is in general area	Site diameter 160 m. Flat top pinnacle with thin sand veneer in eastern high resolution survey area. Smaller outcrops along edges of pinnacle

Table 3.2. (continued).

Site	Area and Megasite	Relief Category	Water Depth and Lat/Long	Leasing Status	Previous Video and/or Photographic Data	Notes
6	Central (Megasite 3)	Low	75-78 m 29°23'52.887"N 87°58'42.610"W	In Main Pass Block 249 which has been leased and has had many exploratory wells, but no production plans	None. First visited during Cruise 1B on 23 March 1997	Site diameter 150 m. Extensive areas of low-relief rock features ranging up to about 1 m in height and covered with a thin layer of fine sediments
7	Western (Megasite 5)	High	69.5-88 m 29°15'24.844"N 88°20'21.455"W	In Main Pass Block 286 which has been leased, but no drilling plans	MAMES Video Station 33; MASPTHMS ROV Dives 1, 2, and 3	Site diameter 200 m. Flat top pinnacle known as 36 Fathom Ridge, in northern high resolution survey area. Feature has more irregular edges than the two other flat top pinnacles (Sites 1 and 5)
8	Western (Megasite 5)	Medium	88-96 m 29°13'53.857"N 88°19'01.565"W	Just east of boundary between Main Pass Block 285 (leased) and Block 286 (leased but no drilling plans)	None. First visited during Cruise 1B on 23 March 1997	Site diameter 100 m. Rugged feature with numerous crevices and overhangs, located in the south-central high resolution survey area. Relief 8 to 9 m
9	Western (Megasite 5)	Low	89-95.5 m 29°14'19.499"N 88°19'36.859"W	In Main Pass Block 286 which has been leased, but no drilling plans	None. First visited during Cruise 1B on 21 March 1997	Site diameter 150 m. Small mounds and outcrops in the south-central high resolution survey area. Generally 0.5 to 2 m in height with diameters of 10 to 15 m. A few features with up to 5 m relief had ledges, overhangs, and crevices

Abbreviations: MAMES = Mississippi-Alabama Marine Ecosystems Study; MASPTHMS = Mississippi-Alabama Shelf Pinnacle Trend Habitat Mapping Study; ROV = remotely operated vehicle.

Overview of Sampling Program

Table 3.3 is an overview of the sampling program, including mooring deployments and retrievals at the monitoring sites. During Cruise 1C (May 1997), subbottom profiling was conducted to geophysically characterize each site in more detail than was possible with the broad-scale geophysical reconnaissance (Cruise 1A). Grab samples were collected for geological and geochemical analyses (see Chapters 4 and 6). Hydrographic profiling was also conducted at each station, including conductivity/temperature/depth (CTD), dissolved oxygen (DO), photosynthetically available radiation (PAR), transmissivity, and optical backscatter (OBS) (see Chapter 7). Hard bottom and fish community monitoring was conducted at each site using the ROV (see Chapter 8). Monitoring included random video/photographic transects and stations and establishment of fixed video/photoquadrats. Voucher specimens were also collected at some sites to aid in species identification.

The overall program consists of repeating the Cruise 1C sampling on three subsequent monitoring cruises (M2, M3, and M4). The only exception is the subbottom profiling at each site, which will not be repeated.

Six physical oceanographic/sediment dynamics moorings were installed during Cruise 1C (see Chapter 7). Three moorings were installed at Site 1, and one each at Sites 4, 5, and 9. Each site will have at least one oceanographic mooring in place throughout the study. Two of the three moorings at Site 1 are "re-locatable" and were subsequently redeployed at Site 5 on Cruise M3. Each mooring includes current meters at 4 and 16 m above bottom (mab), sediment traps at 2, 7, and 15 mab, and an instrument that measures temperature, conductivity, DO, and turbidity.

Eleven "biomoorings" (moorings containing sets of settling plates) were also deployed during Cruise 1C as part of the companion study of epibiont recruitment (see Chapter 11). Eight were deployed at Site 4 and one each at Sites 1, 5, and 9. The biomoorings at Sites 1 and 9 were retrieved on the continuation of Cruise M3 (August 1998); turbidity prevented retrieval of the biomooring at Site 5. Another set of biomoorings was deployed at the same sites on Cruise S2 (January 1998) and will be recovered on Cruise M4 (April-May 1999). The eight biomoorings at Site 4 are for a "time-series" experiment; the original plan was to retrieve one on each subsequent Service Cruise and Monitoring Cruise until all eight were retrieved. However, as explained below, this has been changed so that all biomoorings can be retrieved on monitoring cruises when the ROV is present to cut the anchor line. One Site 4 mooring was retrieved on Cruise M2 (October 1997) and redeployed on Cruise S2 (January 1998). Three of the original Site 4 moorings were recovered on the continuation of Cruise M3 (August 1998) and the remaining five will be recovered on Cruise M4 (April-May 1999).

Table 3.3. Summary of activities conducted on each monitoring cruise and mooring service cruise.

Site	Cruise and Date(s)						
	1C (May 1997)	S1 (Jul 1997)	M2 (Oct 1997)	S2 (Jan 1998)	M3		S3 (Jul 1998)
					(Apr-May 1998)	(Aug 1998)	
1	P H G V D(3) d(1)	S(3)	H G V S(3)	S(3) d(1)	H G V S(1) R(2)	r(1)	S(1)
2	P H G V	--	H G V	--	H G	V	--
3	P H G V	--	H G V	--	H G	V	--
4	P H G V D(1) d(8)	S(1)	H G V S(1) r(1)	S(1) d(1)	H G S(1)	V r(3)	S(1)
5	P H G V D(1) d(1)	S(1)	H G V S(1)	S(1) d(1)	H S(1) D(2)	G	S(3)
6	P H G V	--	H G V	--	H	G	--
7	P H G V	--	H G V	--	H	G V	--
8	P H G V	--	H G V	--	H	G V	--
9	P H G V D(1) d(1)	S(1)	H G V S(1)	S(1) d(1)	H S(1)	G V r(1)	S(1)

Abbreviations:
P = subbottom profiling
H = hydrographic profiling
G = grab sampling
V = video and photography

D(#) = deploy oceanographic mooring(s)
S(#) = service oceanographic mooring(s)
R(#) = remove oceanographic mooring(s)

d(#) = deploy biomooring(s)
r(#) = retrieve biomooring(s)

Phase 2 Cruise Summaries

Phase 2 included two monitoring cruises, M2 (October 1997) and M3 (April-May 1998). (Cruise M3 began in April but was shut down due to weather delays; it was completed in August 1998). In addition, mooring service cruises were conducted in July 1997 (S1), January 1998 (S2), and July 1998 (S3). The survey vessel for all cruises was the R/V TOMMY MUNRO. A Magnavox MX300 differential GPS was used for navigation. The cruises were staged out of Ocean Springs, MS.

The ROV used during monitoring cruises was the Benthos Openframe SeaROVER with a Python multifunction manipulator arm. Video, photographic, and ancillary equipment included a Sony high-resolution videocamera, DeepSea Power & Light Micro-SeaCam 2000 color videocamera, Photosea 1000 still camera and strobe, DeepSea Power & Light lasers, and a Simrad MS900 color imaging sonar.

Cruise S1

The first mooring service cruise, conducted from 27 to 31 July 1997, successfully serviced the oceanographic moorings and collected 11 CTD casts. A problem was encountered with the scheduled recovery of the first biomooring at Site 4, as the acoustic release would not work. An attempt was made to release several of the other identical biomoorings at the site in order to recover one biomooring, but these also would not release. It was decided to attempt to recover two biomoorings during Cruise M2 by cutting the moorings from their anchors using the ROV.

Cruise M2 and Follow-Up Meeting

Cruise M2 was conducted as several legs from 30 September to 31 October 1997. Approximately 21 days of weather downtime were incurred. All samples and data were obtained other than the biomoorings, as explained below.

Each of the nine monitoring sites was sampled during the cruise (Table 3.3). Grab samples were collected for geological and geochemical analyses (see Chapters 4 and 6). Hydrographic profiling was also conducted at each station; a total of 29 CTD casts were collected during the cruise (see Chapter 7). Hard bottom and fish community monitoring was conducted at each site using the ROV (see Chapters 8 and 9).

All six physical oceanographic/sediment dynamics moorings were retrieved and redeployed during Cruise M2. The moorings at Sites 1 and 5 were serviced during the 30 September to 6 October leg. The remaining moorings, including the one at Site 4, were serviced during the 28 to 31 October leg.

As noted above, during Cruise S1, a problem was encountered with the scheduled recovery of the first biomooring at Site 4, as the acoustic release would not work. An attempt was made to release several of the other identical biomoorings at the site in order to recover one biomooring, but these would also not release. It was decided to attempt to recover two biomoorings during Cruise M2 by cutting the moorings from their anchors

using the ROV. However, during Cruise M2, only one of the Site 4 biomoorings was retrieved and another was found to be damaged (due to shackle failure, the biomooring is now resting on the bottom).

Following the cruise, a meeting was held on 20 November 1997 between the COTR (Robert Meyer), MMS Contract Inspector (Robert Rogers), and CSA personnel (David Gettleson, Keith Spring, Bruce Graham, and David Snyder) with significant input from Paul Montagna (Epibiont Recruitment Principal Investigator). The participants discussed problems in retrieving the biomoorings and damage to the unrecovered biomooring. A new plan was developed and later approved to deploy four new biomoorings on the January 1998 service cruise (S2) and to recover the biomoorings with the assistance of the ROV on Cruises M3 (April-May 1998) and M4 (April-May 1999). Chapter 11 explains the revised schedule of biomooring deployment and retrieval and its effect on the experimental design.

Cruise S2

The next service cruise was conducted during 29 to 30 January 1998. All six oceanographic moorings were successfully serviced and 12 CTD casts were made. Four new biomoorings were deployed--one each at Sites 1, 4, 5, and 9. These are all scheduled to be retrieved on Cruise M4 (April-May 1999).

Cruise M3

The first part of Cruise M3 was conducted between 21 April and 2 May 1998. Poor weather delayed departure for two days (21 to 23 May) and interrupted the cruise for about three-and-one-half days on 26 to 28 May. The cruise was shut down by mutual agreement and was completed during 23 to 29 August 1998.

Despite the weather problems during the April-May portion of the cruise, all of the hydrographic profiling was done, and all six of the oceanographic moorings were serviced. The two re-locatable moorings at Site 1 were moved to Site 5. However, ROV sampling of only one hard bottom site was completed (Site 1). Grab samples were collected only at Sites 1, 2, 3, and 4.

During the second part of Cruise M3, ROV sampling was conducted at Sites 2, 3, 4, 7, 8, and 9. Turbidity prevented ROV sampling at Sites 5 and 6 despite repeated attempts. Grab samples were collected at Sites 5, 6, 7, 8, and 9. Biomoorings were retrieved at Sites 1, 4, and 9, but turbidity prevented retrieval of the Site 5 biomooring.

Data Management

A data management program has been established to monitor, control, and facilitate data flow and ensure the integrity of the data through each phase of the program. As part of this process, a program data management plan has been developed which consists of four interrelated elements: (1) data administration; (2) data control; (3) data utilization; and (4) data archiving submission.

The purpose of data administration is to ensure continuous tracking and custody of samples and data. Evidence of data possession, comparison, and security with signatures, dates, times, and location of data are noted. This element also ensures proper formatting and reporting of all data and distribution of data as required among the principal investigators.

Data control consists of monitoring the progress of data flow to identify data gaps and to facilitate further processing. The data control procedures adopted for the data management plan document data availability, data reduction, and data analysis.

Data utilization includes processing and validating data as they are submitted. The processed data are then made available to all study participants.

Available data are being routinely archived to ensure permanency.

Data types, formats, and procedures have been established to insure reliable and accurate data receipt and distribution. Sample inventories from the completed cruises have been developed, and a master inventory of samples received and analyses required has been completed. A sample inventory for all project components has been finalized. This includes expected cruise dates, sampling schedules, and standardized cruise, site, and station nomenclature for all work elements. This will ensure the smooth acquisition of data into the project database.

An inventory of the expected program data has been developed to ensure appropriate processing and availability of data. Data that have been submitted to data management are presented in Table 3.4.

Table 3.4. Data submitted to data management.

Data Description	Cruise and Date	Media
Detailed Mosaics for Sites 1 and 2	Cruise 1A (Nov 96)	Tape
Bathymetric observations	Cruise 1C (Apr 97)	Electronic
Bathymetric observations	Cruise M2 (Oct 97)	Electronic
Random photo locations	Cruise 1C (Apr 97)	Electronic
Random photo locations	Cruise M2 (Oct 97)	Electronic
Survey Videotapes	Cruise 1C (Apr 97)	Videotape
Random Photos	Cruise 1C (Apr 97)	CD ROM
Photo Photo Logs	Cruise 1C (Apr 97)	Electronic
Survey Videotapes	Cruise M2 (Oct 97)	Videotape
Random Photos	Cruise M2 (Oct 97)	CD ROM
Photo Photo Logs	Cruise M2 (Oct 97)	Electronic
Sediment PAHs	Cruise 1C (Apr 97)	Electronic
Sediment TPH, EOM, TOC, and TIC	Cruise 1C (Apr 97)	Electronic
Sediment Trace Metals	Cruise 1C (Apr 97)	Electronic
Sediment Grain Size	Cruise 1C (Apr 97)	Electronic
Sediment Grab Locations	Cruise 1C (Apr 97)	Electronic
Sediment Grab Locations	Cruise M2 (Oct 97)	Electronic
Random Photo Percent Cover Data	Cruise 1C (Apr 97)	Electronic
Random Photo Occurrence Data	Cruise 1C (Apr 97)	Electronic

Abbreviations: EOM = extractable organic matter; TIC = total inorganic carbon; TOC = total organic carbon; TPH = total petroleum hydrocarbons; PAH = polycyclic aromatic hydrocarbons.

Chapter 4
Geologic Characterization

Approach and Rationale

The geologic characterization portion of this project concerns the origin and evolution of, characteristics of, and sedimentation regime around carbonate mounds on the Mississippi-Alabama OCS. These mounds formed in an unknown manner at lower sea level stands of the Pleistocene-Holocene transgression (Ludwick and Walton 1957; Sager et al. 1992) and they have become a substrate upon which a diverse marine ecosystem has evolved (Gittings et al. 1992b).

Much of our current geological knowledge of the Mississippi-Alabama carbonate mounds and their environs come from two prior MMS-funded studies: Mississippi-Alabama Marine Ecosystems Study (MAMES; Brooks 1991) and Mississippi-Alabama Shelf Pinnacle Trend Habitat Mapping Study (MASPTHMS; Continental Shelf Associates 1992), both of which mapped the occurrence of carbonate mounds and the distribution of surficial sediments. Thousands of carbonate mounds ranging from less than a few meters in diameter to nearly a kilometer were found arrayed mostly in two isobath-parallel bands (Sager et al. 1992). Isobath-parallel ridges were also mapped in the shallower of these two depth zones. Both features are thought related to sea level stillstands during the last deglaciation. Surficial sediments are largely related to three late Pleistocene deltas, the Lagniappe Delta (Kindinger 1988; 1989) in the western part of the present study area (Fig. 4.1) and the "eastern" and "western" deltas in the original MAMES study area (Davis 1992). These delta sediments were deposited during sea level lowstands or in the case of the "eastern delta," during the early part of the last deglaciation (Davis 1992). Atop these sediments is a thin, variable layer, consisting mostly of sand, that is thought to have been deposited by reworking of shelf sediments near sea level as it rose across the shelf during the last deglacial transgression (Davis 1992).

The current project seeks to pick up where MAMES and MASPTHMS left off. Those projects were reconnaissance efforts to broadly characterize the Mississippi-Alabama OCS seafloor and to describe the general characteristics and distribution of carbonate mounds such as those reported by Ludwick and Walton (1957). Current project goals are to provide greater detail in the characterization of the mounds and their geologic environment. The objectives of the geological characterization subtask are to (1) use high-resolution side-scan sonar mapping to measure the large-scale physical characteristics, such as shape, locations, and gross roughness; (2) use high-resolution subbottom profiler records and grab samples to examine long term sedimentation; and (3) use ROV videos to characterize the small scale geology. Although understanding the origin and evolution of the mounds was an initial goal of this project, no funding was specifically allotted for this goal, so any progress will rely on clues gleaned from other program elements.

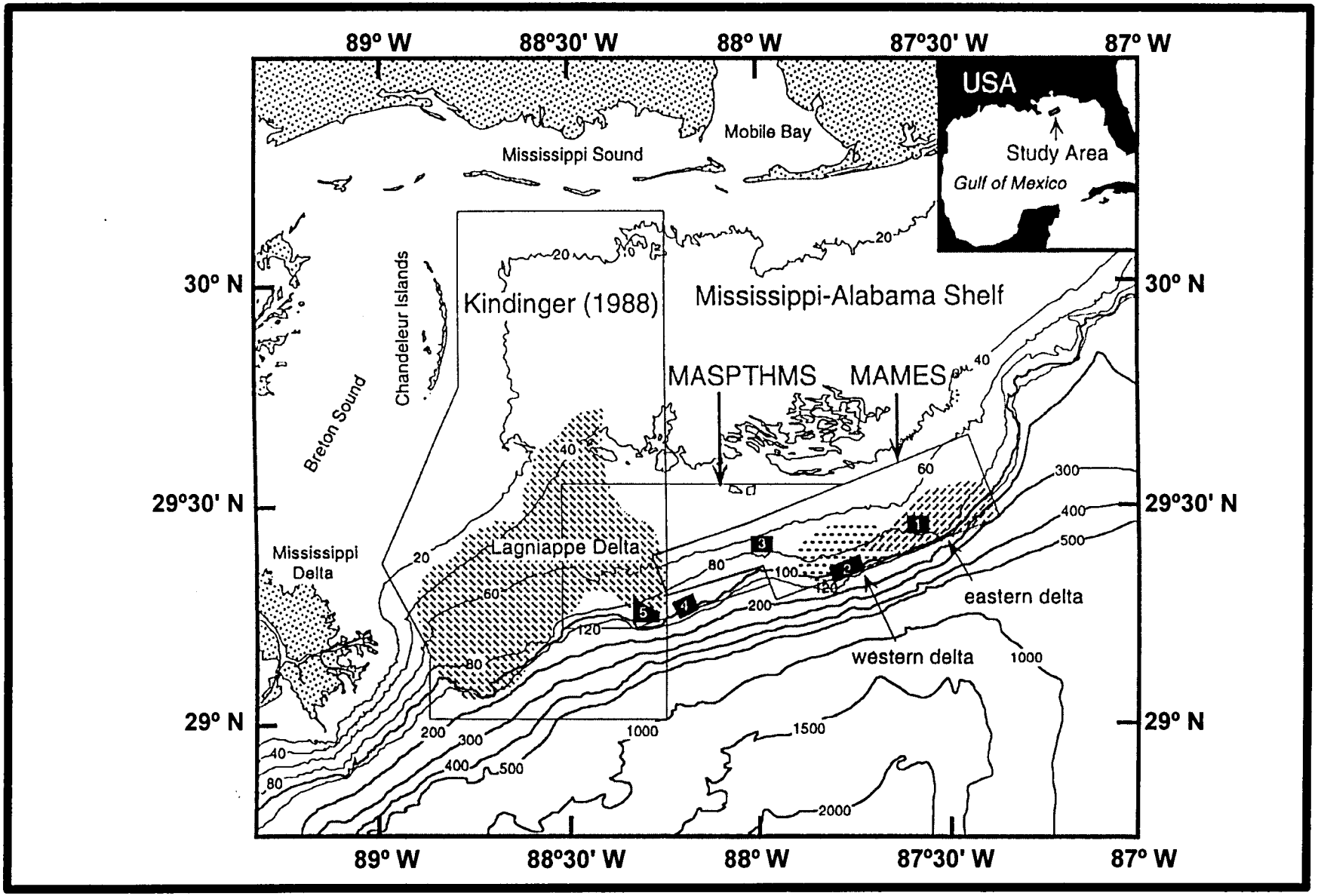

Fig. 4.1. Location map showing the Mississippi-Alabama outer continental shelf. Boxes show prior studies in the area. Hachured areas indicate the locations of deltas described in the text.

To address these goals, four main types of data are used: (1) high-resolution digital side-scan sonar images of the seafloor and bathymetry; (2) high-resolution subbottom profiler data; (3) ROV seafloor photographs; and (4) grab samples. The side-scan sonar images provide data concerning mound locations, sizes, orientations, shapes, and broad-scale roughness. Bathymetry data from the side-scan sonar yield the gross morphologies of the mounds and the surrounding seafloor. ROV bottom photographs give small-scale observations of mound morphology and surface characteristics that complement the larger scale side-scan observations. Sediment cover is shown by the subbottom profiler data as well as ROV bottom photographs whereas sediment types are given by analysis of grab samples. All of these parameters, as well as their correlations to biologic community structure, are being compared by georeferencing and use of a geographic information system (GIS; see Chapter 10).

Methods

High-Resolution Geophysical Baseline Cruise (1A)

One hundred eighty track lines, totaling 797 km in length and covering an area of 144.5 km^2 with side-scan sonar swaths, were collected at the five megasites with the *TAMU*^{2} digital side-scan sonar and an X-STAR 2-12 kHz chirp sonar on Cruise 1A. Ship's tracks were spaced 175 m apart and the ship's speed was approximately 5.5 knots with a sonar layback of about 85 m continuously measured with an ultra-short baseline acoustic tracking system. Navigation was done using *Skyfix* differential global positioning system (GPS), with an accuracy of better than 5 m. On these tracks, which were either oriented at a heading of 0° or 30°, an image swath of 400 m was used to provide ~228% coverage of the seafloor. This allowed features directly beneath the sonar on one ship track to be imaged by adjacent tracks. This duplication was important because features have different appearances depending on the incidence angle of the acoustic waves and because the *TAMU*^{2} sonar has a "blind spot" directly beneath the track. Because the sonar bathymetry swath is limited by the first bottom multiple to 3.4 times water depth, the bathymetry swaths overlapped by 25% to 50% in these surveys.

The sonar digitization rate was typically 1,650 pixels per ping at a ping rate of 2.5 per second. This configuration implies that each pixel is representative of an area of seafloor 1.25 by 0.24 m. Both 72 kHz and 11/12 kHz data were collected along each of the tracks so that the two frequencies could be compared to highlight differences in sediment texture. In addition to these data, slightly higher resolution data were also collected during Cruise 1A on tracks oriented perpendicular to the main survey tracks over areas of particular interest. These "detailed" surveys typically had track spacings of 150 m, sonar swath widths of 200 m, and were digitized with 3,300 pixels per ping, and at up to 5 pings per second. The goal of these data was to provide higher resolution images of likely sites for more detailed study. In all, 34.7 km of data were collected on these "detailed survey" lines covering an area of 5.6 km^2 with side-scan swaths.

Additional chirp sonar data were collected on Cruise 1C. A grid of perpendicular lines was acquired between the lines collected over the "detailed" survey sites from Cruise 1A. Because the original grid had tracks with an east-west spacing of 175 m and north-south spacing of 150 m, the Cruise 1C data filled in the grids at spacings of 87.5 and 75 m. Cruise 1C subbottom lines were positioned by differential GPS with an accuracy of about 5 m. The total length of subbottom data collected on Cruise 1C was 199.8 km.

TAMU^2 Sonar Data Interpretation

Sonar backscatter mosaics were produced by C&C Technologies, Inc. using proprietary image manipulation software. Images for each track were imported, georeferenced, and adjusted for sonar layback. The entire mosaic was built up of images for each of the component lines. Data gaps at the sonar nadir were filled with data from adjacent tracks. Owing to limitations of the proprietary image manipulation software, typical pixel sizes are about 1 m x 5 m. Subsequent analysis of the sonar mosaics has been carried out using ERMapper, a GIS analysis software package.

Bathymetry grids were also produced by C&C Technologies, Inc. Using proprietary software, sonar acoustic raypath takeoff angles were computed from phase angles measured at the sonar acoustic arrays. Takeoff angles and acoustic wave round-trip travel times were used to compute a depth profile perpendicular to the sonar track for each sonar ping. Depth locations and raypaths were corrected for variations in sound speed determined from periodic CTD casts made during the survey. Depth values were binned and plotted using the public domain GMT software package (Wessel and Smith 1995). Megasite bathymetry grids were binned at 15-m intervals whereas detailed survey bathymetry data were binned at 1-m intervals.

The analysis of *TAMU^2* data will include interpretation of side-scan sonar mosaics as well as quantitative studies of mound morphology and roughness from backscatter images and bathymetry. The backscatter patterns will be characterized as a starting point using the analyses from the MAMES and MASPTHMS studies. Interpretation maps for the megasites and detailed monitoring sites will be produced. Morphology will be examined in several ways. To define aspect ratio (length/width) and trends, the best fitting ellipse for a sample of the mounds in each area will be determined. Roughness will be quantified by examining inter-pixel variability and mound outline tortuosity. Flat seafloor, for example, has little pixel variability whereas rough seafloor has a higher degree of variability. Tortuosity can be determined by calculating the ratio of a mound's map-view outline to the area and rougher mounds should have larger values of tortuosity.

TAMU^2 bathymetry data will be used to make contour maps and three dimensional perspective views of each megasite and each monitoring site. These data will address our goals of describing seafloor topography and mound morphology, orientation, and large scale roughness. Depending on data quality, maps will be contoured at 1 to 2 m intervals.

TAMU^2 backscatter images will be used to map surficial sediments as well as surface characteristics of the mounds. These data will address the goal of describing mound

morphology, orientation, and roughness. Mosaics of the side-scan images will be made to allow mapping of sediments with similar backscatter patterns, which are related to texture. From the MAMES survey, backscatter patterns were found to be quite variable and possibly influenced by storm waves (Laswell et al. 1992). These data will also give higher resolution images of mounds in general and the study sites in particular. These images will help biologists better understand the habitat structure.

Subbottom Profile Interpretation

Data from the chirp echosounder will be used to examine thickness and character variations of shallow sediments in the study areas. Subbottom profiles will be analyzed using standard seismic stratigraphic techniques (e.g., Mitchum and Vail 1977). This involves (1) recognition and correlation of acoustic reflectors by their characteristics and (2) mapping and interpretation of seismic facies. The latter step assumes that sediments of different sedimentary facies give a common, recognizable acoustic response. Each subbottom line will be interpreted and the features and sedimentary layer thicknesses will be plotted on charts with survey navigation.

Chirp profiler records will be used to address the goal of understanding mound origin as well as long term sedimentation rates, sediment distribution, and the effects of mounds on sedimentation. Where appropriate, layer thicknesses will be digitized to make maps of sediment distribution. Of particular interest are the uppermost sediments, which consist of Holocene transgressive sands and recent mud from the nepheloid layer. Mounds may have been formed on a surface constructed by sea level lowstand erosion of delta forset beds. The Holocene sediments were therefore deposited around the mounds and their distribution shows the effects of currents perturbed by mound topography. With the chirp profiler data, the thicknesses of Holocene and the most recent sediments within the megasites will be mapped. The detailed study areas will provide information about long term deposition. Horizon characteristics and structure will provide clues about mound origin.

Comparison with Prior Data

To address the goal of assessing sediment texture changes and sedimentation processes around the mounds, the new geophysical data will be compared to existing reconnaissance survey data. Changes may be expected because the sediment backscatter patterns in some areas suggest sediment waves were created by storm waves (Laswell et al. 1992) and several hurricanes have passed over the study site since the last reconnaissance surveys. Reconnaissance subbottom profiler records were precisely navigated and can be compared with new profiles for changes in surficial character owing to changes in seafloor sediments. Likewise, the reconnaissance side-scan images can be compared with the 72 kHz *TAMU*[2] images, but to do this features and bathymetry in the two data sets will have to be matched since the old side-scan images are not as accurately positioned as the new data.

Sediment Grain Size Analysis

Grain size measurements are being done using standard techniques (Folk 1974). Samples are homogenized, treated with bleach to oxidize organic matter, and washed with distilled water to remove soluble salts. Sodium hexametaphosphate is added to deflocculate each sample before wet-sieving with a 62.5 micron (4ϕ) sieve to separate the sand and gravel from the mud fraction. The sand and gravel fraction is dried, weighed, and sieved at 1/2ϕ intervals from -1.5ϕ to 4.0ϕ. Each fraction is examined for aggregates and those found are disaggregated. Sample fractions are weighed to three significant figures. The mud fraction is analyzed for particle size by the pipette settling method at intervals of 4.5ϕ, 5.0ϕ, 5.5ϕ, 6.0ϕ, 7.0ϕ, 8.0ϕ, 9.0ϕ, and 10.0ϕ intervals.

Characterization of Rock Samples

If suitable carbonate rock samples are recovered in grab samples, ROV samples, or other means, a battery of tests may be applied to describe the composition, age, and other characteristics. These include thin section petrographic description, x-ray diffractometery, scanning electron microscopy, and electron microprobe analysis, all of which characterize particle content and composition. Carbon and oxygen isotope ratio measurements yield clues about the formation of the carbonate, and radiocarbon dating determines age. To date, few samples have been recovered and none have been analyzed.

ROV Ground Truth Data

ROV videotapes, still photographs, and grab samples were collected during Cruises 1C and M2 and will be collected on subsequent monitoring cruises. The grabs provide samples of surficial sediments insonified by the side-scan sonar. These are being described for gross characteristics and are also analyzed for particle size distribution (see below). Ten grabs were collected at each site during Cruise 1C to provide a baseline and five of these sites were resampled on Cruise M2. This procedure will be followed during each subsequent monitoring cruise to look for variations. ROV videos and still photos also provide valuable geologic information concerning seafloor features, sediment types, and texture. These are viewed and characterized using the descriptors in Table 4.1. A set of descriptors is chosen for the seafloor at the location of each ROV random photo station in part because these locations are accurately known and because the still photos have a common scale, having been shot at nearly the same distance from the seafloor (about 70 cm). Typically these photos show an area about 0.75 m across. ROV video tapes are viewed to show the approach to each photo station in order to obtain geologic context from larger-scale surroundings. Although it was possible to choose sediment texture, cover, roughness, and small scale relief descriptors at almost all stations, selection of larger scale descriptors [morphology, reef-like mound (RLM) part] was not always possible owing to limited visibility or knowledge of the surrounding terrain.

Table 4.1. Geologic descriptors of the seafloor at ROV photo stations.

General	Morphology (large scale)	RLM part	Relief (scale m)	Roughness (scale cm)	Sediment Texture	Sediment Cover
No rock visible	not desc	not desc	Flat Depression Mound	not desc	Fine Coarse Shell Hash Rubble	not desc
Rock outcrop	Boulder Ridge RLM	Base Face Top Flat Overhang	Low Medium High	Low Medium High	Fine Coarse Shell Hash Rubble	None Partial Complete

Abbreviations: RLM = reef-like mound.

Results

Megasite Side-scan Sonar Mosaics

Mosaics made from *TAMU*[2] side-scan sonar data contain images constructed from the merging of backscatter image strips from individual ship's tracks. The side-scan sonar sends out a fan-shaped acoustic pulse that is narrow and parallel to the ship's track and wide in the orthogonal direction. The sonar then plots a "scan" depicting the amplitude of the backscattered signal for that particular pulse. By sequentially plotting many scans from subsequent pulses, an image is constructed. Typically the image is transformed to appear as if made by an "aerial photograph" illuminated from the ship's track, i.e., "light" areas face the sonar and shadows are on the opposite sides. Usually little of the returned acoustic energy comes from reflection because the incidence angle is such that most such energy continues to propagate away from the sonar. Most of the returned energy is "backscattered," a process that includes diffraction from microtopography and scattering of energy from particles in the uppermost sediments (so called "volume scattering") (Johnson and Helferty 1990). In the images, strong echoes are plotted dark and shadows are white. Much of the returned acoustic signal appears to be related to mound topography and roughness (i.e., shadows, strong returns from faces that are directed towards the sonar, and diffraction from rough areas) and backscatter variations are caused by sediment textural variations.

Megasite 1

Prominent in the Megasite 1 mosaic are numerous groups of medium to large mounds, principally located in the northern, central, and western parts of the survey area (Fig. 4.2). In contrast, much of the seafloor in the southern part of the survey is mostly featureless. The large mound group in the north-central part of the megasite contains several large, flat-top mounds greater than 100 m in diameter. One of these, in the east-central part of the site, is the location of Site 1, atop the flat-topped mound known as "40-Fathom

Fig. 4.2. Side-scan sonar image mosaic for Megasite 1. Dark areas show high-backscatter (acoustic return) and light areas show low backscatter or shadows.

Fishing Grounds." Numerous smaller mounds are associated with these larger mounds. Another large mound group appears at the western edge of the survey. Associated with all of the mounds are areas of high backscatter, which appear dark in these mosaics. These high backscatter features usually are located on the southwest sides of the large mounds and mound groups. In subbottom profiler records, these areas show some erosion of the surficial sediments, so they are probably a textural difference caused by the winnowing current. Many small to medium mounds show high backscatter "tails" extending to the southwest. These appear as shallow gullies in the subbottom profiler records, implying erosion by bottom currents. In the northeast part of Megasite 1 are three linear to sub-linear high backscatter features that appear to be small buried ridges in the subbottom profiler records. The most linear is about 25 m wide by 300 m long. These may be related to the shoreline ridges noted in the original MAMES survey (Sager et al. 1992).

Megasite 2

The Megasite 2 mosaic shows numerous mound clusters in a broad band that trends southwest to northeast across the survey area (Fig. 4.3). In the western part of the survey, areas of medium backscatter define broad, low hard bottoms typically several hundreds of meters across. Detailed examination of the sonar records shows that small mounds, typically less than 10 to 15 m across are associated with these features. These large features appear to be carbonate hard bottoms which may consist of many smaller mounds. In the central and east-central part of the survey, taller mounds are evident by acoustic shadows. These are often irregular in shape and associated with subcircular regions of high backscatter. In the far-eastern part of the survey, small mound clusters are seen associated with subcircular areas of high backscatter. Subbottom profiler records suggest these small mounds are the outcropping parts of larger buried mounds. There is also a suggestion that some of the tall irregular mounds are associated with broad carbonate bases, as if they grew atop hard bottoms similar to those farther west. Unlike high backscatter features in other megasites, those in Megasite 2 are not linear and rarely appear to have a preferred direction or location relative to the mounds. Near the southern edge of the mosaic, a faint, curvilinear higher backscatter feature is the scar of a slump mapped by prior MMS surveys (Laswell et al. 1992).

Megasite 3

The Megasite 3 mosaic shows four main features: mounds, low carbonate hard bottoms, high backscatter areas, and a shoreline ridge (Fig. 4.4). Large mounds are seen clustered in two main areas on the east and west sides of the site. The eastern mounds are mainly subcircular features 50 to 100 m in diameter and many have flat tops. Site 5 is located in the cluster in eastern central part of the megasite. On the west side of the megasite, large and small mounds are clustered into a linear group that trends to the southeast. Two smaller groups appear to its north and northeast. Two areas of broad carbonate hard bottoms appear in the megasite, one in the center of the survey and another in the northeast corner. These low hard bottoms are similar in appearance to those notable in Megasite 2. Both of these hard bottoms have higher backscatter than the surrounding seafloor, although the northeastern one shows more backscatter contrast. In detail, each

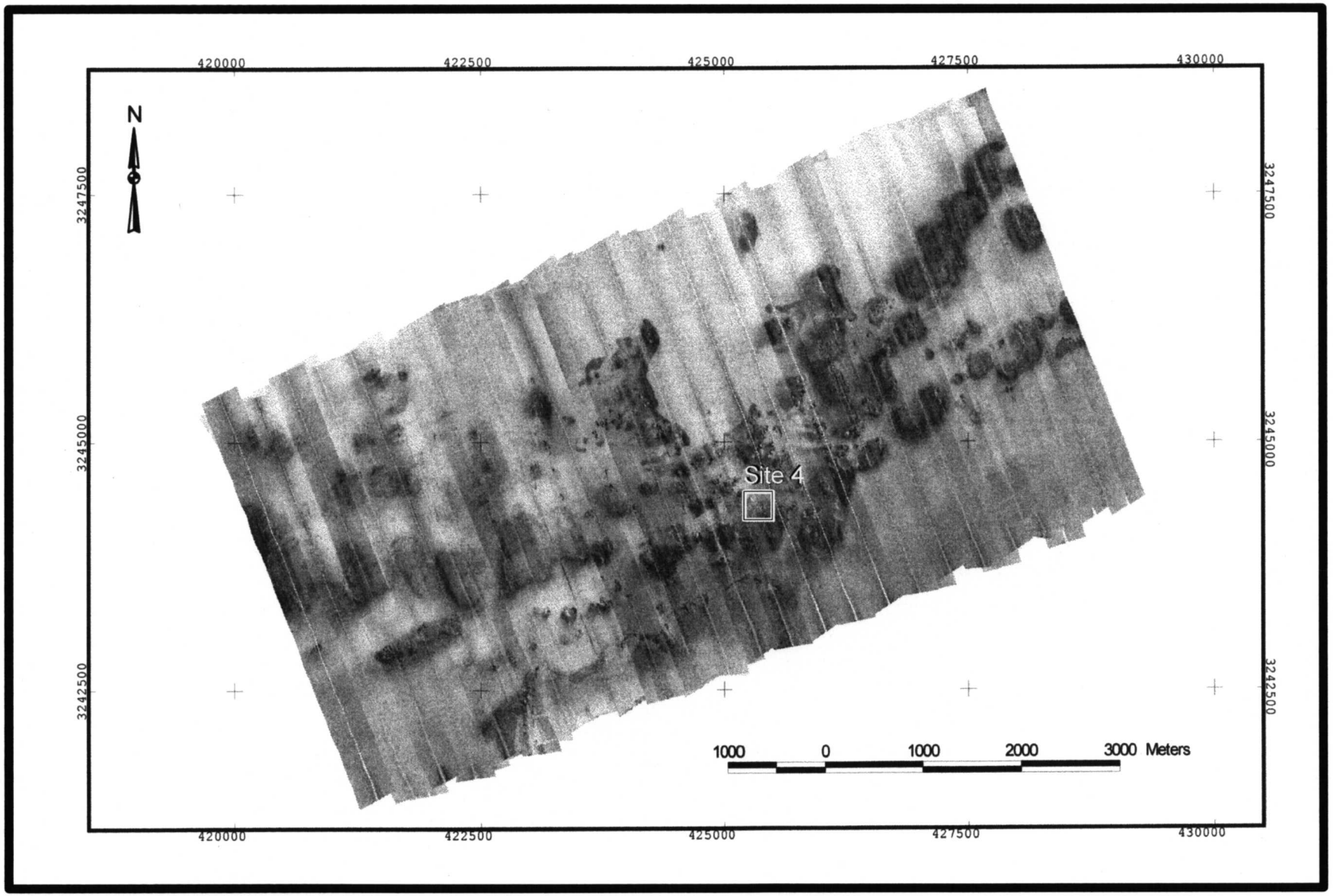

Fig. 4.3. Side-scan sonar image mosaic for Megasite 2. Dark areas show high-backscatter (acoustic return) and light areas show low backscatter or shadows.

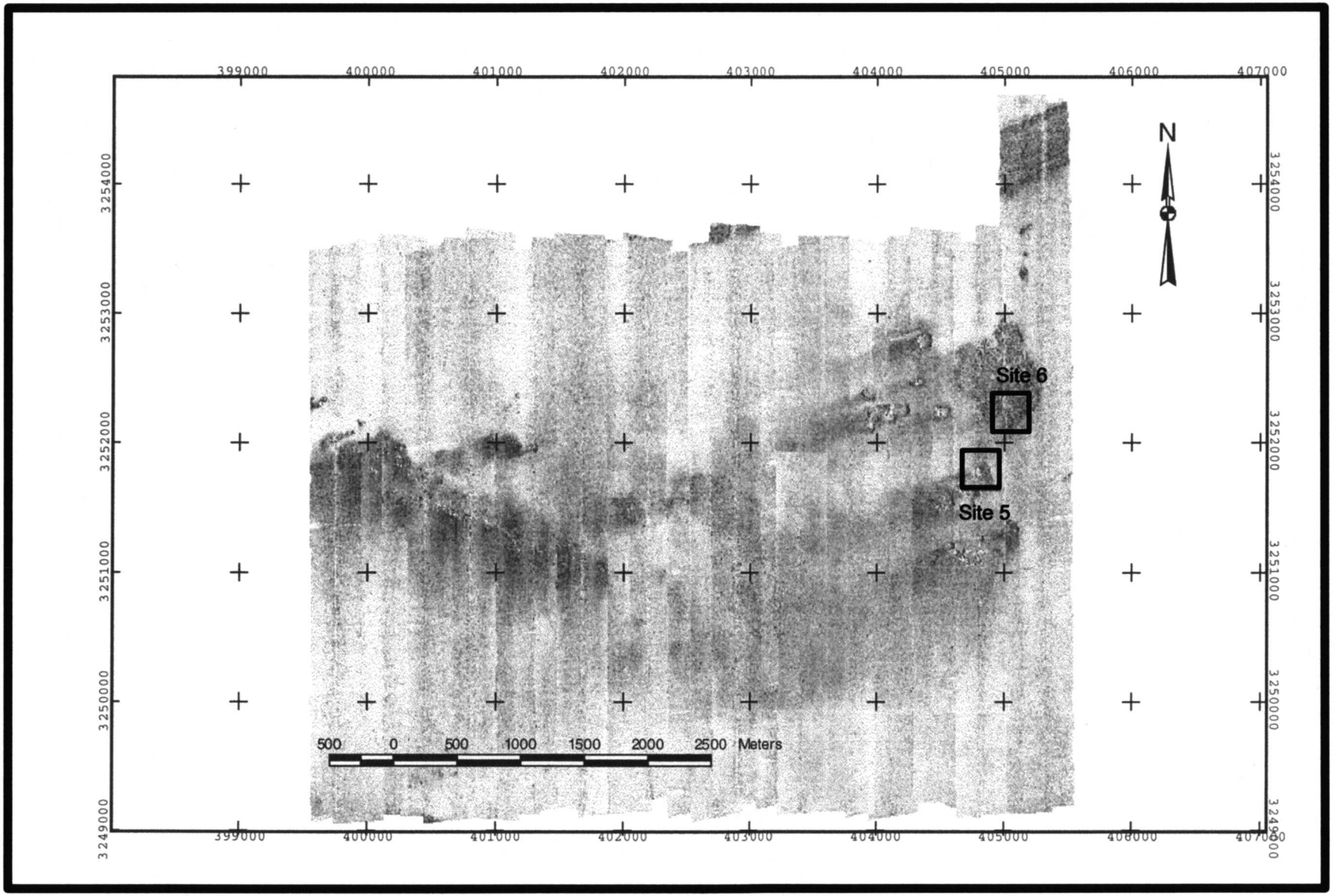

Fig. 4.4. Side-scan sonar image mosaic for Megasite 3. Dark areas show high-backscatter (acoustic return) and light areas show low backscatter or shadows.

hard bottom appears to have many smaller mounds, less than 10 to 15 m across, making up much of its surface. This is also similar in appearance to the Megasite 2 hard bottoms. As at other sites, areas of higher backscatter are associated with the mounds, often on the southwest sides of the topographic features. Also like other sites, many of these high backscatter areas are linear, or have linear edges, with a west-southwest trend. The linear, shoreline ridge feature appears mainly in an extension on the northeast corner of the survey. This extension was added because the ridge was known to be there from previous MMS surveys. The ridge shows high backscatter and has streaks parallel to its trend within. This part of the ridge connects with a larger ridge that extends for over 10 km to the east (Sager et al. 1992).

Megasite 4

The appearance of the Megasite 4 mosaic is unique among all of the sites that were surveyed (Fig. 4.5). Unlike any other site, there are no large mounds. Mounds in this mosaic are seen only as small, subcircular, high backscatter features typically less than 20 m in diameter. Few show any evidence of acoustic shadow, indicating they are also low in height. The most obvious mosaic features are mottled backscatter seafloor in the north and northwest parts of the megasite, and a curvilinear feature that runs from west to east across the southern part of the megasite. The curvilinear feature coincides with an area of slightly greater slope in the bathymetry (see below) and probably indicates the edge of a delta sediment wedge. The patchy backscatter areas in the northern parts of the survey do not match up with features in the subbottom profiler or bathymetry data. These are probably areas of slightly different sediment texture.

Megasite 5

In the Megasite 5 mosaic, a curvilinear group of hundreds of large to small mounds is the most obvious feature (Fig. 4.6). This group contains most of the mounds in the megasite. At its northwest end is a large, rough, linear mound (named "36-Fathom Ridge") whose north-south trend deviates from the overall northwest-southeast trend of the mound group. This mound is about 1,000 m long by about 150 to 300 m wide. Site 7 is at the northeast end of this mound. In the center of the curvilinear mound group are several large mounds, approximately 50 to 100 m across, including two that appear to have flat tops. The number of mounds decreases to the southeast, except for one moderately large group. As at other megasites, high backscatter areas are associated with the mounds. Usually these areas are on the southwest sides of mounds and mound groups and often they are linear with a southwest-northeast trend. A unique feature of Megasite 5 is a curvilinear, high backscatter band that appears seaward of the mound group. This feature is not associated with any mounds nor is it evident in the bathymetry. It appears to be the upper edge of certain sediment layers exposed at the shelf edge (see below).

Megasite Bathymetry

The bathymetry data produced from the *TAMU*[2] sonar far exceed previous similar data sets for accuracy and coverage. Nevertheless, several limitations of this sonar are obvious in bathymetry maps produced to date. To obtain greater depth precision,

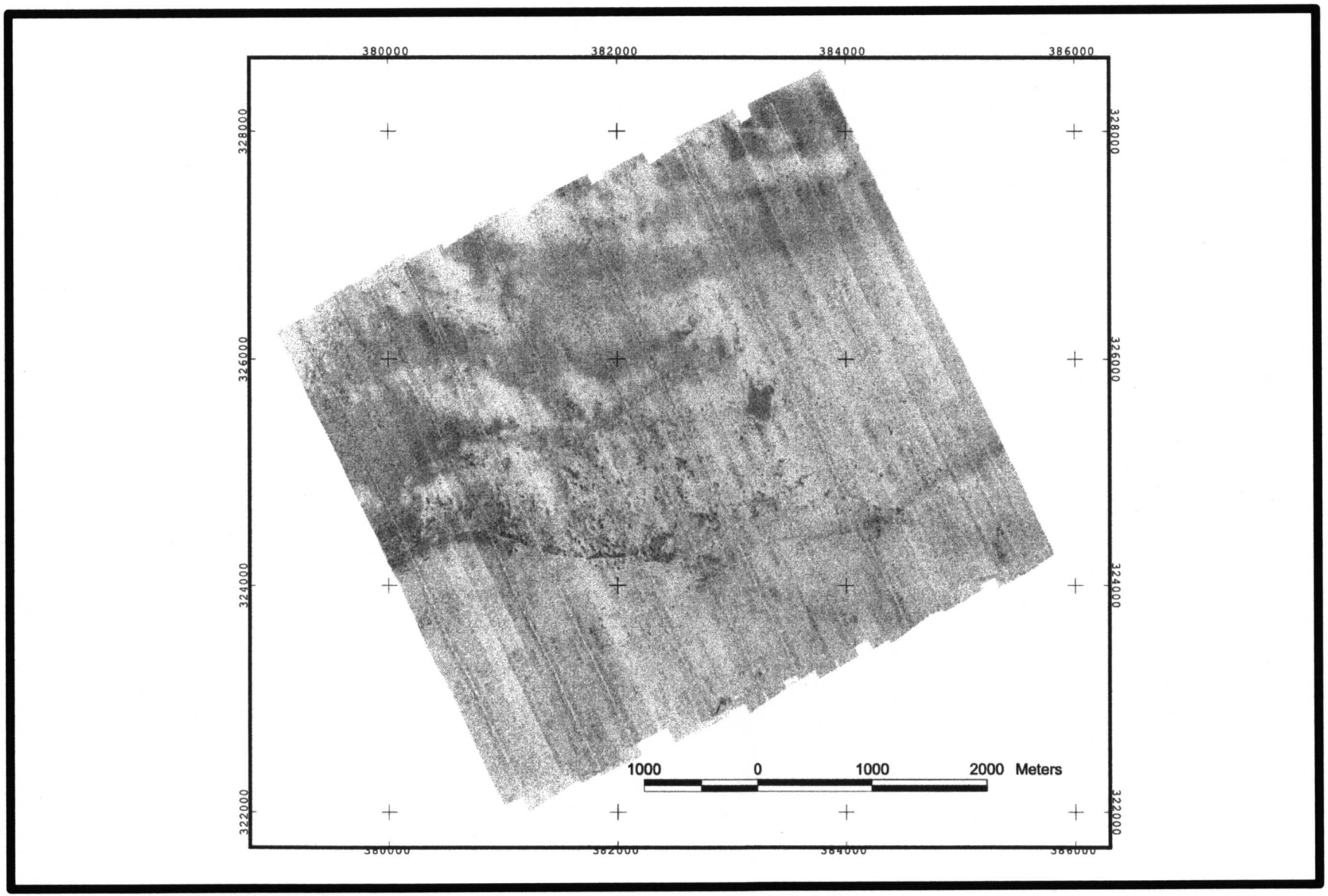

Fig. 4.5. Side-scan sonar image mosaic for Megasite 4. Dark areas show high-backscatter (acoustic return) and light areas show low backscatter or shadows.

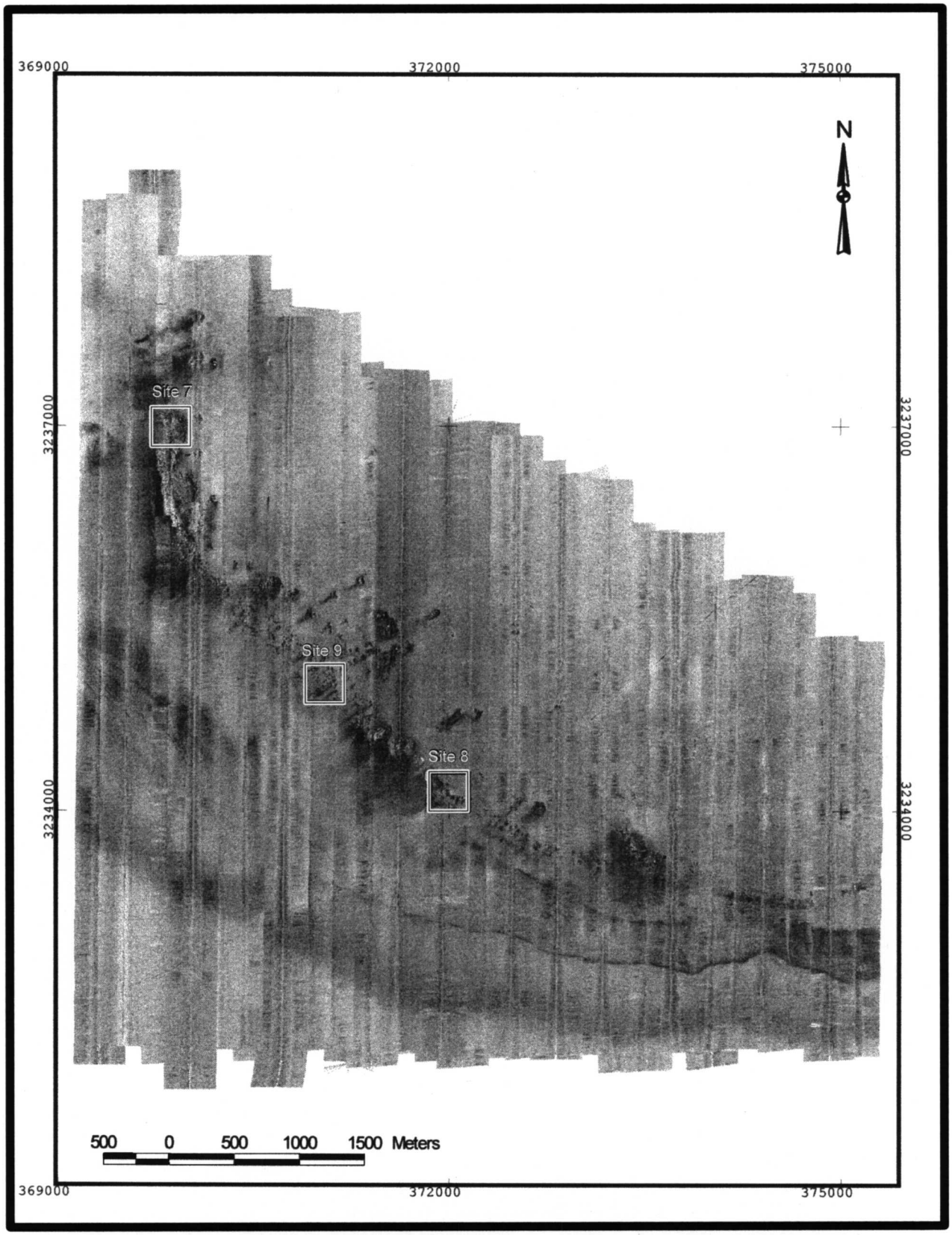

Fig. 4.6. Side-scan sonar image mosaic for Megasite 5. Dark areas show high-backscatter (acoustic return) and light areas show low backscatter or shadows.

adjacent data values were averaged, so mounds have rounded shapes in comparison to their shapes seen in the sonar backscatter images. Furthermore, small mounds do not appear in the data because averaging smoothes them out. Overlapping data from adjacent tracks are typically offset by some 10 to 15 m (and sometimes more), owing to navigation uncertainties, so a small mound on one track is often averaged with a flat patch of seafloor on an adjacent track. Furthermore, smaller mounds are usually averaged with adjacent flat seafloor when their size is much smaller than the depth value bin size. As a result of this smoothing, the megasite bathymetry maps typically show only those mounds greater than about 50 m in diameter. In the detailed survey bathymetry, features with diameters greater than about half that size are preserved.

Two additional artifacts are noted by their along-track trends. First, the data occasionally display offsets of ~1 m from data collected on one track to those adjacent. In some instances this may be a "roll bias" in which the values on one side of the cross-track depth profile are slightly too great or too small. It is most obvious when we examine the data in extreme detail in small areas around the monitoring sites. The second artifact may be related. It appears as a crenulation of the contours in a track-parallel direction caused by the cross-track depth profile being bowed upwards in the center. This is probably a result of imperfect corrections for the refractive effects of sound-velocity variations in the water column because it is worse at some sites (e.g., Megasites 1, 2, and 5) than others (e.g., Megasites 3 and 4). To understand this effect, recall that depths near the track lines are calculated from acoustic waves that travel nearly vertically through the water column and are therefore less affected by refraction. In contrast, depth soundings near the edge of the sonar swath leave the sonar at shallow angles, so their paths are affected by refraction to a greater degree. Consequently, a small error in determining water velocity versus depth profiles can translate to a greater error in determining depth at the edges of the sonar swath. At Megasite 1, for example, the crenulations typically appear as variations of about ±150 m in the lateral position of a particular contour in "flat" areas. The regional slope is about 0.17°, so this suggests an error of about ±0.45 m in depth, which is in turn 0.6% of the water depth in Megasite 1. Thus, the bathymetry data are better than "hydrographic" precision (<1% of water depth), yet because the slope is very shallow, the bathymetry contours appear irregular.

Megasite 1

Megasite 1 shows two large mound clusters near the shelf edge in water depths of 68 to 90 m. The western cluster is subcircular, approximately 600 m in diameter, and contains several smaller, steep-sided mounds. The other cluster is a crescentic band, approximately 800 m wide and 3,000 m long, located in the northeast part of the megasite. It contains two large flat-top mounds, approximately 300 to 400 m in diameter, and about a dozen smaller mounds. One of the two large features is the "40-Fathom Fishing Ground" mound that has been studied in prior MMS projects and is the location of Site 1. The seafloor around the mounds is nearly flat, with a shallow slope to the south. Contours suggest that there is a 3 to 5 m depth difference from north to south across the crescentic mound band. This is in part owing to sediments tending to pile up on the north sides of these features.

Megasite 2

Bathymetry from Megasite 2 ranges from 93 to 194 m depth and shows numerous mounds at the shelf edge. Seafloor north of the mounds is flat and is at about 100 to 103 m depth. To the south, the shelf edge at about 115 m depth separates the mounds from the steeper upper slope. The mounds are subcircular to linear in plan view and seem to have two distinct morphologies. One type occurs as broad, low, round flat-topped topographic features several hundred meters in diameter. The others appear as taller, steeper, less-rounded features. The latter are the "pinnacles" described by Ludwick and Walton (1957) whereas the low features appear to be carbonate platforms. The bathymetry shows that these low platforms are typically flush with the seafloor on their north sides whereas the south sides usually have a drop of 3 to 5 m.

Megasite 3

Megasite 3 shows a gently sloping area of the outer shelf with depths of 64 to 86 m. The main feature is a bulge in the contours which represents a broad, thin dome of sediments surrounding several groups of mounds. One mound group, in the western part of the megasite, is linear with a south-southeast trend. This linear feature is asymmetric, with a shallow slope on its north side and a steeper slope on its south side. To the north and southeast of this linear feature, two other smaller mounds have similar trends, implying some relationship. In the eastern half of the megasite, about a dozen medium mounds appear in several clusters. These are associated with a broad, low mound, similar to those in Megasite 2. This broad mound is about 400 x 800 m in dimension and like its cousins in Megasite 2, it shows a 2 to 3 m drop off its south edge, whereas its northern edge is flush with surrounding seafloor. The side-scan sonar mosaics also show a larger, but less obvious low hard bottom in the central region of Megasite 3. This is seen in the bathymetry contours by slightly steeper slopes on its south edge, in the south-central part of the megasite.

Megasite 4

Depths in Megasite 4 range from 93 to 189 m. This site is similar to Megasite 2 in its shelf-edge position. Slopes in Megasite 4 are somewhat steeper than the others, being about 0.7° north of 120 m depth. The main bathymetric features are curvilinear areas of steeper slope that appear to be the edges of fluvial deltas. The most prominent such feature runs from west to east across the southern part of the megasite at depths of 112 to 133 m. Another obvious feature of the bathymetry in Megasite 4 is the lack of large mounds. This implies that all of the mounds are too small to be seen in the 15-m bathymetry grid.

Megasite 5

The shelf edge is also a prominent feature in the Megasite 5 bathymetry map, which shows depths ranging from 69 to 161 m. Most of the northern two-thirds of the megasite is relatively flat seafloor of the outer shelf. Superimposed is a curvilinear mound group that stretches from northwest to southeast across almost the entire megasite. The

bathymetry shows several large mounds and numerous smaller mounds and mound groups. Most obvious is the large mound at the northwest end of the mound group, which is the location of Site 7. Across the curvilinear mound group, the contours often show a depth offset of about 2 to 4 m.

Monitoring Site Bathymetry

Site 1

Site 1 contains the large flat-topped mound in Megasite 1 and seems well represented in the bathymetry data. The data show a large flat-topped feature with a top depth of about 63 m, a steep flank, and flat seafloor to the northeast at depths of about 75 to 76 m (Fig. 4.7).

Site 2

Bathymetry data from Site 2 show a mainly flat seafloor at a depth of about 77 to 78 m with a medium-sized mound approximately 50 m in diameter along the southern edge of the site (Fig. 4.7). The contours indicate the mound is more than 5 m in height.

Site 3

Site 3 bathymetry contours show no evidence of the small mounds in that area (Fig. 4.7). Instead the depths reflect the relatively flat seafloor, at depths of 78 to79 m, that characterizes the site.

Site 4

Site 4 bathymetry data show a wide, medium-height mound with a northwest trending ridge on its northwest side (Fig. 4.8). Contours indicate the mound is about 10 m in height, but has a relatively flat top. Small areas of closed contours in the northwest corner and on the south side of the area at X=425300 evidently result from a few erroneous depth values.

Site 5

Site 5 bathymetry data show a tall mound near the center and a lower mound at the southwest edge of the area (Fig. 4.8). The large mound seems to consist of two connected mounds, but comparison with the side-scan images indicates that the two mounds are caused by a navigation error in combining bathymetry data from two adjacent tracks.

Site 6

Contours in Site 6 are mainly unclosed, indicating the lack of relief at the site. The seafloor is relatively flat at a depth of about 74 m (Fig. 4.8).

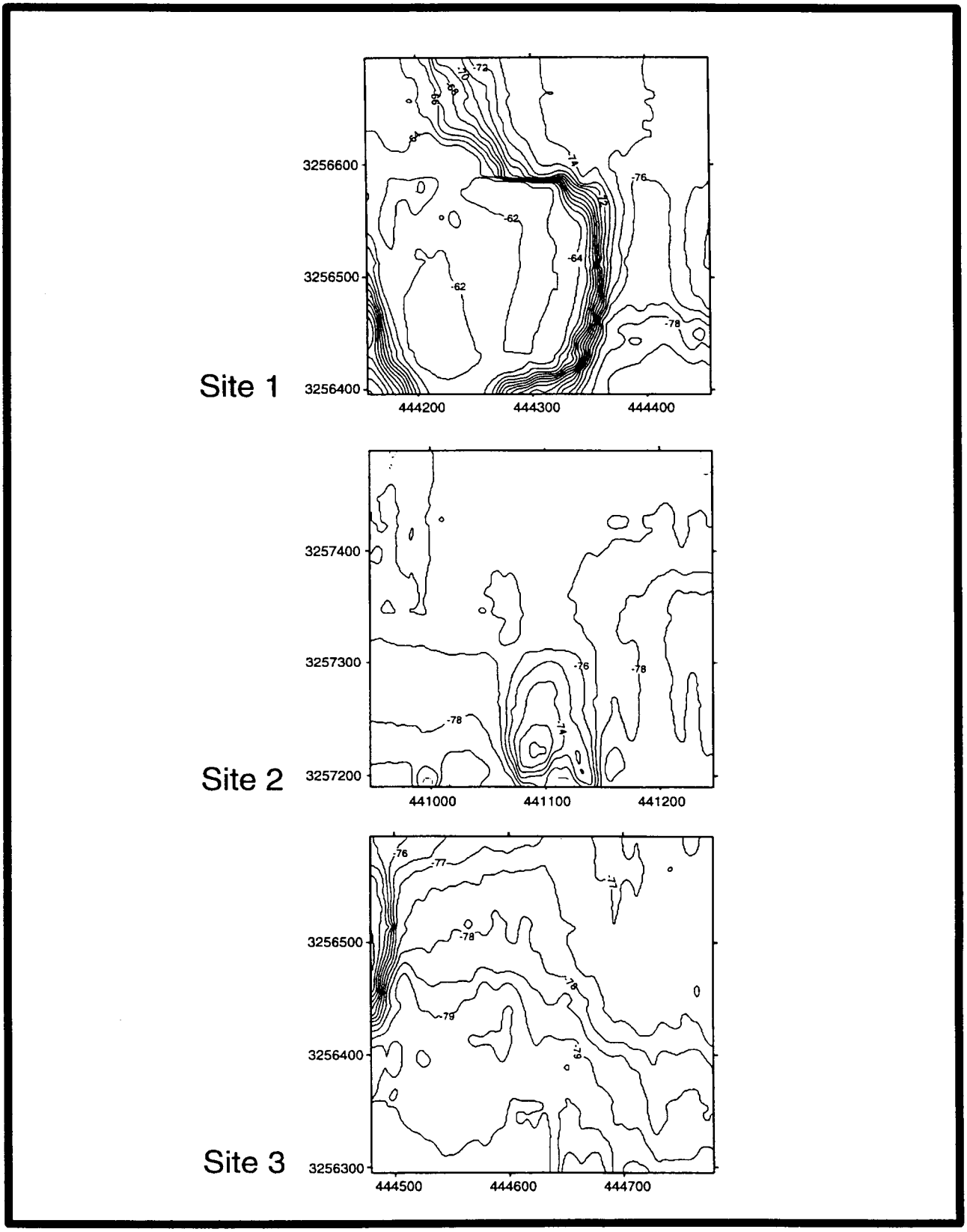

Fig. 4.7. Bathymetry of Sites 1 (top), 2 (middle), and 3 (bottom). Depths are in meters and contours at 1-m intervals. Each box represents an area of 300 by 300 m taken from the TAMU[2] "detailed survey" bathymetry data, which was gridded in x and y with a spacing of 1 m.

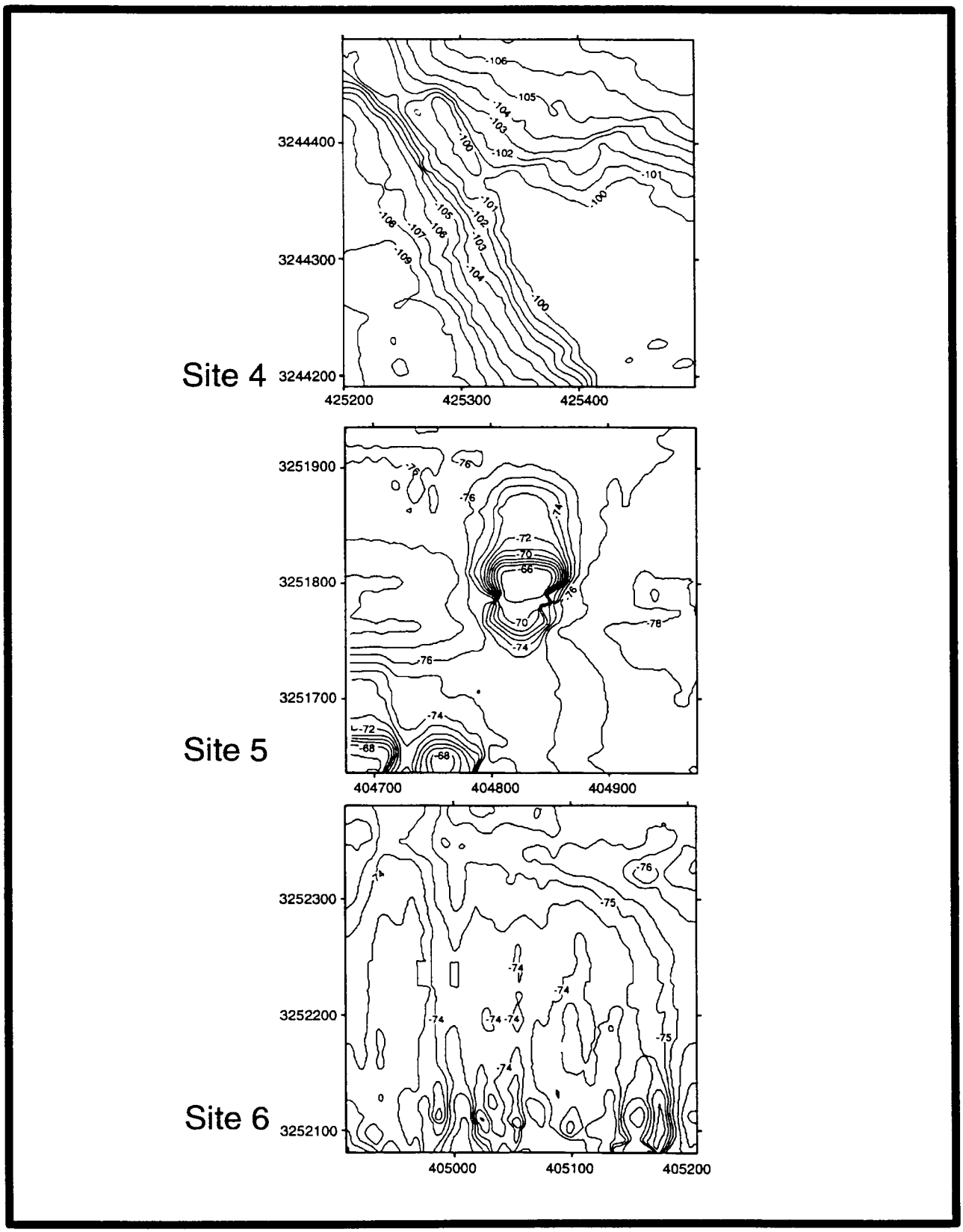

Fig. 4.8. Bathymetry of Sites 4 (top), 5 (middle), and 6 (bottom). Depths are in meters and contours at 1-m intervals. Each box represents an area of 300 by 300 m taken from the TAMU[2] "detailed survey" bathymetry data, which was gridded in x and y with a spacing of 1 m.

Site 7

As at Site 1, the high relief of Site 7 lends itself to bathymetric mapping. The contours show a large, flat-topped mound, elongated north-south, with summit depths of about 70 m and bottom depths of about 86 to 87 m (Fig. 4.9).

Site 8

Site 8 bathymetry shows several closed contours around a medium-sized mound near the center of the site (Fig. 4.9). The mound appears subcircular and several meters in height.

Site 9

Relief at Site 9 is low, so the contours mostly wander unclosed at depths of about 90 m (Fig. 4.9). Several closed contours in the northeast quadrant indicate the presence of a small mound several meters in height.

Megasite Subbottom Profiles

Subbottom profiler records acquired with the X-STAR 2-12 kHz chirp sonar show the seafloor and internal acoustic interfaces within the uppermost sub-seafloor sediments. These records were acquired for two purposes: (1) to provide auxiliary data for the interpretation of side-scan sonar records and (2) to examine the distribution of recent sediments. Although the profiles have been useful for the first purpose, preliminary examination suggests that it may not be possible to create isopach (sediment thickness) maps for all of the megasites owing to geologic factors and limited depth penetration.

In general, most profiles show a thin, relatively transparent layer a few meters thick overlying a deeper horizon. In places, this upper drape layer appears to contain more than one unit. The deeper horizon often appears as an angular unconformity where underlying delta foreset beds are truncated. In most of the survey areas, this horizon may represent erosion that occurred during the last glacial lowstand (Kindinger 1989; Davis 1992). However, in Megasite 1, which sits atop the "eastern delta" of the MAMES study, this horizon may be younger (Davis 1992). Thus, the age of the unconformity at a particular site cannot be determined without additional age information.

One goal of the study was to create isopach maps of sediments overlying the erosional unconformity at all sites to better understand the long-term influence of the mounds on sediment distribution. However, there are two impediments to attaining this goal. First, in most records the upper transparent layer appears relatively uniform, i.e., isopach maps show little of interest. Second, it is difficult to discern this horizon or it is difficult to determine reflector continuity in many places. In some spots, it is evident that the sediments overlying the erosional unconformity constitute more than one layer, of which the upper transparent layer is only the latest. Much of the problem is that acoustic penetration has been inadequate to consistently define sediment layer thicknesses. In part, this may result from unusually impervious seafloor because the X-STAR records show penetration of 15 m or more in Megasite 4, but not in the other areas. The analysis

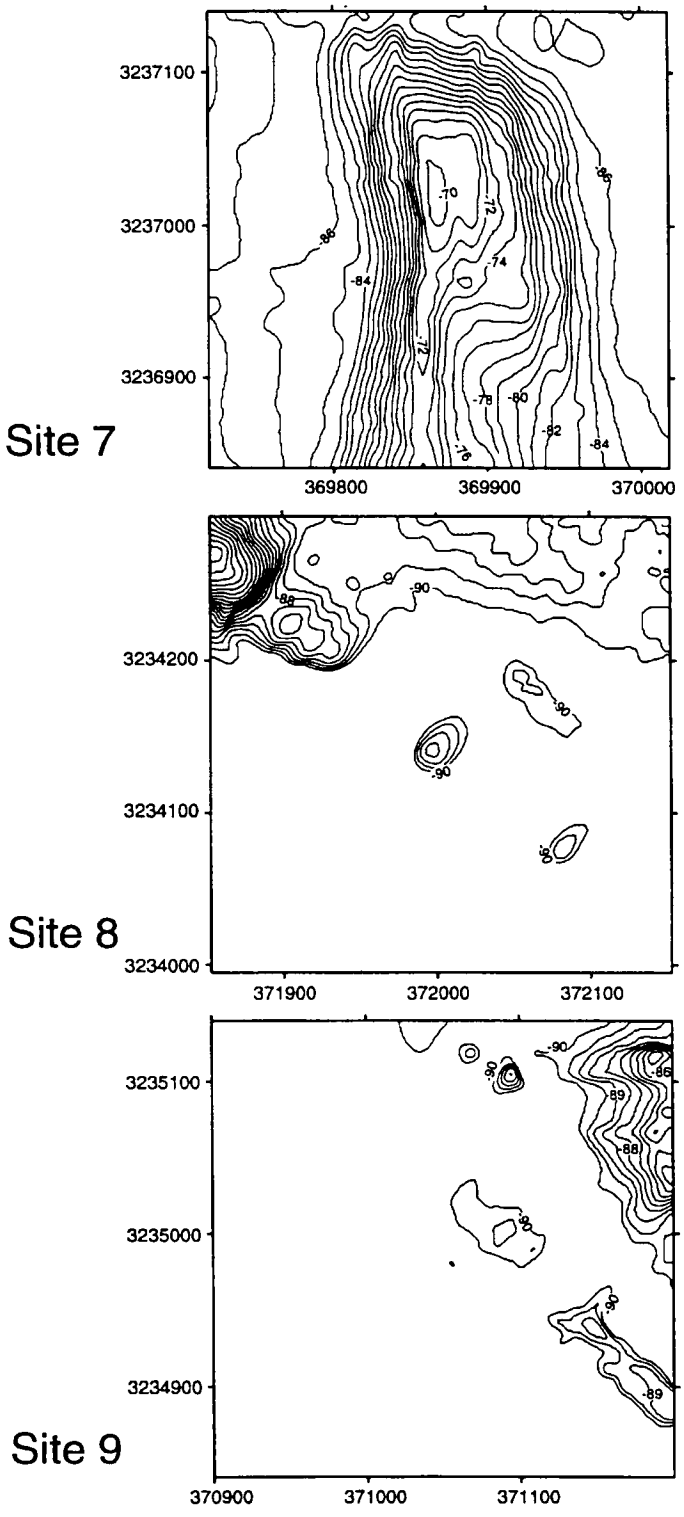

Fig. 4.9. Bathymetry of Sites 7 (top), 8 (middle), and 9 (bottom). Depths are in meters and contours at 1-m intervals. Each box represents an area of 300 by 300 m taken from the TAMU[2] "detailed survey" bathymetry data, which was gridded in x and y with a spacing of 1 m.

has therefore focused on gleaning clues about the relation of the mounds to the sediments, rather than constructing isopach maps.

Megasite 1

Megasite 1 is an area where the bottom of the transparent layer is relatively easy to map. The upper transparent layer is relatively uniform at 1.0 to 2.5 msec (0.8 to 1.9 m; assuming 1,500 m/sec sound velocity) in thickness, but reaches 5.0 msec (4.0 m) at one location. At this megasite there is a notable correlation between areas where this uppermost layer has been eroded and dark (high backscatter) areas in the side-scan sonar mosaic. The high backscatter areas are preferentially located on the southwest sides of the mounds, so most profiles over larger mounds show an erosional hole on the southwest side. Near the largest mounds, erosion occurs over a broad area several hundred meters across to a depth of 1 to 2 m. Behind one mound at the eastern edge of the megasite, the erosional hole has reached the underlying unconformity, but in most places some of the transparent layer remains. On several profiles, linear high backscatter "tails" trailing southwest from small to medium mounds have been matched with gullies, typically 20 to 200 m wide and 1 to 2 m in depth. The cause of the relationship between erosion and high backscatter is not yet clear. It probably represents a current winnowing effect that coarsens the average sediment texture at the seafloor in those areas. This hypothesis can be confirmed by correlation of mean grain size with backscatter intensity.

Subbottom profiles from Megasite 1 also show interesting aspects of mound morphology. Many mounds appear asymmetric in profile with the steepest slopes on the seaward sides. The data show that this is caused by sediment dammed on the landward sides of the topographic features. Furthermore, on some lines there appears to be a 6 to 8 m depth offset across the mounds becoming deeper seaward. Across the large flat-top mound where Site 1 is located, for example, the erosional horizon beneath the transparent layer is at about 70 m depth on the north side of the mound and 76 m on the south side. This observation suggests that some of the mounds may sit atop a scarp.

Within Megasite 1 are three small, linear to sub-linear ridges, located in the northern part of the survey. In the subbottom records, these ridges are asymmetric, with sediment dammed on their north sides and a slight erosional hole on their south sides. Typically the depth offset across these ridges is 1.5 to 2.0 m. The origin of these features is unclear, although previous speculation was that similar ridges are ancient shoreline features (Sager et al. 1992).

Megasite 2

At Megasite 2, the underlying erosional unconformity is not visible in many places. Above this horizon two more-or-less homogeneous layers are visible, the upper one acoustically transparent and the lower acoustically turbid. This configuration is most obvious to the north of the mounds, and is often not seen to the south. These layers are typically about 1 to 2 m in thickness, occasionally 5 to 10 m. The surficial sediments lie atop mound flanks in most places. In particular, the linear, high backscatter area in the northeast part of the megasite is a buried ridge with small mounds on the tops of the

larger mounds showing through. In many places the upper sediment layers are upturned on the mound flanks and pinch out, leaving the mound top exposed. These sediments typically bury the north sides of low, flat carbonate hard bottoms but leave the south sides exposed.

Megasite 2 profiles show no obvious correlation between high backscatter areas and erosion, in contrast to Megasite 1. This fits the observation from the mosaic that the high backscatter areas have no preferred direction. Because these areas fringe the mounds, it is likely that the high backscatter is caused by textural differences owing to material shed from the mounds.

Megasite 3

In Megasite 3, the surficial sediments also appear as a thin transparent layer, typically 1 to 2 m thick. Similar to those of Megasite 2, the two low, flat carbonate hard bottoms are buried on their north sides and show a 1.5 to 2.0 m scarp on their south sides. The tops appear even with surrounding sediments and there are small, thin, transparent areas that suggest sediment ponds.

The linear mounds in the western part of Megasite 3 show an asymmetric profile with low slopes on their north sides and steep slopes on the south sides. In part this is a result of sediments ponded on the north sides. However, the mounds themselves appear asymmetric and often have a low hump on the north sides and a pinnacle on the south side. Many profiles show a small erosional hole at the base of the south side, with a total height of about 10 m from bottom to pinnacle top.

The profiles show that at least one of the mounds in the eastern part of Megasite 3 has an asymmetric shape, but others have flat tops. In this region the dark high backscatter areas to the southwest of the larger mounds can be seen as an erosional feature on subbottom profiles, as at Megasite 1.

Megasite 4

Like its sonar image data, the subbottom data from Megasite 4 are unique. In this area, seaward-dipping delta foreset beds are regularly seen beneath a thin transparent layer, 1 to 2 m in thickness. Penetration here is greater than at any other megasite and it is possible to see delta beds 10 to 15 m below the seafloor.

The curvilinear high backscatter feature in the southern part of the Megasite 4 mosaic corresponds to a zone of steeper slopes in the subbottom profiles. This is consistent with the bathymetry, which shows closer contours at this location. Interestingly, this zone is at different depths on different profiles. It is deepest on the east side of the megasite and shallows approximately 17 m to the west. This is also consistent with the bathymetry data.

In Megasite 4, it was not possible to match high backscatter areas with mounds or other features of the subbottom profiles, such as erosional areas, because the seafloor in the

subbottom profiles usually appears uniform and few mounds are evident. Apparently most of the backscatter features in the side-scan sonar mosaic arise from textural variations at the surface.

Megasite 5

As at other sites, the upper transparent layer in Megasite 5 is nearly uniform and 1 to 2 m thick. In some places this layer is seen atop erosionally-truncated delta foreset beds. According to Sydow and Roberts (1994), these beds are part of the Lagniappe Delta. In the subbottom profiler records, this erosional surface is often irregular, as was reported by Sydow and Roberts (1994).

The shelf edge in Megasite 5 has two unusual features. First, the dark band seen in the side-scan sonar mosaic corresponds to a reflection-free zone in the subbottom records. The seaward edge of this zone often appears as dipping reflectors and the landward edge sometimes matches with erosional "notches" in the seafloor. These observations imply this dark band is an exposed delta-front layer. As the dark band widens to the west, the shelf edge develops a large, flat mound of transparent sediments. The origin of this mound is unclear. The other unusual features are asymmetric troughs near the shelf edge with steep landward and shallow seaward walls. Usually just one is seen on a given line, although occasionally two occur. The depth and widths are several meters by 100 to 200 m. The asymmetric shapes suggest this might be a fault caused by an incipient delta-front slump. Sometimes mounds appear associated with the top of the landward wall of this trough.

Like the dark high backscatter "tails" trending southwest from mounds in other megasites, those in Megasite 5 also appear to be erosional gullies. Similarly, high backscatter areas are preferentially located to the southwest of many of the larger mounds, and the subbottom profiles often show slight erosion, especially on the southwest side of the curvilinear mound trend.

ROV Photo Station Geologic Data

Site 1

Most photo stations from Site 1, located on a large, tall flat-topped mound in Megasite 1, are on the top of the mound (Fig. 4.10), so most geologic observations apply to this special environment. Although sediment cover is partial or complete at most stations, outcropping carbonate rock is also common. Nevertheless, meter-scale relief is typically low and the small-scale roughness is low to medium. Sediments are typically coarse and shell hash is common, implying a significant biogenic component.

Site 2

Located atop a medium-sized mound about 35 m in diameter, approximately half of the photo stations show rock outcrop and these are preferentially on the northeast side of the mound (Fig. 4.11). Such a configuration is consistent with current flow from the

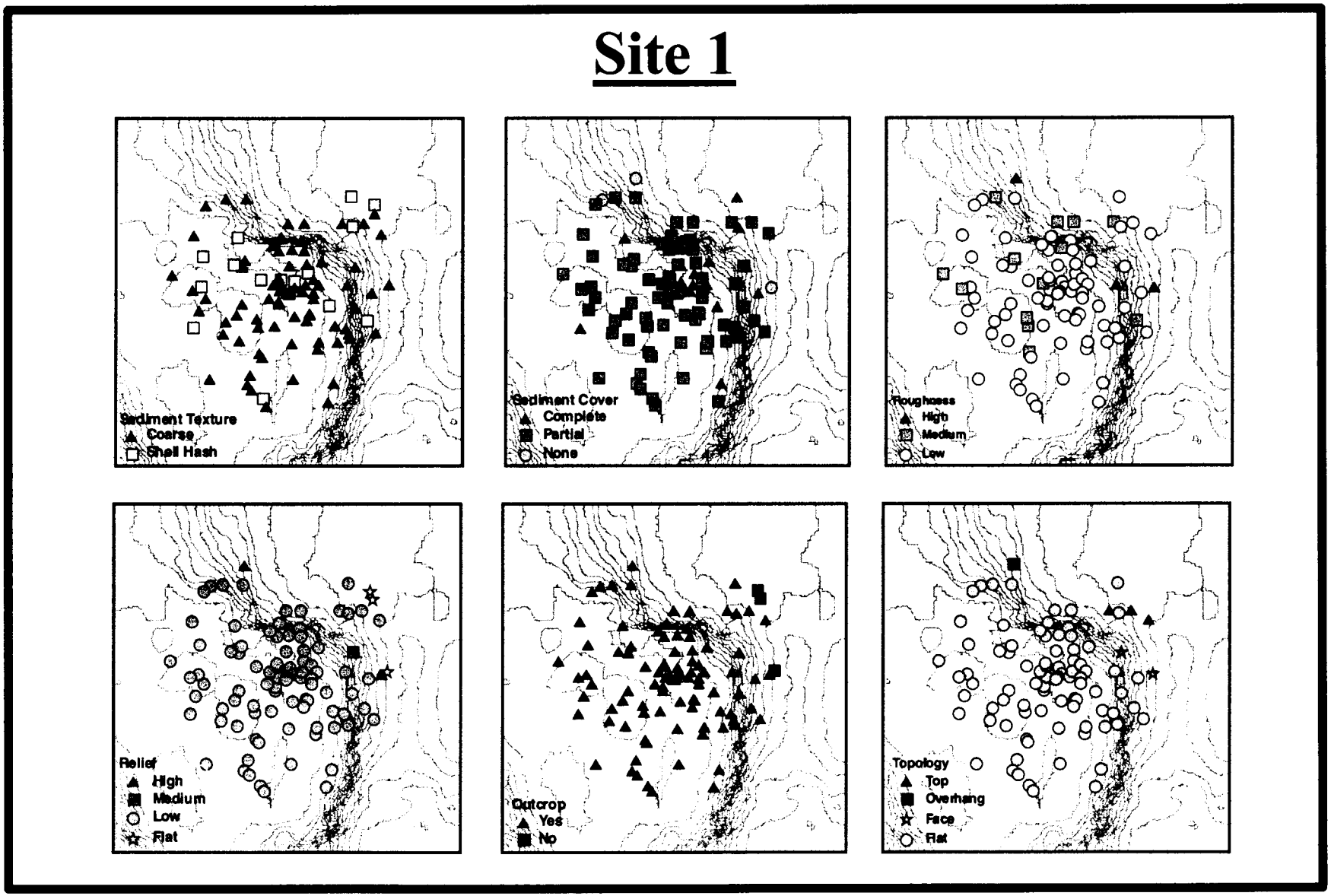

Fig. 4.10. ROV photo station geologic descriptions (see Table 4.1) for Site 1. Each box represents the site with bathymetric contours shown for reference. The sides of the boxes are 300 m in length.

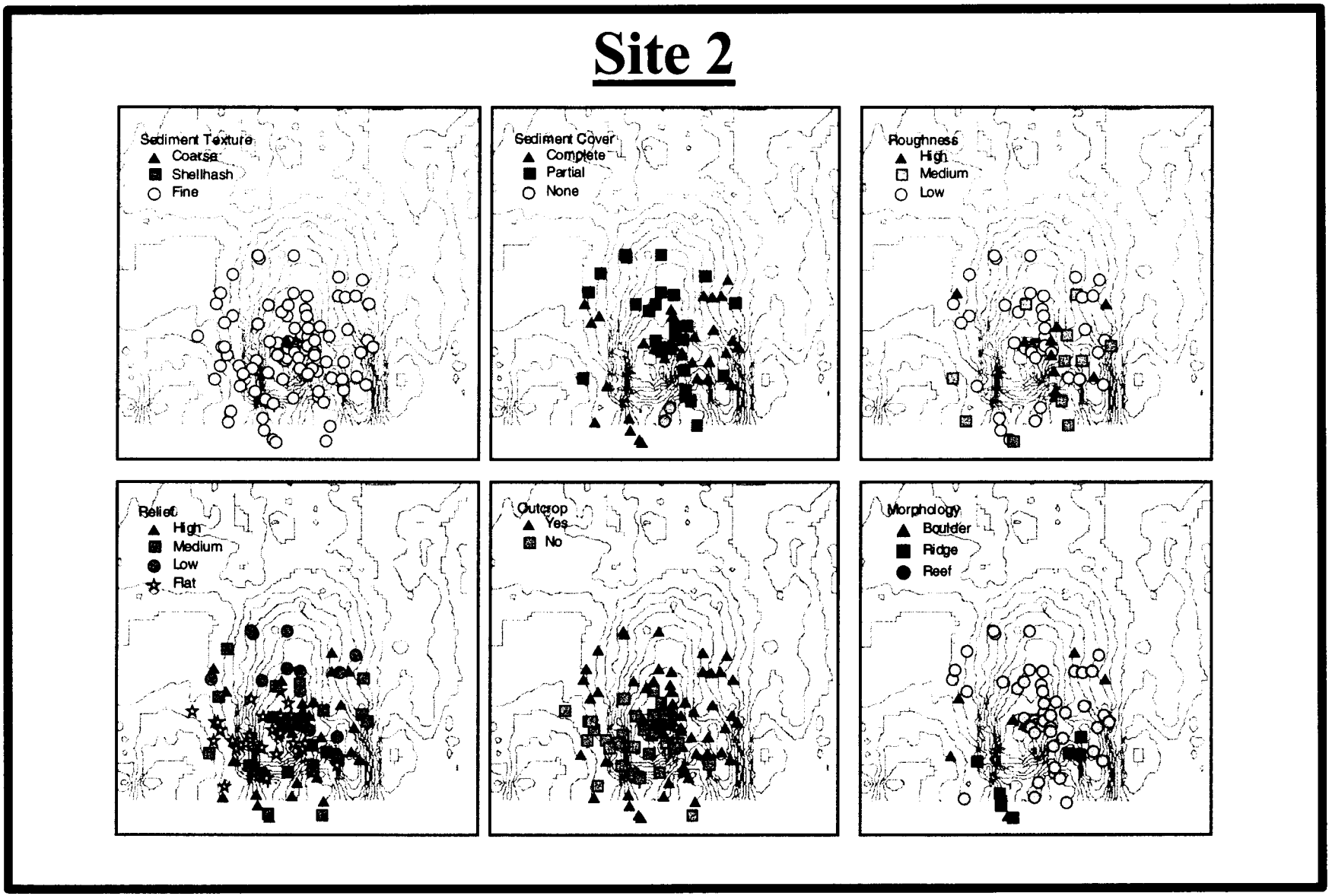

Fig. 4.11. ROV photo station geologic descriptions (see Table 4.1) for Site 2. Each box represents the part of the site with bathymetric contours shown for reference. The sides of the boxes are 200 m in length.

northeast, which would account for the southwestward trending high backscatter "tail" emanating from this mound group (Fig. 4.2), causing sediments to be eroded off the northeast side of the mound and deposited on the southwest side. Most stations, however, show partial sediment cover and the sediments are generally fine, so any currents are not so energetic as to sweep the mound bare of sediments. Both meter-scale relief and centimeter-scale roughness vary from small to large, and aside from a cluster of stations that show flat seafloor on the southwest side of the mound, these parameters are intermixed. This suggests that the character of the mound varies significantly on a lateral scale of meters.

Site 3

Despite the fact that the sonar mosaic for Site 3 shows a loose cluster of low mounds on an expanse of apparently flat seafloor (Fig. 4.2), many of the photo stations showed outcropping rock and many of these were classified as "reefs," meaning mounds larger than the typical ROV-video view (Fig. 4.12). Roughness and relief both vary from low to high, but low to medium values are more common. Sediment texture is mainly fine and sediment cover is usually partial. These observations make a picture of an environment of flat seafloor with many low mounds from boulder to house-size or larger, surrounded by fine sediments.

Site 4

Although Site 4 is located on the northwest side of a wide, medium-height mound in Megasite 2, photo station observations display considerable lateral variability. Stations at which outcrop is visible or not are about evenly divided and sediment types range from fine to coarse with several stations showing shell hash (Fig. 4.13). Roughness ranges from low to high and relief ranges from flat to medium. Stations nearest the center of the site were mainly classified as "reef." Many peripheral stations were classified as "boulder" and several as "ridge." These observations indicate that geological conditions are highly variable laterally at this site.

Site 5

Site 5 is located on a tall, flat-topped mound in Megasite 3. Stations near the center of the site all show outcrop and are surrounded by stations at which no rock is visible (Fig. 4.14). The no-outcrop stations mainly show no relief ("flat") and have fine sediments. This zonation reflects a sharp change from mound flank to flat seafloor nearby. Roughness is mainly low to medium, but some high values occur atop the mound. Meter-scale relief atop the mound is low to medium, consistent with the flat top observed in the side-scan images.

Site 6

ROV videos from Site 6 show an area that appears blanketed by a cover of fine sediments. Consistent with this observation, most photo stations showed no outcrop, particularly near the center of the site. Stations with outcrops were mostly clustered in

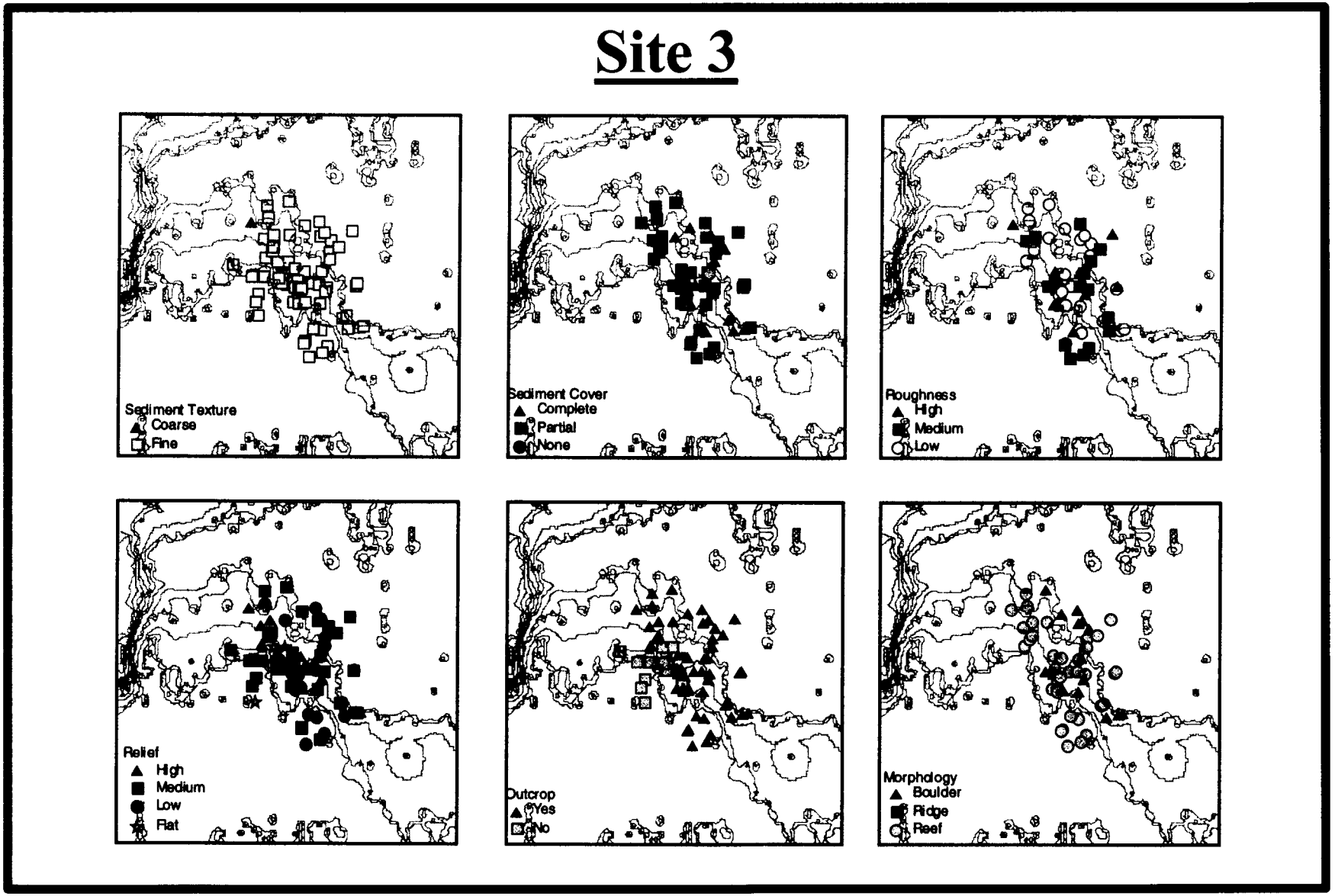

Fig. 4.12. ROV photo station geologic descriptions (see Table 4.1) for Site 3. Each box represents the site with bathymetric contours shown for reference. The sides of the boxes are 300 m in length.

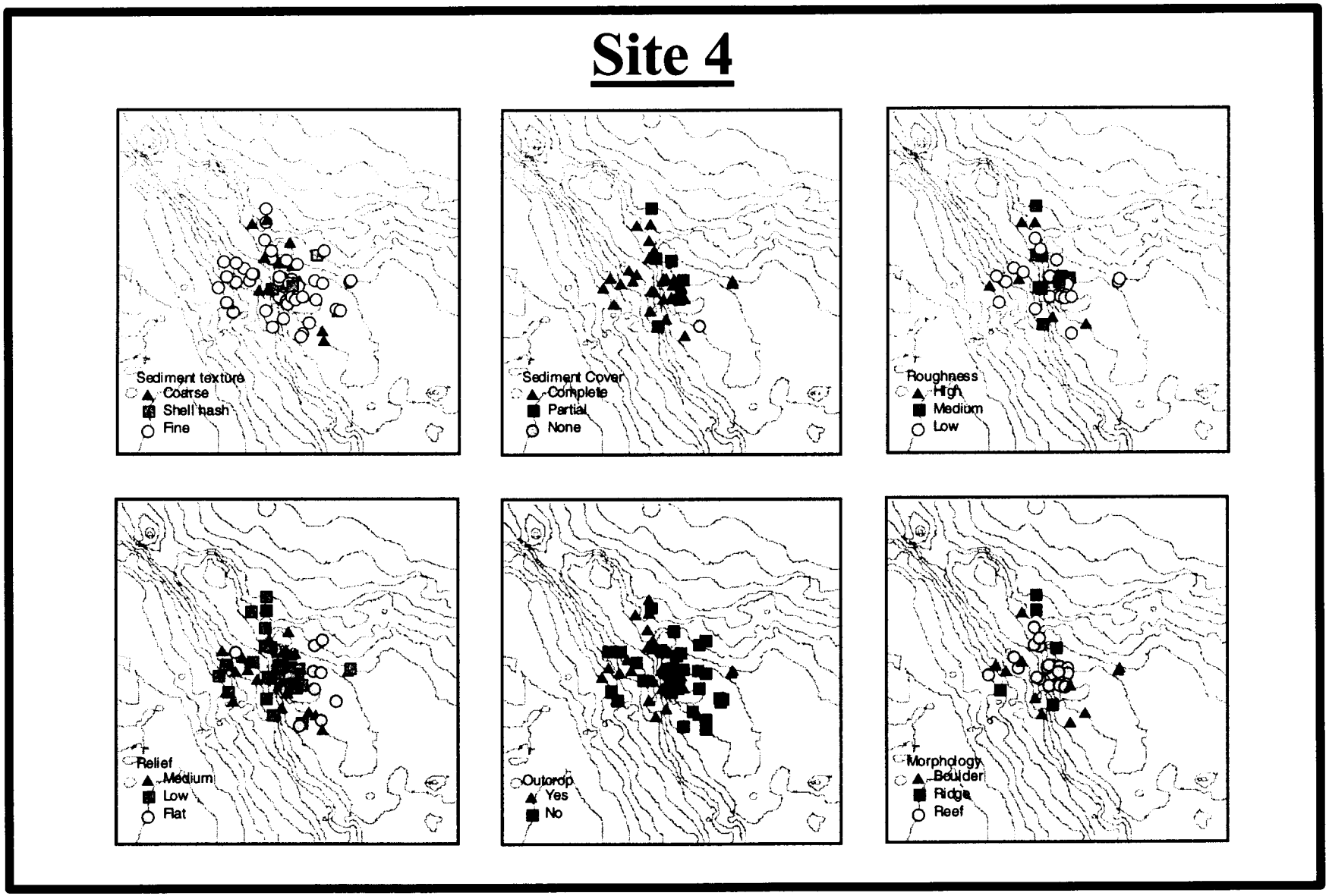

Fig. 4.13. ROV photo station geologic descriptions (see Table 4.1) for Site 4. Each box represents the site with bathymetric contours shown for reference. The sides of the boxes are 300 m in length.

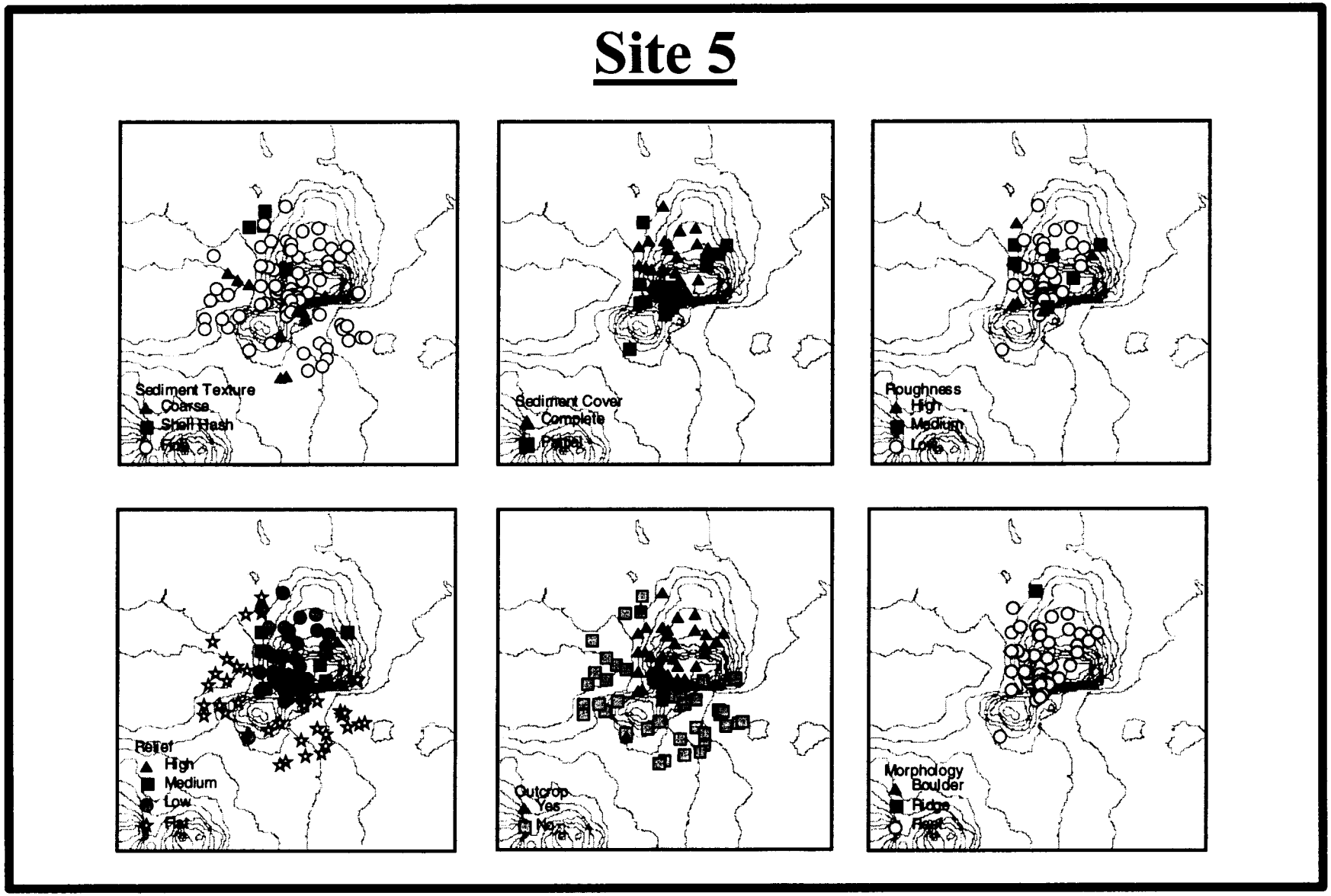

Fig. 4.14. ROV photo station geologic descriptions (see Table 4.1) for Site 5. Each box represents the site with bathymetric contours shown for reference. The sides of the boxes are 300 m in length.

the northwest and southeast quadrants (Fig. 4.15). Although many stations are characterized by fine sediments, coarse sediments are common. Relief and roughness are often medium. These observations are consistent with the side-scan images that suggest the site is a low, wide carbonate hard bottom with a rough upper surface. The fine sediment cover is partial and often limited to sediment pockets within the hard bottom, consistent with subbottom profiler records.

Site 7

Site 7 ROV photos are consistent with the site's location atop the north end of a large, high-relief mound (Fig. 4.6). Most stations show outcrop, many stations are classified as medium to high relief, and the roughness is often medium (Fig. 4.16). Nevertheless, a number of stations, particularly on top of the mound, are characterized by low roughness. Eleven stations on the west side of the site show flat seafloor or depression with shell hash or rubble. These stations are on the seafloor adjacent to and on the west side of the mound that shows high backscatter. These characteristics imply significant input of biogenic material from the mound and the depression suggests erosion.

Site 8

Site 8 is located on a medium mound in Megasite 5 (Fig. 4.6) and consequently most stations show outcropping rock and "reef" morphology (Fig. 4.17). Centimeter-scale roughness is mainly low to medium and meter-scale relief is mostly low, except at the mound edges. Sediment textures are mainly fine except at a few stations atop the mound.

Site 9

Consistent with its location on low mounds in the center of Megasite 5 (Fig. 4.6), Site 9 is characterized by fine sediments, flat to low relief, low roughness, and fine sediments (Fig. 4.18). One station shows shell hash, one shows medium roughness, and several show medium relief, suggesting scattered small mounds.

Grain Size Data

Grain size data show that sediments recovered in grab samples are typically sands with some gravel and clay. The median mean grain size for the 94 samples from Cruise 1C is 2.8ϕ (Fig. 4.19), with most samples having mean grain sizes between 1.75ϕ and 4ϕ. Many samples show a bi- or trimodal distribution, as shown in Fig. 4.20. Often the size distribution is peaked around 1ϕ to 3ϕ (fine sand) with a significant fraction in the smallest size class, >10ϕ (fine clay). Few samples contain a significant silt fraction. Many samples also have a large contribution in the largest size class, <-1.5ϕ (gravel). These particles are typically shells, shell fragments, and other biologic detritus.

Ternary plots echo these characteristics (Fig. 4.21). On a sand-silt-clay plot, samples show a nearly linear scatter from sand to clay. Only those samples with moderate amounts of clay have significant fractions in the silt size range, and even then the largest contribution is less than 20% (Fig. 4.21). The nearly linear trend implies two sediment

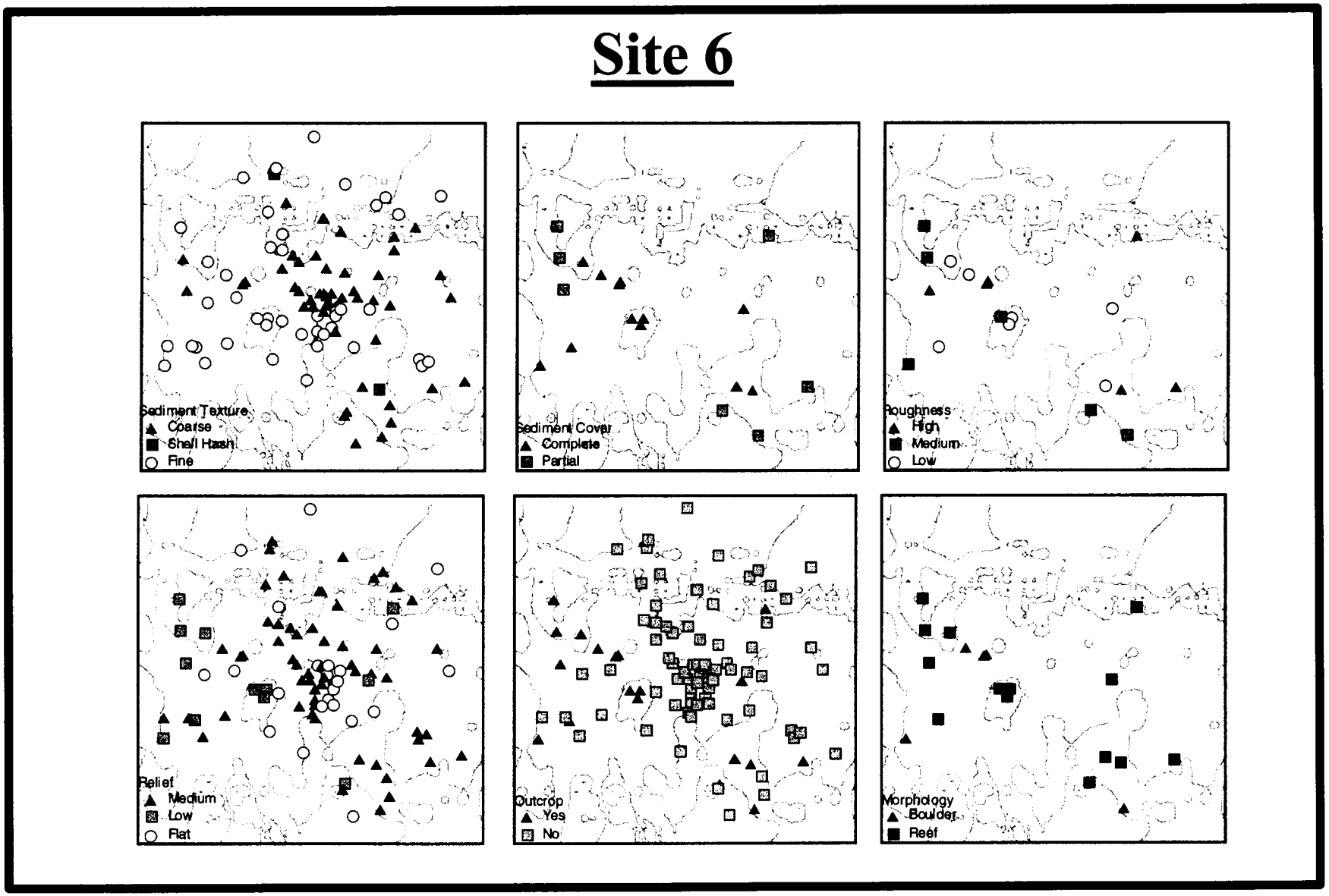

Fig. 4.15. ROV photo station geologic descriptions (see Table 4.1) for Site 6. Each box represents the site with bathymetric contours shown for reference. The sides of the boxes are 300 m in length.

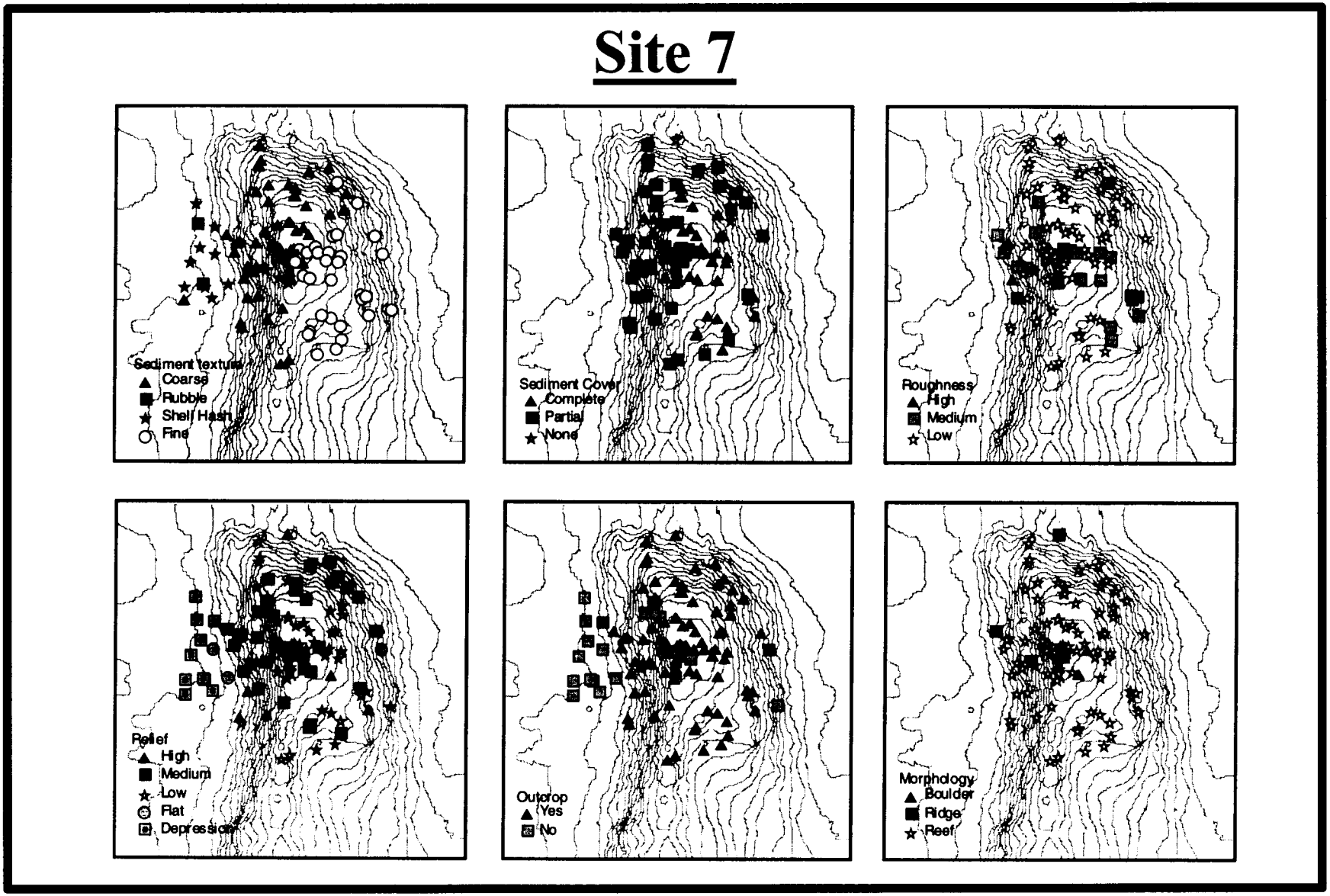

Fig. 4.16. ROV photo station geologic descriptions (see Table 4.1) for Site 7. Each box represents the site with bathymetric contours shown for reference. The sides of the boxes are 300 m in length.

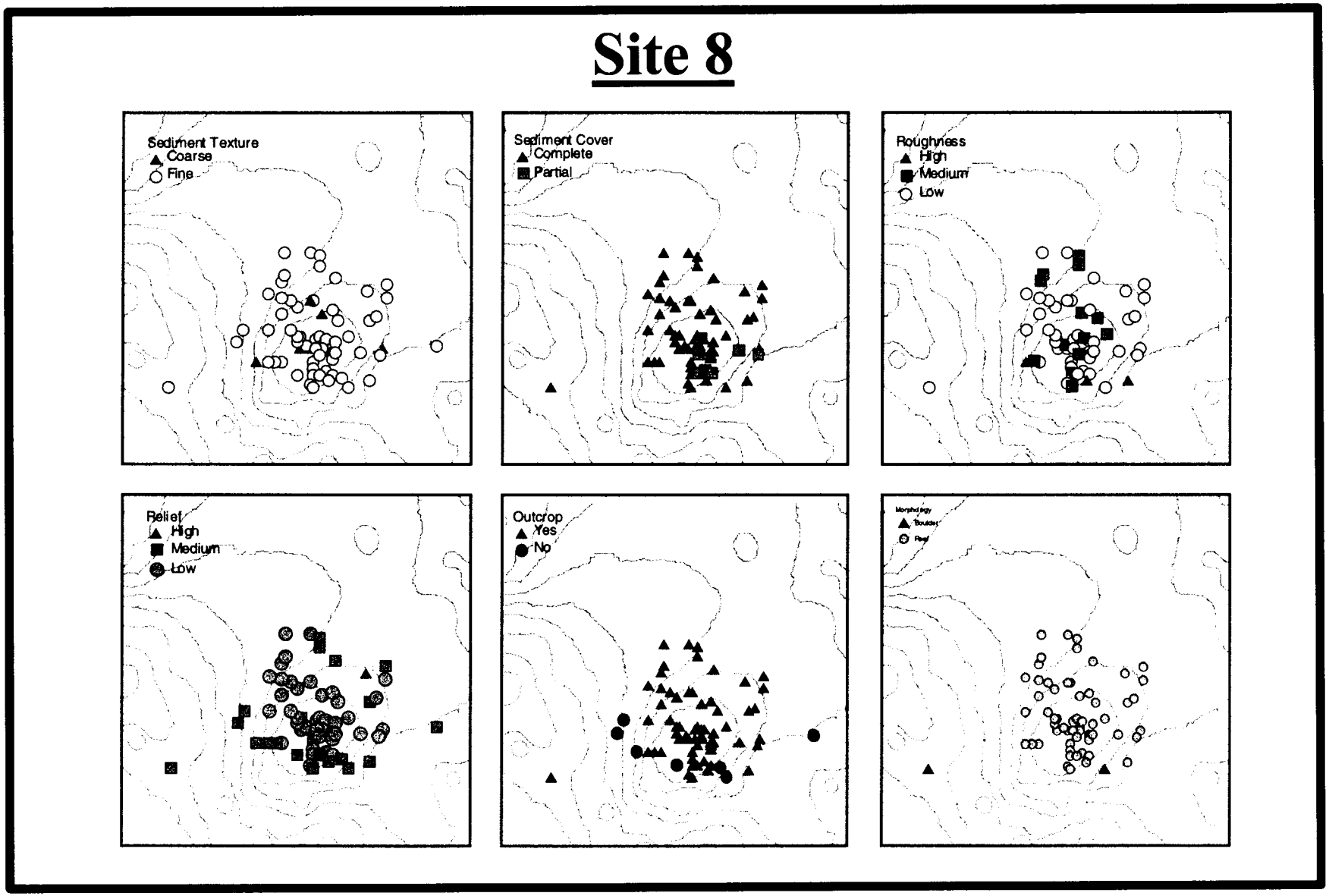

Fig. 4.17. ROV photo station geologic descriptions (see Table 4.1) for Site 8. Each box represents part of the site with bathymetric contours shown for reference. The sides of the boxes are 200 m in length.

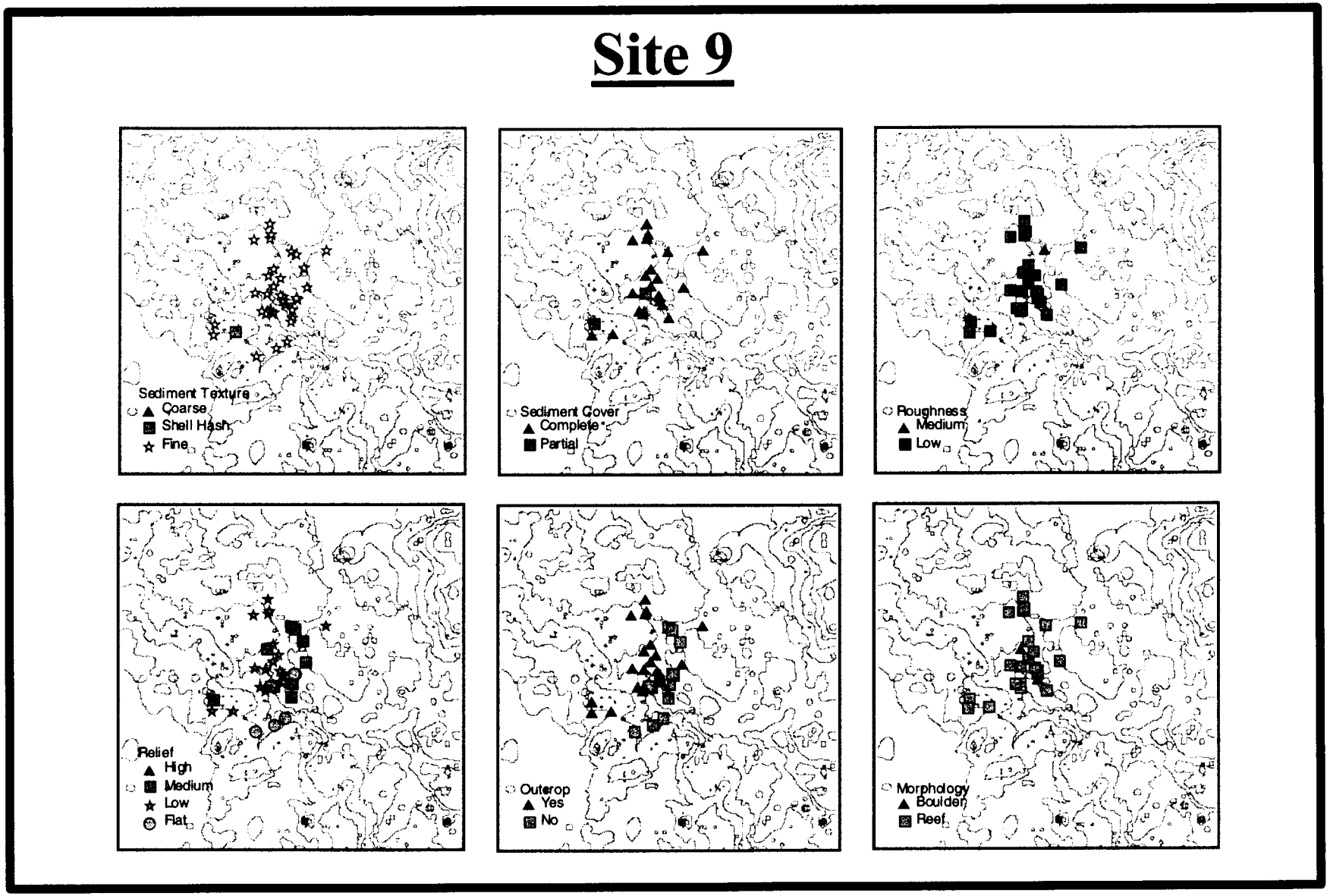

Fig. 4.18. ROV photo station geologic descriptions (see Table 4.1) for Site 9. Each box represents the site with bathymetric contours shown for reference. The sides of the boxes are 300 m in length.

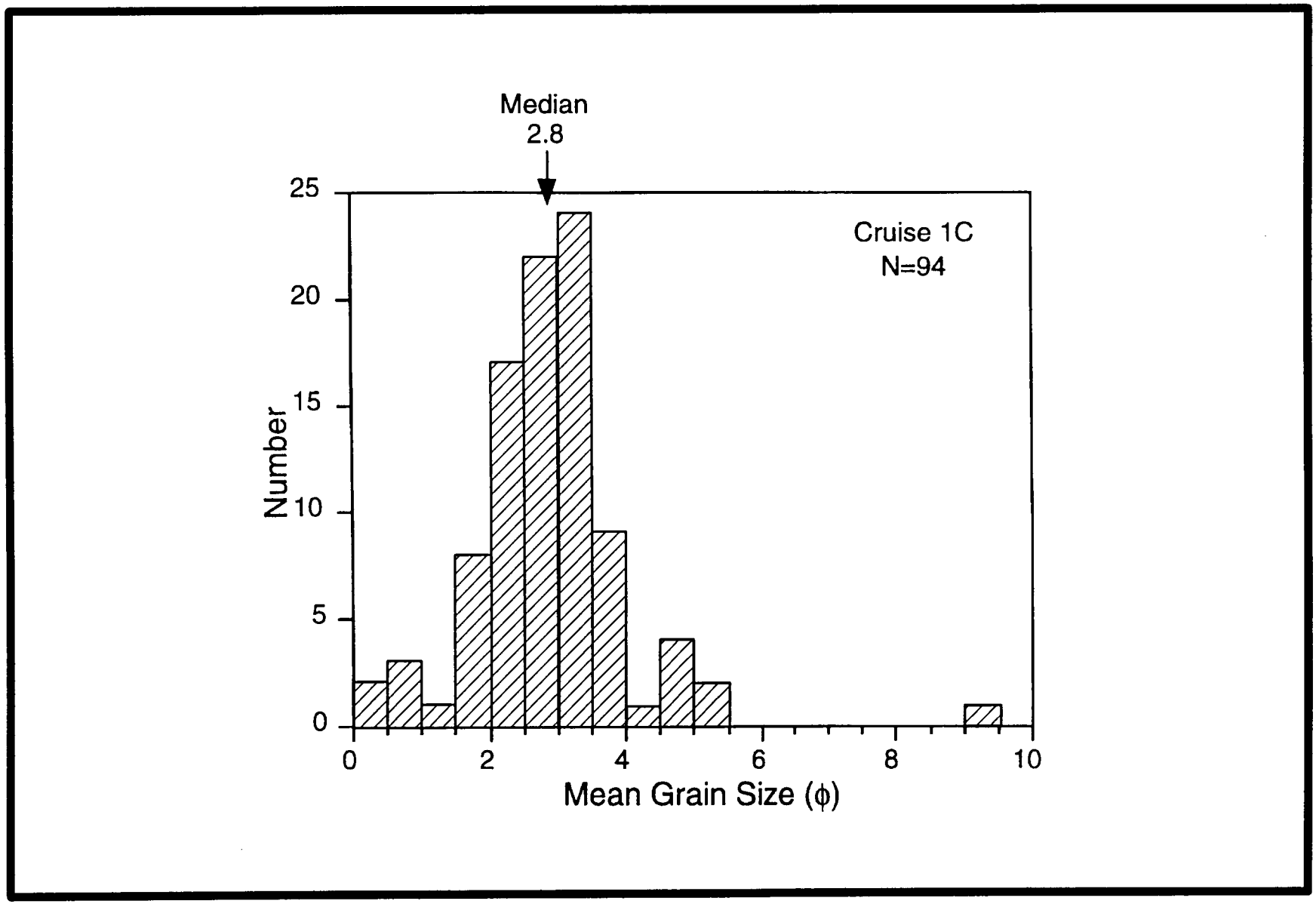

Fig. 4.19. Histogram of mean grain sizes from all grab samples taken on Cruise 1C. Values cluster mainly between 1.75ϕ to 4ϕ.

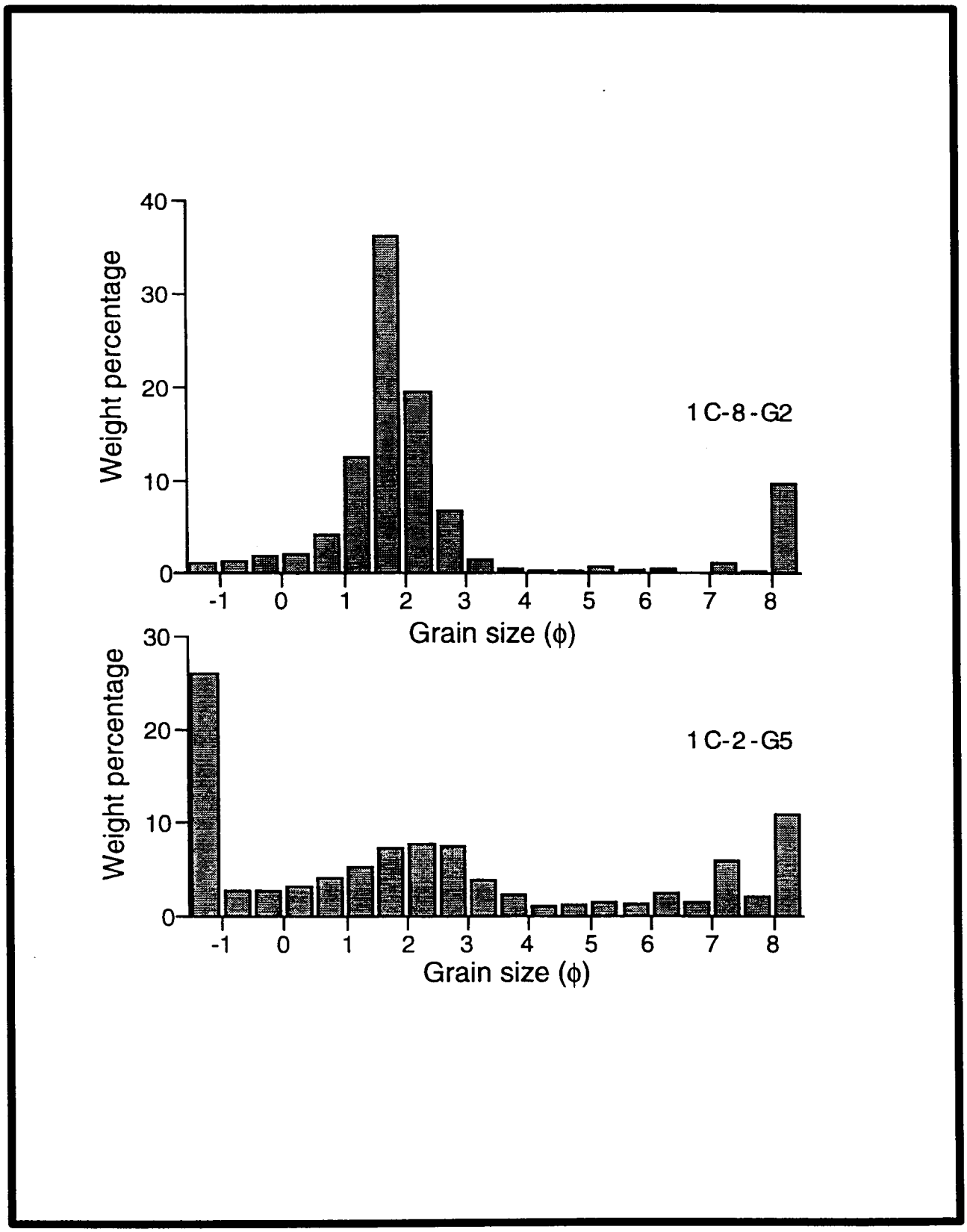

Fig. 4.20. Grain size distributions for two representative grab samples. Sample 1C-8-G2 is from Grab 2 from Site 8 taken on Cruise 1C. Sample 1C-2-G5 is from Grab 5 at Site 2 taken on the same cruise.

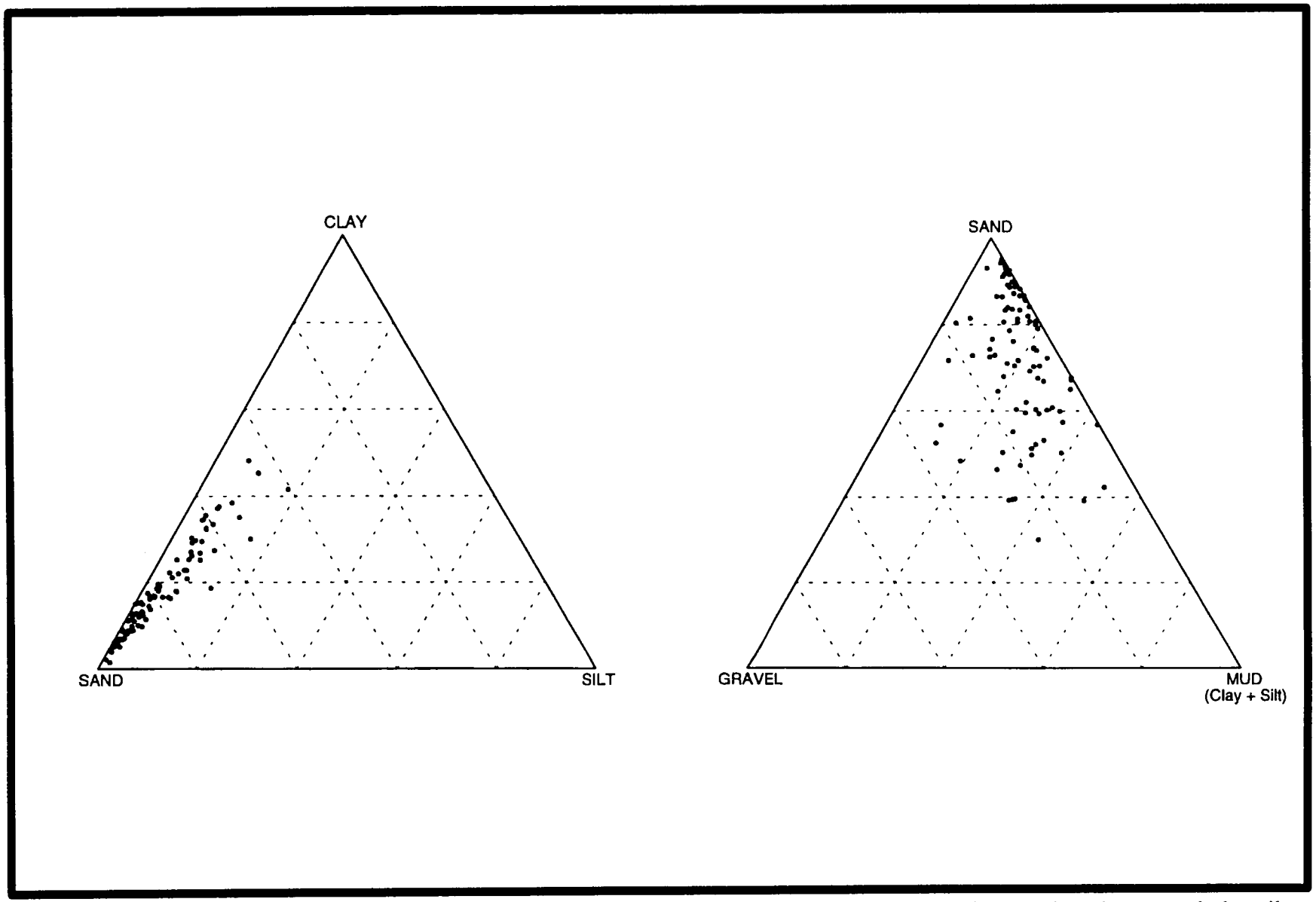

Fig. 4.21. Ternary diagrams showing the composition of Cruise 1C grab samples. At top, all samples are plotted on a sand-clay-silt diagram with values normalized after removal of the gravel fraction. Most samples are sand with a variable amount of clay. The nearly linear trend implies the mixing of sand and clay end-members. At bottom, all samples are plotted on a gravel-sand-mud diagram to emphasize variations in gravel content. Most samples have less than 20% gravel, but some contain up to 50%. The gravel usually consists of small shells, shell fragments, and biogenic debris.

sources, one sand and the other fine clay, that are intermixing. On a gravel-sand-mud ternary plot (Fig. 4.21), samples still tend to cluster near the sand apex, but considerably more scatter is apparent owing to variable gravel fractions up to about 50%. The variability of the gravel fractions and their biogenic compositions implies they are controlled by local factors.

There appears to be no simple correlation between backscatter and grain size. Samples from higher backscatter seafloor tend to be enriched in both gravel and clay. In addition, the highest gravel-content samples tend to be located near mound edges. For example, around the large mound where Site 7 is located, the grain sizes seem to correlate best with position and backscatter. Backscatter is high on the west and north sides of this mound and lighter to the east. Grabs 2, 6, 7, and 10, all located on the west side of the mound on higher backscatter seafloor, show the greatest concentrations of clay and gravel. In contrast, grabs 1, 5, 8, and 9, all located on the east side of the mound, show the lowest clay and gravel contents. Furthermore, grab 7, the sample with the highest gravel content, is located closest to the mound on the western side. At other sites, the correlation is not always as clear. These observations suggest that sediment sorting is a complex process, perhaps involving several mechanisms, but that mound proximity and current direction may play major roles.

Discussion

From prior MMS-funded surveys in the Mississippi-Alabama outer shelf region, we knew that carbonate mounds were often clustered with sizes ranging from several meters on a side to hundreds of meters wide and 10 to 18 m high (Brooks 1991; Continental Shelf Associates, Inc. 1992; Sager et al. 1992). We also knew that areas of high acoustic backscatter were associated with many mounds (Brooks 1991; Laswell et al. 1992) and that in some cases these areas were preferentially located to the southwest of the mounds. This new study has emphasized and broadened these findings. In addition, we are beginning to get a better understanding of the relationship of backscatter to the mounds and the sediment characteristics.

Although we knew previously that many of the carbonate mounds are subcircular in plan view, our new side-scan sonar data show the details of mound flanks and co-occurrences with far-greater resolution than previously. We are still investigating these relationships. Previously we found a difference between mounds at the shelf edge, in water depths of

class of mounds: low, wide, carbonate hard bottoms hundreds of meters in diameter but only a few meters in height. These features are particularly notable near the shelf-edge in Megasite 2, but are also seen in at shallower depths in Megasite 3. These mounds often have tops with bumps a few meters or less in height that make them appear to be made up of many smaller "mini-mounds" and in this sense they are similar to many of the other, shallower subcircular mounds.

The morphologic differences among mounds suggest differences in development. The low, wide carbonate hard bottoms imply slow upward growth over a large area, perhaps indicating stable sea level or slow sea-level rise. We previously speculated that such mounds grew at the shelf-edge during the slow sea level rise after the last ice age (Sager et al. 1992), but now we know them to be even more widespread. The tall, steep-sided "pinnacle" mounds suggest rapid growth during faster sea level rise (Sager et al. 1992). Because many of these mounds apparently sit atop the low, wide hard bottoms, this possibly indicates a switch in mound growth from lateral to vertical aggradation owing to acceleration in sea level rise. The widely-dispersed, shallower mounds, which are highly-variable in size and height, may represent a short period of sea level stabilization in the middle of the deglaciation (Sager et al. 1992).

Our new data also give some insights about the location of mound formation. Prior data implied the mounds formed atop erosional unconformities on the two mounds in the MAMES survey area (Sager et al. 1992). The new data have strengthened this observation. Although layers cannot be traced beneath the mounds, owing to the scattering of acoustic energy they cause, in many places delta foreset beds beneath appear continuous when traced from one side to the other of a mound or mound cluster. This would probably not occur if the mound had formed prior to the deposition of the delta beds; instead the beds would be distorted. Our new data also imply that in some places, larger mound groups formed on bathymetric scarps, as shown by depth offsets across these mounds. Both of these observations imply that the mounds formed where suitable substrates were available. This is consistent, for example, with organisms requiring hard substrates for attachment.

Subbottom profiles over the mounds frequently show asymmetric profiles, another clue about mound formation. Often large mounds have a peak at the seaward edge and have sediments dammed up on their landward sides. These characteristics suggest that mound growth was most intense on the side facing the sea, where perhaps nutrients are highest and sediments least. This is similar to the formation of coral reefs in shallow water and lends credence to the hypothesis that the mounds were formed by biologic action in shallow water. The damming of sediments indicates that the mounds existed when the surficial sediment layer was deposited. Since it is generally accepted that this layer was formed from reworked sediments when sea level was much lower, this implies that the mounds existed when sea level was lower; in other words, they formed nearer to sea level.

Our new findings about sediments give significant insights about sediment distribution and sedimentary processes. The upper acoustically-transparent layer, which apparently represents relict sandy sediments deposited by reworking during lower sea level, is more

uniform than expected. This implies that currents and deposition were not highly variable around the mounds. What is more, the patterns in the sediment distribution and sonar back-scatter suggest a dominant current direction. The high backscatter regions are located preferentially on the southwest sides of the mounds, except in Megasite 2. Particularly telling are long, thin, high backscatter "tails" that trend southwestward from many small and medium mounds. These "tails" are erosional gullies clearly caused by flow disturbance owing to the mounds. This implies a general northeast to southwest current regime. This seems consistent with the damming of sediments on the north sides of many large mounds and erosional holes adjacent to their southwest sides. Like a "snow fence" the mounds evidently slow the currents on their "windward" sides, causing deposition, and cause turbulence and erosion on their "leeward" sides. Whether or not the northeast-southwest trend is dominant current direction, whether it is a special occurrence, such as during large storms, or whether it represents an ancient current regime, is not presently clear.

Sediment grain size data imply the surficial sediments are composed of three end-members. Most sediments are mainly sand, with a smaller variable amount of clay added. The linear nature of the size data on the sand-silt-clay ternary diagram implies two end-members, sand and clay, that are intermixed. Since the sediments currently being deposited in the region are fine clays, this could occur owing to resuspension events that mix the clay with the sand near the surface. The third component consists of gravel-sized fragments, usually shells, shell fragments, or other biogenic debris. The gravel content is usually highest near mounds, indicating the mounds as a potential source or suggesting the mound proximity is an important factor for controlling the presence of organisms. Because we find no simple correlation between mound proximity and gravel content (many near-mound stations show no enhancement in gravel-sized fragments), the gravel may be shed from the mounds.

Grabs located in high backscatter areas sometimes, but not always, showed different grain size characteristics. The lack of a simple pattern suggests that several mechanisms may contribute to the acoustic backscatter. As mentioned above, Site 7 grab data showed that those stations in the high backscatter zone southwest of "36-Fathom Ridge" contain higher concentrations of both gravel and clay. The latter is somewhat surprising because we expected these areas to be erosional, with fine sediments preferentially removed. Site 7 ROV photo data indicate that this zone is also characterized by meter scale surface relief and the common occurrence of rubble and shell hash. This may indicate that the backscatter patterns are partly related to the occurrence of larger fragments and small-scale topography. The intermixing of both gravel and clay with the sand in these erosional areas suggests that the forces causing the erosion may also mix these components. The bias towards southwest flanks implies that debris is preferentially swept to this side of the mounds.

Chapter 5
Sediment Dynamics

Approach and Rationale

The objectives of the sediment dynamics component in collaboration with the geochemistry and geology components are to (1) provide quantitative and qualitative measurements of the extent and occurrence of nepheloid layer; (2) determine sedimentation and resuspension rates; (3) determine how topographic highs affect present-day sedimentation; (4) determine temporal variations in sediment texture; and (5) relate short term sediment dynamics to long term sediment accumulation. To address these goals, sediment traps, optical backscatter (OBS) instruments, and conductivity-temperature-depth/dissolved oxygen (CTD/DO) sensors are used to assess and monitor the extent and variability of the nepheloid layer sediment and resuspension. At the study sites, these processes and their impact on the biological community of the mounds area will be assessed.

The goals as outlined above are being met by documenting particle distributions and dynamics with several techniques. Data on the spatial and vertical distribution, intensity and short time-scale variability of the nepheloid layer are acquired with a transmissometer interfaced to the CTD/DO system. Profiles of beam attenuation are recorded during the cruises. Extended temporal sampling and monitoring of the intensity and temporal variability of the nepheloid layer in conjunction with the current regime at the study sites are measured with OBS instruments interfaced with current meters on the moorings. Sediment traps are deployed with the moorings to quantify particle flux. Together with surface sediment characterization, these data will delineate the origins of the observed seafloor sediment patterns. Vertically-separated sediment traps are used to sample particulates from the nepheloid layer and higher waters to derive short term sedimentation and resuspension rates. Particles from the traps will be compared with sediments from the seafloor to characterize the depositional process. Grab and sediment trap samples are part of the routine monitoring program so that temporal variations are monitored as well. The extent and occurrence of the nepheloid layer is determined by grids of CTD/DO/transmissometer/OBS casts around the study sites during monitoring cruises along with casts taken at each mooring site during the mooring servicing cruises. Long term variations will be addressed by OBS instruments deployed on mooring stations, providing comparisons with current meter records.

Most changes in the optical properties of seawater are caused by particles suspended or settling through the water. Light attenuation as measured with a beam transmissometer is one of the easiest to use and most versatile optical instruments now in use to measure inherent optical properties in seawater. A Seatech 25-cm pathlength transmissometer is used to provide measurements of optical attenuation coincident with CTD casts. Gross, large-scale measurements can be made easily with this instrument, but to make precise quantitative measurements considerable care must be exercised in cleaning the optical windows, in correcting for the decay of the LED light source, and in calibration with in-situ particle concentration from filtered samples (Bartz et al. 1978; Gardner et al.

1983). Beam attenuation is an inherent property of seawater and is the sum of light scattering and absorption (Gordon et al. 1984). At the 660 nm wavelength used in the Seatech transmissometer, the scattering function is small. Attenuation is usually considered to be the sum of attenuation of seawater (c_w), yellow matter (c_y), and particles (c_p). In the open ocean c_y is negligible and c_w is constant, so changes in total attenuation result from changes in particles (Morel 1974; Jerlov 1976; Pak et al. 1988; Gardner et al. 1995; Walsh et al. 1995). The properties of particles that affect attenuation are their concentration, size distribution, index of refraction, and shape, with concentration and size being most important. If the size distribution, index of refraction and shape of particles are constant, beam attenuation is linearly related to particle concentration (Spinrad et al. 1983; Baker and Lavelle 1984; Moody et al. 1986). Particle characteristics vary between regions, however, so in order to estimate particle mass concentration from attenuation data it is necessary to calibrate the data by filtering water for total particle concentration.

Transmissometers are also effective in locating areas of resuspension of bottom sediments and production of bottom and intermediate nepheloid layers (Walsh 1990; Gardner and Walsh 1990). Because resuspended sediments form the bulk of nepheloid layer particles (Gardner et al. 1983, 1985), monitoring of the nepheloid layer by use of beam attenuation data can be used to infer spatial and temporal variability of both particle concentrations and resuspension (Walsh 1990; Gardner and Walsh 1990; Walsh et al. 1995).

Field and Laboratory Methods

CTD/DO/Transmissometer/OBS Data Sets

The use of the R/V TOMMY MUNRO for the field work has resulted in some changes in data gathering. Because of limited work and bunk space, the filtration work was transferred to the mooring service cruises. This limits the number of filtration samples taken during each cruise, but the total number of cruises is larger. With this change, the total number of transmissometer casts during the program has been increased due to use of the CTD/transmissometer package on both monitoring and mooring service cruises.

Using the transmissometer interfaced to the CTD/DO, a minimum of three profiles is collected at each of the monitoring sites per monitoring cruise. These include profiles at mooring locations if they are present at a site. The CTD/DO data will be compared with the OBS instruments used on the moorings so that a robust correlation can be made between the transmissometer signal and the OBS. On each of the mooring redeployments CTD/DO/transmissometer casts are made prior to recovery and after redeployment.

Transmissometer data from a Seatech 25-cm pathlength transmissometer are being collected with each CTD/DO cast as are data from OBS instruments deployed on the moored current meters. CTD data are plotted graphically in real time on board ship to help determine rosette bottle sampling depths and to monitor the quality of the data

stream. Such data are especially helpful in defining the thickness of the nepheloid and bottom boundary layer and the vertical extent of mixing.

Particle concentration profiles for calibration of the transmissometer beam attenuation data are made at each mooring site by filtration from Niskin bottles. One liter samples are drawn from nine bottles from each filtration cast and vacuum filtered onto pre-weighed 47 mm 0.4 μm pore size Poretics filters. The filters are rinsed with distilled water to remove salts and dried. On shore, the filters are weighed again, and the difference between the pre- and post-weighing yields the particle mass concentration per liter. Blank filters are used for quality control at all stages of the analysis.

The first calibration data set was produced on the January 1998 mooring service cruise (S2). Six casts were sampled for particles (three at Site 1, one at each of the other three mooring sites). The average blank value was 0.1 mg. The minimum filtration concentration was 0.03 mg/L. The maximum filtration concentration was 1.46 mg/L. A least squares regression of beam attenuation on particle concentration yielded a relationship with a slope of 1.3897 and an r^2 of 0.89 (Fig. 5.1). The slope is within the range reported for the Texas-Louisiana Shelf Circulation and Transport Process (LATEX) Program data sets [1.2 to 1.9 (Zhang 1997)]. Beam attenuation values for the entire data set were adjusted to yield a c_p of zero for a concentration of zero.

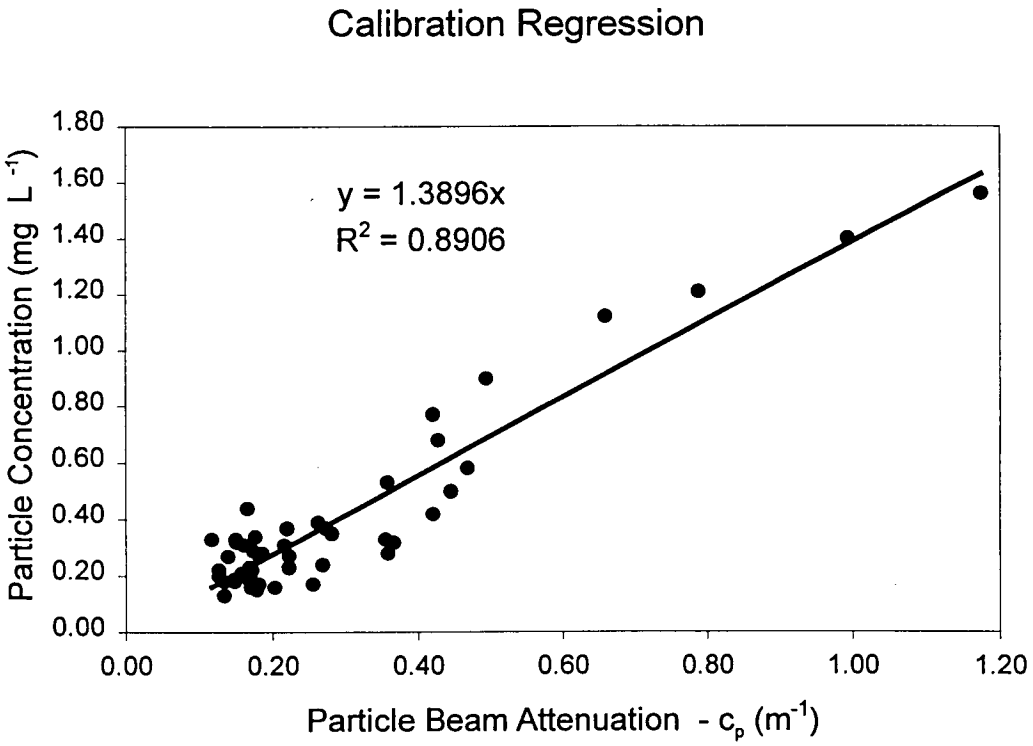

Fig. 5.1. Calibration plot of Niskin bottle particle concentration from the January 1998 mooring servicing cruise against the particle beam attenuation data from the transmissometer for the same depths and casts.

Correlation of the OBS sensor data (a Seatech light scattering sensor [LSS]) on the CTD package with the transmissometer data will be completed with the cross-correlation of the mooring OBS data. Plots of LSS voltage vs. the particle beam attenuation (c_p) as shown for a representative cast in Fig. 5.2 indicate good agreement between the sensors though the upper and midwater LSS data has considerably more data spiking.

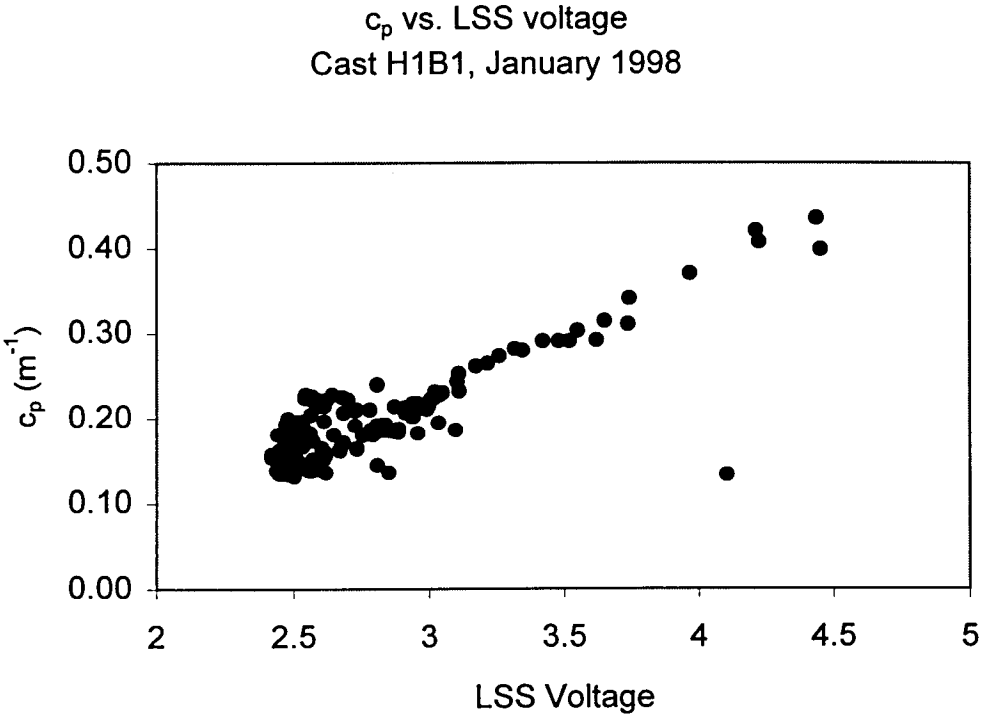

Fig. 5.2. Particle beam attenuation (c_p) plotted against the LSS (Seatech Light Scattering Sensor) data from a representative cast showing the correlation between the two data sets. The high values (i.e., V>3) are from the nepheloid layer.

Mooring Data Sets

Six moorings have been deployed to provide long term data sets and characterize the flow fields, near-bottom oxygen concentrations, and nepheloid layer dynamics with respect to the flow field. Four of the moorings are used for regional coverage, with the remaining two rotating among the study sites for intensive spatial/temporal sampling. An OBS instrument is located a few meters above the bottom of each mooring and interfaced with a current meter to supply power and record data. The nepheloid layer OBS data characterize the intensity and temporal relationships between the current velocities and the nepheloid layer. Simple particle modeling and observational records are being used to determine whether observed nepheloid layer fluctuations are the result of near field

(active) resuspension or are advective features. Combining the point source records of the current meters and optical instruments with the wider areal coverage and discrete full water column profiles from the CTD/DO/transmissometer/OBS work will yield a robust data set describing the temporal and spatial variability of the nepheloid layer over the area and at each of the monitoring sites.

Sediment Traps

The sinking flux of particulate material is collected using sediment traps. Simple core-tube sediment traps have been deployed on each of the moorings to monitor particle flux and resuspension during the monitoring period. This type of sediment trap has been proven both effective and cost-effective during the LATEX Program on the shelf of the western Gulf of Mexico (Zhang 1997). The traps have been placed at 2, 7, and 15 m above the bottom. The resuspended component of the bulk sedimentation rate will be derived by partitioning the bulk sediment sample in the 2 m and 7 m traps using the 15 m trap and the surface sediment samples as end members. Partitioning will be based on bulk sedimentation rate, grain size, and data from a suite of chemical analysis made on each sediment sample [e.g., total inorganic carbon (TIC), total organic carbon (TOC), metals from instrumental neutron activation analysis (INAA); see Chapter 6]. This partitioning scheme has been used effectively in previous sediment trap studies (Walsh et al. 1988; Walsh and Gardner 1992).

Sediment traps were deployed in May 1997 (Cruise 1C). Materials have been collected during Cruises M2 and M3 and two mooring servicing cruises. Additional samples will be collected during future monitoring and servicing cruises. All samples will be analyzed for mass and grain size. TOC and TIC will also be done on the materials from the eight cruises (3 depths x 6 moorings x 8 cruises = 144 samples).

Sediment trap samples are decanted and refrigerated at sea, subsequent processing occurs in the laboratory ashore. In the laboratory, the supernatant is drawn off and the samples are wet sieved through a 1 mm nylon screen. The >1 mm fraction is visually inspected during processing and archived. In all samples to date the >1 mm fraction is a small proportion (<5%) of the total sample. The <1 mm fraction is split into six fractions using a forced air, constant stirring splitter. Two splits are combined and archived at this stage (dark refrigeration). Two splits are used for grain size analysis. The remaining splits are centrifuged in pre-weighed centrifuge tubes at 15 krpm for 10 minutes. Supernatant is drawn off and samples are resuspended with distilled water to remove salts and centrifuged again. The supernatant is drawn off and the tubes with the samples weighed. The samples are frozen and freeze dried for 24 to 48 h depending on the volume of sample. After freeze drying, the tubes are weighed to measure the water loss. The samples are removed from the centrifuge tubes and ground to a powder in a mortar. Ground samples are placed into pre-weighed petri dishes and weighed. The empty centrifuge tubes are also weighed to estimate the remaining sample on the wall and as a double check on the petri dish weight. Mass flux is calculated using the dry weight divided by the area of the tube and the elapsed time of deployment in days. Dry splits of the ground samples are made to provide subsamples for chemical analysis. The concentrations of TIC and TOC are to be measured from the subsamples (methods are

described in Chapter 6). Depending on the amount of subsample available, aluminum, barium, and other metals in the samples will be analyzed from the following:

(1) each mooring and depth from
   (a) Mooring Service Cruise S1 and Monitoring Cruise M2,
   (b) Mooring Service Cruise S2 and Monitoring Cruise M3, and
   (c) Mooring Service Cruises S3, S4, and S5 and Monitoring Cruise M4 will be combined and analyzed for INAA trace metals (3 depths x 6 moorings x 3 combined cruises = 54 samples); or

(2) each mooring and depth from the samples collected on the three monitoring cruises (3 depths x 6 moorings x 3 monitoring cruises = 54 samples).

To date, four sets of sediment trap samples have been recovered. The first two sets, covering May to July 1997 and July to October 1997 have been processed and split for analysis. One trap sample on the first deployment was lost due to a fish bite through the trap endcap. One trap sample was compromised due to spillage during recovery. Trap samples recovered in January and May 1998 are being processed. TIC and TOC analysis for the first two sets of samples have been completed. The first set of combined samples covering the first two periods (May to October) has been submitted for neutron activation analysis of metal concentrations.

Results and Discussion

Water Column

While full analysis of all the data remains to be completed, the data collected to date indicate that the study site is an area of high spatial and temporal variability. Some regional trends are apparent from the data set. The surface layer was characterized by low salinity and a local maximum in the particle concentration reflecting biological activity during both the October 1997 and January 1998 cruises, with lower salinity and higher particle concentrations towards the west. A benthic nepheloid layer was present at all sites in all casts though intensity as measured by the beam attenuation and vertical gradient in attenuation was variable. The benthic nepheloid layer (BNL) was found to be associated with lower bottom water temperatures during both cruises (Fig. 5.3).

Temporal and spatial variability was illustrated at Site 1 during the January mooring servicing cruise (Fig. 5.4). Two casts were made at mooring site B just prior to recovery and immediately after redeployment of the mooring. The two casts, though only a few hours apart, demonstrate that understanding advective processes will be important to interpreting the data set.

Below the surface layer the particle concentration reached a minimum in both casts near 40 m. However, a warm saline layer between 20 and 60 m appears in the H1B2 cast but not the H1B1 cast. An intermediate nepheloid layer (INL) is associated with the base of this layer and is separated from the BNL by a thin layer of lower salinity water. The warm saline layer and its associated INL were found in both of the profiles made at mooring C to the southwest of B while the profiles at mooring site A to the south of B were similar to H1B1.

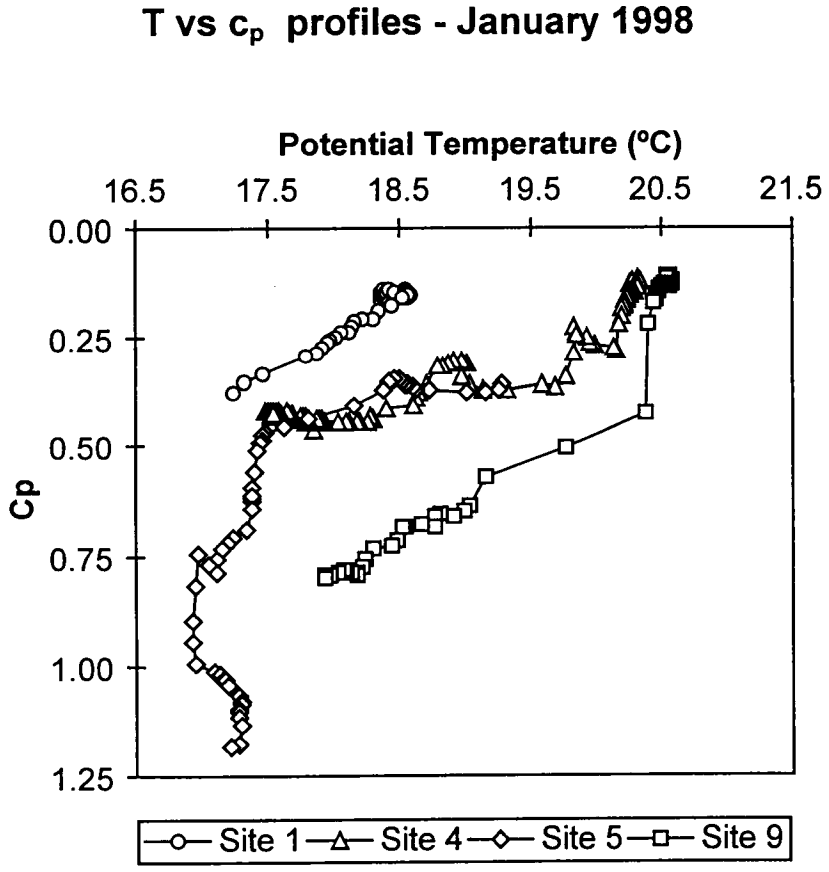

Fig. 5.3. Plot of particle beam attenuation versus potential temperature for selected casts taken during the January 1998 mooring servicing cruise. Note the increase in beam attenuation with decreasing temperature. [Note: Potential temperature is a common oceanographic variable. It is the temperature that a parcel of water would have if it were moved adiabatically (i.e., with no heat added or removed) to the surface where pressure is assumed to be 1 atmosphere.]

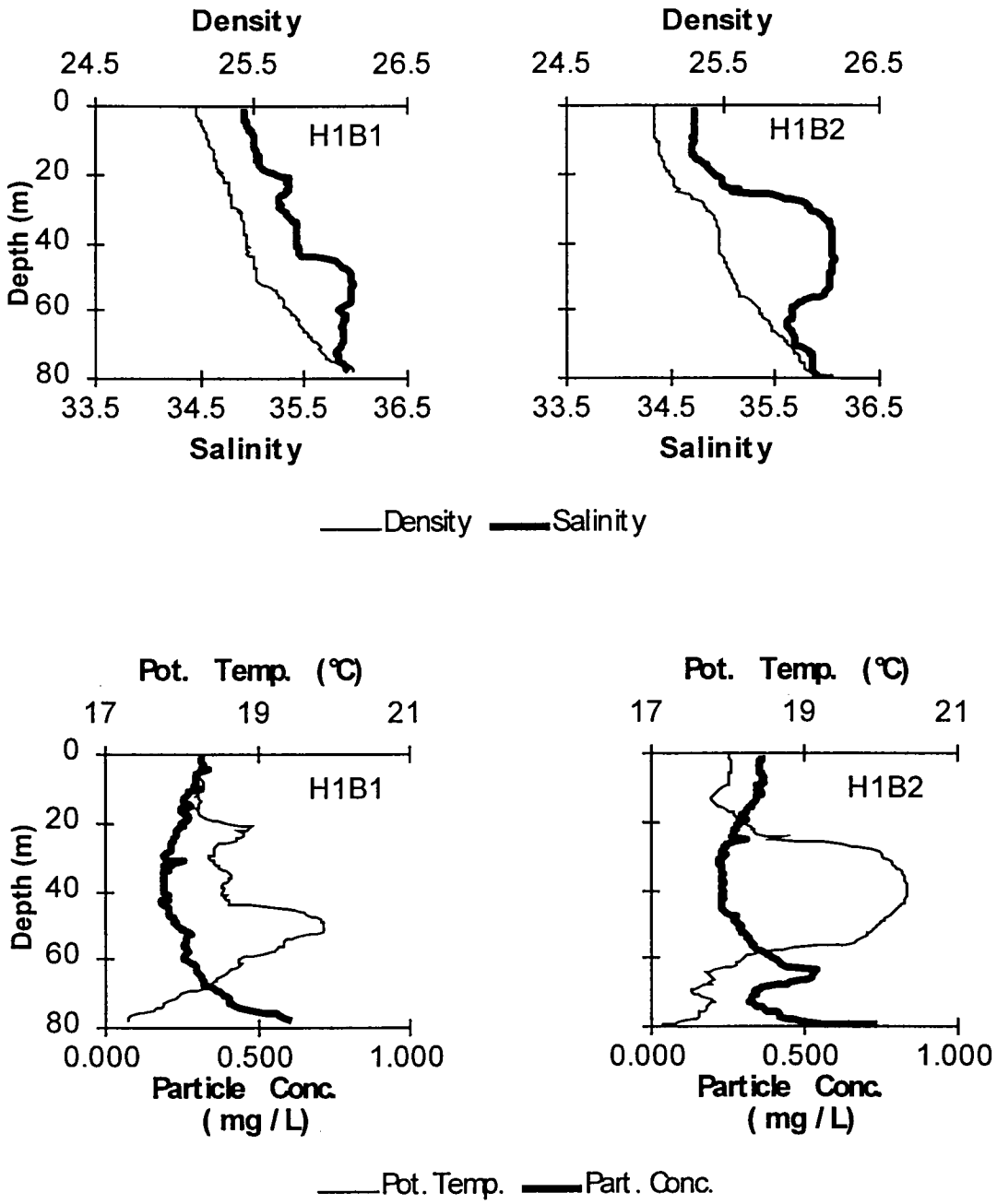

Fig. 5.4. Profiles of density, salinity, potential temperature, and particle concentration from the calibrated beam attenuation data from two casts at Site 1 mooring taken during the January 1998 mooring service cruise (S2). Note the presence of the warm saline intermediate layer in H1B2 and the associated INL.

Sediment Traps

The sediment trap results from the first two mooring periods reflect the influence of resuspension input at the study site with fluxes increasing to the bottom for all moorings and time periods (Figs. 5.5 and 5.6). TOC concentrations decreased towards the bottom, probably reflecting dilution of fresher water column material with resuspended sediment. However, sediment TOC data analyzed from these sites were higher than all but the 15 m above bottom (mab) traps (Chapter 6). At this point no obvious explanation for this conundrum has presented itself.

The bulk flux ranged from 2 to 20 g m^{-2} d^{-1} with all of the fluxes in the 15 mab traps below 5 g m^{-2} d^{-1} while all of the 2.5 mab traps recorded fluxes greater than 5 g m^{-2} d^{-1}. The highest fluxes at all depths were found at Site 5, with decreasing fluxes from 5 to 9 with the lowest fluxes at Sites 1 and 4.

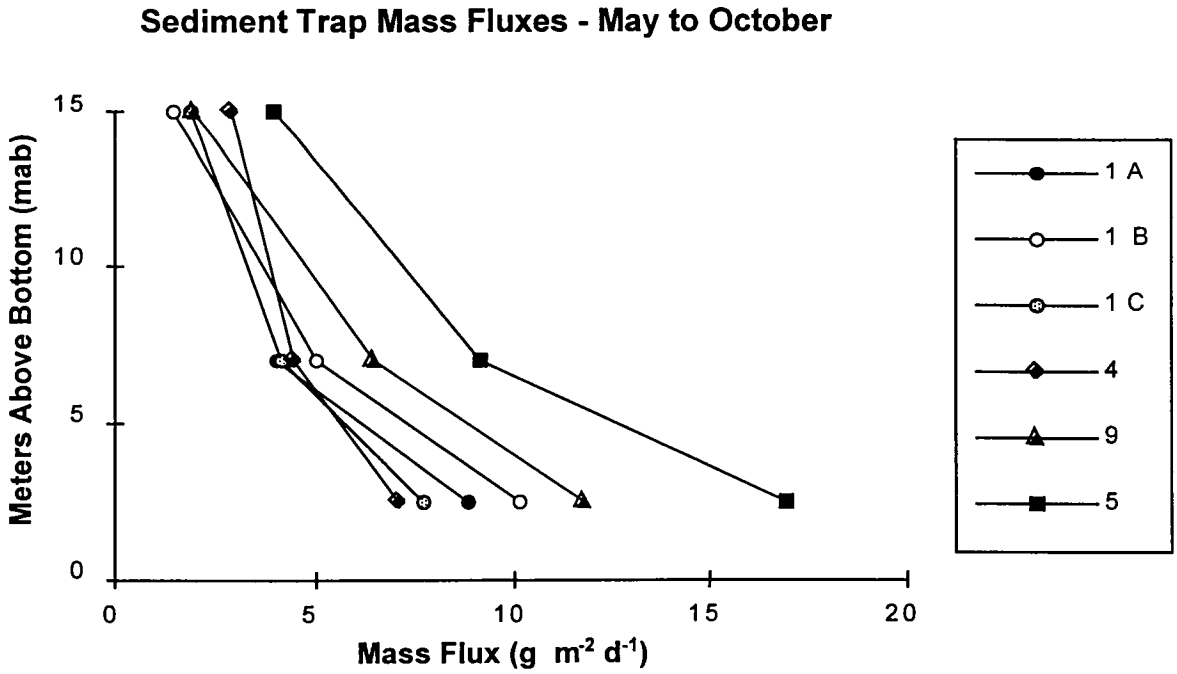

Fig. 5.5. Time weighted average mass fluxes recorded during the first two mooring deployments for all sites covering May to October 1997.

Comparing the two periods the fluxes recorded were similar in the traps 15 mab but generally higher in the deeper traps in the August to October period than May to July. At Site 1 the three moorings recorded similar fluxes at the 7 and 15 mab traps during the May to July period, with increasing fluxes in the bottom traps with A<C<B. In the August to October period, the 7 and 15 mab traps recorded higher fluxes than in the earlier period with a greater degree of variability in the 7 mab traps. The higher fluxes

and higher variability between the two periods may reflect a higher average bed shear stress between the two periods.

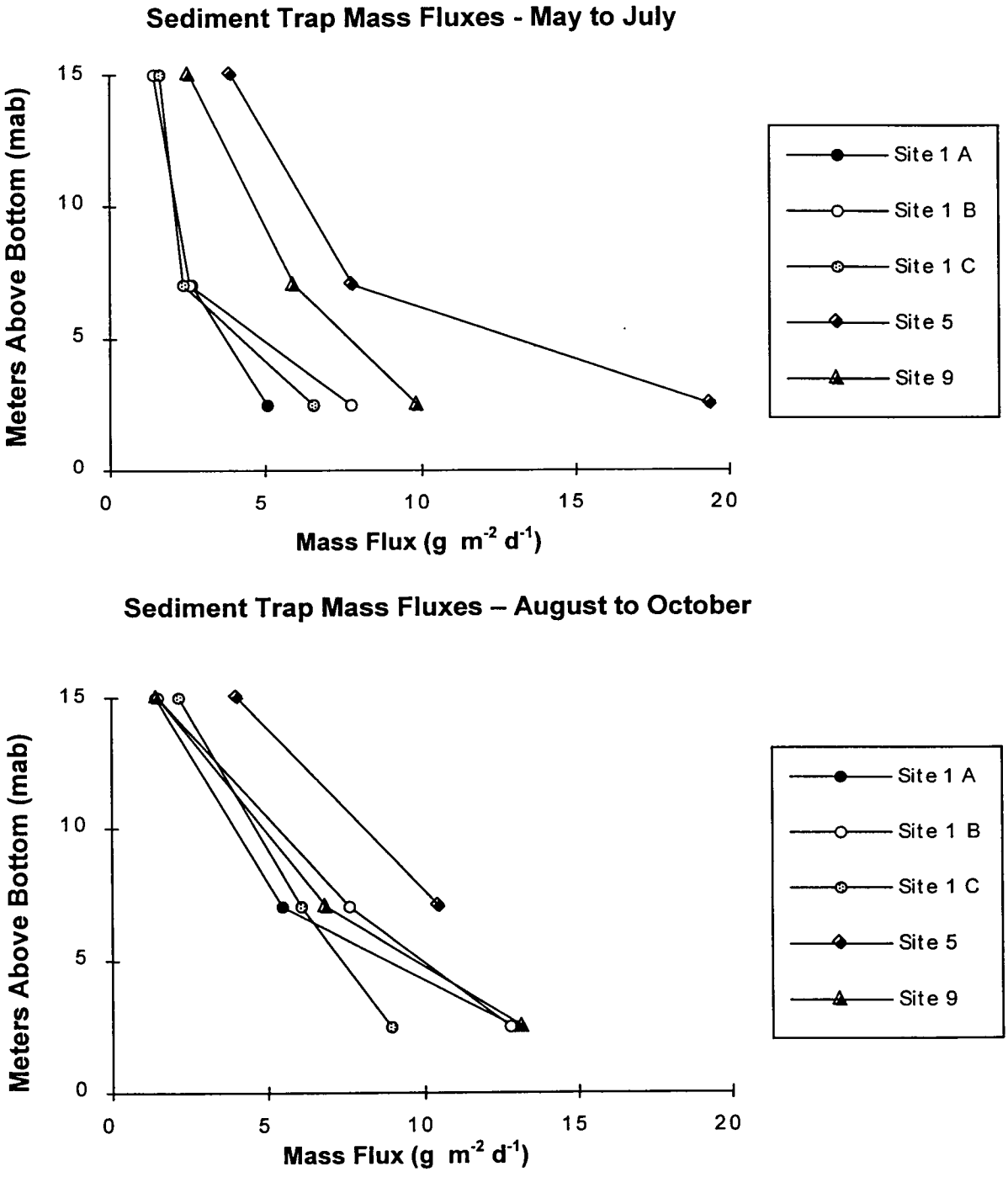

Fig. 5.6. Mass fluxes recorded during the first two mooring deployments for all sites covering May to July and August to October 1997.

Chapter 6
Geochemistry

Approach and Rationale

The geochemistry program component includes a combination of hydrocarbon, trace metal, grain size, total organic carbon (TOC), and total inorganic carbon (TIC) measurements of sediments and sediment trap materials. Contaminant measurements are intended to document the current hydrocarbon and trace metal concentrations within the study sites. Sediment characteristics (grain size, TOC, TIC) aid in the determination of the origins of sediment at the sites and provide a basis for discerning the relationship between sediment texture and biological patterns at the study sites. Trace metals, TOC, TIC, mass, and grain size are being measured in sediment trap materials to aid in determining the origins of sediments at the sites and to document whether contaminants are accumulating at the sites during the duration of the study (see Chapter 5).

There are two objectives related to the geochemistry program component. One objective is to document the presence of any contaminants in the study area due to energy exploration and exploitation. The second objective is to characterize the benthic abiotic environment at the study sites to aid in determining the origins of sediment at the study sites and to define the relationship between sediment texture and biological patterns.

The two most common contaminants associated with platforms are hydrocarbons and metals (Middleditch 1981; Boesch and Rabalais 1987; Boothe and Presley 1987; Continental Shelf Associates, Inc. 1983, 1985b, 1989). The release of petroleum from a platform to the surrounding environment can occur during drilling as well as in the production phase of a platform's lifetime. Petroleum hydrocarbons are potentially present in a variety of discharges including drilling fluids, cuttings, produced water, spills, deck drainage, and other releases (Kendall 1990). Petroleum-derived hydrocarbons released to the environment can be differentiated from naturally occurring background biogenic hydrocarbons (Brassell et al. 1978; Philp 1985; Boehm and Requejo 1986; Kennicutt and Comet 1992). Petroleum contains (1) a homologous series of n-alkanes with 1 to more than 30 carbons with odd and even carbon number n-alkanes present in nearly equal amounts; (2) a complex mixture of branched and cycloalkanes; and (3) an extensive suite of polycyclic aromatic hydrocarbons (PAHs). Aliphatic hydrocarbons synthesized by organisms (both planktonic and terrestrial) include a suite of normal alkanes with odd numbers of carbons from 15 to 33. Complex branched and cycloalkanes are rare in organisms. Petroleum PAH mixtures are easily differentiated from PAHs synthesized by organisms by the structural complexity of the mixture and the presence of substantial amounts of alkyl substituted PAHs. PAHs are some of the more toxic components of oil and as such indicate the potential for biological effects. Based on considerations of petroleum chemistry, biological occurrences, and toxicological effects, aliphatic and aromatic hydrocarbons were chosen as tracers of petroleum contamination (Kennicutt 1995).

Trace metals are also released in discharges from offshore drilling activities (Lake Buena Vista Symposium 1981; Boesch and Rabalais 1987; Boothe and Presley 1987). Metal contamination can potentially affect both infauna and epifauna in the vicinity of platforms (Southwest Research Institute 1978). Many trace metals are priority pollutants (antimony, arsenic, cadmium, chromium, copper, lead, mercury, nickel, selenium, silver, and zinc) and are known to be toxic to organisms. These metals are often constituents of drill muds (Houghton et al. 1981; Rubinstein et al. 1981; Tornberg et al. 1981). Tin is known to be toxic and is present in antifouling paints used on platform structures. Barium is an ideal tracer of the settleable particulate fraction of discharged drilling fluids and cuttings because it occurs in high concentrations in drilling muds and has a low, natural background in ambient sediments (200 to 500 ppm dry weight; Chow and Snyder 1981; Boothe and James 1985; Boothe and Presley 1987). Barium (as barite, barium sulfate) is the dominant component of drill mud (up to 90% on a dry weight basis). Aluminum and iron are major constituents of alumino-silicate minerals and can be used to detect changes in sediment type. Vanadium is another metal of interest because it can occur in significant concentrations in crude oil.

In order to characterize the benthic geochemical environment at the proposed study sites, a variety of inorganic and organic attributes are being measured. The origins and regional distribution of sediment characteristics are ultimately a function of abiotic and/or biotic processes and anthropogenic activity. Some characteristics tend to covary due to common origins and thus can confirm or contradict the importance of an inferred process. For example, TOC and silt/clay content covary and may suggest the prevailing depositional environment. Other parameters are indicators of the origins of materials that have accumulated at the site. For example, PAHs are a measure of petroleum contamination. The origins and movement of sediments and their associated constituents on continental shelves are particularly important in predicting the impact of human activities with reference to the longevity of an "unnatural" perturbation and possible "natural" mitigation or enhancement of environmental effects (i.e., removal or concentration of a contaminant; disruption of sedimentary processes). The detection of perturbations due to anthropogenic activities can only be recognized if the natural variability of the system is understood. The benthic setting is a key determinant in defining the ecology of biological communities.

Measures of sediment characteristics can provide quite different information. Often bulk characteristics, the chemistry of a select subfraction of the sediment, or compositional information is determined. Each type of measurement provides important information, however, each has its limitations in inferring origins and processes. Bulk measurements characterize a large percentage of the total sample. However, depending on the measurement, these characteristics can be generic in nature with multiple inputs unresolved (e.g., TOC). On the other hand more specific tracers can be useful in defining the origins of materials (e.g., $\delta^{13}C$). If a subfraction of the sample is characterized, the subfraction may or may not be representative of the bulk of the associated materials (e.g., alkanes). Often a specific chemical composition is preferentially associated with a single or unique source of materials (e.g., PAHs and petroleum). Quantitative determinations are needed if the relative importance of multiple inputs is to be determined. It is also key

to measure flux to the benthos based on analyses of sediment trap materials in conjunction with measurements on the accumulated sediment.

The approach and rationale for the geochemistry portion of the study optimizes application of resources by using prior study information and a hierarchical approach to analysis selection. For hydrocarbons, a simple cost effective measure of the presence or absence of oil is needed. Total petroleum hydrocarbons (TPH) determined by gas chromatography/flame ionization detection (GC/FID) and a gravimetric measurement of extractable organic matter (EOM) has been shown to accurately reflect oil contamination on the Gulf of Mexico continental shelf (Kennicutt et al. 1996). The best application of resources is to provide simple, cost effective measurements and increase sample coverage to assure representativeness. The origin of hydrocarbons within a site is of interest and is determined on a single composite of all samples collected at a site. Fingerprinting techniques using PAH composition are the method of choice. In addition it is clear from previous studies that many indicators of platform discharges covary, providing equivalent information about the presence or absence of drilling discharges. A select set of metals (barium, cadmium, chromium, lead, mercury, and zinc), most closely related to platform discharges, is being measured. As an indicator of sediment mineralogy, aluminum and iron are also being measured. Crustal elements are used to normalize the concentration of trace metals to detect anthropogenic additions.

Methods

Sediments are collected by grab as described in Chapter 4, Geologic Characterization. The top 5 cm are sampled. Samples for geochemistry are collected concomitantly with geological samples. The collection of sediment trap materials is described in Chapter 5.

Total Inorganic and Organic Carbon

Sediment carbonate content (0.2 to 0.5 g) is determined by treatment with concentrated HCl. Residual organic carbon is converted to CO_2 and analyzed with a non-dispersive infrared spectrophotometer (Leco WR-12 Total Carbon System). Calcium carbonate is determined as the difference between a treated (acidified) and untreated carbon determination. The acidification is carried out in the crucible used for analysis and the residual acid is evaporated in place to avoid loss of acid soluble organic matter.

Hydrocarbon Analyses

The analytical procedures that provide quantitative hydrocarbon concentrations in sediments have been described in detail elsewhere (Wade et al. 1988; Brooks et al. 1990). The method was adapted from MacLeod et al. (1985) as modified by Wade et al. (1988). Sediment samples are freeze-dried, ground, and stored frozen until analysis. Each set of samples (six to eight) are accompanied by a complete system blank and a spiked blank, which is carried through the entire analytical scheme in a manner identical with the samples. System blanks only include reagents and internal standards. Spiked blanks are system blanks plus known amounts of the analytes of interest. Approximately 15 g of

sediment (dry weight) is extracted with methylene chloride for 12 h in a Soxhlet apparatus. Extracts are concentrated with a Kuderna-Danish evaporative concentrator to 0.5 to 1 mL (60°C) and stored refrigerated (4°C), if not immediately fractionated by column chromatography.

Aromatic hydrocarbons are separated from interfering lipids by alumina/silica gel chromatography. Copper powder is added to the column to remove sulfur. The methylene chloride is replaced with hexane, and the extract, in 1 mL of hexane, is transferred to the column. The column is then eluted with 50 mL of pentane (f_1, aliphatic), and 200 mL of 1:1 CH_2Cl_2-pentane (f_2, aromatic). The aliphatic fractions are analyzed by gas chromatography with flame ionization detection. The detector is calibrated by triple injections of authentic standards (n-C_{11} to n-C_{34}). The aliphatics are separated on a DB-5 fused-silica capillary column by using the following temperature program: T_1 = 60°C, t_2 = 0 min, rate = 12°C/min, T_2 = 300°C, and t_2 = 10 min.

Quantitation of the aromatic (f_2) fraction is by gas chromatography/mass spectrometry (GC/MS) using the selected ion monitoring (SIM) mode. Mass fragmentation is accomplished by electron impact at 70 eV. Sample components are separated on 30-m (DB-5, 0.25 mm i.d.) fused-silica capillary columns with carrier flow (He) of 2 to 3 mL/min. Sample injections are cold trapped on the capillary column for 1 min at 40°C. The oven is then heated to 300°C at 12°C/min. The detector is calibrated for the molecular ion of each analyte. Deuterated surrogates are readily differentiated with no interferences due to differences in the molecular ions monitored (i.e., naphthalene, m/z 128; naphthalene-d_8, m/z 136). Two GC/MS systems are used: Hewlett-Packard (HP) 5996 GC/MS/DS and HP 5970 GC/MSD/DS. The HP Aquarius software is calibrated at five concentrations for each component of interest. Blanks and spiked blanks are run with each sample set. Analyte concentrations are corrected for blank levels and surrogate recovery.

Surrogate recoveries are maintained between 60% and 90%. Method detection limit (MDL) calculations are based on 15 g sample size, 1 mL final volume, and 1-µL injections provide values of 1 to 4 ppb for all aromatic analytes. Blanks are maintained at less than three times the MDL or corrective action is taken (i.e., reinjection or reextraction as necessary). Analytical precision of ±20% for individual analytes on replicate samples is maintained at a concentration of five times MDL.

Trace Metal Analyses

All labware is pre-cleaned by soaking for 24 h in Micro® cleaning solution followed by extensive rinsing with distilled water. The rinsed labware is then soaked for 24 h in 50% nitric acid, rinsed with reagent water, and air-dried. Each set of samples is accompanied by quality assurance/quality control (QA/QC) samples (i.e., method blank, spiked blank, duplicate, matrix spike duplicate, and standard reference material).

The method to be utilized involves wet digestion of a dry homogenized sample in a closed Teflon® bomb. Three mL of Ultrex nitric acid are added and the lid loosely

replaced. The Teflon® bomb is allowed to react for 24 h at room temperature with the lid securely tightened and digestion proceeds at 130°C. Following digestion, 17 mL of ultrapure water are added to the Teflon® bombs and the samples are transferred to clean 1 ounce Nalgene® sample bottles.

The analytical methods are optimized for each element/matrix type to ensure high quality data. The analytical methods to be used are summarized in Table 6.1.

All sediments are stored frozen. Sediment samples are thawed, homogenized, and a representative aliquot is taken for freeze-drying. After freeze-drying, the samples are homogenized by grinding to a powder prior to digestion.

For most elements in sediments, National Oceanic and Atmospheric Administration (NOAA) National Status and Trends Mussel Watch methodologies, which incorporate a closed Teflon® bomb acid digestion, are used (Lauenstein et al. 1993). These are sensitive (low detection limit), total digestion methods (i.e., MDLs for most elements in the 0.01 to 1.0 ppb dry weight range) developed for use in baseline monitoring programs. These methods are capable of accurately measuring trace element levels in uncontaminated, pristine areas. Mercury is determined according to U.S. Environmental Protection Agency (EPA) method 245.1 (U.S. EPA 1991), which involves a separate sulfuric/nitric acid and permanganate/persulfate digestion followed by cold vapor atomic absorption spectrophotometry (CVAAS).

For certain elements of special interest to this study (e.g., barium), specialized analytical techniques are needed. For example, sediment barium is the most important elemental tracer of drilling mud discharges and is a critical parameter for interpreting the chemical gradients observed in the vicinity of drilling locations. To maximize data quality, sediment barium concentrations are determined by instrumental neutron activation analysis (INAA). INAA is the analytical method of choice for sediment barium determination because barium is difficult to dissolve by normal acid digestion procedures. INAA is a nuclear technique that is free of chemical interferences, and has an essentially unlimited linear dynamic range. INAA determinations are made using the method of Boothe and James (1985), which is optimized for marine sediments. Other elements (chromium, iron) are determined simultaneously by this multi-element technique.

Trace element analyses are conducted under a comprehensive QA project plan designed to consistently produce high quality, verifiable data. All sample processing and analysis procedures are performed to minimize contamination and maximize data quality (accuracy and precision). All procedures are conducted by properly trained personnel according to approved laboratory standard operating procedures (SOPs). Good laboratory practices (e.g., daily refrigerator/freezer temperature checks, balance calibrations, etc.) are consistently followed.

Table 6.1. Trace element analytical methodologies.

Element	Grab Samples	Sediment Trap Samples
Barium (Ba)	INAA	INAA
Cadmium (Cd)	GFAAS	--
Chromium (Cr)	INAA	INAA
Iron (Fe)	INAA	INAA
Lead (Pb)	FAAS	--
Zinc (Zn)	FAAS	--
Mercury (Hg)	CVAAS	---

Abbreviations: FAAS = flame atomic absorption spectrophotometry; GFAAS = graphite furnace or flameless AAS; INAA = instrumental neutron activation analysis; and CVAAS = cold vapor AAS.

All sample handling is done using new or acid-cleaned, metal-free containers and implements. Cleaning procedures and sample processing are performed in a clean room to avoid sample contamination. Also, all containers are kept closed or covered except when material is being added or removed. Distilled-deionized high purity water is used to prepare all detergent and acid cleaning solutions and for all rinses during cleaning procedures. Double-distilled, ultra-pure water is used for all dilutions and to prepare all sample digestion/processing reagents. Ultra-pure reagents are used whenever necessary to ensure that the procedural blank for a given analytical procedure is below the MDL for that procedure.

A detailed log is prepared for each digestion, specifying all aspects of the procedure (e.g., SOP to be used, matrix spike levels, QA samples, etc.). As the digestion is performed, all information is recorded in a bound, pre-printed logbook for the specific digestion procedure being used. A full suite of laboratory QA samples is analyzed with each set of 30 to 45 samples digested. These include certified reference materials, laboratory control samples (blank spikes, matrix spikes, laboratory duplicates ±5%), and procedural blanks.

All standards are traceable to National Institute of Standards and Technology standards and are replaced when expiration dates are exceeded. The preparation of all standard solutions (including lot numbers, measuring devices, and amounts used, etc.) are recorded in a single log book and all solutions are clearly labeled and traceable to a logbook entry.

During each analytical procedure, the instrument is calibrated at the beginning of the analysis and the calibration is checked (or re-calibrated) frequently during the analysis.

Full re-calibrations are performed as necessary if the calibration changed more than 5% between any two checks. All data entered are verified independently by a second person.

Each analytical batch is evaluated based on the results of the QA samples and stringent QA acceptance criteria consistent with those recommended by the EPA (U.S. EPA 1989). The acceptance criterion for percent recovery (i.e., QA parameter for CRM, matrix spikes, blank spikes) is 80% to 120%. The acceptance criterion for relative percent difference for duplicates at 10 times the MDL is ±20%. The acceptance criterion for procedural blanks is less than twice the MDL. Finally, 95% of all QA analyses performed for each batch of samples must meet the acceptance criteria. When one or more QA parameters fall outside the acceptance criteria for a given digestion set and element, the samples are re-analyzed. If re-analysis does not bring the QA parameter(s) within acceptable ranges, the samples are re-digested and re-analyzed.

Results and Discussion

To survey the monitoring sites for the presence of contaminants, 10 grab samples were collected at each site during the first monitoring cruise (1C). Each grab sample was analyzed for EOM, TOC and TIC content, gas chromatographically resolvable and unresolvable (UCM) hydrocarbons, and selected trace metals (Ba, Cd, Cr, Fe, Hg, Pb, and Zn). A composite of the grab sample at each site was also analyzed for total PAHs. The measures of hydrocarbons at the sites were low and relatively uniform. Little or no evidence of petroleum related hydrocarbons was observed at any of the nine study sites (Table 6.2). The slight increase in EOM and PAH towards the west most likely represents a general fining of sediments. Trace metals indicative of contamination were observed to be at or near background levels at all sites as well (Table 6.2). In particular, barium, a tracer of drill mud discharges, was observed to be at background levels with only a very few samples that might be interpreted as slightly elevated. The slight increase in a few metals (Ba, Cr, Fe, Zn) towards the west most likely represents a general fining of sediments. In conclusion, the sediments collected at the study sites exhibited little or no evidence of a significant history of contamination from drilling related or other activities and only a slight geographic trend in concentrations.

Heterogeneous distributions of organic and inorganic carbon in sediments were observed (Table 6.3, Figs. 6.1 to 6.4). The relationships between environmental conditions and sediment composition is unclear. Significant variability in sediment carbon content was apparent between cruises, most likely representing small scale heterogeneity in sediments at the sites.

Table 6.2. Summary of average sediment characteristics at the study sites during Cruise 1C.

Site	EOM (ppm)	TPH (ppm)	PAH (ppb)	UCM (ppm)	Total Resolved Hydrocarbons (ppm)
1	43.2	11.2	8.2	7.7	9.5
2	35.7	12.0	8.3	9.7	3.2
3	42.1	10.4	10.8	8.6	1.8
4	74.1	20.1	21.5	12.7	7.5
5	59.2	18.4	15.3	13.7	4.7
6	59.2	16.2	15.5	11.3	4.9
7	73.1	21.2	25.7	16.3	4.9
8	33.6	13.2	12.2	10.2	3.0
9	70.9	20.0	20.4	12.7	7.3

Site	Ba (ppm)	Cd (ppm)	Cr (ppm)	Fe (ppm)	Hg (ppm)	Pb (ppm)	Zn (ppm)
1	123.3	0.10	21.0	8858	0.02	7.8	26.2
2	120.1	0.05	21.0	7616	0.02	7.9	22.8
3	111.2	0.07	26.8	8665	0.02	6.7	24.7
4	357.1	0.12	40.0	18,729	0.03	15.0	60.4
5	499.5	0.08	33.8	17,316	0.03	12.3	50.6
6	471.6	0.08	32.0	17,578	0.03	12.5	60.0
7	497.3	0.07	38.0	18,344	0.03	15.3	58.4
8	240.0	0.05	23.5	10,397	0.02	10.6	30.1
9	465.9	0.07	40.6	19,565	0.03	15.3	60.8

Abbreviations: EOM = extractable organic matter; TPH = total petroleum hydrocarbons; PAH = polycyclic aromatic hydrocarbons; UCM = unresolved complex mixture.

Table 6.3. Summary of the average carbon content of sediments at the study sites during Cruises 1C and M2.

Site	Total Organic Carbon (%)		Total Inorganic Carbon (%)	
	Cruise 1C (n=10)	Cruise M2 (n=5)	Cruise 1C (n=10)	Cruise M2 (n=5)
1	3.4	1.2	3.3	7.1
2	3.7	1.1	2.8	5.3
3	2.6	0.8	3.7	5.1
4	3.5	1.2	9.1	7.9
5	3.6	1.7	4.1	4.4
6	3.1	1.3	3.5	3.5
7	3.1	2.0	1.9	3.6
8	0.6	1.0	2.9	3.3
9	3.1	1.5	4.8	4.8

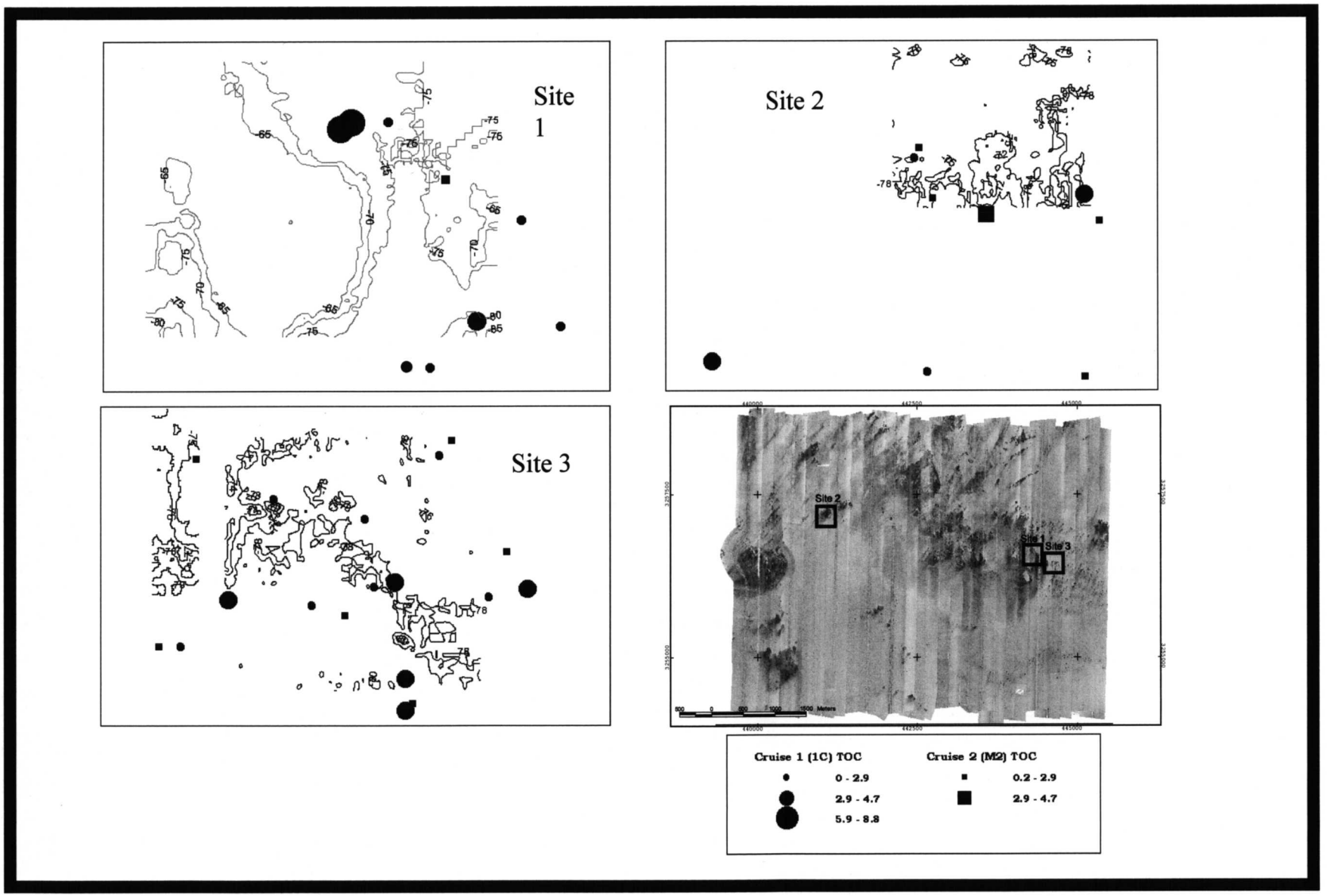

Fig. 6.1. Total organic carbon (%) concentrations at Sites 1, 2, and 3.

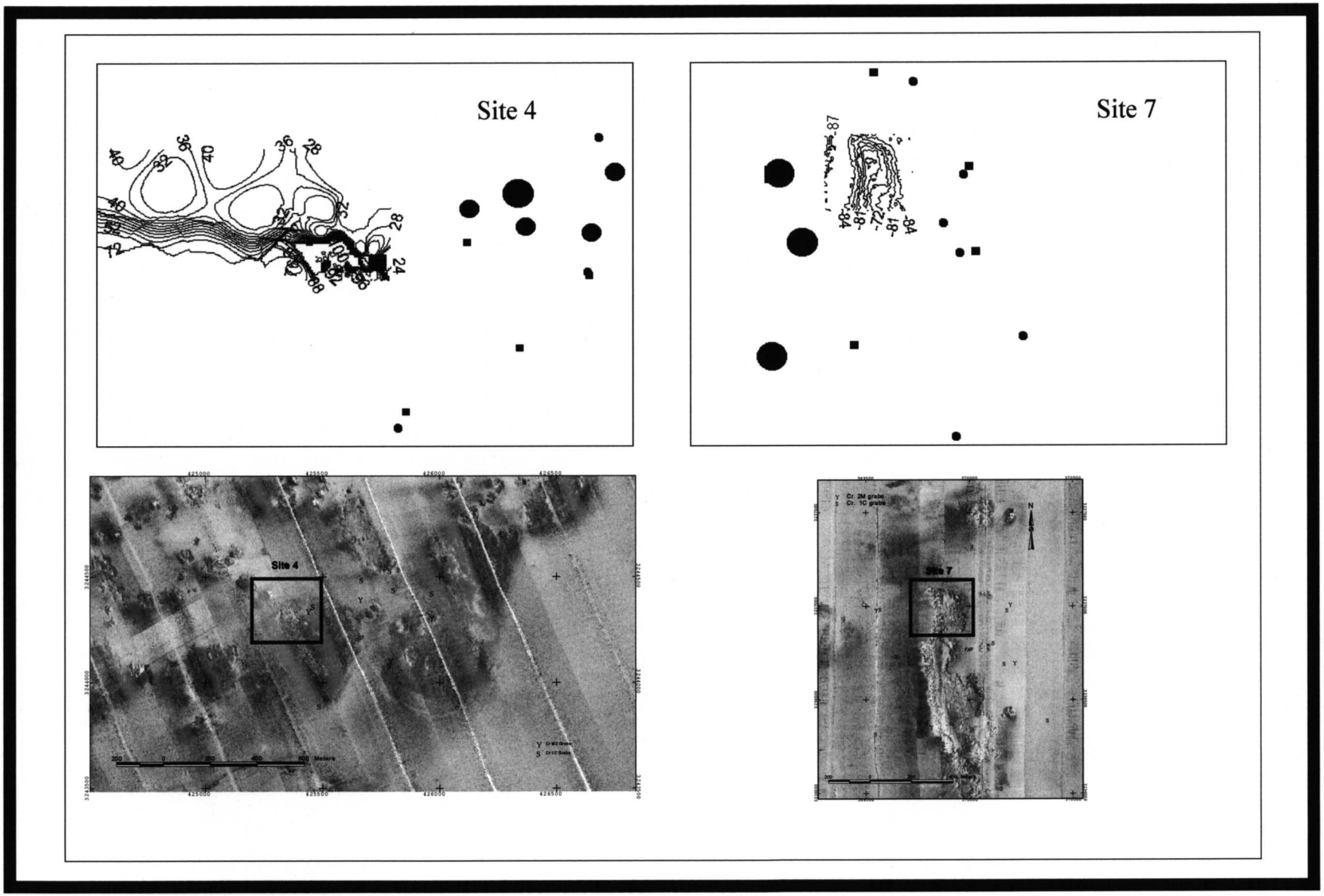

Fig. 6.2. Total organic carbon (%) concentrations at Sites 4 and 7.

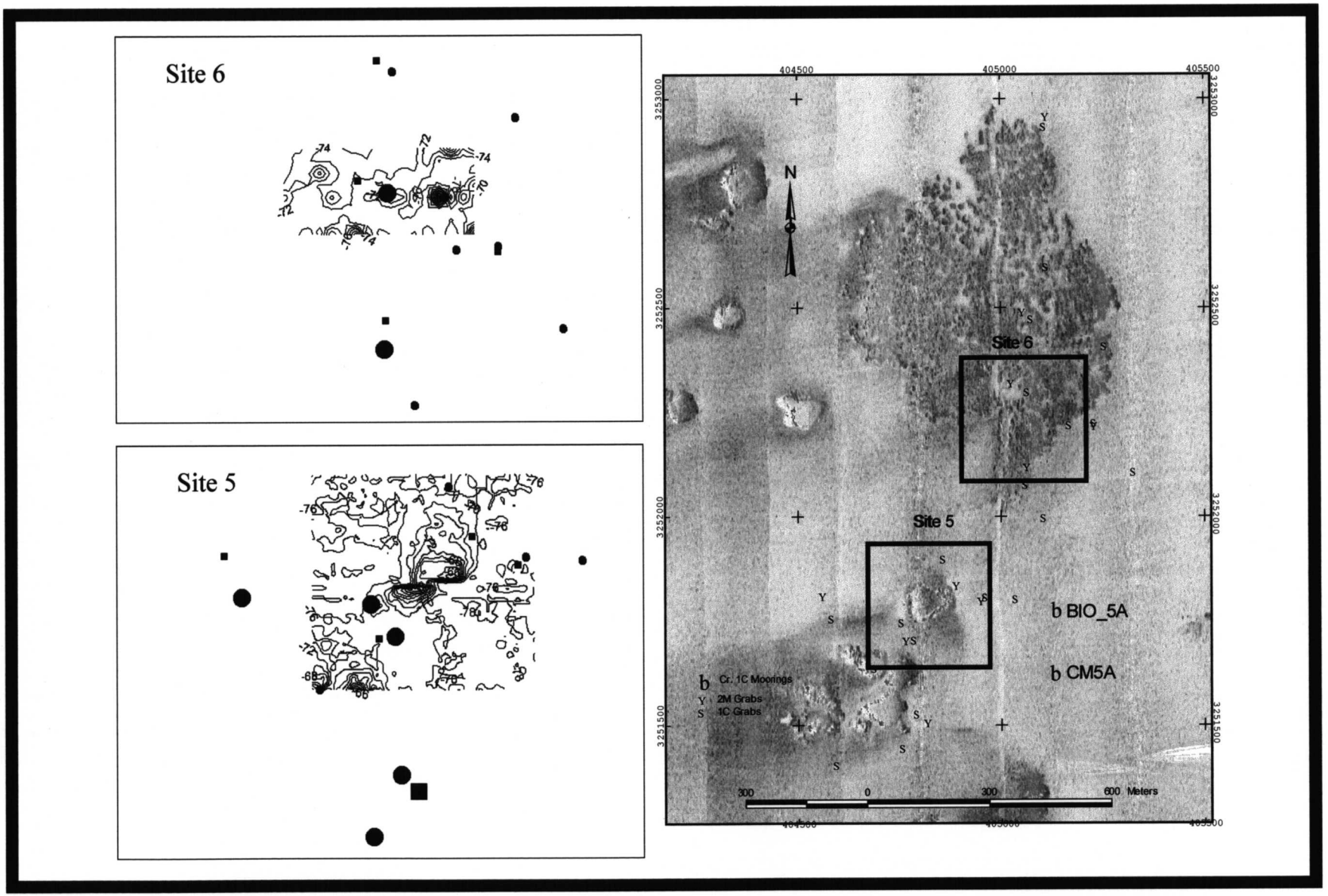

Fig. 6.3. Total organic carbon (%) concentrations at Sites 5 and 6.

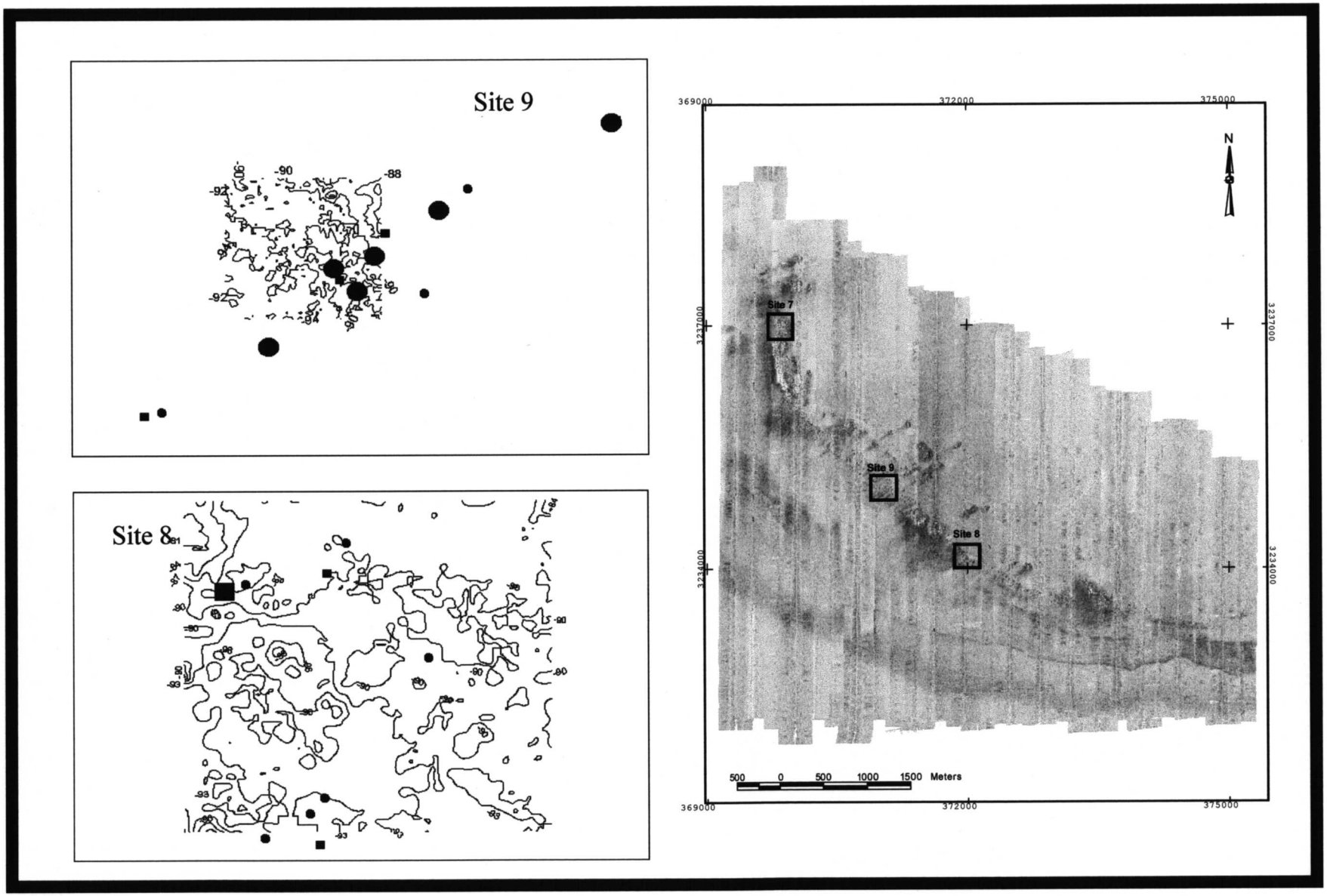

Fig. 6.4. Total organic carbon (%) concentrations at Sites 8 and 9.

Chapter 7
Physical Oceanography/Hydrography

Approach and Rationale

The purpose of this component of the program is to monitor environmental conditions (i.e., dissolved oxygen, turbidity, temperature, salinity, etc.) at the three types of topographic features along the Mississippi-Alabama OCS. Other work elements can then relate observed seasonal and inter-annual changes in community structure and zonation to changes in environmental conditions. The specific objectives that focus on the details of this relationship are as follows:

- to characterize the regional and local current dynamics in the study area, which lies on the outer portion (60 to 100 m water depth) of the Mississippi-Alabama continental shelf;

- to determine the dynamics of important environmental parameters, including temperature, salinity, dissolved oxygen and turbidity; and, most important,

- to define the relationship of the current dynamics and environmental conditions to the geological and biological process occurring at these hard bottom features.

To address the objectives, the oceanographic-processes effort consists of three elements: instrument moorings, hydrographic stations, and collateral data. Six 18-m high, bottom-mounted, instrument moorings are deployed at selected hard bottom sites to continuously measure current velocity, temperature, conductivity/salinity, dissolved oxygen, and turbidity. The moorings also have sediment traps to collect suspended samples of settling suspended particulate matter. Discrete vertical profiles of CTD/DO/transmissivity/light are collected by the same instrument package used during the LATEX study. Collateral data, such as satellite advanced very high resolution radiometer (AVHRR) images, satellite altimetry, river discharge, coastal wind and sea level data, and buoy observations of wind, waves, barometric pressure, air and sea temperature, will be used during the synthesis study to describe the primary physical forcing mechanisms. In this report we focus on data collected by the moored instruments during the first three deployment periods and the CTD data collected on the four cruises that deployed and recovered the moorings.

Instrument Moorings

Moored instruments provide information about the temporal scales of physical processes that affect the biota associated with the bottom features in the study area. The variables of greatest interest are currents, suspended sediments, water temperature, dissolved oxygen, and salinity. The semi-annual monitoring cruises observe the cumulative results of the interactions on various time scales among the physical and chemical variables and the biological communities of the hard bottom features. Time-series data provide

information about the time scales and also capture the details of events, such as the passage of a hurricane or an intrusion associated with the Loop Current.

The hard bottom features addressed here include pinnacles that extend up to 15 m above the bottom. Water depth in the region ranges from 70 to 120 m. Six moorings are deployed in the study area to measure currents, conductivity/salinity, temperature, dissolved oxygen, turbidity, and sediment flux. The mooring design is illustrated in Fig. 7.1. The dissolved oxygen and turbidity sensors are located as close to the bottom as possible. Time-series measurements of dissolved oxygen and turbidity are difficult to obtain because even minor fouling degrades data quality. However, these are important ecological parameters, and the new technologies used by the instruments are providing time series of up to 3 months duration. Sediment traps are attached at three heights above the bottom. Current, temperature, and conductivity/salinity are recorded about 2.5 m above the bottom and at 16 m above the bottom.

One mooring is placed at each of four of the nine study sites. Three of the sites (Sites 1, 4, and 5) are medium and high relief features located near the 100 m isobath. The fourth (Site 9) is a low relief site in shallower water near the 60 m isobath. (See Chapter 4 for maps of the pinnacle sites.) These four mooring locations are permanent, i.e., they will be maintained throughout the program to provide continuous long-term, time-series data at each of the four sites. The three deeper sites will provide significant along-isobath coverage of the outer shelf, which in turn will provide data about the cross-isobath exchange of water-mass properties between the outer shelf and the slope/open ocean. The shallower site when paired with a deeper site will yield some information about cross-isobath correlations.

The fifth and sixth moorings are re-locatable. During the first year, they were placed at the eastern-most high relief site (Site 1) to form, in conjunction with the permanent mooring, a triangular pattern. The two re-locatable moorings were moved to Site 5 in May 1998 (Cruise M3).

Hydrography

Physical factors that affect the biota in the region include currents, temperature, salinity, dissolved oxygen, turbidity, and light levels. Moored instruments produce time series of all of these variables except light levels, but only at two depths for current, temperature, and salinity and one depth for dissolved oxygen and turbidity and only at a few discrete locations. Vertical profiles of these variables taken during the monitoring and servicing cruises provide valuable information on the vertical distribution of these properties. Previous studies (Kelly 1991) indicate that water masses in the study area can undergo changes both at the surface and at depth. CTD profiles indicate the presence of near bottom nepheloid layers that vary quite markedly over the area.

Vertical variations are induced by Loop Current intrusions, seasonal heating and cooling, wind forcing, fresh water input from the local rivers, and the passage of storms. To assess the effect of these variations at each study site, multiple vertical profiles of conductivity, temperature, photosynthetically active radiation (PAR), transmissivity,

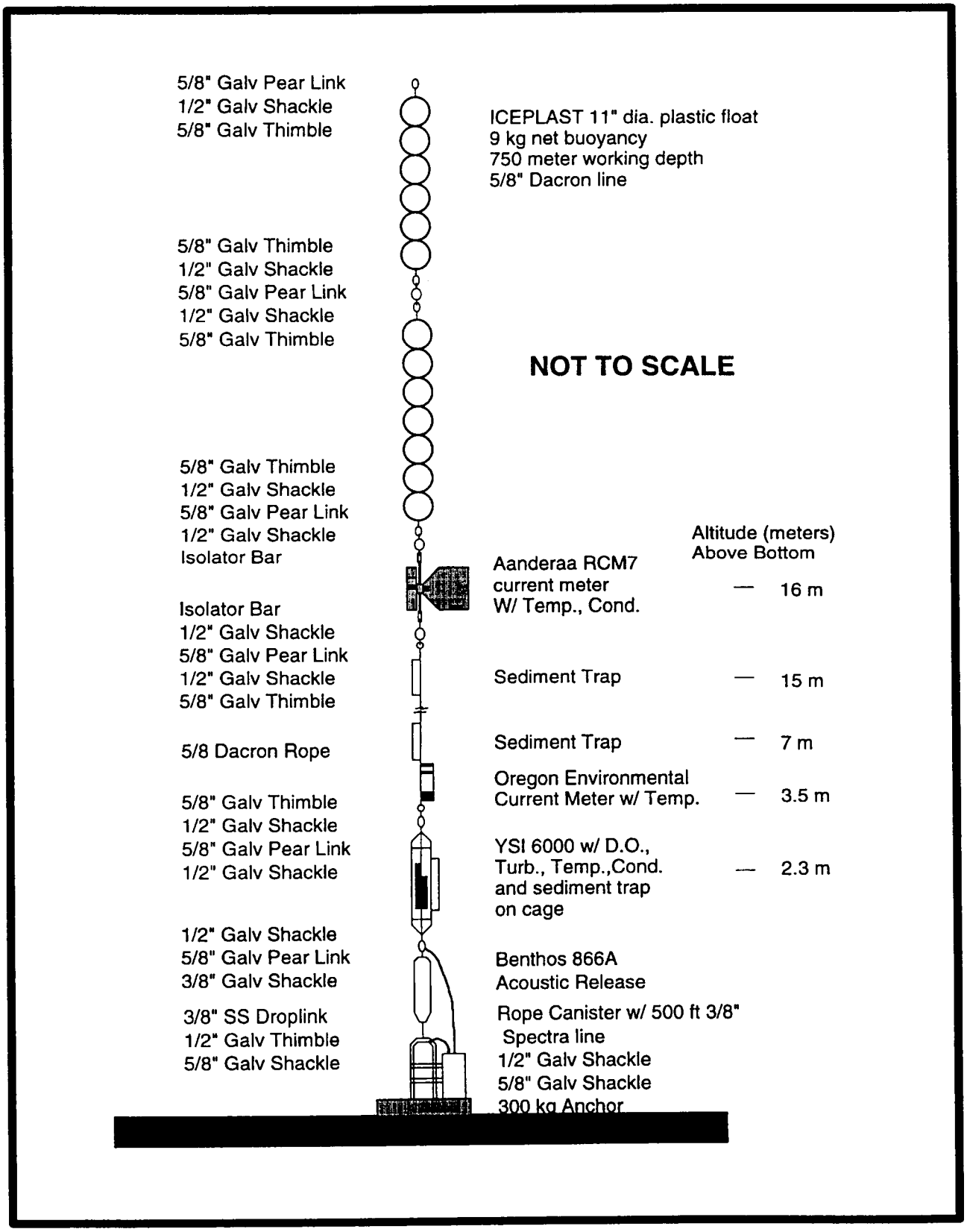

Fig. 7.1. Schematic drawing of the instrument mooring.

backscattered light, and oxygen concentrations are collected. Vertical profiles are made at three locations around each site to determine if changes in water properties are induced by flow past the topographic features. Water samples are collected for determination of total suspended matter and for calibration of the oxygen sensor. Salinity samples are used as a check on the depth at which the bottle actually closed. Sampling depths focus on the depth from feature height to the regional bottom depth, with fewer samples in the overlying water. From these measurements, we hope to infer the depth of the nepheloid layer and characterize the water masses enveloping the features. The basic measurements of temperature, salinity, light levels, oxygen, and suspended sediment loads are available for use as environmental variables in statistical models applied to the biological assemblages. These data will also be useful for calibration and quality control of the time series measurements made at the moorings.

Methods

Four cruises have been conducted to collect CTD profiles and to deploy and service the moorings over three deployment periods. Cruise dates, type of CTD and number of casts by cruise are summarized in Table 7.1. CTD casts were made at all nine sites during monitoring cruises, but only at the four sites with moorings during service cruises. Chapter 3 provides the details of the operations and logistics for each cruise. The locations, dates, and times of deployment of the instrument moorings are provided in Table 7.2.

Table 7.1. Ecosystems monitoring: Mississippi/Alabama shelf cruises.

Name	Seq.	Start	End	CTD Casts	Instrument type
1C	c1	5/21/97	5/24/97	29	SBE-911
S1	c2	7/28/97	7/29/97	11	SBE 19 SEACAT
M2	c3	9/30/97	10/31/97	26	SBE-911
S2	c4	1/29/97	1/30/97	11	SBE-911

The 20 to 24 May 1997 leg of Cruise 1C deployed six instrument moorings and conducted 29 casts with the CTD system. The first mooring service cruise, conducted on 28 to 29 July, rotated five moorings and collected 11 CTD casts using a SBE-19 SEACAT. During this cruise, the acoustic release on the instrument mooring at Site 4 would not respond, and so the service of this mooring was postponed until the next cruise, when an ROV would be available to cut the rope drop-link. Cruise M2 was conducted in several legs during 30 September through 31 October 1997 because of poor weather. The moorings at Sites 1 and 5 were rotated during the 30 September to 6 October leg. The remaining moorings, including the one at Site 4, were rotated during the 28 to 31 October leg. A total of 29 CTD casts were collected with the LATEX CTD

Table 7.2. Locations, dates, and times of deployment of the instrument package.

ID	Depth	Data In	Time (UTC)	Date Out	Time (UTC)	Easting	Northing	Lat Degree	Lat Min	Lat Sec	Lon Degree	Lon Min	Lon Sec
CM 1A1	78	05/23/97	0339	07/28/97	1231	444520.7	3256839.9	29	26	28.75	87	34	19.32
CM 1A2	79	07/28/97	1433	10/03/97	0230	444555.0	3256881.2	29	26	30.09	87	34	18.05
CM 1A3	80	10/04/97	0826	01/29/98	1656	444532.0	3256877.9	29	26	29.98	87	34	18.91
CM 1B1	83	05/23/97	0457	07/28/97	1509	444544.5	3256163.9	29	26	6.79	87	34	18.31
CM 1B2	81	07/28/97	1637	10/03/97	0140	444608.6	3256226.7	29	26	8.84	87	34	15.95
CM 1B3	83	10/04/97	0717	01/29/98	2104	444581.1	3256249.9	29	26	9.59	87	34	16.97
CM 1C1	82	05/23/97	0109	07/28/97	1739	443761.2	3256406.8	29	26	14.56	87	34	47.43
CM 1C2	81	07/28/97	1913	10/03/97	0333	443793.8	3256445.8	29	26	15.83	87	34	46.23
CM 1C3	83	10/03/97	1206	01/30/98	0027	443792.9	3256456.9	29	26	16.18	87	34	46.26
CM 4A1	115	05/21/97	2121	10/29/97	1730	426583.3	3244597.2	29	19	47.66	87	45	22.15
CM 4A2	112	10/30/97	0643	01/30/98	0540	426551.2	3244767.9	29	19	53.20	87	45	23.38
CM 5A1	82	05/23/97	1303	07/29/87	0206	405132.8	3251628.7	29	23	30.94	87	58	39.59
CM 5A2	82	07/29/97	0340	10/06/97	0426	405132.8	3251592.8	29	23	29.77	87	58	39.58
CM 5A3	82	10/06/97	0717	01/30/98	1221	405119.8	3251578.2	29	23	29.29	87	58	40.06
CM 9A1	93	05/23/97	2030	07/29/97	0718	371417.2	3235151.9	29	14	24.89	88	19	23.29
CM 9A2	94	07/29/97	0900	10/31/97	0600	371400.2	3235151.4	29	14	24.78	88	18	23.92
CM 9A3	94	10/31/98	0858	01/30/98	1818	371134.1	3235538.5	29	14	37.35	88	19	33.94

Abbreviations: UTC = Coordinated Universal Time.

System during the two legs. The next service cruise was conducted during 29 to 30 January 1998. All moorings were successfully rotated and 12 CTD casts were made using the LATEX CTD System. This CTD system was used instead of the SBE-19 SEACAT so that water samples for filtration together with profiles of transmissivity and turbidity could be obtained (Chapter 5).

Equipment

Moorings

Six multi-parameter physical oceanography moorings were deployed. Their principal components are shown in Fig. 7.1.

A mooring is constructed using 5/8" Dacron rope. The linkage between the acoustic release and the anchor is rope rather than chain so that it can be cut by an ROV should the release fail. ICEPLAST Model 1102 plastic floats provide flotation. Each float has 9 kg of net buoyancy and a maximum working depth of 750 m. Static mooring analysis was computed for the mooring using the program BUOY2.41 developed by Specialty Devices Inc. The amount of flotation has been selected to assure that mooring "blow-over" is less than 1.0 m for current profiles up to 40 cm/s. The rope canister contains 152 m of 3/8" Spectra line, a length that will permit the mooring to rise to the surface and be recovered before pulling up the anchor.

Acoustic Releases

Benthos Model 866A Continental Shelf Releases are used on the current moorings. Billings Industries, Inc. Model ATR-397 acoustic releases are used on the bio-moorings.

Current Meters

The bottom current meter on each mooring is an Oregon Environmental, Inc. (OEI) Model 9407 with temperature sensor. The top current meter on each mooring is an Aanderaa Model RCM7 with conductivity and temperature sensors. Both types vector average currents, record into battery-backed solid-state memory, and download directly to PC-type computers. Each instrument is serviced according to the manufacturers' instructions before and after deployment.

Dissolved Oxygen and Turbidity Recorders

A YSI Model 6000 recording system with oxygen, turbidity, temperature, and conductivity sensors lies immediately below the OEI current meter. This unit records internally. It includes an external battery pack to extend battery life up to 4 months. The oxygen system uses rapid pulse technology. This measures oxygen current in small pulses only when the measurement is actually being made, which not only limits power drain but also reduces the effect of fouling on the measurement. The turbidity sensor is of the backscatter type. It contains a small wiper that cleans the optical window before each sample. The rapid-pulse technology and the wiper have proven to significantly

extend the period of good data collected by these types of sensors before biofouling finally takes hold.

To further reduce biofouling, the standard sensor-guard of the YSI 6000 (conceptually, a cup with holes in it) have been replaced with a "poison sensor-guard" custom manufactured by Oceanographic Industries of Miami Beach, FL. The inside of the guard is covered with a poisoned gel. The poison slowly diffuses from the gel into the small interior region surrounding the sensors. Freshly coated guards are installed during each service cruise. Used guards are returned to the manufacturer for re-coating.

The dissolved oxygen sensor is calibrated to 100% saturation, following the manufacturer's instructions, just prior to deployment. In addition, water samples are collected at the depth of the sensor for analysis by the modified Winkler titration method on most cruises. The turbidity sensor is calibrated using distilled water and a solution of standard turbidity provided by the manufacturer. The standard is a 100 nephelometric turbidity unit (NTU) ± 2% solution made with Styreen/DVB Copolymer. The turbidity sensor is quite linear between 0 and 100 NTU, but the turbidity in the study region is low, usually less than 10 NTU. Therefore, a second calibration point obtained using a 10 NTU substandard is created by precision dilution.

CTD/DO/Transmissivity/Light-Profiling Instruments

The primary system for continuous measurements is a Sea-Bird Electronics, Inc. SBE-911 CTD system used with a SBE-11 deck unit. This is essentially the same system used during the MMS LATEX A program. The Sea-Bird SBE-911 CTD is a research grade CTD system which offers high quality profiles of oceanic temperature, salinity, and density to all ocean depths. The SBE-911 uses ultra-stable time-response matched sensors and fast, high-resolution parallel sampling for data acquisition.

In addition to providing precise measurements of temperature and salinity with depth, the Sea-Bird CTD is also used as a general-purpose data acquisition and telemetry system. Dissolved oxygen is measured with a "Beckman" polarographic type *in situ* dissolved oxygen sensor connected to the Sea-Bird Electronics SBE-911 CTD. Downwelling irradiance is measured with a Biospherical Instruments, Inc. Model QSP-200L irradiance profiling sensor. Particle scattering is measured with a Sea Tech light scattering sensor. In addition to the light scattering sensor, the CTD is equipped with a SeaTech, Inc. 25-cm transmissometer.

Water Samples

Samples for discrete measurements of dissolved oxygen and salinity are drawn from the 10-liter PVC Niskin bottles mounted on the General Oceanics Rosette sampler, which is part of the CTD profiling system.

Samples for dissolved oxygen analysis are collected in 125-mL, calibrated glass-stoppered bottles. Samples are collected from all stations. At least 10% of the oxygen analyses are duplicated to establish sampling and analytical precision, and assure

data reliability. Samples are collected and analyzed for dissolved oxygen by the microwinkler technique (Carpenter 1965). This method has been the world standard for major oceanographic programs for decades. The microwinkler method has a precision of 0.01 mg/L oxygen at STP. Most analyses were performed aboard ship. Some of the samples from the last few stations plus duplicates from samples analyzed aboard ship were analyzed in the laboratory after the cruise.

Samples for salinity analysis are collected in 350-mL citrate bottles that have been triple rinsed with sample water before collection. These bottles are air tight. A salinity sample is collected from every Niskin bottle that is tripped. Samples are taken for salinity analysis from at least half of the stations during a given cruise and returned to the laboratory for analyses.

Results

Time-Series Data

Each mooring nominally has three different instruments recording time series data. The upper one, at 16 meters above bottom (mab), is always an Aanderaa RCM7 current meter with temperature and conductivity sensors (one vector and two scalar series). The current meter at 4 mab is usually an OEI 9407 current meter with a temperature sensor (one vector and one scalar series). Just below it is a YSI 6000 Monitor with temperature, conductivity, dissolved oxygen, and turbidity sensors (four scalar series). For record keeping and graphical display purposes, a naming convention is used that identifies instrument type, site, position at site, deployment period, and for current meters, the height above bottom, e.g., C1B2 16 mab. The coding is as follows:

Instrument type:	C = current meter, O = oxygen/turbidity system
Site:	1, 4, 5, or 9
Position at site:	A, B, or C; generally, A is NNE of pinnacle, B is SSE, C is W
Deployment:	1, 2, or 3
Height:	16 mab, or 4 mab (for instrument type C)

Each instrument's time series data are plotted and reported as a group by deployment. It would be premature at this time to join the time series of sequential deployments and then estimate a seasonal division of the records. Three types of graphical displays illustrate the results. A summary page (e.g., Fig. 7.2) for a current velocity record displays basic statistics, a scatter plot, and a table of joint frequency for speed and direction, which is the tabular version of a current rose. The start and stop times at the top of the summary page include all times for which the instrument's sensors produced good records. The number of points refers specifically to the velocity record, which may be shorter. Current velocity data are then plotted in time series format, together with scalar data collected at the same time by the current meter (e.g., Fig. 7.3). The scale is one month per page to resolve visually the tidal and inertial fluctuations in speed and direction. The four parameters measured by the YSI 6000 are also plotted as a time series group, but at a

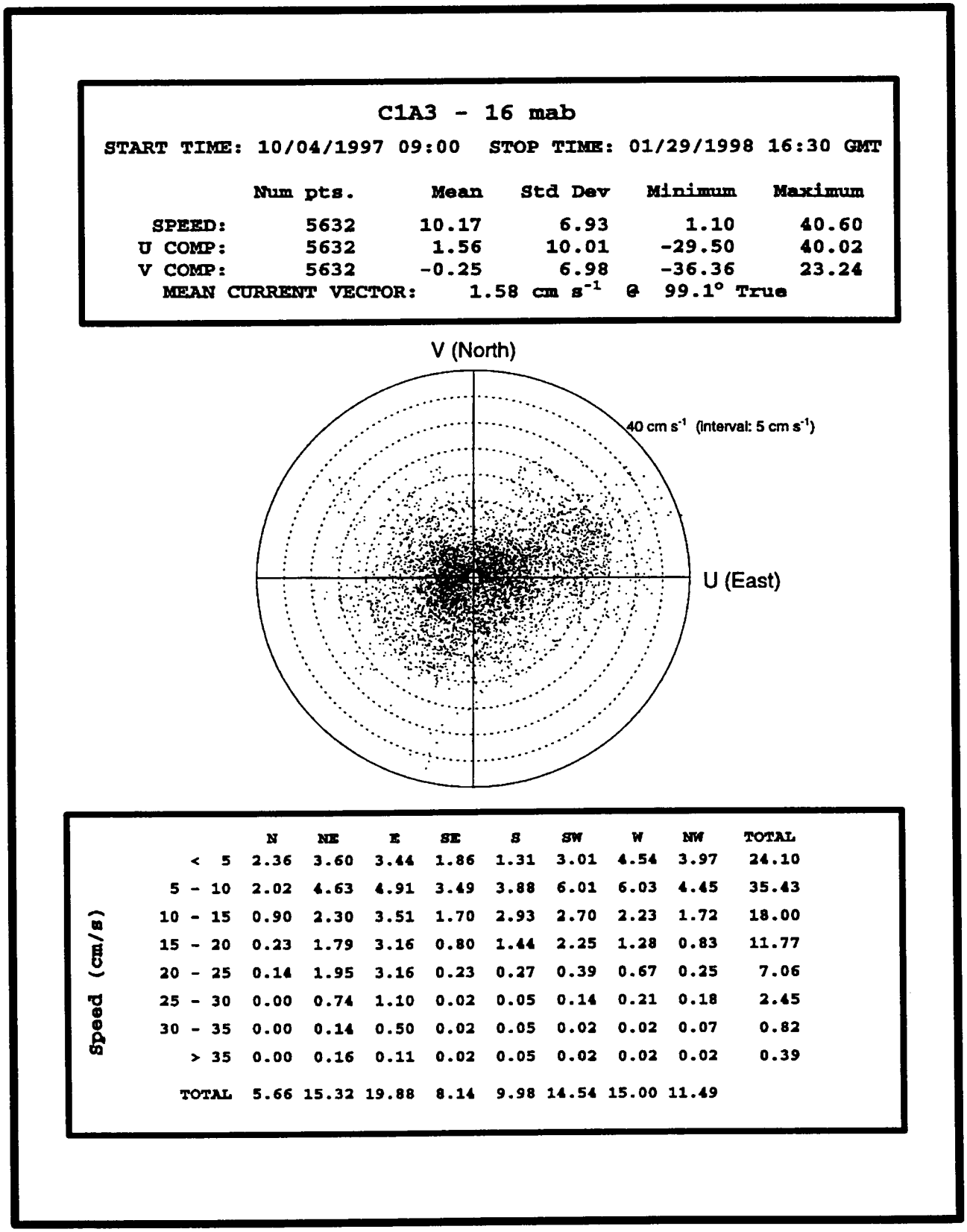

Fig. 7.2. Example of a Summary Page (C1A3) for a current velocity time series.

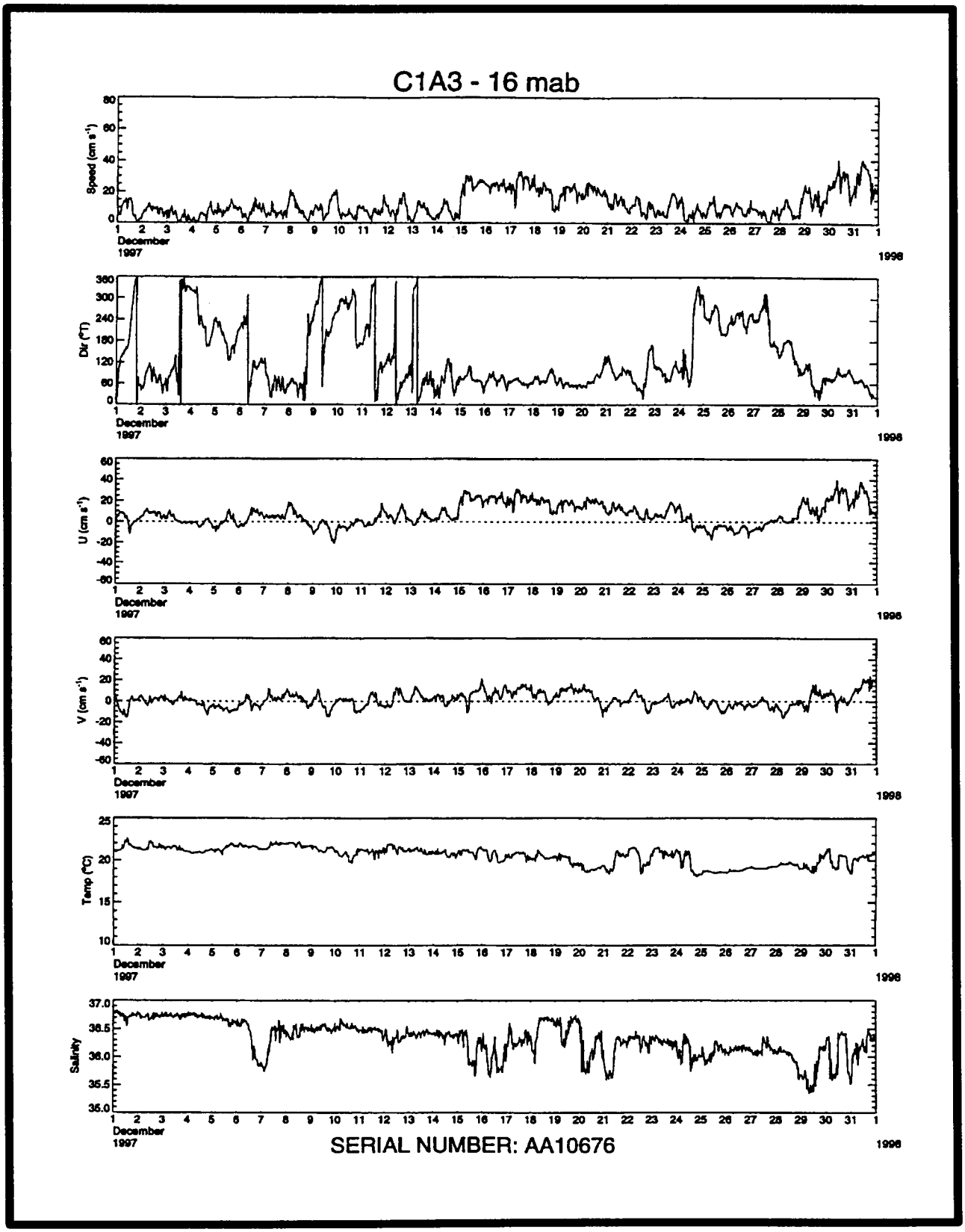

Fig. 7.3. Example of a monthly time-series plot (C1A3) for data recorded by a current meter.

scale of one deployment period per page. With this format, the variability in dissolved oxygen and turbidity during the deployment can be seen (e.g., Fig. 7.4).

This work element of the report uses only selected examples of the graphical records to illustrate the principal features in the time-series records. A complete set of the data is maintained on an Internet Website in both graphical postscript and ASCII tabular formats. The Website address is http://www.gerg.tamu.edu/mames. The site will be maintained for the duration of the project. Upon completion of the project, it is planned to publish a CD-ROM containing all project data.

The time-series data return, sorted by deployment period and instrument location is summarized in Table 7.3. Note that the period of a time-series record is usually shorter than the total period of deployment (Table 7.1) because of instrument equilibration at the beginning or other editing. The data gap between recovery and redeployment of instruments is usually a few hours, but can be several days in duration because of the logistical demands of the multidisciplinary monitoring cruises. Data gaps in the total potential record length of an instrument location are also caused by fouling, individual sensor failure, and total instrument failure. Fouling mainly affects speed and/or direction sensors, causing drag or complete lock-up of the mechanical sensors. Each instrument is carefully inspected upon recovery and notes about the degree and effects of fouling are noted on the mooring log sheet. Several velocity records have been manually truncated after initial processing, based on these recovery notes and a subjective inspection of the time series plot. Some of the OEI 9407 and YSI 6000 meters have suffered total instrument failure. In the case of the OEI 9407, a firmware bug caused no data to be recorded if the instrument was initialized with certain parameter settings. The problem has been resolved. The YSI 6000 has had some problems with waterproof connectors and fittings. Saltwater leakage has caused some individual sensors to fail or the main logger to loose all data. The manufacturer has repaired these units under warranty.

Vertical Profiles

Seventy-seven CTD stations measurements were completed during four cruises at the end of this reporting period (Table 7.1). The data have been processed using the Seabird standard software. Plots of temperature, salinity, and sigma-theta have been prepared for all casts and are available on the Website. Composite plots of temperature and salinity for each cruise and two representative salinity-temperature profiles are shown in Figs. 7.5 to 7.10. Composite plots for each site for each cruise are available on the web site. A discussion of the optical properties measured by the CTD on the first, third, and fourth cruises is found in Chapter 5.

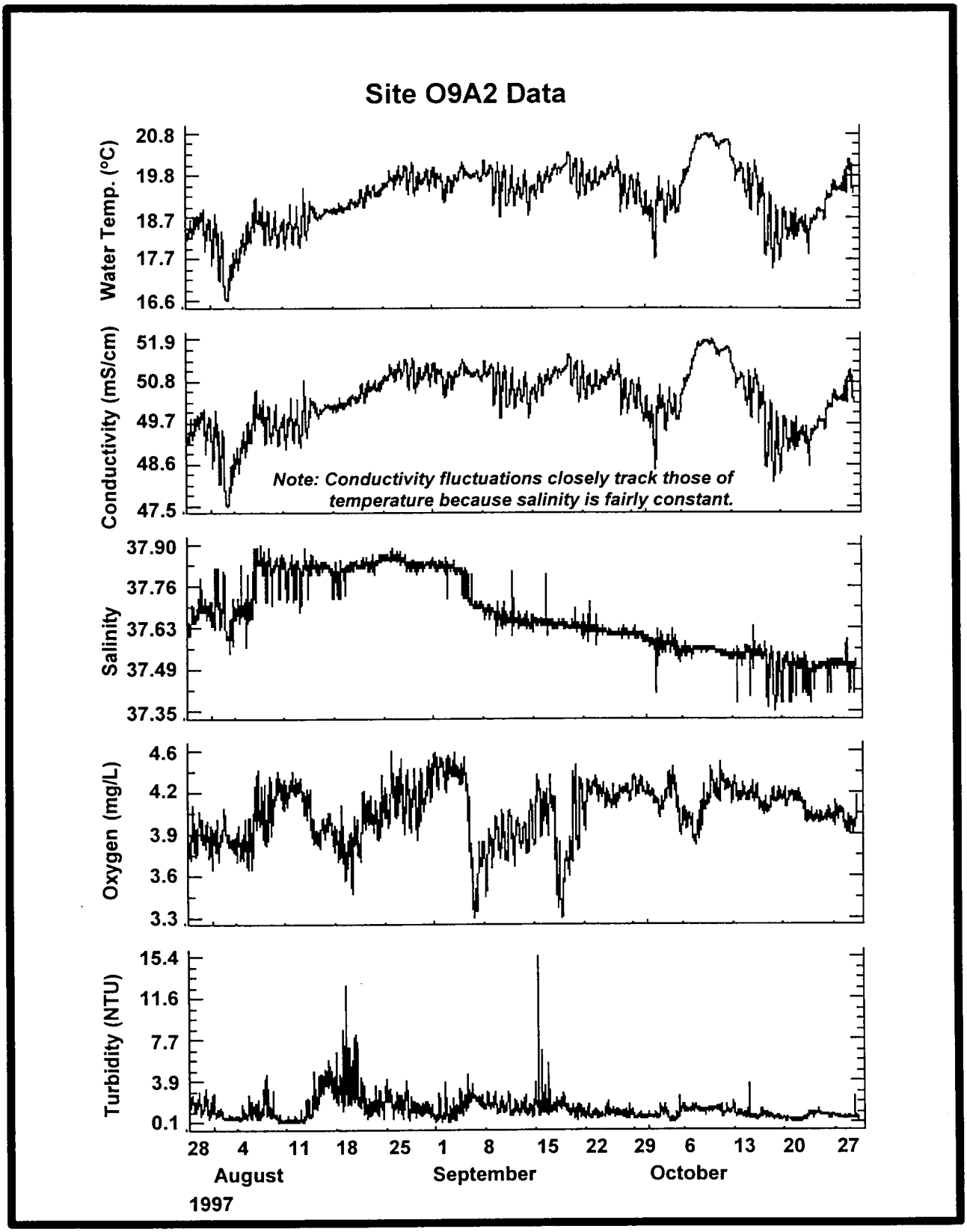

Fig. 7.4. Example of a plot of data (O9A2) collected by the YSI 6000.

Table 7.3. Summary of the time-series data return, sorted by deployment period and instrument locations.

ID	START	UTC	STOP	UTC	SENSORS	COMMENTS
C1A1 16 mab	05/23/97	4:30	07/28/97	12:00	V,T,C	
C1A2 16 mab	07/28/97	16:00	10/03/97	1:30	V,T,C	Data gap 8/4 - 9/3
C1A3 16 mab	10/04/97	9:00	01/29/98	16:30	V,T,C	
C1A1 4 mab	05/23/97	4:00	07/28/97	12:00	V,T	
C1A2 4 mab	07/28/97	15:00	10/03/97	2:00	V,T	
C1A3 4 mab	10/04/97	9:00	01/29/98	15:30	V,T	
O1A1	05/23/97	4:00	07/28/97	12:00	O2,Turb,T,C	
O1A2	07/28/97	15:00	10/03/97	2:00	O2,Turb,T,C	Oxygen bad; turbidity ends 9/13/97
O1A3	na	na	na	na	na	Connector leaked - no data
C1B1 16 mab	05/23/97	4:00	07/28/97	13:00	V,T,C	
C1B2 16 mab	07/28/97	17:30	10/03/97	0:30	V,T,C	No cond. data
C1B3 16 mab	10/04/97	8:00	01/29/98	20:30	V,T,C	
C1B1 4 mab	05/23/97	5:30	07/28/97	15:00	V,T	
C1B2 4 mab	07/28/97	17:00	10/03/97	0:00	V,T	Velocity ends 9/18/97 due to fouling
C1B3 4 mab	10/04/97	8:00	01/29/98	20:00	V,T	Velocity ends 1/17/98 due to fouling
O1B1	05/23/97	5:30	07/28/97	15:00	O2,Turb,T,C	Turbidity data bad after 7/16/97
O1B2	07/28/97	17:00	10/03/97	0:00	O2,Turb,T,C	Turbidity bad
O1B3	10/04/97	8:00	01/29/98	20:30	O2,Turb,T,C	Turbidity bad
C1C1 16 mab	05/23/97	7:00	07/28/97	17:30	V,T,C	
C1C2 16 mab	07/28/97	19:30	10/03/97	3:00	V,T,C	
C1C3 16 mab	10/03/97	12:30	01/30/98	0:00	V,T,C	
C1C1 4 mab	na	na	na	na	na	No data recorded by OEI 9407
C1C2 4 mab	na	na	na	na	na	No data recorded by OEI 9407
C1C3 4 mab	10/03/97	12:30	01/30/98	0:00	V,T,C	RCM7 instead of 9407; velocity ends 10/29/97 - fouling

Table 7.3. (Cont.)

ID	START	UTC	STOP	UTC	SENSORS	COMMENTS
O1C1	05/23/97	7:00	07/28/97	17:00	O2,Turb,T,C	
O1C2	07/28/97	17:00	10/03/97	3:00	O2,Turb,T,C	
O1C3	10/03/97	12:00	01/30/98	0:00	O2,Turb,T,C	Oxygen questionable
C4A1 16 mab	05/22/97	3:00	08/04/97	12:30	V,T,C	Recording stopped by low battery; cond. sensor failed
C4A2 16 mab	na	na	na	Na	na	Mooring not rotated during July 97 cruise
C4A3 16 mab	10/30/97	7:00	01/30/98	5:00	V,T,C	
C4A1 4 mab	na	na	na	na	na	No data recorded by OEI 9407
C4A2 4 mab	na	na	na	na	na	Mooring not rotated during July 97 cruise
C4A3 4 mab	10/30/97	7:00	01/30/98	5:00	V,T	
O4A1	05/22/97	3:00	09/19/97	12:00	O2,Turb,T,C	Turbidity bad beginning 8/1/97
O4A2	na	na	na	na	na	Mooring not rotated during July 97 cruise
O4A3	na	na	na	na	na	Connector leaked - no data
C5A1 16 mab	05/23/97	18:30	07/29/97	2:00	V,T,C	
C5A2 16 mab	07/29/97	4:30	10/06/97	4:00	V,T,C	
C5A3 16 mab	10/06/97	7:00	01/30/98	11:00	V,T,C	
C5A1 4 mab	05/23/97	18:00	07/29/97	1:30	V,T	
C5A2 4 mab	07/29/97	4:00	10/06/97	4:00	V,T	
C5A3 4 mab	10/06/97	7:30	01/30/98	11:00	V,T	Velocity ends 12/1/97 due to fouling
O5A1	05/23/97	18:00	07/29/97	1:30	O2,Turb,T,C	
O5A2	07/29/97	4:00	10/06/97	4:00	O2,Turb,T,C	Turbidity bad
O5A3	10/06/97	7:30	01/30/98	11:00	O2,Turb,T,C	
C9A1 16 mab	05/24/97	2:00	07/29/97	7:00	V,T,C	
C9A2 16 mab	07/28/97	10:00	10/02/97	2:30	V,T,C	
C9A3 16 mab	10/31/97	9:30	01/30/98	18:00	V,T,C	

Table 7.3. (Cont.)

ID	START	UTC	STOP	UTC	SENSORS	COMMENTS
C9A1 4 mab	05/24/97	2:00	07/29/97	7:00	V,T	
C9A2 4 mab	na	na	na	na	na	No data recorded by OEI 9407
C9A3 4 mab	10/31/97	9:30	01/30/98	18:00	V,T	
O9A1	05/24/97	2:00	07/29/97	7:00	O2,Turb,T,C	Turbidity questionable
O9A2	07/28/97	10:00	10/02/97	2:30	O2,Turb,T,C	
O9A3	10/31/97	9:30	01/30/98	18:00	O2,Turb,T,C	

Abbreviations: mab = meters above bottom; na = not applicable; V = velocity; T = temperature; C = conductivity; UTC = Coordinated Universal Time.

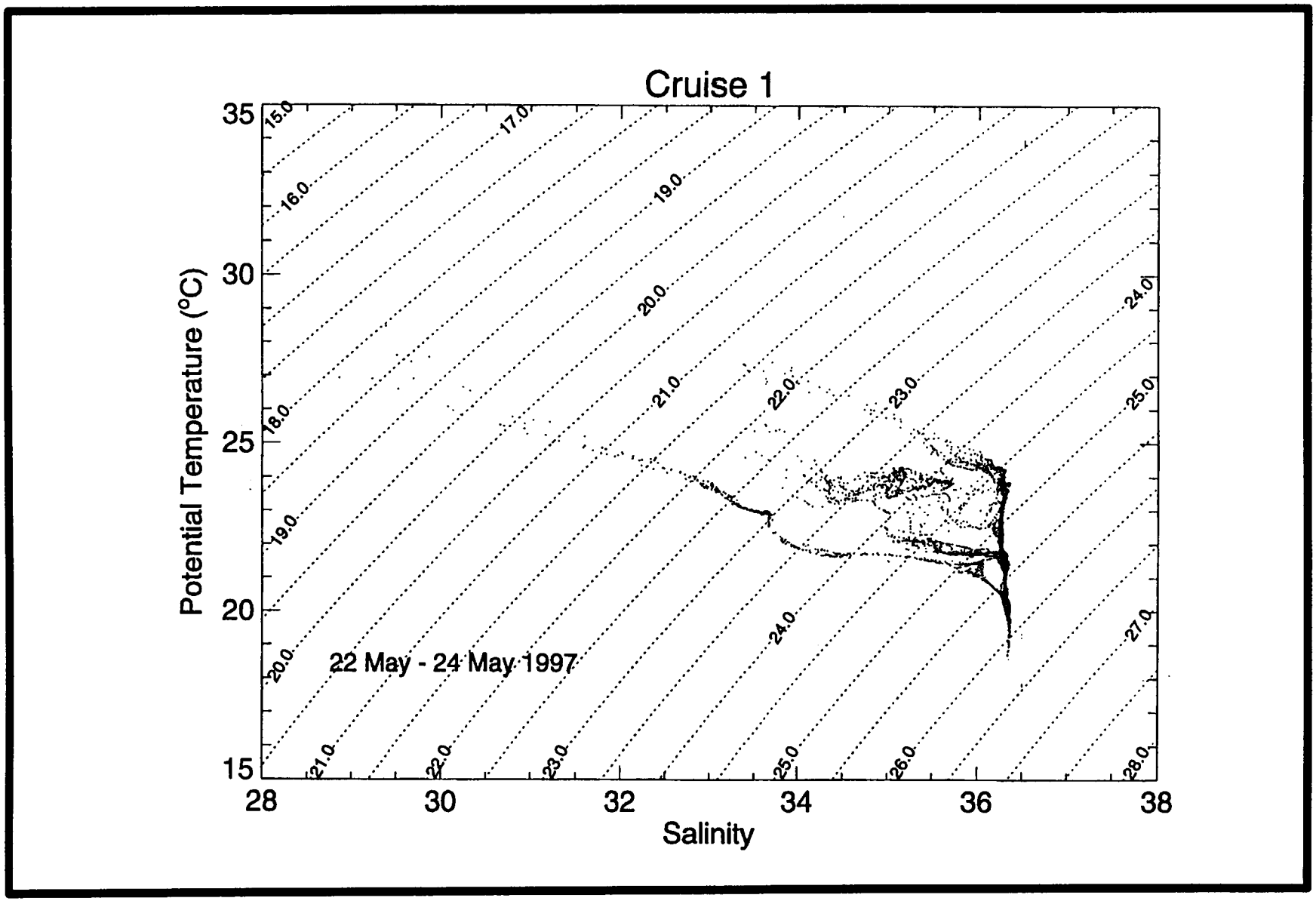

Fig. 7.5. Composite plot of temperature versus salinity for Cruise 1C.

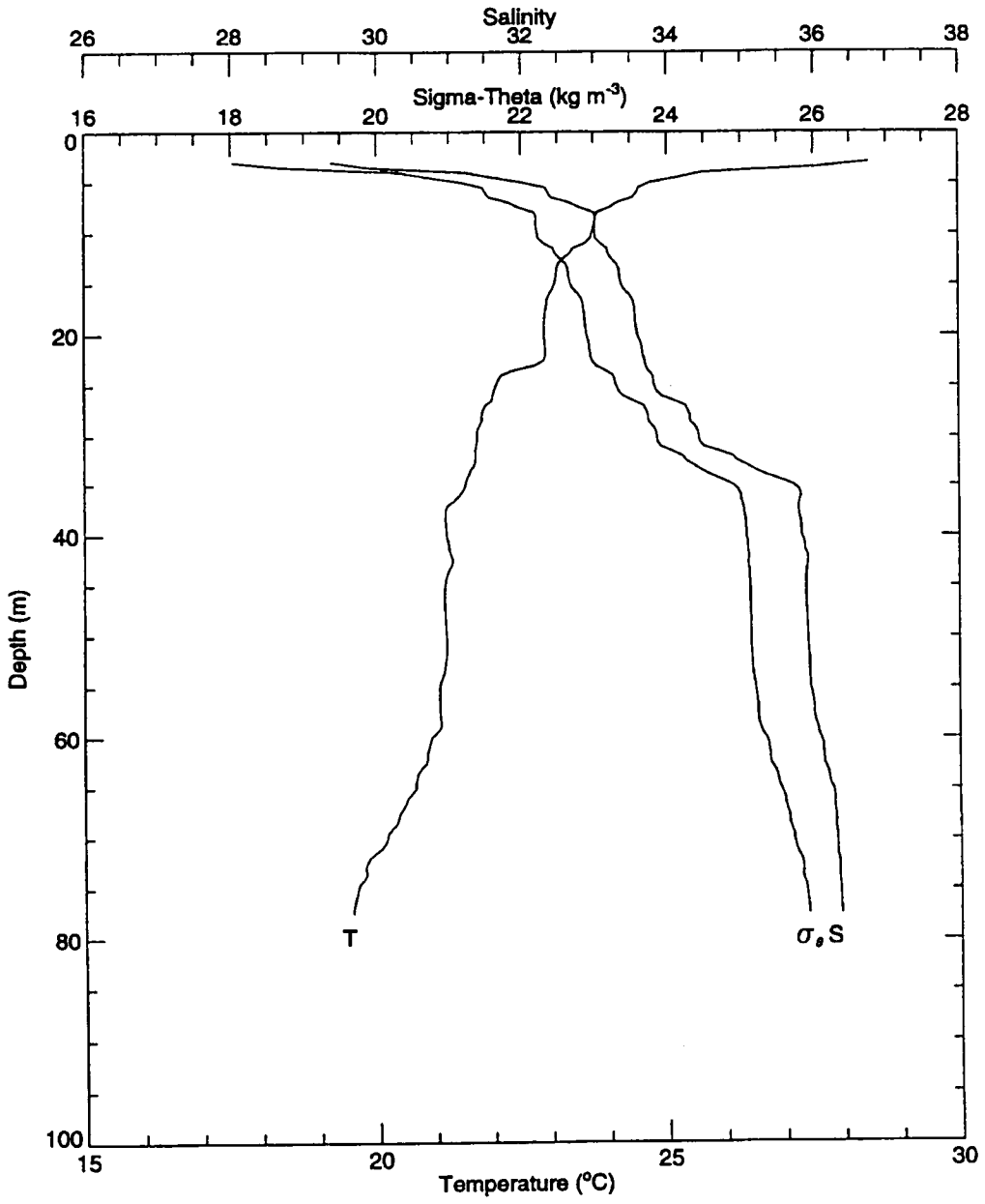

Fig. 7.6. Temperature, salinity, and sigma-theta profiles for CTD cast at station H5B1 during Cruise 1C.

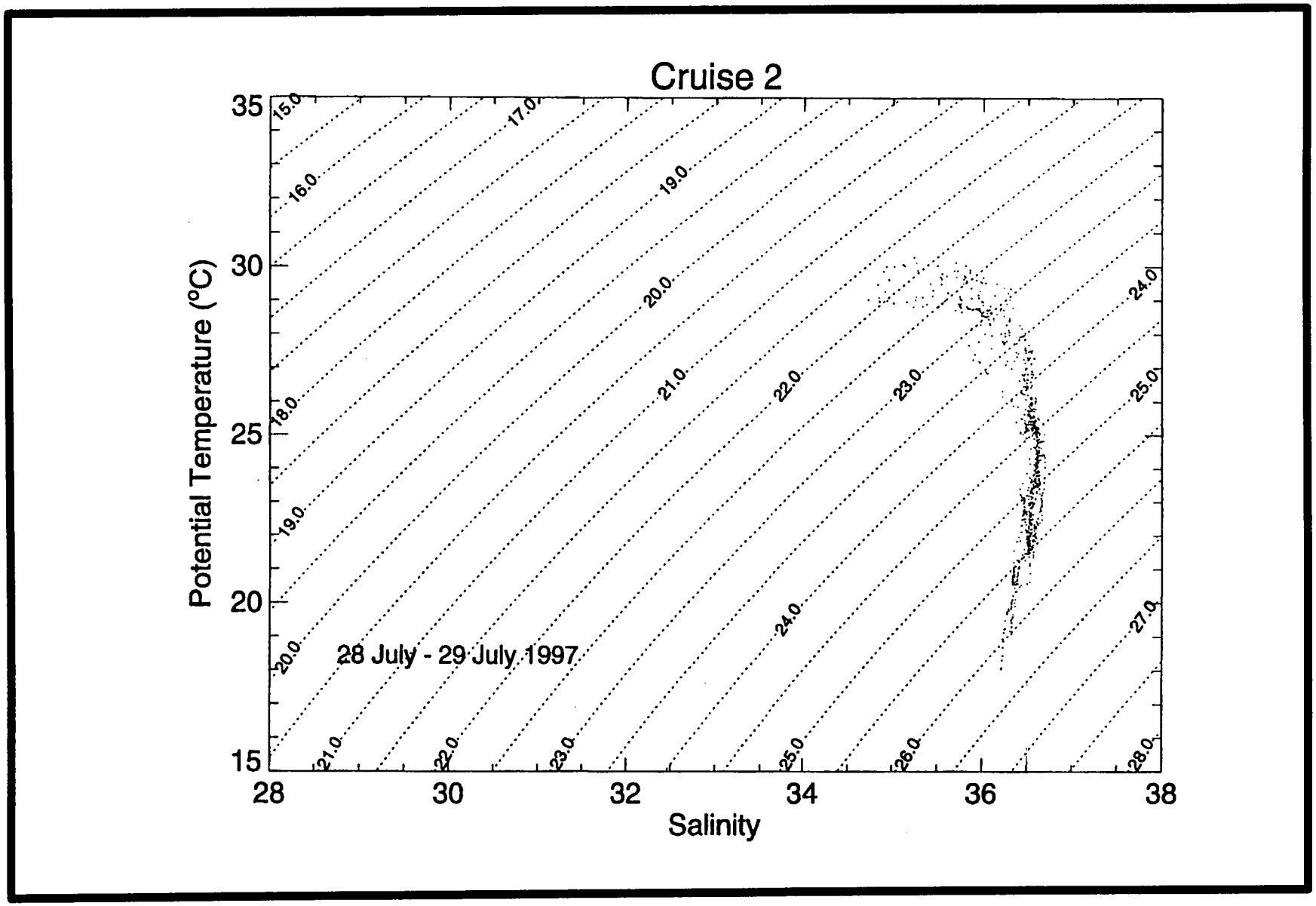

Fig. 7.7. Composite plot of temperature versus salinity for Service Cruise S1.

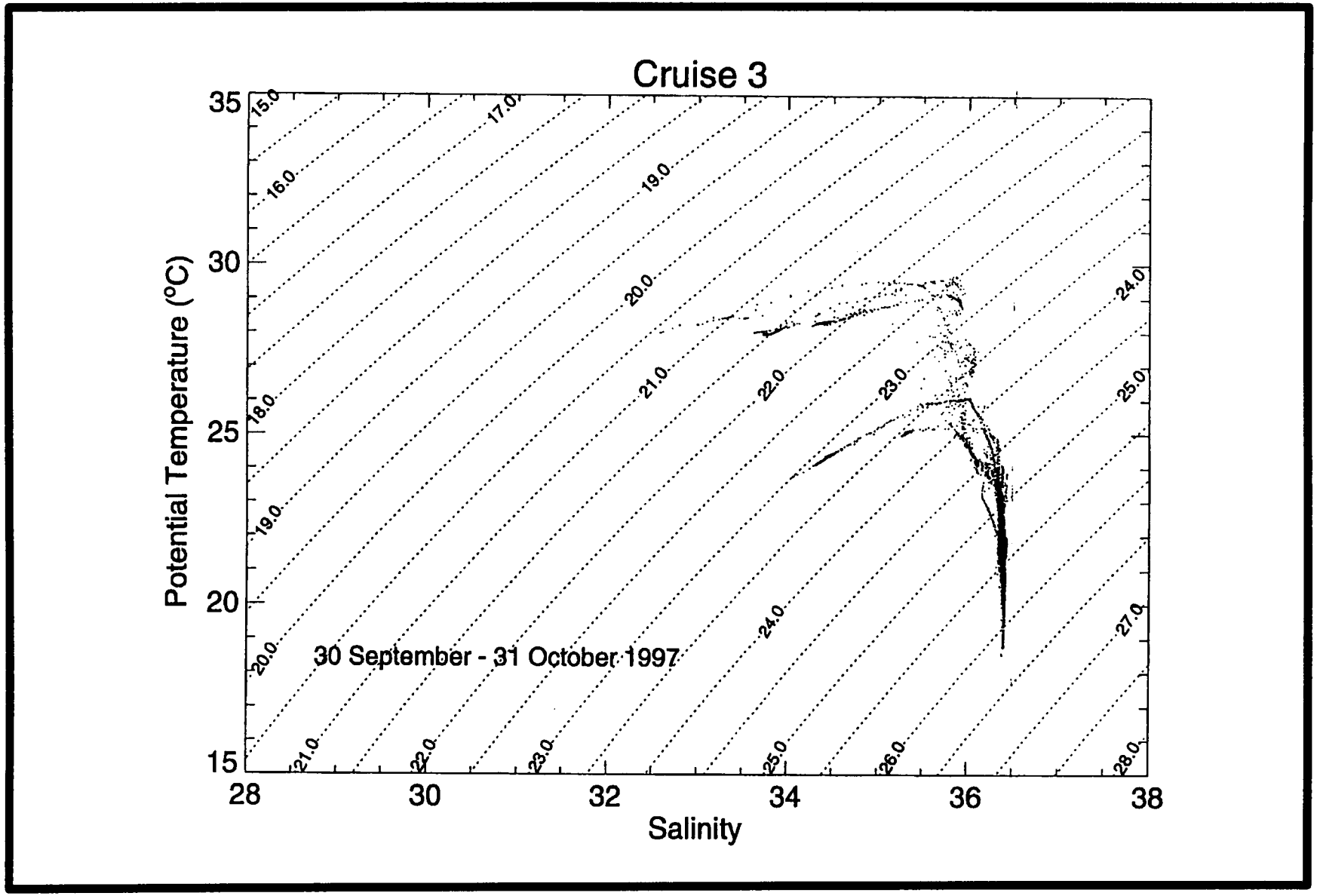

Fig. 7.8. Composite plot of temperature versus salinity for Monitoring Cruise M2.

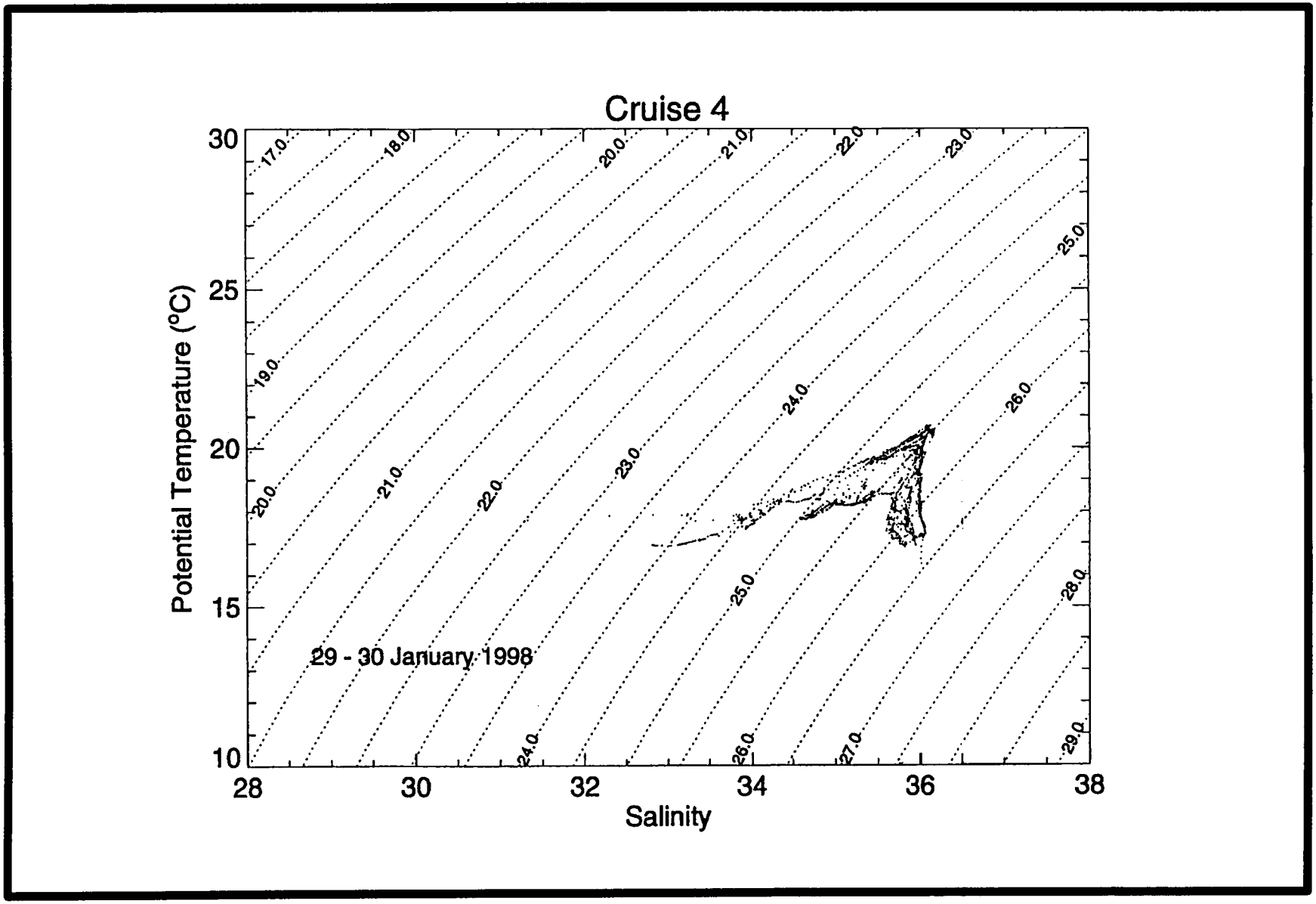

Fig. 7.9. Composite plot of temperature versus salinity for Service Cruise S2.

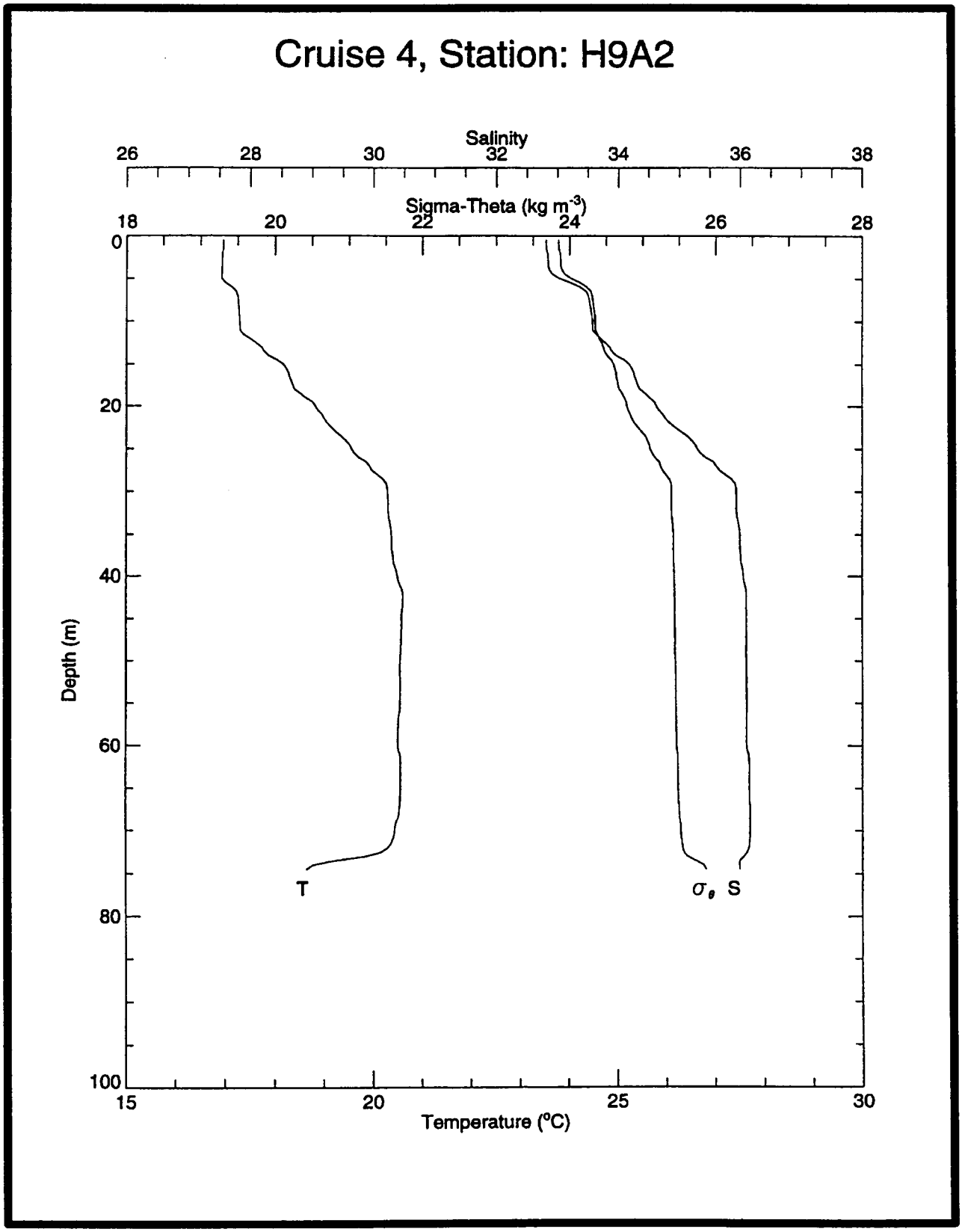

Fig. 7.10. Temperature, salinity, and sigma-theta for CTD cast at station H9A2 during Service Cruise S2.

Discussion

Time-Series Data

Flow at 16 mab

The current meters at 16 mab measure the mesoscale flow just above the pinnacles. This height is above the bottom Ekman layer. The larger pinnacles may slightly perturb the flow, a possibility that will be examined during the synthesis phase. Across the entire pinnacle study region there is substantial similarity in the observed flow fields. For example, Figs. 7.11a and 7.11b show the scatter plots at Sites 1 and 9 for the first deployment period. The principal direction sectors are east and northeast. To further condense the information content of the velocity series, six statistics have been extracted from the individual summary pages and placed in Table 7.4. Note that the vector mean speed and the scalar average speed can be quite different, which indicates the amount of directional variability in the flow. Maximum speeds during this period were in the 30 to 40 cm/s range, but occurred briefly and infrequently.

During the second deployment period (mainly August and September), flow at 16 mab was generally weaker and more directionally variable, resulting in lower vector mean and scalar mean values. The principal direction sectors of east and northeast were balanced to some degree by currents in the south and southwest sectors. Maximum speeds were in the 25 to 30 cm/s range. As an example, Fig. 7.11c shows the scatter plot for C5A2.

During the third deployment period (mainly October through January) currents were more energetic than during the previous two periods. Currents were greater than 20 cm/s more frequently, but maximum speeds were still in the 30 to 40 cm/s range. The principal direction sectors were still east and northeast, but vector means were low because flow was to the south and southwest a significant amount of the time. The scatter plot for C1A3 and C9A3 are shown in Figs. 7.2 and 7.11d, respectively.

Flow at 4 mab

Information about the near bottom flow is summarized in Table 7.5, and four examples of scatter plots are shown in Fig. 7.12. Compared with the flow at 16 mab, the near-bottom flow is more site specific (cf., Figs. 7.11 and 7.12). Bottom friction and the local topography influence flow. The most frequent direction octants are those with a southerly component (Table 7.5). Average scalar speeds are comparable at times to those at 16 mab, and mean vector speeds sometimes exceed the overlying flow because of greater directionality.

Dissolved Oxygen and Turbidity

Time series of dissolved oxygen and turbidity were collected at a height of about 2.3 mab at each mooring. Data return is quite good for dissolved oxygen, but not for turbidity. Sensor or instrument malfunction rather than fouling are responsible for data loss. Plots of dissolved oxygen for the three deployment periods are shown in Figs. 7.13, 7.14, and

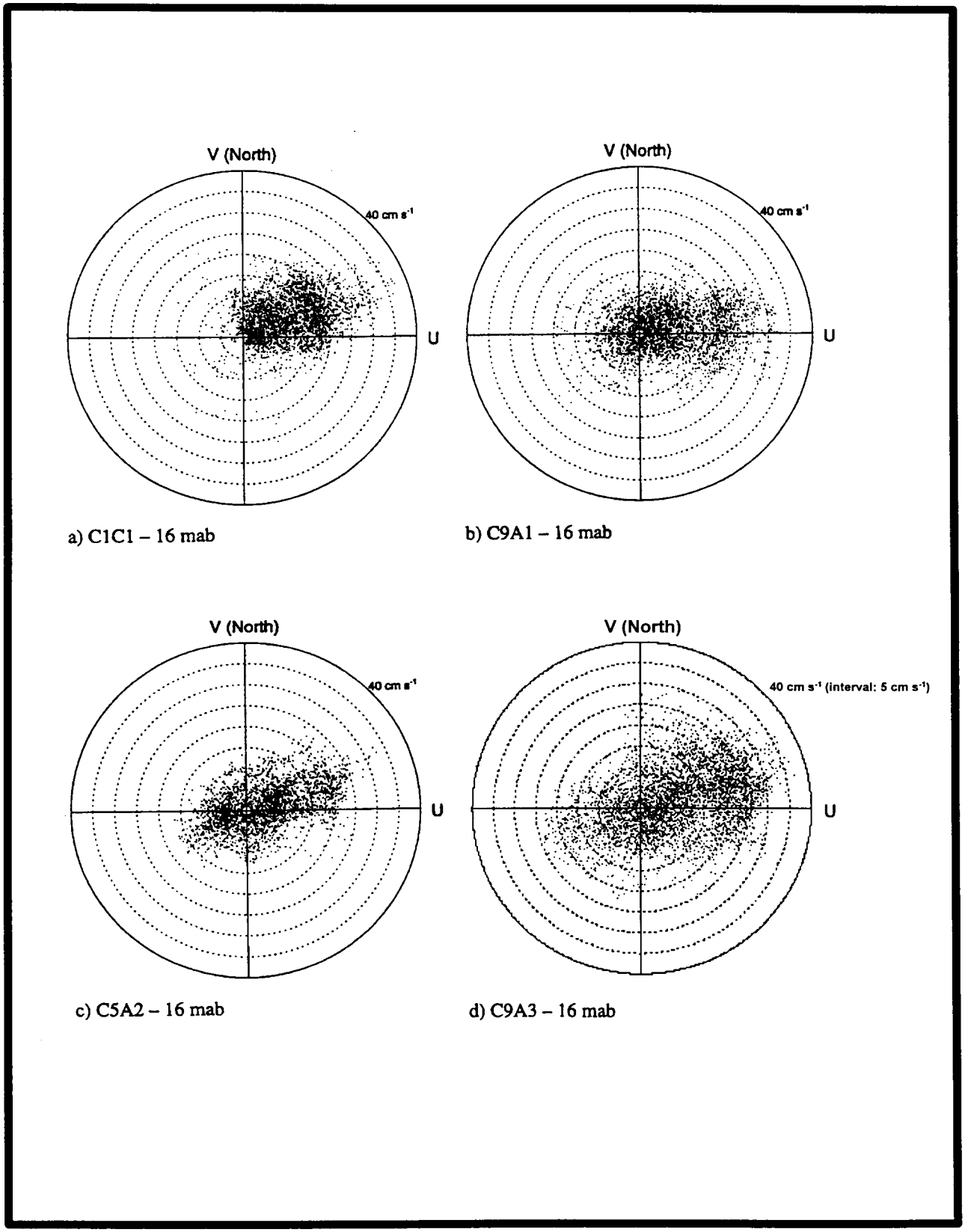

Fig. 7.11. Scatter plots of current velocity from Summary Pages for a) C1C1 - 16 mab; b) C9A1 - 16 mab; c) C5A2 - 16 mab; and d) C9A3 - 16 mab.

Table 7.4. Statistics for the velocity time series at 16 mab.

	Scalar Avg. Speed (cm/s)	Scalar Max Speed (cm/s)	Scalar Std. Dev. (cm/s)	Vector Mean Speed (cm/s)	Vector Mean Dir. (Deg. T)	Most Frequent Octant	%
C1A1	14.7	37.1	7.9	13.1	68.6	E	47.1
C1B1	13.3	41.1	7.7	12.0	69.8	E	48.8
C1C1	12.7	37.1	6.9	11.4	65.7	E	44.6
C4A1	11.9	34.8	6.3	8.3	81.2	E	54.0
C5A1	10.1	30.7	5.6	7.1	65.3	NE	33.5
C9A1	10.4	33.4	7.1	6.8	80.9	E	39.5
C1A2	5.0	23.8	4.7	1.5	129.2	E	24.8
C1B2	6.9	27.5	4.8	2.3	103.4	E	20.8
C1C2	6.1	25.2	4.5	1.6	73.4	NE	16.6
C4A2	--	--	--	--	--	--	--
C5A2	8.1	32.8	5.8	3.4	76.6	E	29.0
C9A2	7.3	30.7	5.5	1.2	52.2	NE	21.5
C1A3	10.2	40.6	6.9	1.6	99.1	E	19.9
C1B3	9.1	36.8	6.9	1.7	110.1	SW	19.6
C1C3	8.2	34.2	6.1	1.5	81.2	NE	18.6
C4A3	11.2	41.7	7.4	2.1	170.6	E	26.0
C5A3	11.0	42.7	7.2	1.2	66.1	E	22.3
C9A3	14.2	36.8	7.9	8.6	75.2	E	33.0

Abbreviations: mab = meters above bottom.

Table 7.5. Statistics for the velocity time series at 4 mab.

	Scalar Avg. Speed (cm/s)	Scalar Max. Speed (cm/s)	Scalar Std. Dev. (cm/s)	Vector Mean Speed (cm/s)	Vector Mean Dir. (Deg. T)	Most Frequent Octant	%
C1A1	5.7	30.8	4.1	2.3	96.5	SE	19.5
C1B1	11.6	34.1	6.8	6.9	63.4	NE	45.9
C1C1	--	--	--	--	--	--	--
C4A1	--	--	--	--	--	--	--
C5A1	10.4	30.6	5.9	1.1	176.9	SW	23.6
C9A1	10.6	35.0	6.5	6.9	125.3	SE	33.3
C1A2	4.6	19.5	3.5	2.3	162.2	S	24.2
C1B2	8.0	22.5	5.6	3.9	191.8	S	28.6
C1C2	--	--	--	--	--	--	--
C4A2	--	--	--	--	--	--	--
C5A2	7.1	29.7	5.6	1.2	183.3	SW	23.5
C9A2	--	--	--	--	--	--	--
C1A3	5.3	28.5	4.4	2.1	176.4	S	26.7
C1B3	10.0	30.2	6.1	3.6	184.4	S	26.5
C1C3	7.9	29.9	7.0	6.1	201.7	S	36.9
C4A3	7.3	41.8	6.1	2.3	181.2	SW	27.5
C5A3	8.9	25.8	6.0	2.6	240.4	SW	23.2
C9A3	10.9	49.6	7.3	7.7	140.9	S	27.6

Abbreviations: mab = meters above bottom.

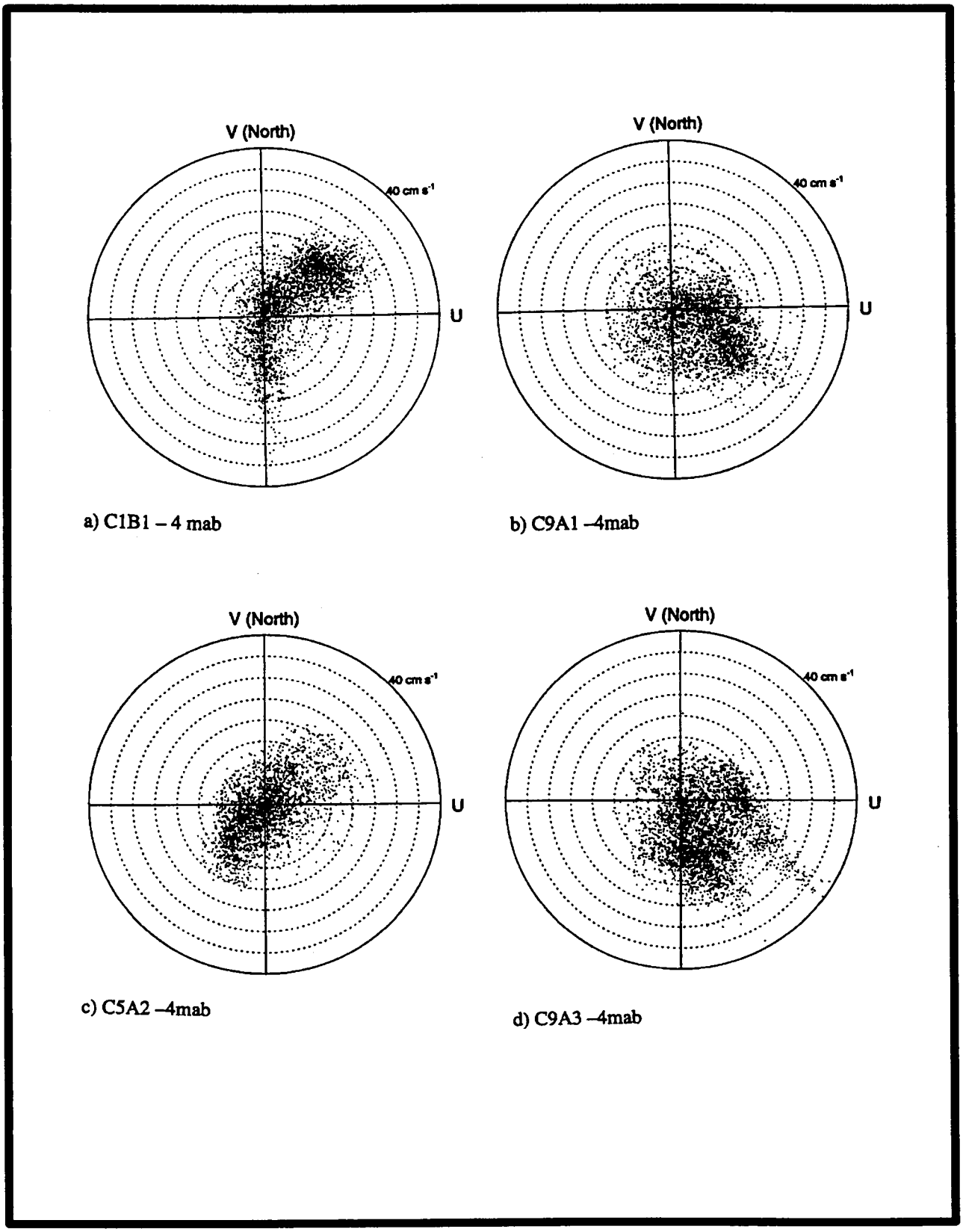

Fig. 7.12. Scatter plots of current velocity from Summary Pages for a) C1B1 - 4 mab; b) C9A1 - 4 mab; c) C5A2 - 4 mab; and d) C9A3 - 4 mab.

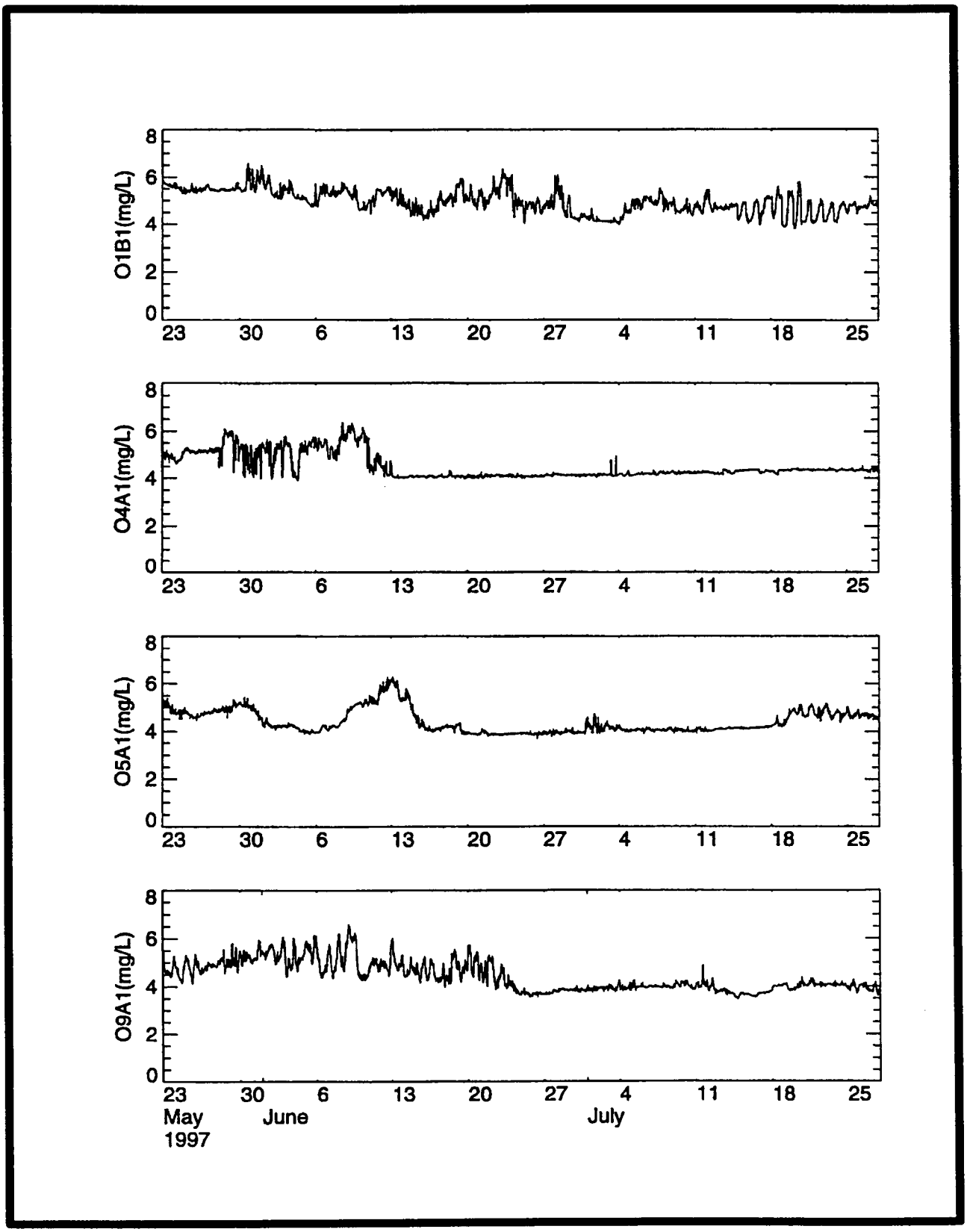

Fig. 7.13. Time-series plots of dissolved oxygen for the first deployment period for O1B1, O4A1, O5A1, and O9A1.

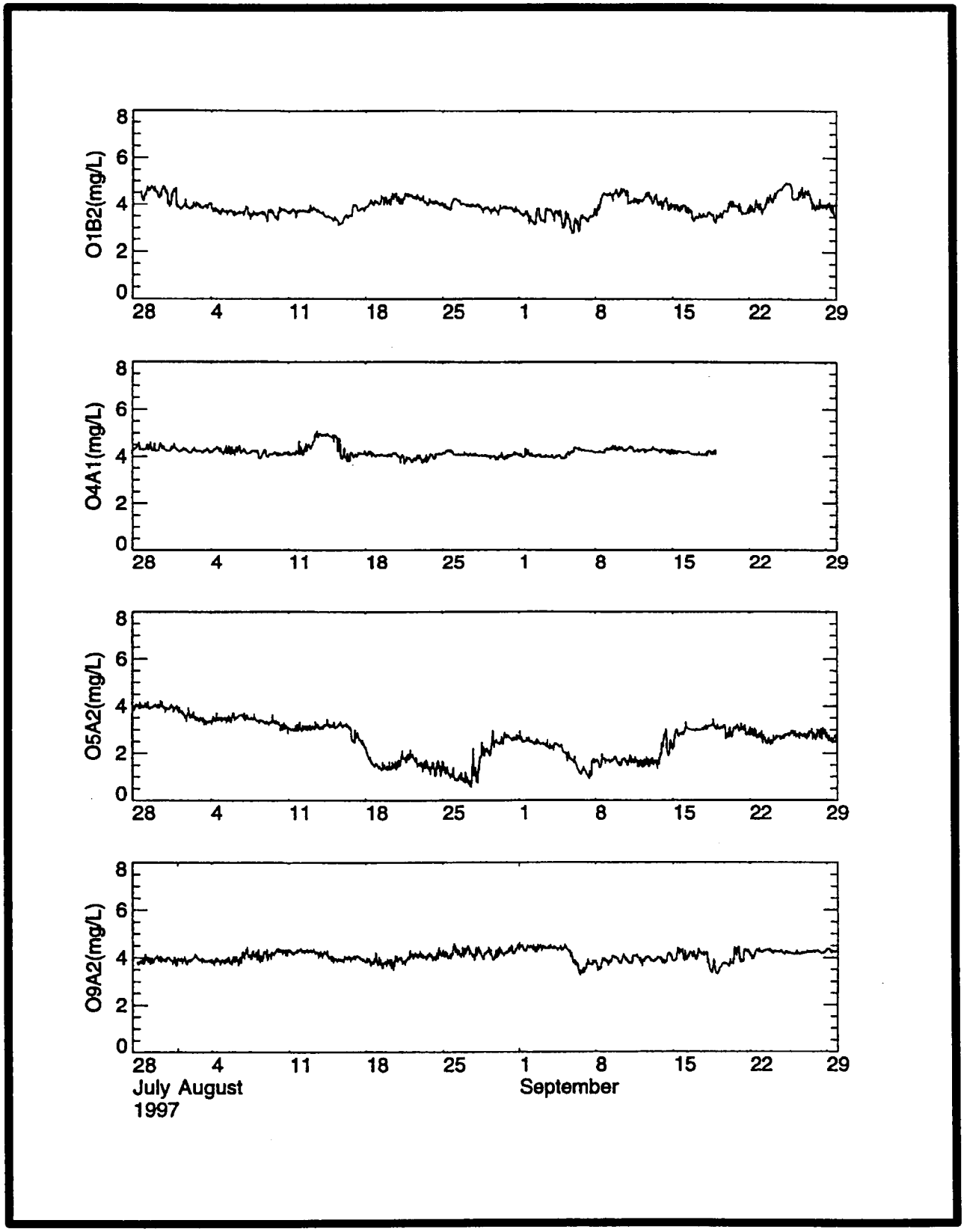

Fig. 7.14. Time-series plots of dissolved oxygen for the second deployment period for O1B2, O4A1, O5A2, and O9A2.

7.15, respectively. Values are generally near or above 4 mg/L, except at Site 5, the shallowest site, during the second deployment period. Values were below 3.0 mg/L much of the time. They fell below 2.0 mg/L during 18 to 28 August and 5 to 13 September.

Available time series of turbidity are shown in Figs. 7.16, 7.17, and 7.18 for the three deployment periods, respectively. Values are generally quite low, i.e., 0 to 2 NTU, with brief periods during which turbidity rises to the 2 to 10 NTU range.

Temperature and Conductivity/Salinity

The moored instruments collected time series temperature and conductivity, which together yield a time series of calculated salinity. The basic statistics for each deployment-length record of temperature and salinity are detailed in Tables 7.6 and 7.7, respectively. Temperature follows a seasonal trend with superimposed variability caused by advective changes from tidal and inertial currents and possible intrusions by mesoscale water mass motion. Salinity generally falls in the 36.2 to 36.4 range. Values fall as low as 34.0 and rise as high as 36.8. Values above 36.5 suggest possible intrusion of Loop Current related water.

Vertical Profiles

Almost all the water sampled on the four cruises had a density less than 26.25 sigma-theta.

During the 22 to 24 May 1997 period (Cruise 1C, Fig. 7.5), Sites 5 and 6 had surface salinities below 30. The other sites during this period had surface salinities as low as 33.5. Bottom water salinities during this period were close to 36.4. The profile at station H5B1 (Fig. 7.6) shows that the water with salinity less than 30 extends down to about 5 m below the surface.

During Cruise S1 on 28 to 29 July 1997 (Fig. 7.7), the setting was very different. No salinities below 34.5 were observed. Bottom salinities were around 36.2 to 36.4 with a salinity maximum of around 36.6 found at midwater depths.

During Cruise M2 between 30 September and 31 October 1998 (Fig. 7.8), bottom salinities were between 36.4 and 36.5. Lowest salinities were found at Site 1 where the surface mixed layer was around 34.6.

During Cruise S2 on 29 to 30 January 1998 (Fig. 7.9), bottom salinities varied between 35.8 to slightly above 36. Lowest salinities were at Site 9 (Fig. 7.10) where the surface layer extending down to 5 m depth was about 33.

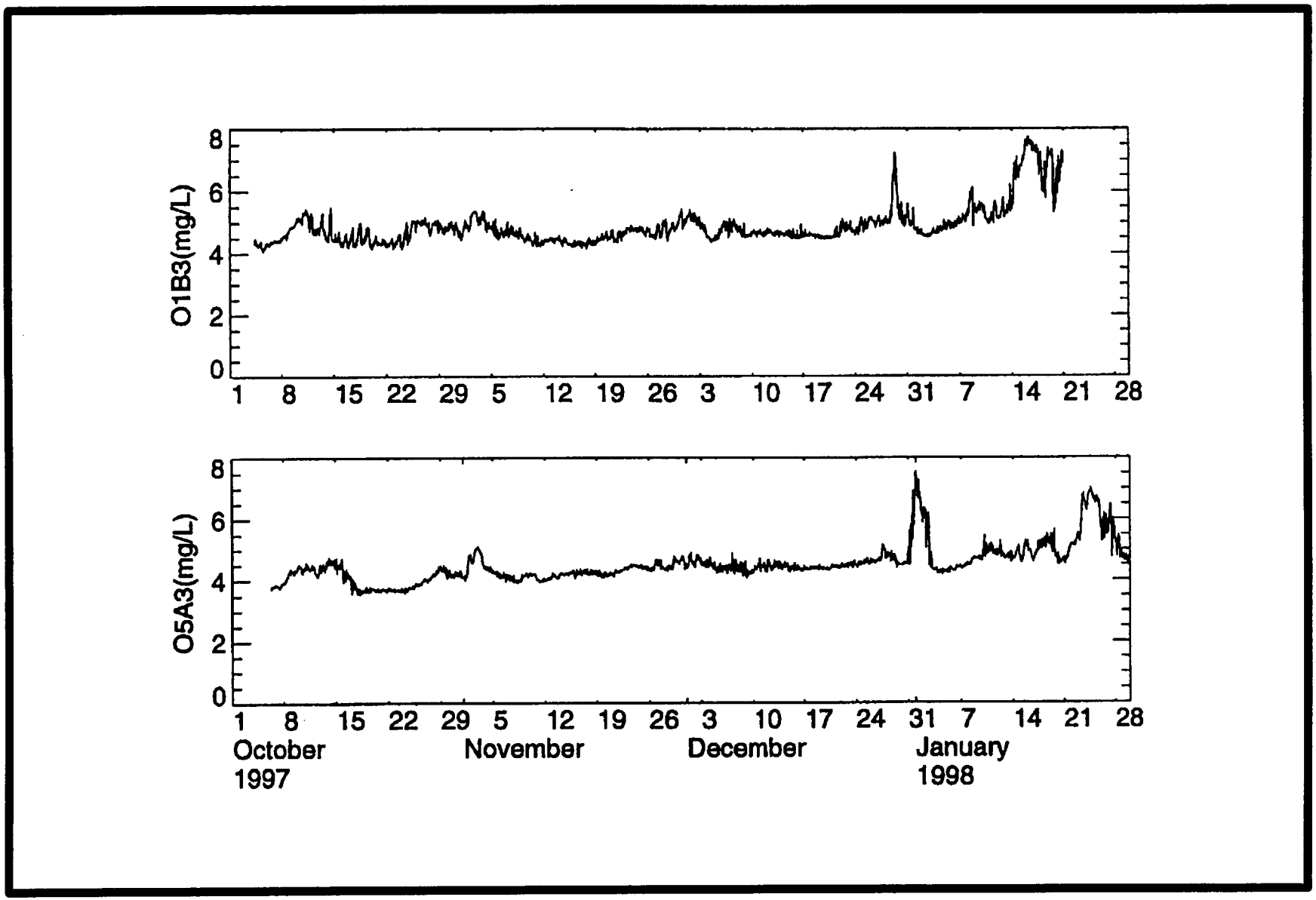

Fig. 7.15. Time-series plots of dissolved oxygen for the third deployment period for O1B2 and O5A2.

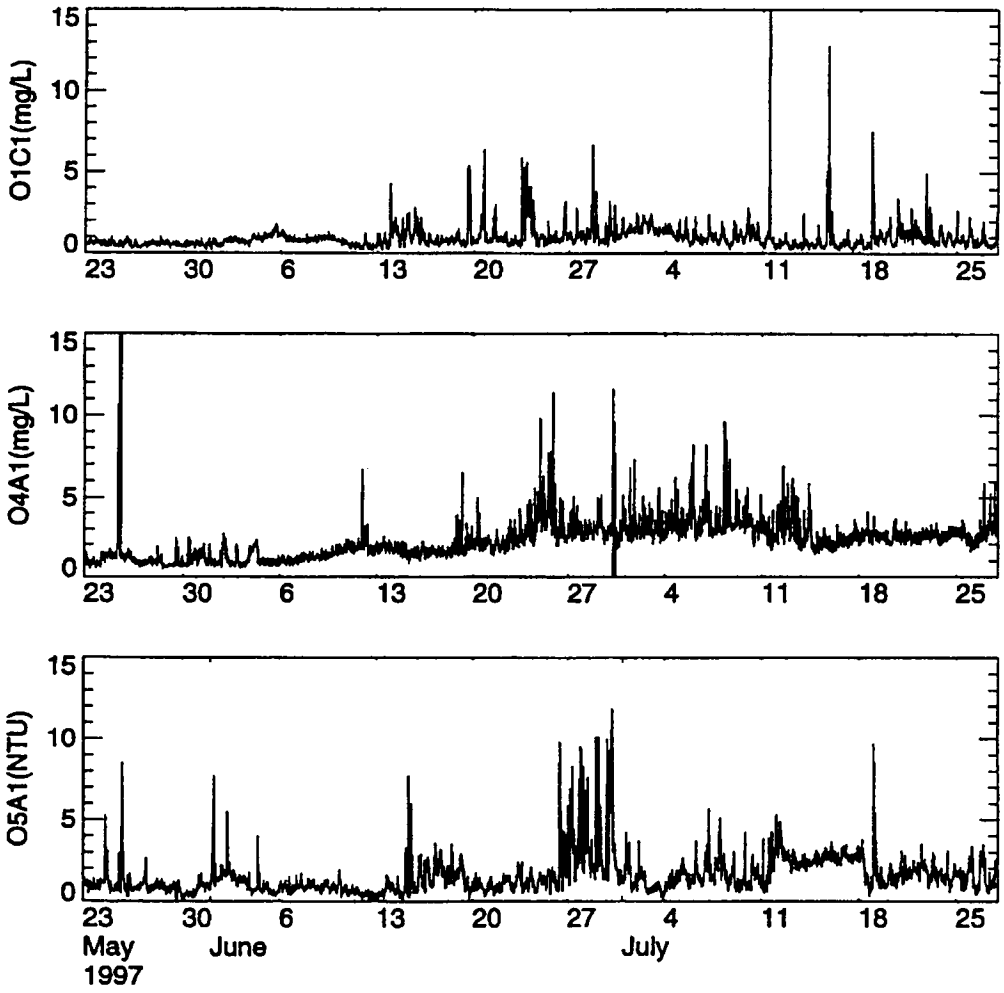

Fig. 7.16. Time-series plots of turbidity for the first deployment period for O1C1, O4A1, and O5A1.

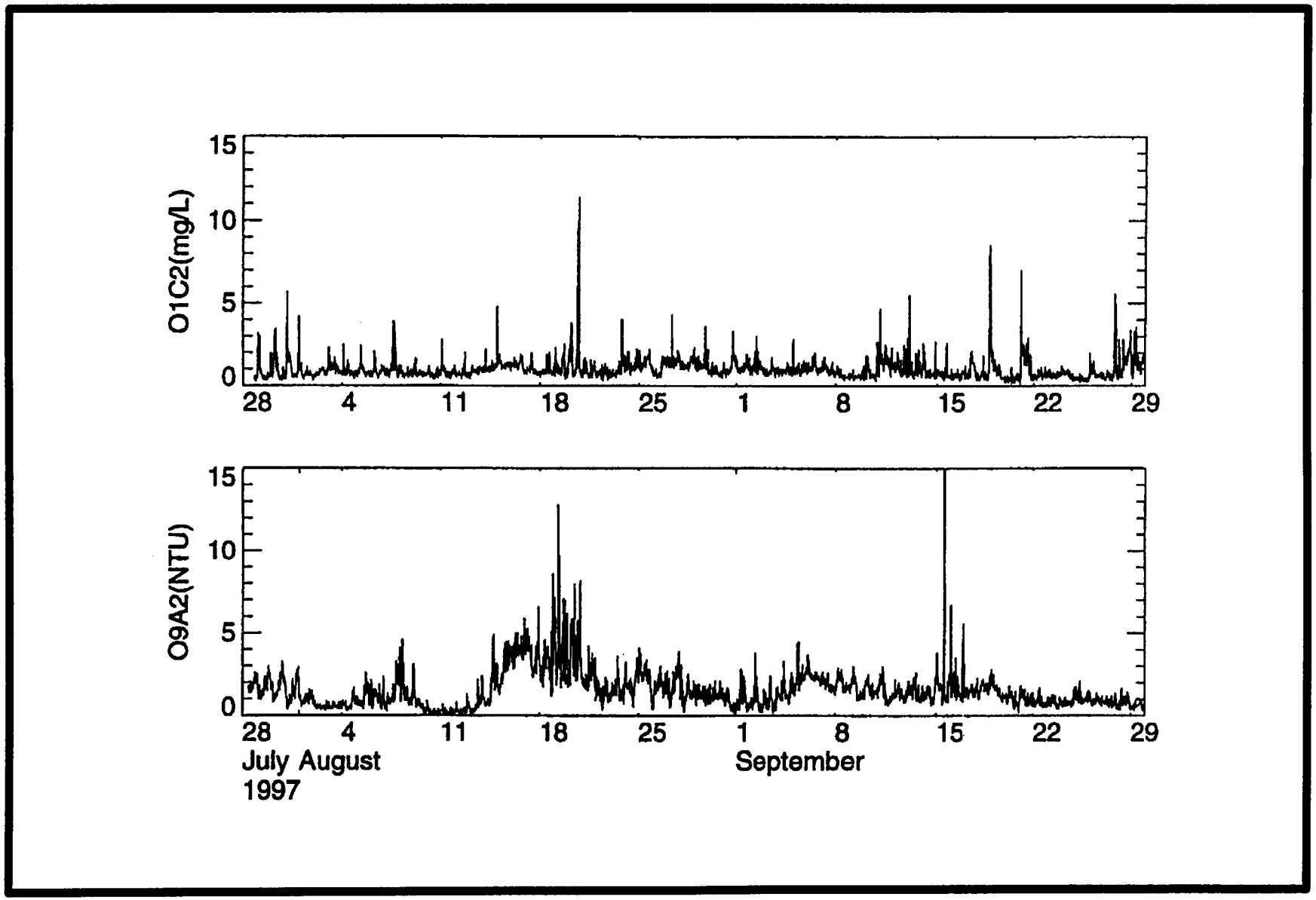

Fig. 7.17. Time-series plots of turbidity for the second deployment period for O1C2 and O9A2.

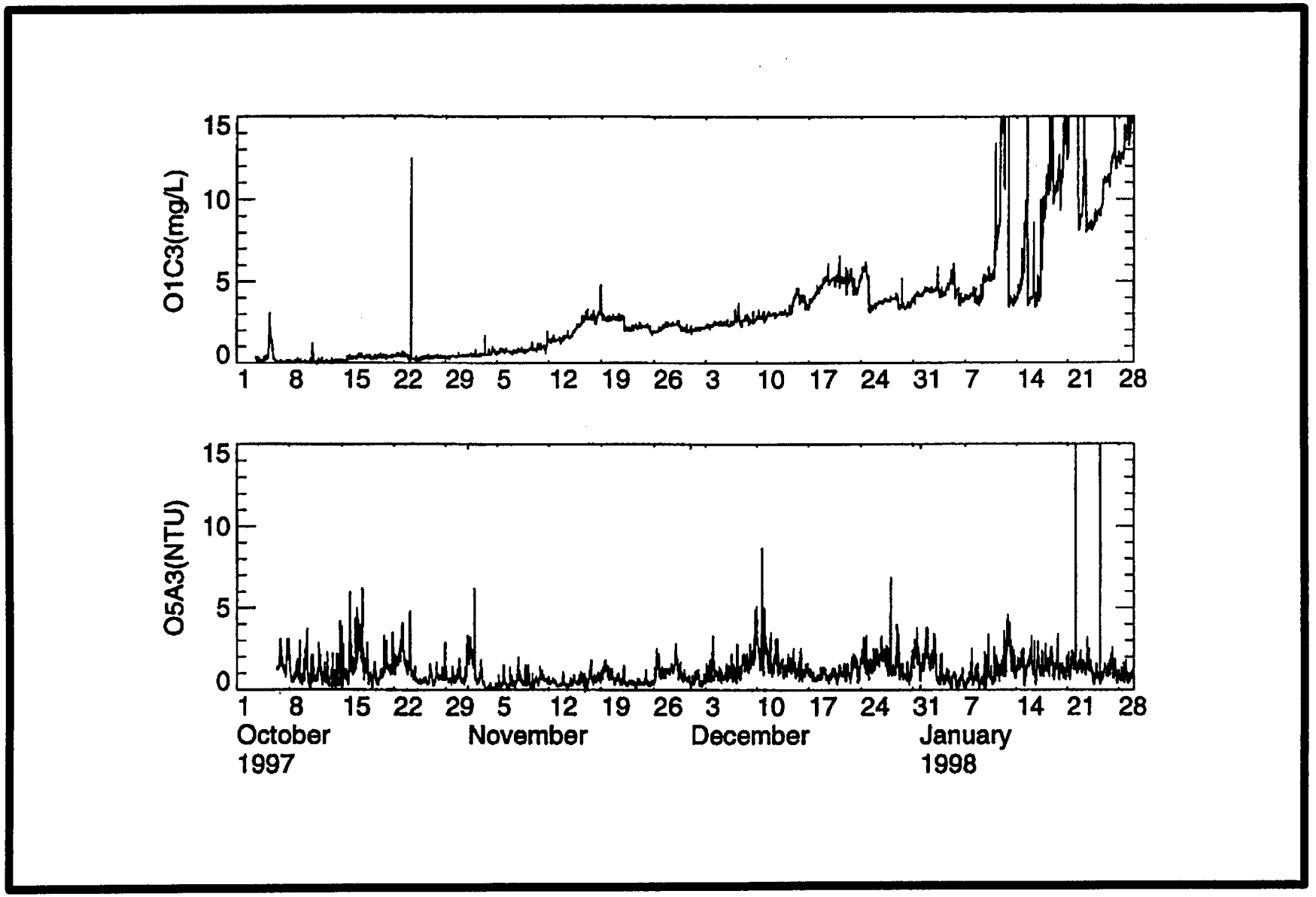

Fig. 7.18. Time-series plots of turbidity for the third deployment period for O1C3 and O5A1.

Table 7.6. Statistics for the temperature time-series data collected by the current meters at a) 16 m above bottom (mab) and b) 4 mab.

a)

	Mean	Standard Deviation	Minimum	Maximum
C1A1	21.48	0.45	20.30	23.40
C1B1	21.25	0.43	19.71	22.82
C1C1	21.19	0.45	19.68	23.05
C4A1	19.16	1.22	15.85	21.44
C5A1	20.70	0.85	18.36	22.24
C9A1	20.36	0.92	17.10	21.87
C1A2	21.00	0.48	19.81	22.59
C1B2	20.51	0.58	18.77	22.34
C1C2	20.56	0.56	18.96	22.49
C5A2	20.73	0.40	18.99	21.91
C9A2	20.32	0.45	18.08	21.50
C1A3	20.40	1.56	15.61	23.35
C1B3	20.13	1.56	15.34	23.24
C1C3	20.18	1.54	15.62	23.29
C4A3	17.90	1.92	10.93	21.05
C5A3	20.20	1.50	13.76	22.77
C9A3	19.69	1.43	15.38	22.57

b)

	Mean	Standard Deviation	Minimum	Maximum
C1A1	20.38	0.67	17.48	21.69
C1B1	20.08	0.76	16.93	21.66
C5A1	18.90	0.88	16.84	21.25
C9A1	18.87	1.09	16.60	21.20
C1A2	19.91	0.77	17.73	21.15
C1B2	19.78	0.81	17.42	21.14
C5A2	19.67	0.78	17.71	21.06
C1C3	18.88	1.97	12.33	21.71
C1A3	19.12	2.05	12.49	21.94
C1B3	19.03	1.97	12.32	21.81
C4A3	17.00	2.15	10.78	20.23
C5A3	18.92	1.77	13.42	21.73
C9A3	18.34	1.38	13.77	21.33

Table 7.7. Statistics for the salinity time-series data collected by the current meters at 16 m above bottom.

	Mean	Standard Deviation	Minimum	Maximum
C1A1	36.29	0.11	35.92	36.79
C1B1	35.86	0.58	34.83[a]	36.52
C1C1	36.29	0.10	35.92	36.74
C5A1	36.27	0.05	36.01	36.47
C9A1	36.42	0.05	36.26	36.64
C1A2	36.40	0.09	36.20	36.76
C1C2	36.45	0.10	36.27	36.81
C5A2	36.46	0.09	36.29	36.76
C9A2	36.47	0.07	36.32	36.76
C1A3	36.42	0.49	35.04	36.99
C1B3	36.26	0.30	35.29	36.59
C1C3	36.14	0.46	34.81[a]	36.65
C4A3	36.35	0.25	35.54	36.79
C5A3	36.26	0.34	35.21	36.66
C9A3	36.33	0.16	35.91	36.71

[a] The minimum values of 34.83 (C1B1) and 34.81 (C1C3) are suspect, but the beginning and end of these records agree with the CTD casts.

Chapter 8
Hard Bottom Communities

Approach and Rationale

Hard bottom communities at greater than 50 m water depth are assumed to be slow growing, have low rates of recruitment, and be sensitive to physical disturbance. Studies near several offshore petroleum platforms off Point Conception in California (Hyland et al. 1994) measured decreased abundances of some epifaunal species associated with fluxes of drilling muds near the seabed. Observations within the current study region by Gittings et al. (1992b) indicated variation in epibiota associated with longitude (proximity to the Mississippi River), vertical relief of hard bottom, and position on hard bottom features (perhaps related to current exposure and near-bottom fluxes of suspended sediments). Hardin et al. (1994) also found variation in the distribution and abundance of epibiota related to depth, vertical relief of hard bottom features, position on hard bottom features, and flux of suspended sediments. The slow growth, low recruitment rates, and possible sensitivity to drilling muds and/or suspended sediments of hard bottom epibiota suggest the importance of investigating the factors that may control these communities in areas affected by petroleum development.

Hard bottom communities are being sampled at nine sites by ROV. Sampling sites were chosen to fall within three categories of relief (i.e., low, medium, and high; see Chapter 3) in three regions from east to west. Site selection was based on data from geophysical surveys and ROV reconnaissance surveys. At each site, random photographs are taken and random video transects are being surveyed during each monitoring cruise. The random photographs are used to estimate the abundances of sessile and motile epibiota, whereas video images are used to quantify larger and more widely dispersed organisms and to broadly characterize substrates and species composition. In addition, fixed video/photoquadrats have been established that are resampled on subsequent cruises; the data will be used to describe temporal changes related to growth, recruitment, competition, and mortality. Voucher specimens are also being collected to aid in species identification. Together with geological and oceanographic data collected during the program, these data will be analyzed and interpreted to describe hard bottom community dynamics, variation within and among sites, and relationships between the biota and physical variables.

Field Methods

Field sampling includes qualitative data collection, random photographic stations and video transects, fixed video/photoquadrats, and voucher specimen collection. The ROV being used for field sampling is a Benthos Openframe SeaROVER with a Python multifunction manipulator arm. Video, photographic, and ancillary equipment include a Sony high-resolution video camera, DeepSea Power & Light Micro-SeaCam 2000 color video camera, Photosea 1000 35-mm still camera and strobe, DeepSea Power & Light

lasers, and a Simrad MS900 color imaging sonar. The location and track of the ROV on the seabed is determined with a precision acoustic navigation system.

Both qualitative and quantitative video and still photographic data are collected at each site. The ROV equipped with two independent video camera systems and one still camera system was used to collect video and still photograph data. One of the video cameras is aimed forward to help maneuver the ROV and collect qualitative video images for identifying substrates, epibiota, and fishes. The second video camera and the still camera are used to collect either qualitative or quantitative video and still photographs. These two cameras are aligned to have the same field of view and are able to be remotely positioned to be perpendicular to the targeted substrate or subject. The second video camera and still camera also allow the scientific observer and ROV pilot to observe the four lasers which are used to determine distance above the bottom and scale within the video and still photographs. Video and photographic data, ROV position, and observations concerning specific features of interest are correlated using the Mission Manager software system (C-Map Systems, Inc.) and written logs.

Due to the small sizes of many of the more abundant species, the camera-to-subject distance for still photographs is set at 60 cm. This is the closest distance from which an in-focus photograph can be taken. This provides the highest resolution possible with the Photosea camera for discerning small biota.

Random Photographic Stations and Video Transects

At each of the nine monitoring sites, the ROV collects video footage and still photographs at pre-selected random locations and along transects between these locations. Prior to the monitoring cruise, 100 locations were randomly selected for each of the nine monitoring sites. These random locations were selected using the digital elevation models for each of the sites that were created from the detailed bathymetric data collected during Cruise 1A.

The results of an analysis of the digital elevation data were considered in determining the size of the nine sites (see Appendix B of the First Annual Interim Report; Continental Shelf Associates, Inc. and Texas A&M University, Geochemical and Environmental Research Group 1998). In this analysis, the standard deviation of the slope magnitude, slope direction, and depth were iteratively calculated for progressively larger areas of each feature, starting at the center of the study site. Plots of these calculated standard deviations versus area were examined to ascertain the areas around the study site central locations over which the standard deviations stabilized. This insured that the variability in elevation that the feature added to the surrounding background elevation was appropriately considered in the site boundary evaluation process.

Each of the nine monitoring sites is defined as a circular area with a site-specific diameter. Each circular site is divided into eight sectors (Fig. 8.1), with 16 points randomly positioned in each sector. The ROV maneuvers between each of the random locations in a sector, collecting a quantitative still photograph with a camera orientation perpendicular to the substrate at each random location. Both qualitative and quantitative

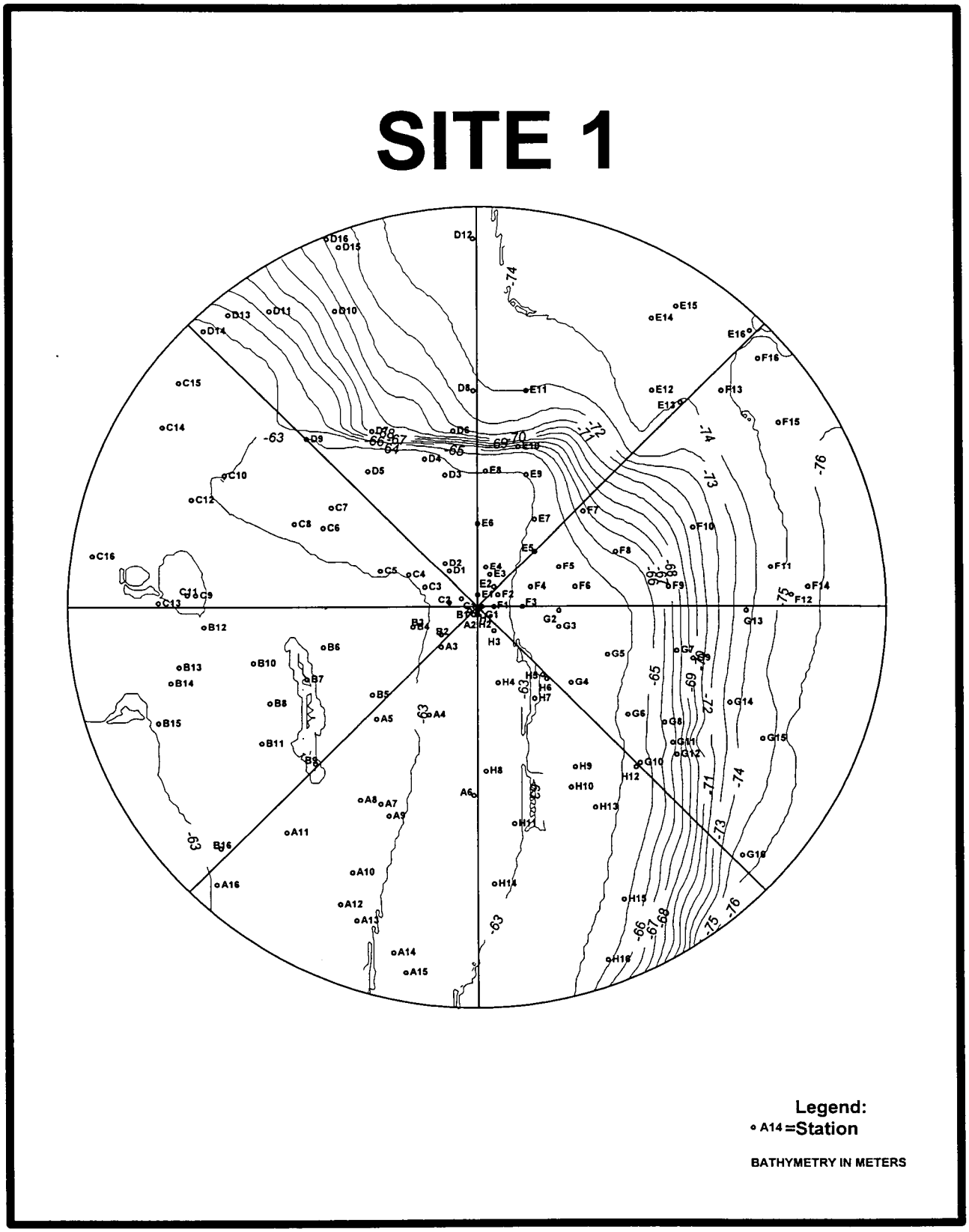

Fig. 8.1. Example of random point allocation within eight sectors of a site. A quantitative photograph was taken at each random point. Qualitative and quantitative video and additional photographs were collected along transects between random points.

video data are collected along the transects between each of the random still photo locations, with one video camera (qualitative) aimed ahead for navigating the ROV and the second video camera (quantitative) oriented perpendicular to the substrate. Upon the completion of a sector, the ROV moves to the next adjacent sector and resumes collecting video and still photo data until each of the eight sectors are covered. Additional photographs are taken of specific features or biota along the transects to aid in bottom characterization or individual species identifications.

The quantitative video and still cameras are maintained at a specific distance from the bottom by the use of four lasers mounted on the ROV. This laser system consists of three lasers mounted around the video and still cameras with their beams parallel and aimed to fall within the cameras' fields of view. The three lasers are oriented in the shape of an equilateral triangle with the resultant beam pattern providing a constant scale in all video and still photo data. The fourth laser was mounted at a convergent angle to coincide with one of the three parallel lasers when the quantitative video camera and still camera lenses are 60 cm from the bottom. All four lasers are visible to the ROV pilot in the quantitative video camera field of view, enabling him to maneuver the ROV at a constant height above the bottom along the transects.

The sampling procedures and criteria for the collection of random still photographs changed slightly during the monitoring survey in Cruise 1C based upon the type of feature being surveyed. Initially, for all of the low, medium, and high relief pinnacle sites, if a sandy or sediment-covered bottom was present at the pre-selected random photograph location, a photograph was not taken. In this case, the ROV's forward-looking sonar was used to guide the vehicle to the nearest adjacent hard bottom location within the sector where a photograph was taken. If sufficient hard bottom was not present in the sector, additional random points were sampled in subsequent sectors. This worked well at sites where the bathymetry data collected during Cruise 1A matched up well with the features actually present at the site. But at Sites 2, 5, and 8 there were mismatches between actual observations and the bathymetry data. The sizes of the circular sampling areas established at these sites were significantly larger than the actual diameter of the features, causing a majority of the random photograph locations in some sectors to fall on sand bottom areas tens of meters from the edge of the pinnacles. Additionally, the features at Sites 5 and 8 were also offset to the north relative to the positions shown in the bathymetry data set. Because of the lack of nearby adjacent hard bottom in many of the random photograph locations at these sites, additional random positions were regenerated for the site following the completion of the eight sectors and the ROV collected photographs at these new locations.

Fixed Video/Photoquadrats

During Cruise 1C, five fixed video/photoquadrats were established at random locations within each site. The video/photoquadrat markers for each site consisted of the numbers 1 through 5 made from lead, with dimensions of approximately 10 cm in height by 6 cm in width. The numbers were deployed at the random locations using the manipulator arm of the ROV. The actual position of each video/photoquadrat marker was recorded with the precision navigation system to allow relocation of the markers on subsequent

monitoring surveys. For each of the first two monitoring sites visited, Sites 1 and 3, the five fixed video/photoquadrat markers were deployed at five different random locations. Silty conditions observed while deploying several of the markers at other sites raised concerns the markers may become obscured with sediments. Consequently, it was decided to deploy the markers around a single random location identified by a 12-cm diameter buoy coated with antifouling paint and highly reflective tape. The fixed video/photoquadrat markers for six of the seven subsequent monitoring sites (Sites 2 and 4 through 8) were deployed in this manner. Fixed video/photoquadrat markers were not deployed at Site 9 due to high turbidity that prevented the collection of video or photographic images of acceptable quality. At Site 7, only fixed video/photoquadrat markers 1 and 2 were deployed and only marker 1 was photographed due to ROV video camera problems and the subsequent loss of use of the ROV manipulator arm upon recovery of the vehicle.

After each fixed video/photoquadrat marker was deployed, still photographs and video images were recorded of the marker and the surrounding substrate from a distance of 60 cm. Video images were also recorded at distances of up to 2 m from the markers to provide a wider view of the surrounding features to facilitate relocation of the marker on future surveys. During collection of the still photographs and video images, the cameras were oriented perpendicular to the substrate and the heading or orientation of the ROV was recorded in the log for each shot or image grab.

Voucher Specimen Collection

Epibiota and rock samples are collected when feasible to provide a specimen inventory to aid in the identification of species appearing on video and in photographs and to provide information to help characterize the substrates. Selected specimens are picked up with the ROV's manipulator arm, placed in the sample basket that is lowered to the seabed, and the basket is returned to the surface by the ROV. At the surface the specimens are assigned a unique identification number, photographed, and then labeled and preserved.

Laboratory Methods

Random Photographic Stations and Video Transects

For analysis purposes a replicate video transect consists of a standardized time increment of visually acceptable video data. Time is counted only when the ROV is in motion and remains at the proper distance from the bottom, and when visibility is acceptable. Video images recorded along each replicate transect are reviewed to characterize substrates and determine species composition. Video data are reviewed using an S-VHS videocassette recorder interfaced with a 20-inch color monitor and Mission Manager software system. All recognizable substrate features and epibiota are listed as either present or absent. Biota is identified to the lowest practical taxonomic grouping. Substrate types are separated into the following categories:

- soft bottom;
- hard bottom with a sediment veneer;
- low relief hard bottom;
- medium relief hard bottom (vertical to irregular topography);
- high relief hard bottom (flat-topped); and
- high relief hard bottom (vertical to irregular topography).

Areal coverage of substrate and epibiota within the random quantitative photographs is estimated using the quantitative analysis method developed by Bohnsack (1976, 1979). Each photograph (slide or photo CD image) is analyzed in one of two ways. If using the original slide film, the image is projected onto the 30 cm by 40 cm screen of a slide viewer and a clear acetate overlay containing 50 randomly located points is superimposed on the screen over each frame. If using photo CDs made from the original slide film, the stored image is pulled up onto the screen of a high-resolution monitor and a set of 50 randomly generated points is added to the display.

For each analysis method the number of points that covers each taxon and/or substrate type is recorded for each frame or image. The percent coverage of each taxon and substrate type is the percentage of the total points that contact each taxon and substrate type. Since some points may fall on deep shadows and be unreadable, the denominator in the percent cover calculations is reduced by the number of points overlaying shadowed areas. These percentages are combined for all frames from each site to obtain the average percent coverage for each taxon and substrate type. The numbers of individuals of solitary species are also counted and all species that are present in the photographic frame are recorded. The data for point contacts, numbers of individuals, and species presence are directly entered into a computer database for subsequent calculation of percent cover, density, and diversity.

Epifauna such as sponges, hydroids, octocorals, and antipatharians may be attached at a single point and their morphologies are commonly ascending and branched or expansive above the point of attachment. This morphology creates a canopy effect when viewed from above during quantitative photography. Therefore, their cover as viewed in quantitative photographs is more correctly termed "areal cover" rather than percent cover of substrate provided by the individual biota.

Due to difficulties in taxonomic identification, certain epifauna observed in the photographs are given descriptive names only, which are assigned to specific morphological forms that can be consistently distinguished. Groupings based on specific morphology can result in either overestimation or underestimation of the abundance of the correct species. Conversely, because some descriptive groupings may contain several species that cannot be distinguished from one another, an underestimation of the species richness may result. These uncertainties are unavoidable, and are being minimized by the careful collection and identification of voucher specimens and the construction of the voucher photographic image catalogue.

Fixed Video/Photoquadrats

Fixed video/photoquadrats are analyzed using a method similar to that used by Gittings et al. (1992a) for fixed photoquadrats on the Flower Garden Banks. A single representative video frame is selected from images collected at each fixed video-photoquadrat location to serve as a baseline image. The selected image is projected on a high-resolution color monitor and the percent cover of epibiota and substrate types is estimated using the same random point analysis method used for the random photographs. The thickness of the sediment veneer is estimated, if possible, when it is present. Supplemental photographs of the fixed quadrats taken at the same time as the video images are also used to assist in the identification of epibiota. The number of species in the projected images is counted and their densities are calculated. The borders of all conspicuous epibiota and distinctive physical features are traced onto a sheet of clear mylar. The mylar overlay will be used as a baseline template for selecting identical video images collected during subsequent monitoring cruises and as a means to detect temporal change within each video/photoquadrat. Changes in the border dimensions of each colony or individual species from the baseline tracing may represent growth or retreat and possible evidence of disease or stress, sediment inundation, or inter- and intraspecific competition. All changes in border dimensions will be categorized and enumerated during future analyses. New colonies that appear within the video/photoquadrats during the program will be documented and traced on the mylar overlay. The small sizes, three-dimensionality, and possibility of parallax error in video/photoquadrat images may preclude the measurement or estimation of epibiota growth rates.

Statistical Analyses

Because this report is based on analysis of samples from a single cruise (1C), statistical analyses were performed to provide an initial broad scale evaluation of the effects of certain physical variables on the distribution and abundance of epibiota and the correlations of taxa to each other. These results will help guide future analytical approaches. Linear regressions (Statview 4.5.1, ABACUS Concepts) were performed to determine whether selected taxa vary according to site depth, vertical relief, distance from the Mississippi River, or flux of suspended sediments. These four independent variables were approximated as follows:

- Depth = the mid-point of the depth range recorded for each site (see Chapter 3);
- Vertical relief = the total depth range recorded for each site (see Chapter 3);
- Distance from the Mississippi River = the approximate distance from the river to each site; and
- Flux of suspended sediments = the average flux among the sediment traps occurring within the depth range for the four sites at which traps were deployed (see Chapter 5).

Correlations (Statview 4.5.1, ABACUS Concepts) between selected taxa were determined as a preliminary way of evaluating the presence of biotic associations or assemblages.

A list of the 10 taxa with highest density (number/m^2) at each site was generated and ranked in order of highest overall mean density among all sites. The statistical analyses were performed on the 10 taxa with the highest mean density over all sites, as well as the remaining taxa on the list that were present at a minimum of six sites. Because of taxonomic questions that will be resolved for future reports, only density data were analyzed for this report.

Results

A total of 790 random photoquadrats was analyzed from Cruise 1C (Table 8.1). Most sites had at least 98 random photoquadrats for analysis, but high turbidity at Site 9 resulted in all but six samples being rejected due to poor image quality.

A total of 43 taxa comprise the 10 taxa with the highest density at each site (Table 8.1). Cnidaria was the most-represented phylum with 13 taxa of octocorals, 10 taxa of ahermatypic corals, 4 taxa of antipatharians, and single taxa of hermatypic corals and actinarians (anemones). Porifera was the next most-represented phylum with five taxa, followed by Ectoprocta with four taxa. The phylum Echinodermata was represented by two taxa (one crinoid and one echinoid). The phyla Urochordata, Arthropoda, and algae were represented by single taxa of ascidians, galatheids, and Rhodophyta, respectively.

Although octocorals were represented by the most taxa, ahermatypic corals had the highest mean density of 327.97 organisms per m^2 over all sites, due to the numerical dominance of *Rhizopsammia manuelensis* (Table 8.1). Octocorals had the second highest mean density over all sites, 9.43 per m^2, followed by poriferans, ectoprocts, and antipatharians with 5.30, 3.17, and 2.75 organisms per m^2, respectively.

Only 21 taxa were recorded at at least six sites (Table 8.1). Two taxa, the yellow encrusting poriferan, Didemnidae, and the octocoral *Bebryce* sp., were observed at all nine sites. The yellow encrusting poriferan and didemnid ascidian taxa may be comprised of more than one species that are difficult to distinguish in the photos, so we are not certain that any species except *Bebryce* sp. occurs at all of the sites. Five taxa were recorded at eight sites, four taxa were recorded at seven sites, and nine taxa were recorded at six sites.

The high biological variability among sites suggested by the low number of taxa that were observed at all sites is also indicated by the highly variable group aggregate densities among sites for the list of dominant taxa (Table 8.1). The densities of ahermatypic corals ranged from 0.96 to 895.74 per m^2 and the densities of octocorals ranged from 0.79 to 20.29 per m^2. Densities of poriferans, ectoprocts, and antipatharians ranged from 0.02 to 25.03, 0.00 to 15.34, and 0.00 to 11.31 organisms per m^2, respectively. The total number of taxa at each site was also highly variable, ranging from 20 at Site 9 to 90 at Site 3, although the low number of taxa at Site 9 are probably the result of the small number of photographs that was analyzed.

Table 8.1. Physical characteristics (depth, relief, distance from the Mississippi River delta, mean flux of suspended sediment), number of slides analyzed, and dominant epibiota at hard bottom sites ordered according to overall mean density.

		Site 1	Site 2	Site 3	Site 4	Site 5	Site 6	Site 7	Site 8	Site 9		
Depth Range (m) →		63-76	69-81	76-80	95-107	62-78	75-78	69-88	88-96	89-95		
Depth - Midpoint of Depth Range (m) →		69	75	78	101	70	77	79	92	92		
Relief Category →		High	Medium	Low	Medium	High	Low	High	Medium	Low		
Approx. Distance from Miss. Delta (km) →		145	142	145	126	105	105	70	72	71		
Mean Flux of Susp. Sediment ($g/m^2/day$) →		4.98	-	-	4.83	10.00	-	-	-	9.15		
Number of Slides Analyzed →		98	99	85	102	102	99	101	98	6		
Taxon	Group[a]	Mean Density Within Each Site ($number/m^2$)									Overall Mean Density	Number of Sites
Rhizopsammia manuelensis	Aherm.	0	182.85	38.95	221.78	448.31	42.30	621.45	836.82	307.80	300.03	8
Scleractinia (tan/purple-solitary)	Aherm.	0	0	0	0.38	66.50	32.41	0.25	34.17	2.84	15.17	6
Scleractinia (white - solitary)	Aherm.	0	0	5.16	1.59	12.31	4.13	0.55	16.02	0	4.42	6
?Paracyathus pulchellus	Aherm.	0.48	0.47	1.05	0	14.60	2.36	0	5.82	0	2.75	6
Stenogorgiinae (tan/orange)	Octo.	4.34	4.90	9.31	0	2.54	0	0	0	0	2.34	4
Porifera (yellow encrusting)	Porif.	p	p	p	1.84	p	p	8.93	p	9.22	2.22	9
Nicella goreaui	Octo.	9.12	2.06	3.00	4.63	0	0	0.25	0	0	2.12	5
10-armed crinoids	Crinoid	1.17	0.64	2.50	5.13	0.54	0	7.84	0.26	0	2.01	7
Didemnidae	Ascid.	0.04	0.13	0.45	3.05	0.04	1.12	2.86	0.09	9.93	1.97	9
Thesea sp. (small - whitish)	Octo.	0	0	0	0.21	0.42	14.44	0	0.48	0	1.73	4
Bebryce sp.	Octo.	0.52	0.64	1.65	1.67	0.08	4.47	1.10	1.48	3.55	1.68	9
Idmidronea sp.	Ecto.	1.26	0.43	0.15	0	1.67	10.57	0	0	0	1.56	5
Scleractinia (yellow - solitary)	Aherm.	0	0	0	0	0	0	1.60	0	11.35	1.44	2
Galatheidae	Galath.	0	3.18	0.15	0	0.04	8.04	0	0.35	0	1.31	5
Antipathes ?furcata	Antipath.	0.09	0.47	0.40	9.35	0.17	0.26	0.08	0.30	0	1.24	8
Porifera (orange - encrusting)	Porif.	p	p	p	0	p	p	6.83	0.65	3.55	1.22	8
Ellisella sp.	Octo.	0	0.82	0	5.59	0	0.56	0.63	1.95	1.42	1.22	6
Porifera (yellow - boring)	Porif.	0	p	p	0.63	p	0	9.27	0	0	1.10	5
Madracis myriaster	Aherm.	0	0.39	1.60	0.58	3.13	0.09	1.01	1.43	0	0.91	7
Scleractinia (solitary)	Aherm.	0	8.21	0	0	0	0	0	0	0	0.91	1
Scleractinia (large white solitary)	Aherm.	0	0	0.30	5.01	0.04	0.04	0.21	0.39	2.13	0.90	7
?Stylopoma spongites	Ecto.	0.04	4.47	p	0	0.25	3.14	0	0.04	0	0.88	6
Madrepora carolina	Herm.	0	0.43	2.35	2.21	1.17	0.09	0	1.09	0	0.81	6
Nicella ?guadalupensis	Octo.	0	0	0	0	0	0	0	7.08	0	0.79	1

Table 8.1. (continued).

Taxon	Group[a]	Site 1	Site 2	Site 3	Site 4	Site 5	Site 6	Site 7	Site 8	Site 9	Overall Mean Density	Number of Sites
		Mean Density Within Each Site (number/m^2)										
Antipathes sp.	Antipath.	0.04	1.29	0.65	1.96	1.29	0.30	0.38	0.61	0	0.73	8
Stylocidaris affinis	Echinoid	0.09	0.09	0.30	0.38	1.13	0.09	1.26	2.95	0	0.70	8
Ellisella ?barbadensis	Octo.	5.73	0	0.45	0	0.08	0	0	0	0	0.70	3
Stenogorgiinae	Octo.	0	0	0	0	0	0	0	5.34	0	0.59	1
Peyssonnelia sp.	Rhodo.	0	0	0	0	0	0	4.72	0	0	0.52	1
Thesea sp. (pink)	Octo.	0	0.52	1.25	0.04	0.21	0.82	0	1.82	0	0.52	6
?Cellaria sp.	Ecto.	1.52	0.26	1.15	0	0.25	1.33	0	0	0	0.50	5
Stenogorgiinae (grey/white)	Octo.	2.43	0.26	0.60	0	0.29	0	0	0	0	0.40	4
Antipathes ?atlantica	Antipath.	0	0.77	0.40	0	0.58	0.13	1.47	0.22	0	0.40	6
?Stichopathes lutkeni	Antipath.	0.13	1.29	1.25	0	0.25	0.13	0.42	0.09	0	0.40	7
?Scleracis/Thesea (red-orange)	Octo.	0	0	0	0.13	0	0	0.51	0	2.84	0.39	3
Dysidea sp.	Porif.	3.43	0	0	0	0	0	0	0	0	0.38	1
?Halichondriidae	Porif.	3.17	0	0.05	0	0	0	0	0	0	0.36	2
Scleractinia (tan - solitary)	Aherm.	0.48	0	2.55	0	0	0	0	0	0	0.34	2
Ellisella ?elongata	Octo.	0.13	0	2.50	0	0	0	0	0	0	0.29	2
Zoantharia (anemone)	Actin.	0	0.04	0	0	0	0	0	2.56	0	0.29	2
Scleractinia (orange solitary)	Aherm.	0	0.30	0.30	0.13	0.17	0.17	1.47	0	0	0.28	6
Stenogorgiinae (pink-purple)	Octo.	0	0.30	1.95	0	0	0	0	0	0	0.25	2
?Crisia sp.	Ecto.	1.17	0.26	0.05	0	0.21	0.30	0	0	0	0.22	5
Total Density of Dominant Taxa	All	35.39	215.47	80.50	266.25	556.28	127.27	673.10	922.01	354.61	358.99	
Total Density of Dominant ahermatypic corals	Aherm.	0.96	192.65	52.27	231.66	546.22	81.58	626.54	895.74	324.11	327.97	
Total Density of Dominant octocorals	Octo.	15.50	4.04	8.86	12.27	0.79	20.29	2.49	12.81	7.80	9.43	
Total Density of Dominant antipatharians	Antipath.	0.26	3.83	2.70	11.31	2.29	0.82	2.36	1.22	0.00	2.75	
Total Density of Dominant poriferans	Porif.[b]	6.63	0.03	0.08	2.46	0.03	0.02	25.03	0.66	12.77	5.30	
Total Density of Dominant ectoprocts	Ecto.	3.99	5.42	1.36	0.00	2.38	15.34	0.00	0.04	0.00	3.17	
Total number of Taxa		80	67	90	59	78	70	62	68	20		

Abbreviations: Aherm.=ahermatypic coral; Octo.=octocoral; Porif.=poriferan; Ascid.=ascidian; Galath.=galatheid; Antipath.=antipatharian; Rhodo.=Rhodophyta; Actin.=actinarian; and p = (present) values estimated at 0.01 per m^2.

Little of the biological variation among sites is apparently due to water depth, vertical relief, distance from the Mississippi River, or suspended sediment flux (Table 8.2). Eight of the 21 taxa that were recorded at a minimum of six sites had statistically significant regression coefficients for one or more of these physical variables. Densities of *Antipathes ?furcata*, *Ellisella* sp., and the large white solitary scleractinian all increase with increasing depth. Densities of *Bebryce* sp. increase as vertical relief decreases. Densities of *Rhizopsammia manuelensis* and the orange encrusting poriferan increase with decreasing distance from the Mississippi River, and densities of the tan/orange Stenorgorgiinae and *Nicella goreaui* increase with increasing distance from the Mississippi River. None of the taxa had significant regression coefficients for mean sediment flux. The total density of ahermatypic corals and of all the 43 dominant taxa also increased with decreasing distance from the Mississippi River, probably due to the numerical dominance of *R. manuelensis*.

Significant correlations occurred between 20 pairs of taxa, with two groupings of taxa being apparent (Table 8.3). The highly significant correlations among *Antipathes ?furcata*, *Ellisella* sp., and the large white solitary scleractinian are probably the result of their common significant positive association with depth (Table 8.2). The tan-purple solitary scleractinian, the white solitary scleractinian, *?Paracyathus pulchellus*, and *Madracis myriaster* were also significantly correlated, but with no apparent effect of the four physical variables.

Discussion

The paucity of significant regression coefficients between numerically dominant taxa and depth, relief, distance from the Mississippi River, and the flux of suspended sediments probably reflect the preliminary nature of the data set that was analyzed. Several of the descriptive taxa and questionable genus or species designations will be more clearly defined as the study progresses, allowing better quantitative evaluations of species-specific relationships between biological and physical variables. The analytical approach that was taken for this report could also obscure such relationships. For instance, each of the sampling sites encompasses substantial physical variation due to the large size, complex topography, and vertical relief of the hard bottom features. Large ranges of potentially important physical variables such as distance above unconsolidated seabed, exposure to currents, slope, and topographic variation affecting sedimentation are incorporated into each site; the physical and biological variations within sites may be nearly as large as those between sites. Therefore, an important objective in deducing the causes of between-site variation in epibiota will involve accounting for this within-site variation.

Accounting for the within-site variation will require a more sophisticated analytical approach than was taken for this report. The approach in this report was to examine the relationships between mean densities of epibiota and broadly generalized estimates of physical variables such as depth, vertical relief, and flux of suspended sediments for each

Table 8.2. Regression coefficients and probabilities that are different from zero for regressions of biological variables against four physical variables.

Taxon	Depth		Relief		Distance from Miss. River		Mean Sediment Flux	
	Coefficient	*p*	Coefficient	*p*	Coefficient	*p*	Coefficient	*p*
Rhizopsammia manuelensis	8.523	0.3900	19.989	0.3128	-6.916	0.0135*	58.190	0.1576
Scleractinia (tan/purple - solitary)	-0.523	0.5324	0.210	0.9027	-0.212	0.4544	8.478	0.2958
Scleractinia (white - solitary)	0.023	0.9146	-0.097	0.8180	-0.056	0.4228	1.359	0.3776
?Paracyathus pulchellus	-0.133	0.4278	0.199	0.5611	-0.026	0.6605	1.768	0.3346
Stenogorgiinae (tan/orange)	-0.151	0.1643	-0.104	0.6562	0.077	0.0182*	-0.126	0.8380
Porifera (yellow encrusting)	0.115	0.3992	0.170	0.5411	-0.080	0.0544	0.594	0.6316
Nicella goreaui	-0.049	0.6582	0.078	0.7249	0.069	0.0311*	-1.432	0.1092
10-armed crinoids	0.052	0.5890	0.283	0.1183	-0.009	0.7799	-0.609	0.2887
Didemnidae	0.155	0.1423	-0.100	0.6615	-0.051	0.1612	0.525	0.6942
Thesea sp. (small - whitish)	-0.062	0.7150	-0.438	0.1696	-0.009	0.8786	0.029	0.6018
Bebryce sp.	0.047	0.3384	-0.197	0.0215*	-0.015	0.3849	0.081	0.8575
Antipathes ?furcata	0.185	0.0499*	0.052	0.8121	0.019	0.5967	-1.004	0.4107
Porifera (orange - encrusting)	0.028	0.7398	0.177	0.2817	-0.051	0.0416*	0.307	0.5294
Ellisella sp.	0.140	0.0023**	0.006	0.9649	-0.004	0.8632	-0.485	0.5012
Madracis myriaster	-0.021	0.5610	0.059	0.4126	-0.003	0.8100	0.326	0.4057
Scleractinia (large white solitary)	0.126	0.0060**	-0.008	0.9462	-0.001	0.9629	-0.356	0.5904
?Stylopoma spongites	-0.047	0.4218	-0.060	0.6197	0.016	0.4210	0.027	0.3966
Madrepora carolina	0.020	0.5669	-0.019	0.7811	0.016	0.1543	-0.095	0.7584
Antipathes sp.	0.017	0.4533	0.035	0.4466	0.007	0.3787	-0.057	0.8410
Stylocidaris affinis	0.020	0.5538	0.037	0.5845	-0.017	0.1158	0.090	0.5221
Thesea sp. (pink)	0.006	0.7807	-0.067	0.1167	-0.001	0.8967	0.022	0.4084
Antipathes ?atlantica	-0.015	0.3626	0.056	0.0713	-0.003	0.5579	0.072	0.3233
?Stichopathes lutkeni	-0.018	0.2949	-0.006	0.8614	0.009	0.1361	0.018	0.5957
Scleractinia (orange solitary)	-0.007	0.6704	0.047	0.1163	-0.004	0.4318	0.007	0.7831
Total Density Dominant Ahermatypic Corals	8.068	0.4425	20.215	0.3342	-7.221	0.0149*	70.606	0.1497
Total Density Dominant Octocorals	0.106	0.6396	-0.731	0.0738	0.099	0.2437	-2.480	0.1580
Total Density Dominant Antipatharians	0.166	0.1404	0.140	0.5650	0.033	0.4164	-0.970	0.5049
Total Density Dominant Poriferans	0.047	0.8782	0.762	0.1855	-0.144	0.1307	0.161	0.9217
Total Density Dominant Ectoprocts	-0.190	0.2595	-0.370	0.2784	0.036	0.5463	-0.110	0.8463
Total Density All Dominant Taxa	8.244	0.4285	19.966	0.3369	-7.290	0.0123*	67.218	0.1532
Total Number of Taxa	-1.041	0.1011	0.311	0.8261	0.366	0.0891	-3.134	0.6938

* Regression coefficient is significantly different from zero ($p<0.05$).
** Regression coefficient is highly significantly different from zero ($p<0.01$)

Table 8.3. Correlation coefficients between hard bottom epifaunal taxa.

	Rhizopsammia manuelensis	Scleractinia (tan-purple solitary)	Scleractinia (white solitary)	*?Paracyathus pulchellus*	Stenogorgiinae (tan/orange)	Porifera (yellow encrusting)	Crinoids (10-armed)	Didemnidae	*Antipathes ?furcata*	Porifera (orange encrusting)	*Ellisella* sp.	*Madracis myriaster*	Scleractinia (large white solitary)	*Madrepora carolina*	*Antipathes* sp.	*Stylocidaris affinis*	*Thesea* sp. (pink)	*Antipathes ?atlantica*	*?Stichopathes lutkeni*
Scleractinia (tan-purple solitary)	0.363																		
Scleractinia (white solitary)	0.595	**.794***																	
?Paracyathus pulchellus	0.380	**.943****	**.784***																
Stenogorgiinae (tan/orange)	-0.521	-0.240	-0.089	-0.054															
Porifera (yellow encrusting)	0.310	-0.364	-0.433	-0.363	-0.452														
Crinoids (10-armed)	0.201	-0.431	-0.338	-0.350	-0.132	0.456													
Didemnidae	0.051	-0.320	-0.414	-0.358	-0.430	**.824****	0.054												
Antipathes ?furcata	-0.103	-0.220	-0.154	-0.204	-0.252	-0.061	0.424	0.104											
Porifera (orange encrusting)	0.466	-0.290	-0.304	-0.286	-0.408	**.916****	0.600	0.536	-0.211										
Ellisella sp.	0.143	-0.222	-0.068	-0.251	-0.466	0.083	0.325	0.269	**.923****	-0.084									
Madracis myriaster	0.436	**.692***	**.727***	**.846****	0.203	-0.254	0.030	-0.395	-0.105	-0.114	-0.206								
Scleractinia (large white solitary)	-0.047	-0.304	-0.244	-0.295	-0.365	0.239	0.324	0.492	**.910****	-0.023	**.926****	-0.228							
Madrepora carolina	-0.298	-0.067	0.071	0.077	0.477	-0.324	0.258	-0.175	0.603	-0.411	0.375	0.399	0.471						
Antipathes sp.	0.051	0.145	0.153	0.254	0.031	-0.361	0.228	-0.287	**.706***	-0.395	0.607	0.377	0.509	**.666***					
Stylocidaris affinis	**.899****	0.455	**.804****	0.456	-0.325	-0.067	0.070	-0.284	-0.110	0.152	0.083	0.509	-0.171	-0.182	0.052				
Thesea sp. (pink)	0.270	0.255	**.679***	0.171	0.220	-0.497	-0.356	-0.434	-0.239	-0.359	-0.110	0.241	-0.326	0.075	-0.054	0.565			
Antipathes ?atlantica	0.401	-0.038	-0.074	0.054	0.047	0.339	0.583	-0.188	-0.312	0.621	-0.332	0.326	-0.409	-0.138	0.057	0.230	-0.125		
?Stichopathes lutkeni	-0.280	-0.306	-0.165	-0.169	**.802****	-0.258	0.036	-0.372	-0.281	-0.145	-0.382	0.142	-0.392	0.329	0.177	-0.227	0.265	0.441	
Scleractinia (orange solitary)	0.312	-0.242	-0.269	-0.206	-0.104	0.533	**.806****	-0.002	-0.131	**.783***	-0.169	0.101	-0.198	-0.123	-0.072	0.127	-0.249	**.905****	0.233

* Correlation coefficient is significant ($p<0.05$)

** Correlation coefficient is highly significant ($p<0.01$)

site. A more fruitful approach may involve estimating important physical variables for each photograph and testing the entire data set for significant relationships. This will be especially important for defining assemblages of epibiota that may co-occur within random photographs. For example, taxa may contribute only moderate amounts to the overall density at a site, but their distribution within the site may be very restricted (e.g., within the zone consistently exposed to a nepheloid layer).

A tiered analysis strategy is planned. Generally, physical variables will be reduced/simplified using canonical and partial correlation analysis. Ordination and classification analyses will be used to explore patterns and structure in the biological data and to identify species groupings for further analysis. Strong relationships between biological groupings and physical variables will be identified through discriminant analysis and canonical correlation analysis. Finally, statistical testing for relationships to environmental variables will be conducted using a general linear/non-linear models approach. Prior to statistical analyses, assumptions will be tested and, if necessary, data will be transformed or nonparametric methods will be used, depending on the nature of the data.

Despite the preliminary nature of the results presented in this report, several of the findings conflict with those reported by others. For example, Gittings et al. (1992b) reported abundances of *Rhizopsammia* and overall organism abundances were positively related to distance from the Mississippi River at a range of 27 to 70 km, but we report abundances of this species and the combined densities of the 43 dominant taxa are negatively related to distance from the river at a range of 70 to 145 km. We do not know whether this contradiction is enigmatic or whether it indicates abundance maxima at approximately 70 km from the Mississippi. Also, in contradiction to the high organism abundances and species richness associated with high vertical relief by Pequegnat (1964), Genin et al. (1986), Messing et al. (1990), Gittings et al. (1992b), and Hardin et al. (1994), the results presented here do not indicate increases in the density of epibiota or number of taxa with increasing vertical relief. Moreover, the only significant regression coefficient for the association between a taxon and vertical relief was negative (Table 8.2, *Bebryce* sp.). The influence of vertical relief was observed within 1 to 2 m of the seabed at 105 to 212 m water depth off California (Hardin et al. 1994), and we do not know whether the range of vertical relief at most of the sites in the current study is much greater than that over which the effect might occur in the Gulf of Mexico, as well. The more detailed statistical analyses planned for future reports should help address these questions.

Chapter 9
Fish Communities

In this program component, fish communities are being studied by analyzing photographs and videotapes recorded from an ROV during hard bottom community monitoring (see Chapter 8). Trophic interrelationships are being studied by reviewing literature from the Gulf of Mexico and South Atlantic Bight. In future reports, these data and literature will be used to describe fish communities associated with the pinnacle features and delineate their ecological roles.

Approach and Rationale

The objectives of this program component are to

- describe fish community composition, taxonomic richness, and temporal dynamics at each monitoring site;
- identify differences in fish community composition among sites differing in relief and location;
- identify relationships between fish communities and environmental parameters such as small-scale habitat variability, rock type, sediment cover, etc.; and
- identify trophic relationships among fishes, as well as between fishes and the epibenthic community.

These objectives are being addressed by analyzing photographs and videotapes recorded by the ROV during routine hard bottom monitoring (see Chapter 8). The program does not include any "dedicated" fish censusing or sampling. Nevertheless, the photographs and video collected while performing other tasks will provide images suitable for qualitative analysis of fish assemblages. The data obtained will consist of species occurrences that can be partitioned by site, time (cruise), and habitat (substrate). This report provides the ongoing results of the first two objectives.

Methods

Field Methods

Because qualitative data are being extracted opportunistically from video transects not specifically made for fishes (i.e., epibiota), the field methods will be identical to those described for hard bottom community assessment in Chapter 8. Only the aspects of these methods most important to fish assessment need to be restated. Two video cameras simultaneously record the path taken by the ROV during its operations; one is forward-viewing for piloting the ROV, the other is downward-viewing perpendicular to the substrate for recording quantitative benthic data. A 35 mm Benthos camera equipped with a Nikkor 28 mm lens and a 200 watt-second electronic strobe is being used to collect

the photographs. The camera is aligned perpendicular to the substrate for all quantitative photographs, and aligned parallel with the downward-viewing video camera. A coordinate laser system mounted on the ROV is being used to estimate proper distance. Still photographs have the high resolution needed for accurate identifications of fishes, particularly small ones, and the video provides redundant images should the still camera fail during a dive.

The most important field task pertaining to the fish data is the collection of random photographs (Chapter 8). Random photographs are collected within eight sectors of a circular plot located within each site. The paths recorded on video by the ROV as it moves from photograph to photograph provide the best data available for characterizing the fish taxa present at each site.

Laboratory Analysis

In the laboratory, videos from both video cameras (forward-viewing and downward-viewing) were examined simultaneously for the presence of fishes. Videotapes from both of these cameras are useful because they produce complementary observations. The forward-viewing camera will often record larger fishes such as amberjacks, snappers, groupers, or sharks that are not seen by the downward camera. On the other hand, the downward-viewing camera records small reef associated species (anthiins, damselfishes, squirrelfishes) not discernable by the forward-viewing camera. Fish species occurrences were recorded for each random path taken within a sector of a site. Also, within each sector, the time spent by the ROV over soft bottom and hard bottom was recorded, and when on hard substrate, the time spent along the vertical face, the surface, or the base of a feature was also recorded. The photographs (35 mm transparencies) are viewed on a large screen film viewer. All fish in the quantitative photographs are identified to the lowest practical taxon and added to the species list for a particular site or sector from which the photograph was taken. All photographic data (including still photographs) collected during ROV operations were reviewed for new species to add to the master species list for the hard bottom features. The final data include frequency of occurrence at all features by area and cruise.

Data Analysis

All data analyzed for this report, with the exception of the overall species list (Table 9.1) which included taxa observed in still photographs, are from videotape analyses. These data consist of presence-absence and frequency of occurrence of fish taxa by transect within the nine study sites. Frequency of occurrence was examined graphically for each cruise separately and for the two cruises combined. The total number of taxa recorded for each site within both cruises was used as an estimate of taxonomic richness. Relationships between richness and two variables (shallowest water depth and sample area) were examined for each site with Pearson's product-moment correlation. Patterns of co-occurrence or association among taxa and similarity among stations were related to pre-defined location (east, central, and west) and relief (high, medium, and low) categories using multivariate analyses. These analyses included classification (cluster analysis) and Correspondence Analysis (CA) ordination of the taxa-by-samples data

matrix. This matrix, consisting of species presence and absence (summed across the eight transects for each site), was constructed for all stations and cruises with only taxa occurring at more than one station-time. This produced a matrix of 18 samples (9 sites x 2 cruises) by 43 taxa, which was entered directly into the correspondence analysis. This same data matrix was converted to a resemblance matrix using a qualitative similarity index, the Phi index (Rohlf 1997), and then clustered. The Phi index measures the degree of association (ranging from -1.0 to 1.0) among samples (normal analysis) or taxa (inverse analysis). This index has been tested with field data and is not greatly influenced by the frequency of occurrence of taxa (Jackson et al. 1989). Both normal and inverse cluster analyses were performed using the Unweighted Pair Group of Averaging (UPGMA) (Sneath and Sokal 1973).

Results

Analysis of videotapes and still photographs from the first two monitoring cruises (1C and M2) revealed a total of 69 fish taxa from 28 families (Table 9.1). The most speciose families were sea basses (Serranidae), squirrelfishes (Holocentridae), lizardfishes (Synodontidae), jacks (Carangidae), wrasses (Labridae), and butterflyfishes (Chaetodontidae). The most frequently occurring taxa in video transects for the combined cruises were roughtongue bass (*Pronotogrammus martinicensis*), short bigeye (*Pristigenys alta*), bank butterflyfish (*Chaetodon aya*), and red barbier (*Hemanthias vivanus*) (Fig. 9.1). Rank occurrence plots of taxa differed between the two cruises as shown in Fig. 9.2. Video transects from Cruise 1C yielded 44 taxa, whereas those taken during Cruise M2 produced 67 taxa. The similarity in taxonomic composition measured by the Phi coefficient for each site between the two cruises ranged from 0.30 at Site 4 to 0.51 at Site 2 as shown in Fig. 9.3. The most frequently occurring taxa showed similar patterns across sites between cruises. Fig. 9.4 shows the frequency of occurrence of the top species by site and cruise.

Taxonomic richness recorded from videotapes for each cruise differed across all sites (Fig. 9.5). During Cruise 1C, the number of taxa observed ranged from 5 at Site 9 to 22 at Site 7 and averaged 15.3 taxa per site. Cruise M2 yielded an average of 20.7 taxa per site, ranging from 13 taxa at Site 6 to 30 taxa at Site 1. The number of taxa was weakly correlated with sample area for the nine sites during both Cruise 1C ($r = 0.38$) and M2 ($r = 0.51$). The correlation between shallowest depth at each site and number of taxa was higher, but still relatively weak for Cruise 1C ($r = 0.55$) and M2 ($r = 0.69$).

The influence of relief category (high, medium, and low relief) and location (east, central, west) on fish assemblage composition in videotapes was examined by cluster analysis and ordination. CA ordination axes 1 and 2 accounted for 15.6% and 13.1% of the variation in the data matrix. When the site scores plotted on CA axes 1 and 2 were labeled as high, medium, or low relief, no distinctive patterns emerged (Fig. 9.6a). When the same site scores were labeled by location (east, central, or west), three eastern sites appeared to separate from the rest along axis 1, while three western sites separated along axis 2 (Fig. 9.6b). Taxa responsible for these patterns observed in the site scores are

shown in the ordination of taxon scores for CA axes 1 and 2 (Fig. 9.7). Normal cluster analysis of the Phi matrix produced four sample groupings, each with differing combinations of location and relief categories (Fig. 9.8). The inverse cluster analysis of the Phi matrix resolved three weakly associated species groups (Fig. 9.9).

Discussion

Qualitative video data collected during the first two monitoring cruises show that the ichthyofauna inhabiting the pinnacle features consists primarily of reef fishes. Pelagic (e.g., sharks, jacks, and bluefish) and demersal (flounders) fishes also were observed, but infrequently when compared with reef species. The most commonly occurring reef fish species including roughtongue bass, tattler, short bigeye, yellowtail reeffish, bank butterflyfish, red barbier, and various scorpionfishes represent the deep reef fish assemblage reported for water depths of 50 to 100 m in the western Atlantic. Similar species were reported by previous investigations of the pinnacle features (e.g., Continental Shelf Associates, Inc. 1985a; Darnell 1991). Similar deep reef fish assemblages have been documented off the southeastern U.S. (Miller and Richards 1980; Parker and Ross 1986; Gilmore et al. 1987), within the lower portion of the Algal-Sponge Zone of the west Flower Garden Banks in the northwestern Gulf of Mexico (Bright and Pequegnat 1974; Boland et al. 1983; Dennis and Bright 1988a), and near the head of De Soto Canyon (Shipp and Hopkins 1978; Continental Shelf Associates, Inc. 1987b). The total of 78 taxa represents about half of the fish fauna known from the hard banks and reefs of the northern Gulf of Mexico (Cashman 1973; Bright and Pequegnat 1974; Smith et al. 1975; Smith 1976; Sonnier et al. 1976; Boland et al. 1983; Dennis and Bright 1988a,b).

The sea bass family (Serranidae) was the most speciose group observed at the study sites. The streamer basses (*Pronotogrammus martinicensis*; *Hemanthias vivanus*) were the most frequently occurring fishes and they probably numerically dominate the pinnacle habitats. These species feed upon plankton and were commonly observed hovering above the substrate picking plankton from the water column. Streamer basses provide forage for a number of piscivorous species (e.g., amberjacks, groupers, sharks, and mackerels). Other serranids frequently observed in the videotapes were tattler (*Serranus phoebe*), blackear bass (*Serranus atrobranchus*), and wrasse bass (*Liopropoma eukrines*). Few larger groupers were seen, with the scamp (*M. phenax*) and snowy groupers (*Epinephelus niveatus*) represented by some large individuals. These species have probably endured heavy fishing pressure along the pinnacle trends. Other frequently occurring species such as short bigeye (*Pristigenys alta*), bank butterflyfish (*Chaetodon aya*), and yellowtail reeffish (*Chromis enchrysurus*) were more closely associated with the substrate.

The cluster analysis of the taxa-by-samples data matrix did not resolve distinctive patterns with respect to location and relief. Inverse and normal cluster analysis produced several groups that reflect the occurrence of species in various samples, but clear associations among species or samples did not emerge in these groupings. The CA

ordination showed some differences related to location, with eastern samples separating from central and western along CA axis 1. Also, western samples showed more variability than the eastern or central samples. High relief sample scores clustered together, but not tightly when compared with low and medium relief sample scores. Qualitative data on the scale of the study area as used here may be too coarse to resolve any differences or similarities that may exist among the sites with respect to location or relief. A closer examination, at the level of transects within sites, along with an analysis of substrate preference of the dominant species, will be undertaken for the final synthesis report. This approach should provide greater insight into the processes structuring these assemblages.

Table 9.1. Preliminary list of fish taxa observed in still photographs and videotapes from each site during Cruises 1C and M2.

Taxa	Site								
	1	2	3	4	5	6	7	8	9
Relief Category:	H	M	L	M	H	L	H	M	L
CARCHARHINIDAE									
Mustelus sp.	--	--	--	--	●	--	--	--	--
Rhizoprionodon terranovae	--	--	--	--	--	--	●	--	--
RAJIIDAE									
Raja olseni	--	--	--	--	--	--	--	--	●
MURAENIDAE									
Gymnothorax kolpos	--	--	--	●	--	--	--	--	--
Muraena retifera	--	--	●	--	--	--	--	--	--
Muraenid sp.	--	●	--	--	--	--	--	--	--
SYNODONTIDAE									
Saurida sp.	--	--	●	--	--	---	--	--	--
Synodus intermedius	--	●	●	--	--	--	--	--	--
Synodus sp.	--	--	●	--	--	●	--	--	--
BATRACHOIDIDAE									
Opsanus pardus	●	--	●	--	--	--	--	●	--
OGCOCEPHALIDAE									
Ogcocephalus corniger	--	--	●	--	--	--	●	●	●
Ogcocephalus sp.	●	●	--	●	--	--	--	●	●
GADIDAE									
Urophycis sp.	●	--	--	●	--	--	--	●	--
OPHIDIIDAE									
Brotula barbata	--	--	--	●	--	--	--	--	--
HOLOCENTRIDAE									
Corniger spinosus	--	--	--	●	--	--	--	--	--
Holocentrus adscensionis	●	--	--	--	--	--	--	--	--
Holocentrus bullisi	●	--	--	--	--	--	--	--	--
Holocentrus sp.	--	--	--	●	--	--	--	--	--
FISTULARIIDAE									
Fistularia petimba	●	--	●	--	--	--	--	--	--
SCORPAENIDAE									
Scorpaena sp.	●	●	●	●	●	●	●	●	--
Scorpaena sp. b	--	●	--	●	--	--	●	--	--
SERRANIDAE									
Anthiin sp.	--	●	--	--	●	●	--	●	●
Centropristis ocyurus	--	--	●	--	●	●	--	--	--

Table 9.1. (continued).

Taxa	Site								
	1	2	3	4	5	6	7	8	9
Relief Category:	H	M	L	M	H	L	H	M	L
Centropristis striata	--	--	--	--	●	--	--	--	--
Epinephelus niveatus	--	--	--	--	--	●	--	●	--
Epinephelus adscensionis	--	--	--	--	●	--	--	--	--
Gonioplectrus hispanus	--	●	●	●	--	--	--	●	●
Hemanthias vivanus	●	●	●	●	●	●	●	●	●
Pronotogrammus martinicensis	●	●	●	●	●	●	●	●	●
Liopropoma eukrines	●	●	--	--	●	●	●	●	●
Mycteroperca phenax	●	●	--	--	--	●	●	--	--
Paranthias furcifer	●	--	--	--	--	--	--	--	--
Rypticus saponaceous	--	--	--	--	--	●	--	--	--
Rypticus sp.	--	--	--	--	--	●	--	--	--
Serranus atrobrancus	--	●	●	●	●	--	--	--	--
Serranus phoebe	●	●	●	●	●	●	●	--	--
PRIACANTHIDAE									
Priacanthus arenatus	●	--	--	--	●	●	●	--	--
Pristigenys alta	●	●	●	●	●	●	●	●	●
APOGONIDAE									
Apogon pseudomaculatus	●	●	●	●	--	●	--	--	--
MALACANTHIDAE									
Caulolatilus sp.	--	--	--	●	--	--	--	--	--
Malacanthus plumieri	●	--	--	--	--	--	--	--	--
CARANGIDAE									
Seriola dumerili	●	●	--	●	●	●	●	--	--
Seriola rivoliana	●	●	--	--	●	--	●	--	--
Trachurus lathami	●	--	●	●	--	--	--	--	--
LUTJANIDAE									
Lutjanus campechanus	--	--	--	●	●	●	●	--	●
Rhomboplites aurorubens	●	--	--	●	●	●	●	--	--
SPARIDAE									
Calamus sp.	--	●	--	--	●	--	--	--	--
SCIAENIDAE									
Equetus iwamotoi	●	●	●	●	●	●	--	●	--
Equetus umbrosus	--	--	--	●	--	●	●	●	●
CHAETODONTIDAE									
Chaetodon aya	●	●	●	--	●	●	●	--	--
Chaetodon ocellatus	--	●	--	--	--	--	--	--	--
Chaetodon sedentarius	●	--	--	--	●	--	●	--	--

Table 9.1. (continued).

Taxa	Site								
	1	2	3	4	5	6	7	8	9
Relief Category:	H	M	L	M	H	L	H	M	L
POMACANTHIDAE									
Holacanthus bermudensis	●	●	--	--	●	●	●	●	--
Holacanthus tricolor	●	--	--	--	--	--	--	--	--
POMACENTRIDAE									
Chromis enchrysurus	●	--	--	--	●	●	●	●	--
LABRIDAE									
Bodianus pulchellus	●	●	--	--	--	--	--	--	--
Decodon puellaris	●	--	●	--	--	--	●	--	--
Halichoeres sp.	●	--	●	--	--	--	--	--	--
BOTHIDAE									
Bothid sp.	--	--	●	●	--	--	--	--	--
Cyclopsetta sp.?	--	●	--	--	--	--	--	--	--
Syacium sp	--	--	--	--	--	--	●	--	--
BALISTIDAE									
Balistes capriscus	--	--	●	--	--	--	--	--	--
Monacanthus sp.	●	--	--	--	--	--	--	--	--
OSTRACIIDAE									
Lactophrys polygonia	●	--	--	--	--	--	--	--	--
Lactophrys quadricornis	--	--	--	●	--	--	--	--	--
TETRAODONTIDAE									
Canthigaster rostrata	●	--	--	--	--	--	●	--	--
Sphoeroides spengleri	●	--	--	--	--	--	--	--	--
DIODONTIDAE									
Chilomycterus sp.	--	--	--	●	--	--	--	--	--
Diodon holocanthus	--	--	--	●	--	--	●	--	●
TOTAL TAXA	34	24	23	26	23	23	24	16	12

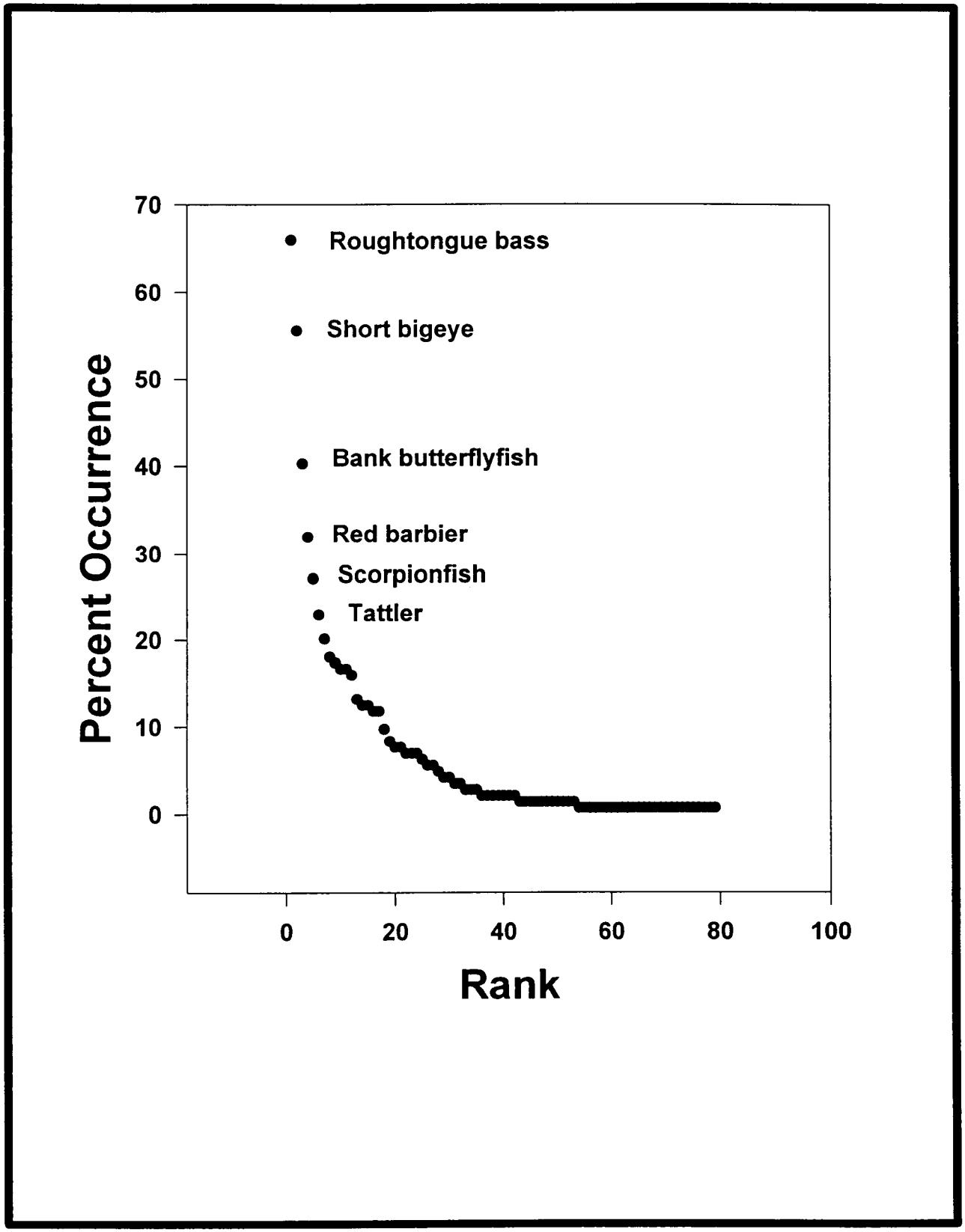

Fig. 9.1. Rank frequency of occurrence of fish species observed in video transects from Sites 1 through 9 for Cruises 1C and M2 combined.

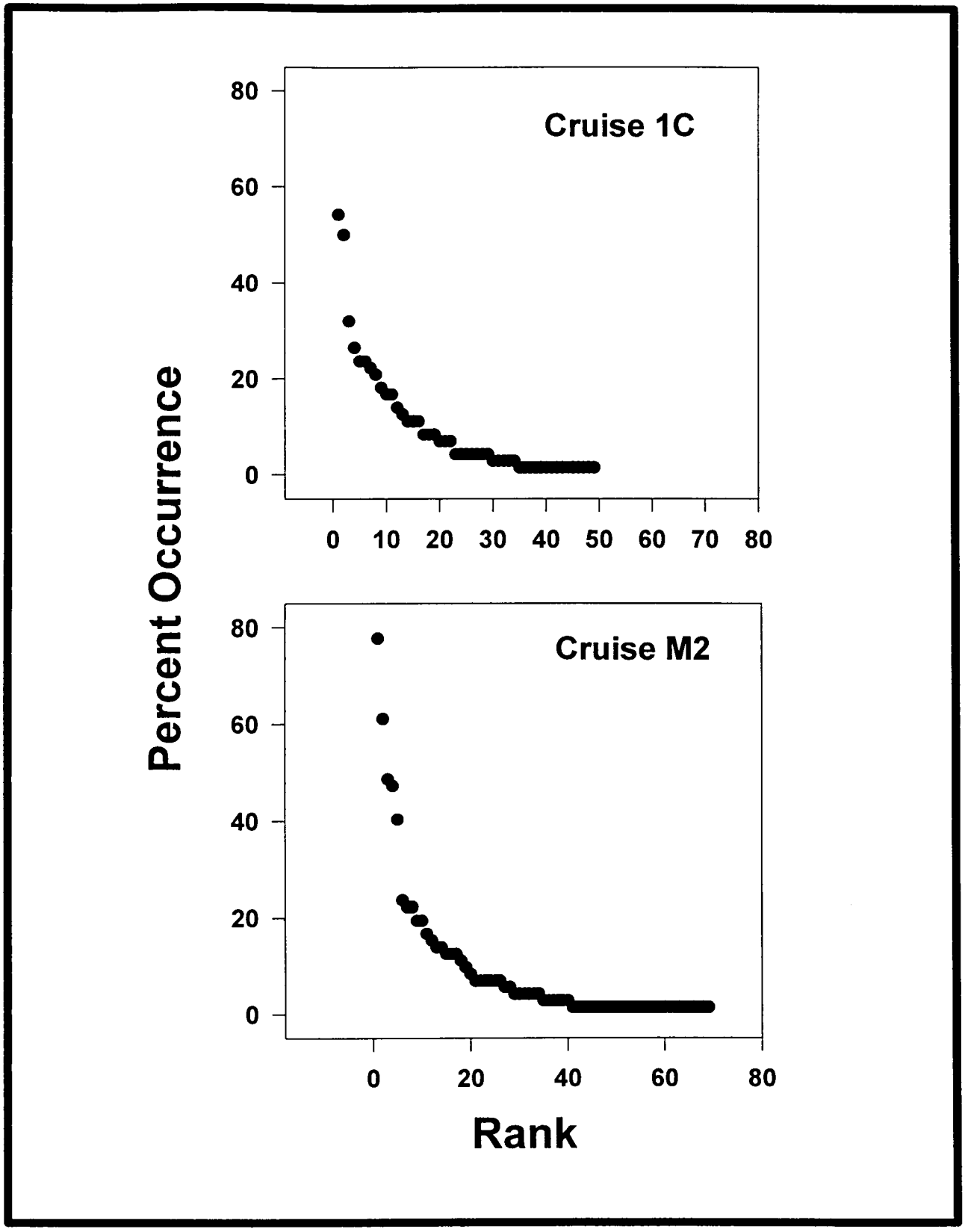

Fig. 9.2. Rank frequency of occurrence of fish species observed in video transects from Sites 1 through 9 for Cruises 1C and M2.

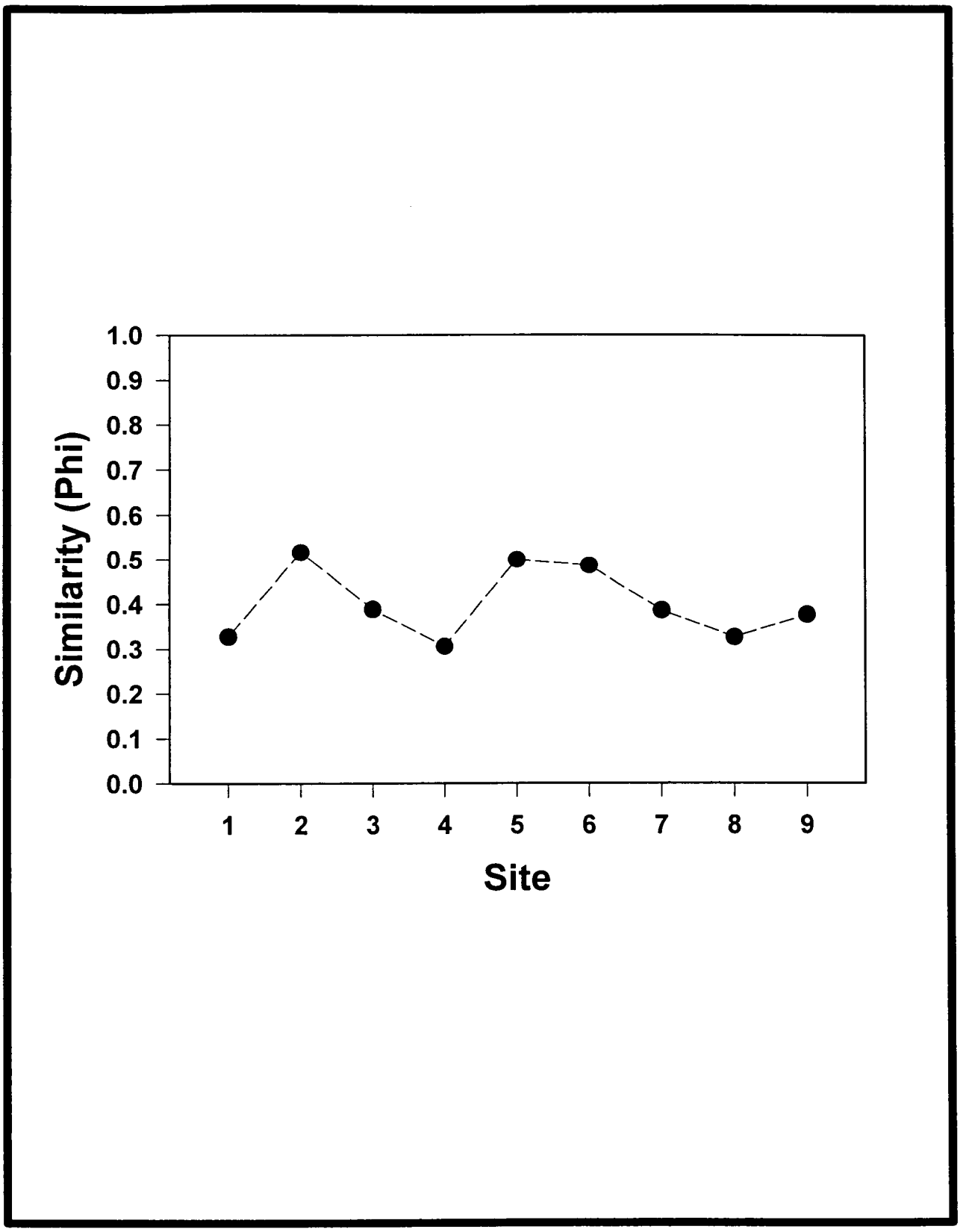

Fig. 9.3. Similarity in fish species composition between Cruises 1C and M2 at all sites.

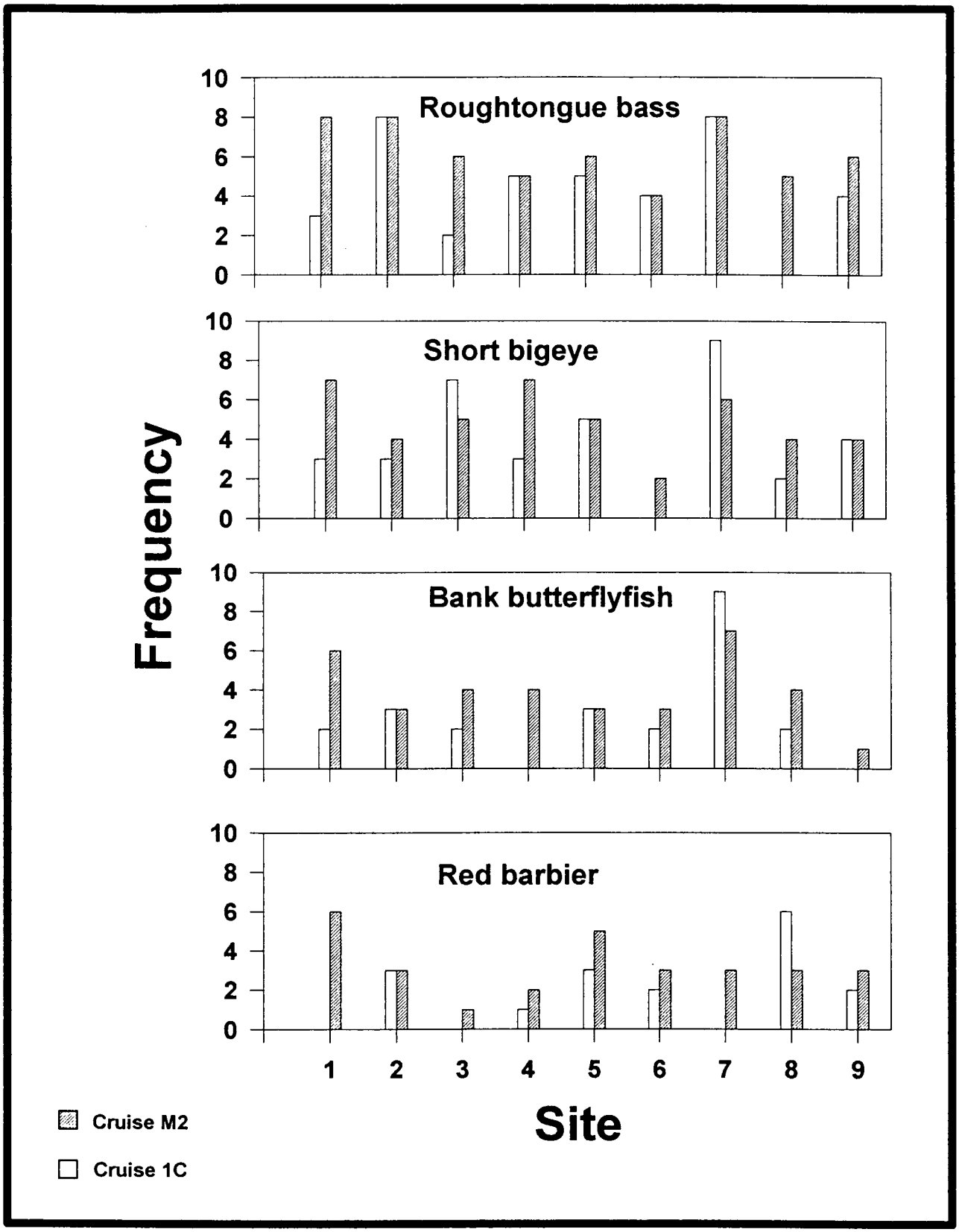

Fig. 9.4. Frequency of occurrence for common fish species in video transects across study Sites 1 through 9 for Cruises 1C and M2.

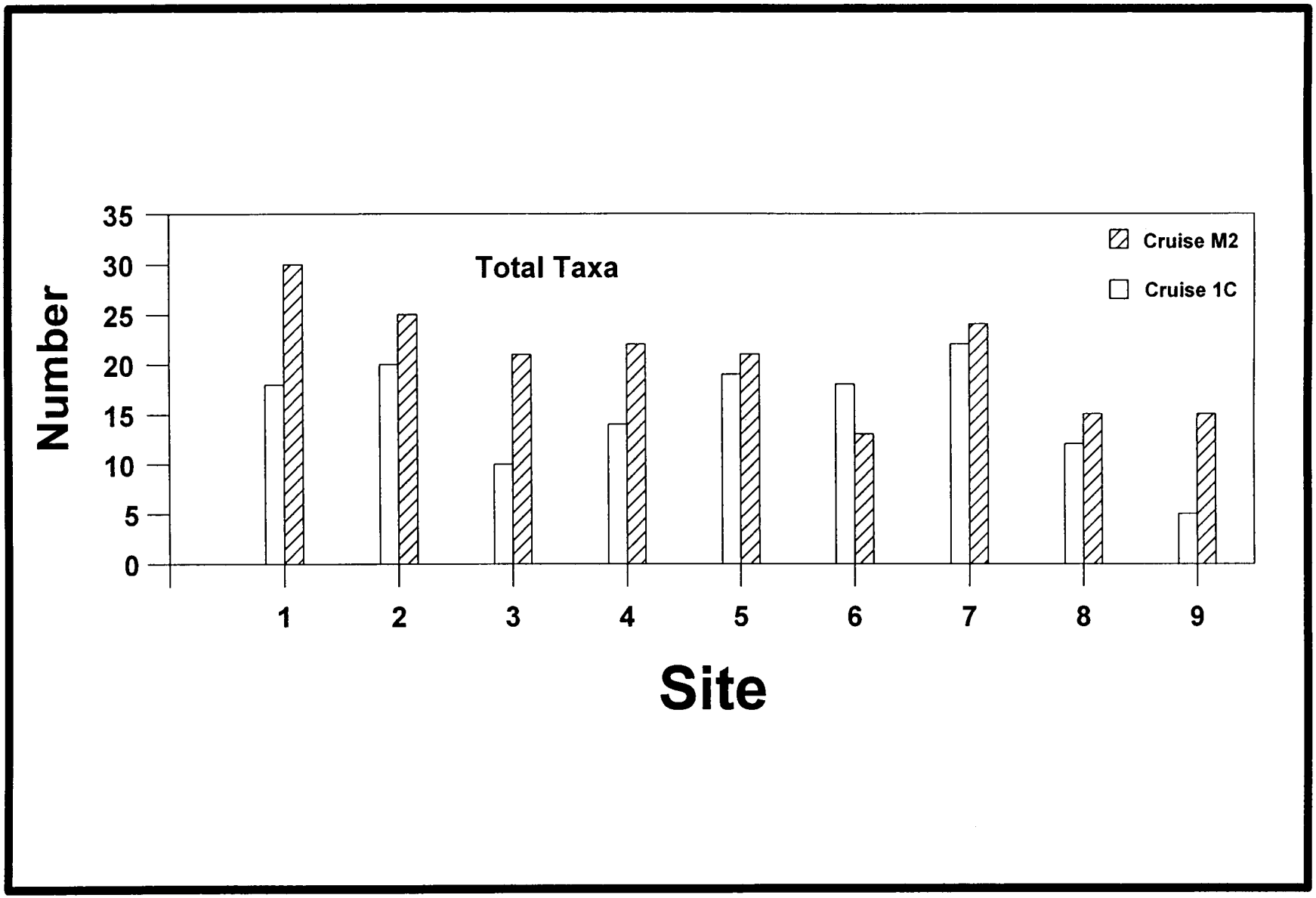

Fig. 9.5. Total fish taxa observed in video transects across study Sites 1 through 9 for Cruises 1C and M2.

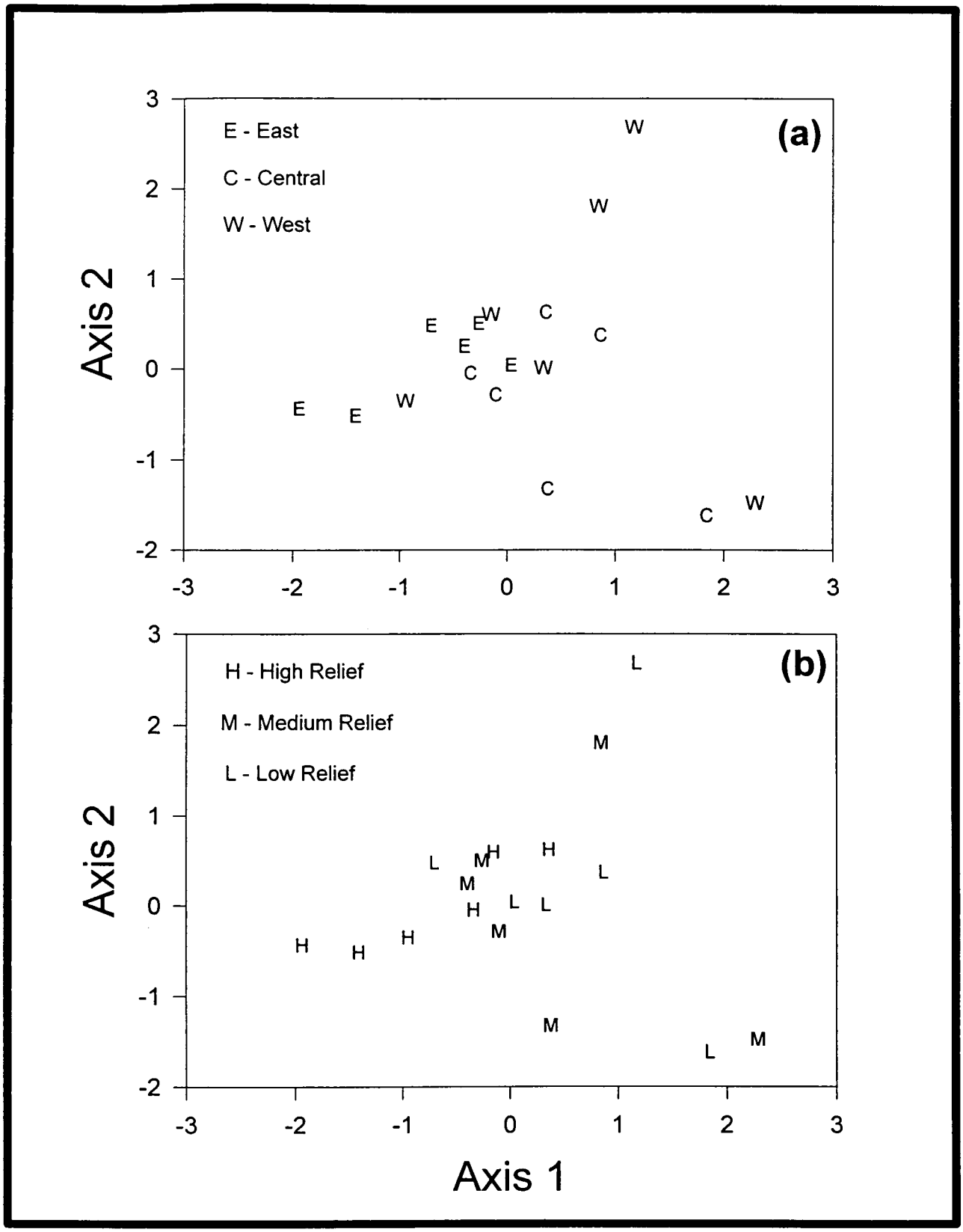

Fig. 9.6. Sample scores from correspondence analysis of a presence-absence matrix based on video transects plotted on Axes 1 and 2. (a) scores labeled by location (east, west, and central); (b) same scores labeled by relief category (high, medium, and low).

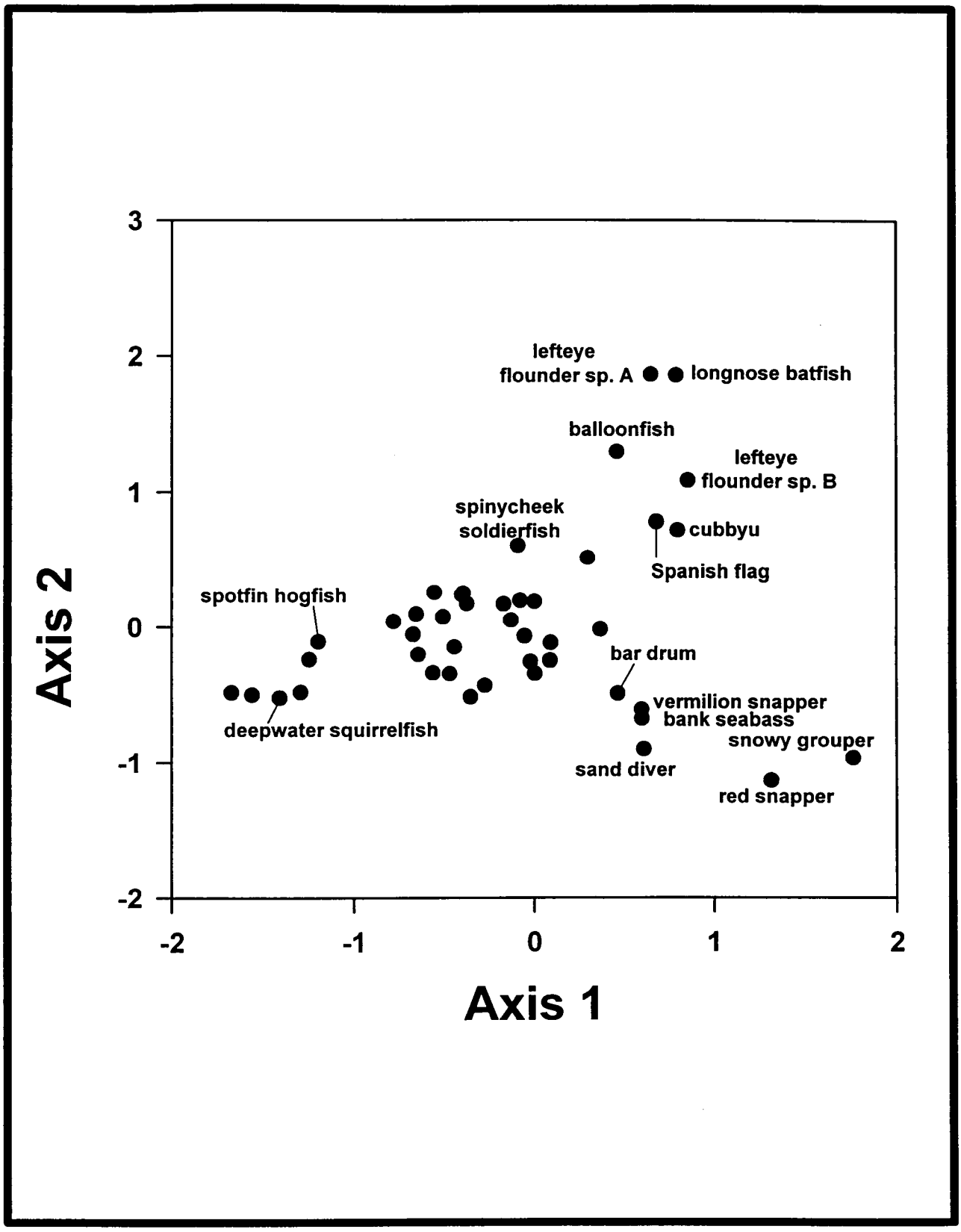

Fig. 9.7. Taxa scores from correspondence analysis plotted on Axes 1 and 2.

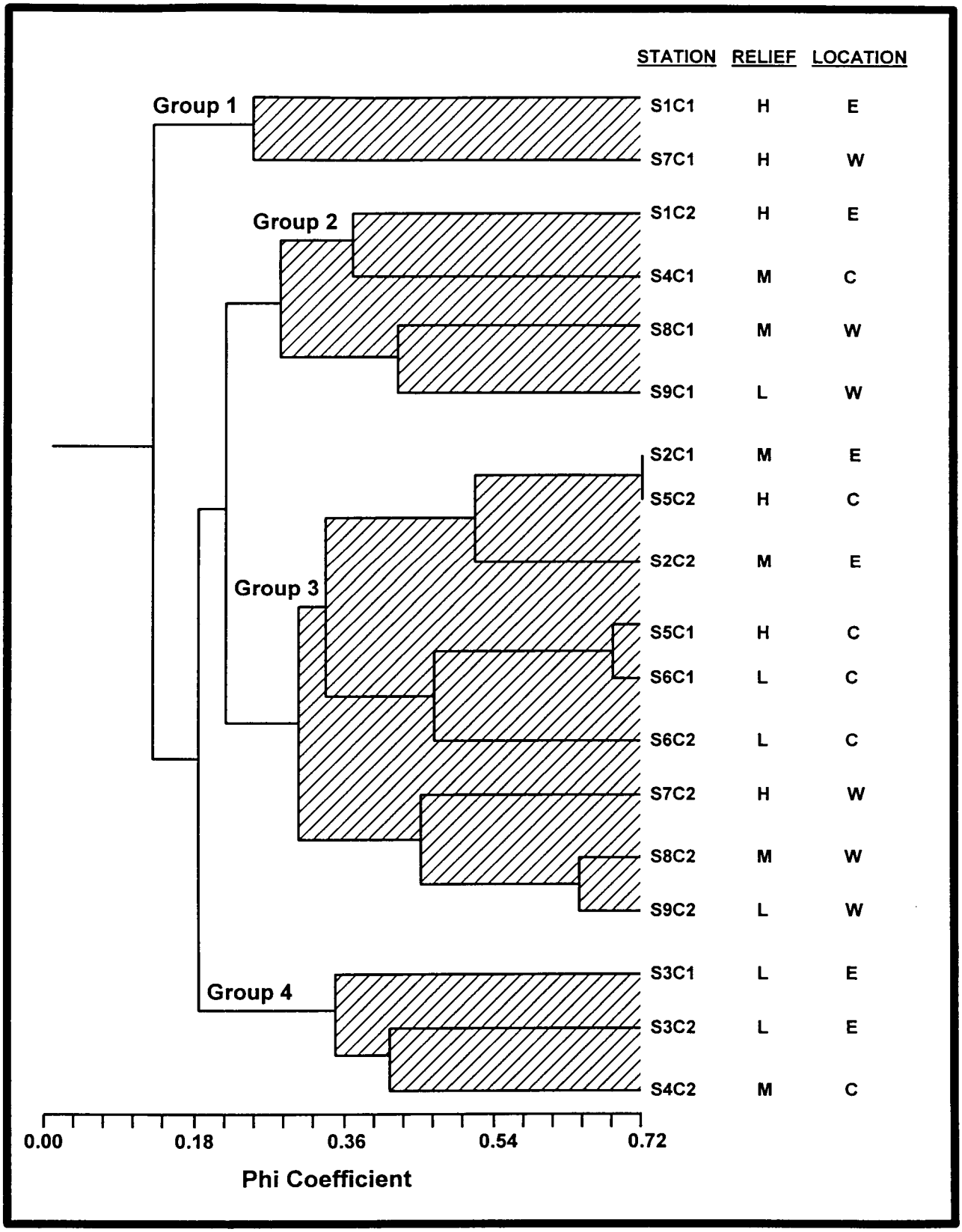

Fig. 9.8. Dendrogram from normal cluster analysis of fish taxa observed in video transects. (Relief: H = high; M = medium; L = low. Location: E = east; W = west; C = central).

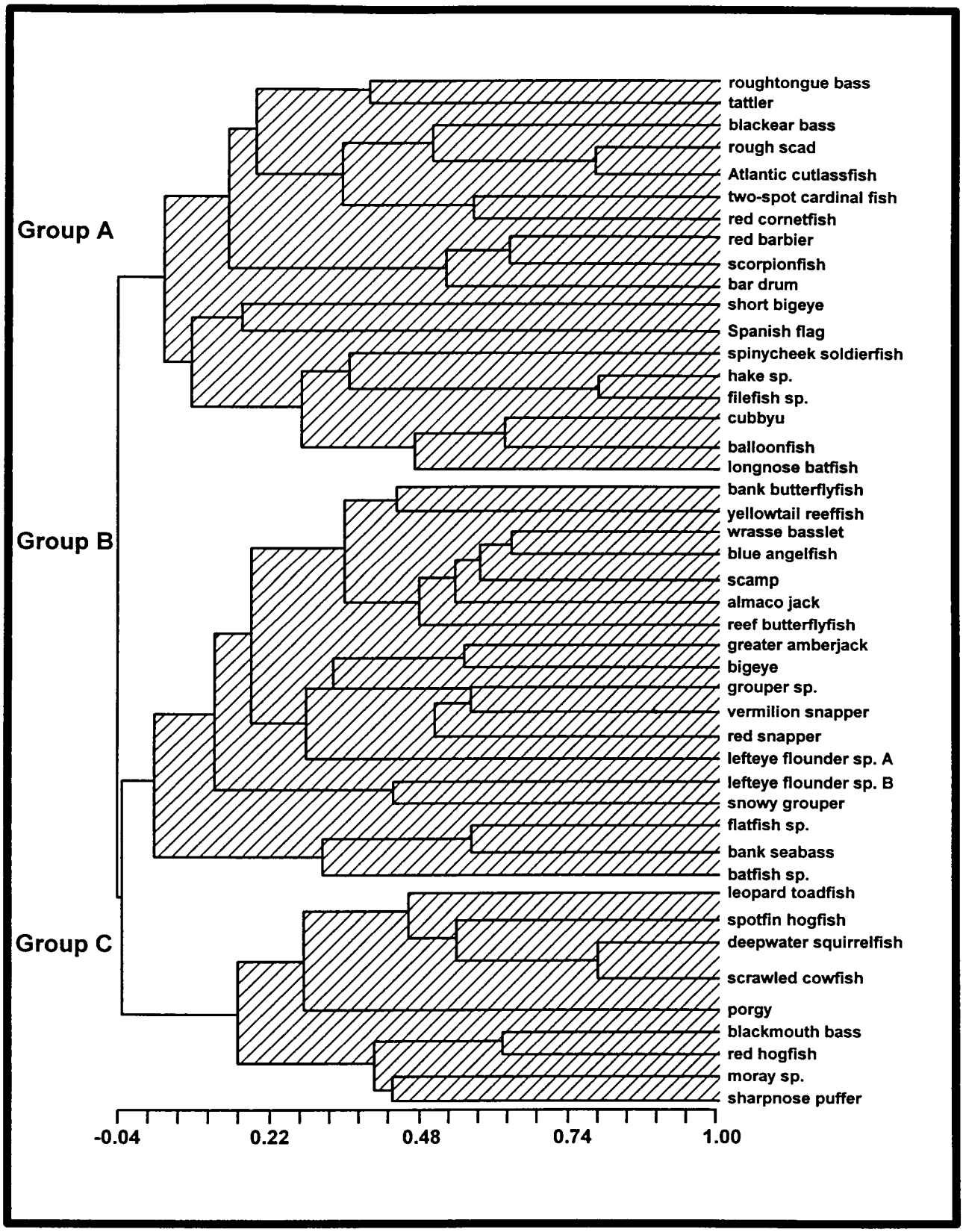

Fig. 9.9. Dendrogram from inverse cluster analysis of fish taxa observed in video transects.

Chapter 10
Companion Study: GIS and Micro-Habitat Studies

Approach and Rationale

This program component focuses on relationships between the physical environment and the composition, abundance, and health of a marine, hard bottom ecosystem. Study sites consist of bottom regions, approximately 1 to 5 ha in area, centered on structures that belong to the low, medium or high relief categories. Measurements for hard bottom community structure and dynamics include fine-scale photographs collected in a randomized design across the sites during each cruise and the video record while the ROV is transiting between photo stations. Hard bottom community structure and dynamics results are suitable for general description of the individual sites as a whole, for determination of ecosystem health, and for statistical comparison among sites and seasons. One goal of the program is to test hypotheses concerning differences in the major fauna within sites that result from specific abiotic factors.

GIS techniques have been used to integrate available data into consistent map formats and standardized displays. Essentially, what GIS allows is construction of maps with multiple overlays, e.g., depth contours with random photo stations displayed as symbols that indicate the local geology. GIS provides one means by which further integration among the various program elements can be achieved as new results are forthcoming. In this application, inter-layer comparisons are used to develop new data--for example, to evaluate abiotic differences among random stations that were sampled quantitatively by photography. For this report, GIS was used to determine the average exposure to currents at random photo stations in Megasite 1 as a demonstration of the application. Subsequent analyses will make more extensive use of this technique.

Eventually, the micro-habitat study will incorporate appropriate physical measurements with biological observations. These results will combine the descriptive statistics from the hard bottom community structure and dynamics effort with the micro-habitat categorizations in a cross-cutting design. The micro-habitat study will provide a control on the within-site variability of the sessile community that can be used to determine the influence of abiotic factors--particularly current direction and the effect of pinnacle slope on current intensity.

The direct influence of current direction upon benthic fauna has been documented in several previous studies. Rowe and Menzies (1968) predicted the seafloor extent of the Gulf Stream on the continental slope off North Carolina based on photographs of two decapod species that tended to face into the current. Heezen and Hollister (1971) published numerous photographs in which fish, sponges, or other deep-sea animals act as current vanes. Time-averaged effects become evident when sessile animals have a fixed and axially asymmetric growth form that enhances survival if turned into prevailing currents. Such effects have been noted in scleractinian corals such as *Agaricia agaricites*, which can display bifacial growth forms (Helmuth and Sebens 1993). Orientation is particularly distinctive among the fan-shaped gorgonians in which the

colony of polyps occupies ramie arrayed from a central holdfast along a predominant vertical axis or blade (Barham and Davies 1968). Early investigators proposed that turning the plane of the fan normal to a current would minimize tortional stress to the holdfast (Wainwright and Dillon 1969; Grigg 1972). Subsequent work showed that it also maximized feeding efficiency by the colony of polyps (Leversee 1976; Velimirov 1983; Dai and Lin 1993). MacDonald et al. (1996) have recently measured precisely the distribution and orientation of almost 1,000 gorgonians in an area of approximately one square kilometer and therefore compiled a more comprehensive data set than had been previously available. They also obtained a diverse set of physical measurements to validate and complement the biological observations. Together, these results demonstrated the influence of circulation patterns at a community level and considered the role of fine-scale topographic features in determining this effect.

Methods

Geographic Information System

The data available from the different program elements are either raster type, such as side-scan sonar images or bathymetric grids, or point type data--primarily locations where samples were collected. To compile a complete GIS, the raster data were first processed to a common Universal Transverse Mercator (UTM) projection at meter scale. The north-UTM zone was 16 and the spheroid was Clark 1866. The side-scan sonar images were geo-rectified with ER Mapper software by applying the registration points provided by the side-scan subcontractor (C&C Technologies). The rectified images were imported to series of ARC View 3.0a projects projected as backdrops over which point-type data from mooring locations, grab samples, or random photo stations could be overlain.

Subsets of all bathymetric data were compiled in 300 by 300 m areas centered on the pinnacle or pinnacles in the candidate sites. These data, which contained unavoidable gaps because of the limits of the swath side-scan bathymetry methodology, were fitted to a 1 m grid by use of routines in PV Wave. These 300 by 300 m grids were then contoured to provide base maps for use during ROV operations and analyzed to objectively determine the boundaries of the sites. This procedure has been described in detail in previous reports. For the GIS, depth contours were calculated and saved as separate GIS layers.

Modeling Current Direction

A simple flow model was derived as a preliminary step toward using regional current meter data in conjunction with a realistic hydrodynamic model to approximate current flow on a scale that is compatible with the spatial resolution of other data sets. This will serve as a foundation for more detailed modeling efforts as well. This model can provide a crude approximation of current intensity on a several meter scale across each of the detailed survey sites.

Three hundred square meter details of side-scan sonar data encompassing each of the nine monitoring sites served as a basis for the model. Using a 300 x 300 element grid of 1 m resolution bathymetric data, values for depth, slope, and direction were obtained for each element (pixel) of the matrix.

A first order polynomial fit through 5 m lengths centered on each pixel provided values for change in depth (dz) in both the X and Y directions. A slope was then calculated and assigned to each pixel.

$$Slope = \tan^{-1}(\mathrm{sqrt}\{(dz_x^2 + dz_y^2) / 5\})$$

The current velocity in a direction perpendicular to each point could then be calculated using the pixel orientation along with a mean current vector taken from the most appropriately positioned current meter.

$$\textit{Perpendicular component of current velocity} = \textit{current velocity x } [\cos(\textit{pixel direction} - \textit{current direction})]$$

The geometry of this formulation results in perpendicular current velocities that are positive for pixels facing into the current and negative for those facing away. This sign convention establishes a distinction between "upstream" and "downstream" regions. The degree to which any given pixel is exposed to these perpendicular currents would then depend upon its slope value. As a way of determining relative exposure to the flow of current, the slope and geometry of each pixel were used to calculate a cross-sectional area in the direction of flow.

$$\textit{Area} = (\textit{pixel length}) \times (\textit{pixel width}) \times (\tan(\textit{slope}))$$

By multiplying this value with the current velocity, a flux representing the hypothetical flow of water across the pixel area was obtained and employed as an indicator of relative current exposure.

$$\textit{Flux or relative exposure} = (\textit{perpendicular velocity}) \times (\textit{area})$$

Exporting the data generated by this model into a GIS format allows current flow characteristics to be easily associated with any other data point.

Results and Discussion

Geographic Information System

The ARC View GIS analysis completed for this report incorporated data from Cruises 1A, 1B, and 1C as well as limited information from Cruise M2 (sediment grabs). Data were included where analyses were complete or substantially complete and where transcription into digital files was finished. Table 10.1 summarizes the GIS data set.

Table 10.1. Summary of mapped data presently incorporated in ARC View GIS. All data are positioned with UTM XY meter coordinates.

Layer Type	Study Areas	Comments
Side-scan sonar mosaics	Megasites 1, 2, 3, and 5 Monitoring Sites 1, 2, 3, 4, 5, and 6	Discussed in Chapter 4
Bathymetric grid at 1-m resolution	Monitoring Sites 1 through 9	Displayed as bathymetric contours
Geologic interpretations of Cruise 1C photo stations	Monitoring Sites 1 through 9	Discussed in Chapter 4
Cruise 1C and M2 grabs	All locations	Discussed in Chapters 4 and 6
Cruise 1C mooring locations	All moorings	Discussed in Chapters 5, 7, and 11

The side-scan sonar mosaics included large images of the entire megasite areas as well as smaller detailed mosaics that were collected in areas of special interest, some of which were later selected as monitoring sites (see Chapter 3, Site Selection). All bathymetric grids were derived from the smaller mosaics and these grids were crucial for site selection. A minor problem was encountered due to slight but noticeable navigation offsets between the large and small mosaics. The cause was most likely the fact that the track-lines for the large mosaics were north-south while track-lines in the small mosaic ran east-west. This produced slight differences in the correction used for the lay-back of the side-scan sonar tow vehicle. The result was that sampling locations plotted on the uncorrected large mosaics were 20 to 35 m away from the pinnacle in some cases. This was corrected, where necessary, by re-registering the large mosaics to the positions of identical features present in the small mosaics.

As the program progresses, additional data will be incorporated into the GIS. This can be readily accomplished with tabular data as long as the data are stored in spread sheet format and UTM XY coordinates are provided for each line of data. The entire GIS data set will be distributed to program participants at regular intervals and will be delivered on CD ROM, following QA and client review, at the conclusion of the program.

Preliminary Current Exposure Model

The purpose of this effort was to produce a preliminary analysis of pinnacle bathymetry and current direction that would delineate regions of monitoring sites that are subject to qualitatively different exposure to prevailing current. Bathymetric grids from monitoring Sites 1, 2, and 3 were processed. Average current vectors recorded by the Cruise 1 deployment of the meters 16 m above bottom at moorings 1B and 1C were applied to determine current direction. These stations are designated as high relief, medium relief, and low relief pinnacles according to program guidelines.

The results for the three sites are shown in Figs. 10.1, 10.2, and 10.3. Generally, these plots show a relatively uniform exposure in the middle range, with localized pockets of relatively higher or lower exposure. It needs to be emphasized that each plot shows relative values for comparison within a given monitoring site, not absolute values that could be compared between monitoring sites. Overall, the values suggest that bathymetry exercises the greatest influence to create variable current exposure at monitoring Site 2, where the spread of random photo stations encompasses all sides of the pinnacle. At monitoring Site 1, the high relief site, much of the actual study area is the flat top of the pinnacle, which was toward the up-current side of the site. There were, however, areas of apparent shadowing on the northwest margin of the feature. As might be expected, the low relief site showed the least variability at spatial scales that could be detected in the bathymetric grid. It is likely that more pronounced differences in current exposures do occur--on the up-current and down-current sides of a boulder for example--but it is not possible to model these differences with the available bathymetric data.

This highly simplified model does not take into account differences due to turbulent flow across the pinnacles. Nor does it delineate topographic steering that evidently occurs in the near-bottom layer. Data presented in Chapter 7 show that the uniform current vector in Megasite 1 was consistently to the northeast throughout the first deployment period. A mean current vector would be less valid for determining exposure if there were frequent reversals in flow direction as occurred during subsequent intervals. The data do show which regions of the sites would be most prone to local turbulence.

Use of the GIS software will make it possible to extract the current exposure at each random photo station. This information will be another independent variable that can be used to distinguish among factors that may control the local attributes of the benthic communities within the study sites.

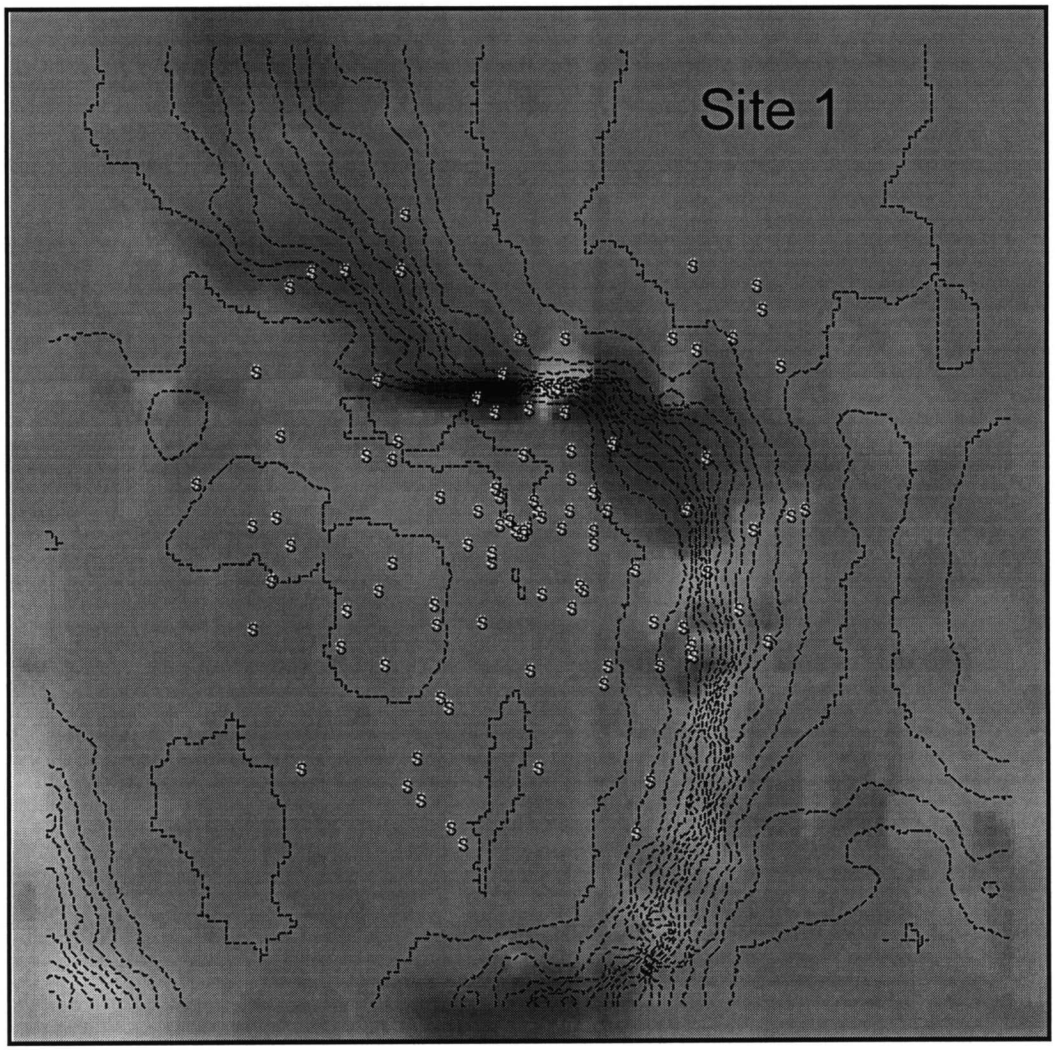

Fig. 10.1. Relative current exposures at Cruise 1C random photo stations for Site 1. Contours are 1 m.

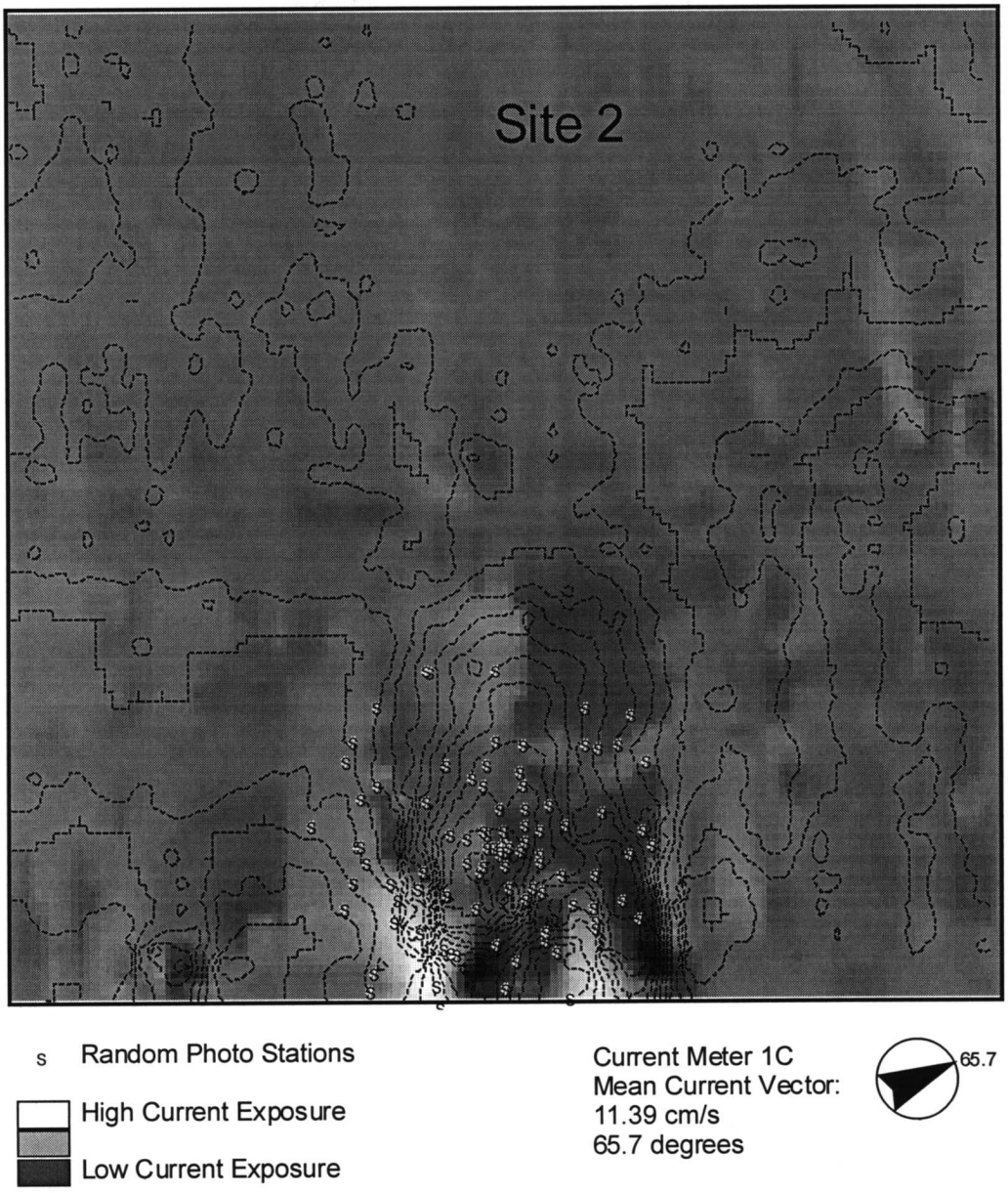

Fig. 10.2. Relative current exposures at Cruise 1C random photo stations for Site 2. Contours are 0.5 m.

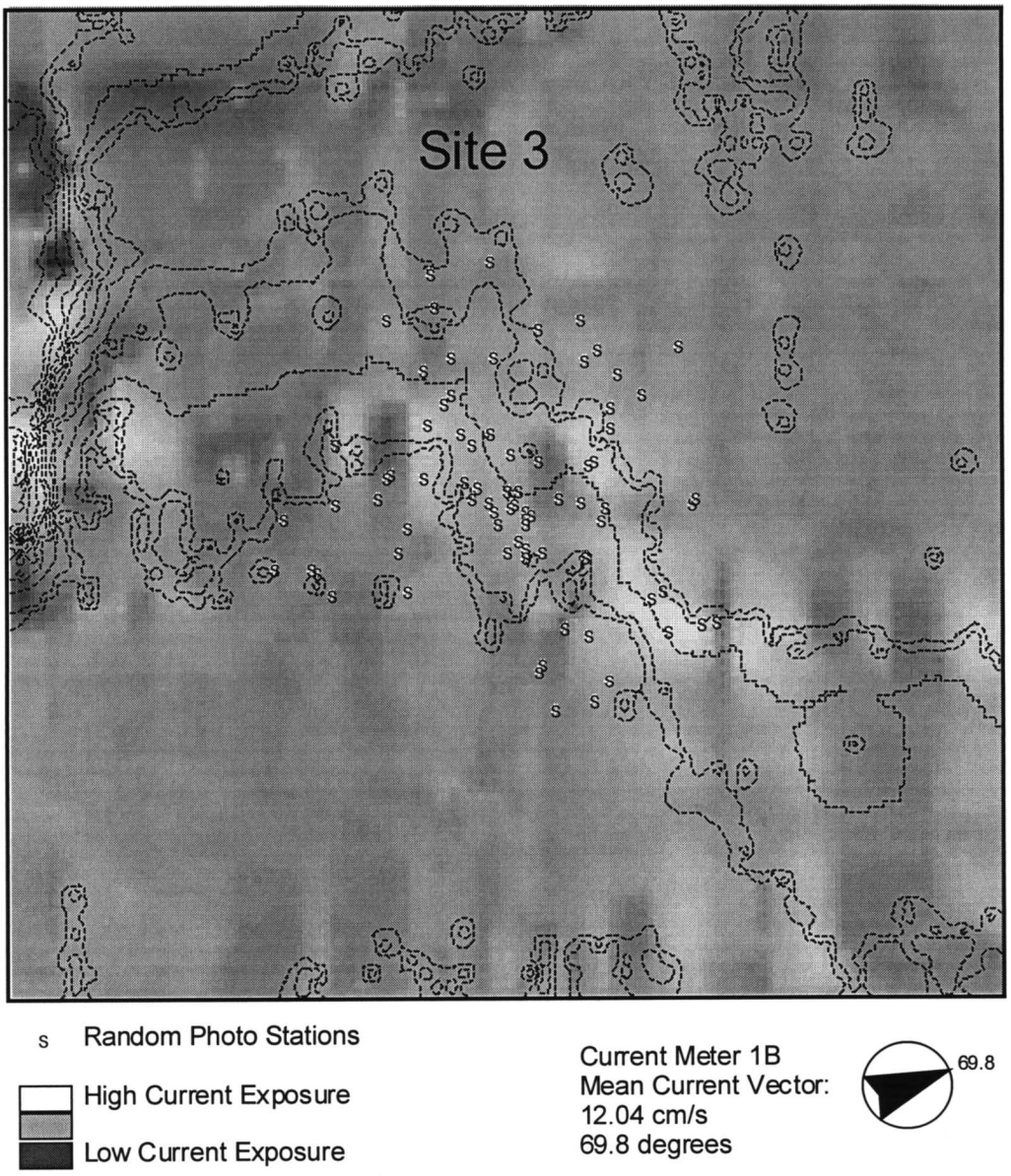

Fig. 10.3. Relative current exposures at Cruise 1C random photo stations for Site 3. Contours are 0.4 m.

Chapter 11
Companion Study: Epibiont Recruitment

Approach and Rationale

The goal of this companion study is to support the descriptive and monitoring portions of the program with experiments (based on testable hypotheses) that define ecological mechanisms responsible for spatial and temporal changes in hard bottom epifauna. Spatial and temporal variation of hard bottom communities are functional responses to biotic and abiotic processes. There are primarily three biological processes: recruitment, competition, and predation. Abiotic processes affecting spatial and temporal variability in shallow coastal zones include seasonal temperature and salinity changes, desiccation, abrasion due to waves, turbidity due to resuspended sediments, turbulence, and stochastic disturbance events. In deep water (e.g., the pinnacle habitat) temperature, salinity, and desiccation are not important determinants, but abrasion, turbidity, turbulence, and stochastic disturbance events may play an important role in the changes of abundance and biomass of epibionts.

Mechanisms that control biotic processes (e.g., recruitment, competition, and predation) in shallow environments are well known due to accessibility, controllability, and replicability.

Experimental studies in deep, hard bottom habitats are rare. Larval recruitment is controlled by size of the adult reproductive population and reproductive rates. Recruitment rates involve substrate selection, settlement, and growth of invertebrate larvae onto hard bottom habitats. Substrate selection and settlement is controlled by various environmental cues, which include biofilms, interactions with adults of the same and different species, and physical processes. The most important factor regulating recruitment and recruitment rates in hard bottom habitats is the availability of open space for colonization and competition for that space (Connell 1961a,b).

The mechanisms that control abiotic processes (i.e., seasonal temperature and salinity changes, abrasion, turbidity, small-scale turbulence and stochastic disturbance events) are also relatively well known in shallow water environments. Abrasion and disturbance play a role in removing epibionts or retarding the natural succession of community development. The movement of currents may cause abrasion across the surface, and stochastic disturbance events are generally related to storms (Dayton 1971). Both of these processes are very important in the intertidal zone but they are probably of minimal importance in the deep sea pinnacle habitat. Turbidity and turbulence are more likely the two physical processes that have a recruitment effect in deep water.

Development of an epibiont community is the net result of the interactions between biotic and abiotic processes. Following creation of open niche space, as simulated by the placement of an artificial surface for colonization, a community of organisms colonizes substrate and develops through time by the process called succession. Succession is a directional process in which pioneering species alter the environment, making it

amenable to colonization by climax species. Climax species make up stable communities achieved over time (Sutherland 1974). Only stable communities are resistant to perturbations, and from which succession is not possible (Connell and Slayter 1977). In a non-stable community, disturbance may open up enough space to allow succession to again take place. However, climax communities may change over time due to differences in recruitment and predation events (Sutherland 1974).

Consequently, the ecological companion study adapts designs used in the intertidal zone to the pinnacle habitat. Settling plate experiments with exclusion, settlement, and control treatments were used to study the biotic and abiotic interactions that regulate ecological processes. The settling plates are attached to a mooring, and the entire device is called a "biomooring." There are two major deployments: one for a spatial and one for a temporal study. The original major elements of the settling plate experiment studies were as follows:

1. Spatial study at four stations to last for one year;
2. Replication of the spatial study during the second year;
3. Two settling surface treatments: hard and soft;
4. Three settling plate treatments: uncaged, caged, and partially-caged;
5. Two heights, or distances from the bottom (2 m, 13 m); and
6. Time series study at one station, retrieval every 3 months for two years.

Although details of the project were modified because of equipment failure and bad weather, the original hypotheses will still be tested. Only elements 5 and 6 have changed:

5. Three heights, or distances, from the bottom (0 m, 2 m, 13 m)
6. Time series study at one station, cruise every year for retrieval

Sites were chosen to correspond with the physical oceanography experiments (see Chapter 7) in order to gather as much information about the ambient environment as possible. Sites 1 and 5 are characterized by high relief features, Site 4 by medium relief features, and Site 9 by low relief features. Site 1 is in the eastern part of the pinnacle habitat, Sites 4 and 5 are in the central part, and Site 9 is in the western part. The selection of these four sites ensures that the biomoorings are well distributed throughout the pinnacle habitat and allows for the representation of all relief types found throughout the study area.

The temporal experiment was designed to test for differences in recruitment and growth over time, with quarterly retrievals over a two-year period. Eight biomoorings were deployed at Site 4 during Cruise 1C and one biomooring was to be retrieved on each of the subsequent cruises (Table 11.1). Due to shackle failure, the first set of biomoorings deployed are resting on the bottom substrate (0 m height) while the second set of biomoorings deployed are suspended at the previously planned heights of ~2 m and ~13 m from the bottom. This change enhances the project because we are now sampling three heights from the bottom (0 m, 2 m, and 13 m). Due to sampling difficulties and

logistical problems, one cruise per year has been allotted for retrieval of the temporal set (Table 11.1). Replicate biomoorings will be retrieved on each cruise, which increases the power to determine change over time and space. The slow recruitment rates observed from the first set of samples also indicate the design has been improved. Sampling more frequently would not have shown significant differences among treatments because of the slow growth rates.

The spatial experiment is designed to test for differences among habitats. One biomooring each was deployed at Sites 1, 5, and 9 at approximately the same water depth (Table 11.1). This experiment is proceeding as originally planned.

Table 11.1. Time line and sampling schedule for experimental studies. For each cruise, the table gives the study, number of stations being sampled, and the duration of the deployment over the entire study period, where D = deployed, --- = submerged, and R = retrieved.

Study and Location(s)	Revised Cruises (No., Date, and Months Exposed)								
	1C	S1	M2	S2	M3	M3	S4	S5	M4
	May 97	Jul 97	Oct 97	Jan 98	Apr 98	Aug 98	Oct 98	Jan 99	Apr-May 99
	0	3	6	9	12	16	18	21	24
Time Series (Site 4)	D	-------	R (B4E)						
	D	-------	-------	-------	-------	R			
	D	-------	-------	-------	-------	R			
	D	-------	-------	-------	-------	R			
	D	-------	-------	-------	-------	------	-------	-------	R
	D	-------	-------	-------	-------	-------	------	-------	R
	D	-------	-------	-------	-------	-------	-------	-------	R
	D	-------	-------	-------	-------	-------	-------	-------	R
				D	-------	-------	-------	-------	R
Spatial (Sites 1, 5, & 9)	D	-------	-------	-------	-------	R[a]			
				D	-------	-------	-------	-------	R
Total Deployed	11	0	0	4	0	0	0	0	0
Total Retrieved	0	0	1	0	0	5[a]	0	0	9

[a] Turbidity prevented retrieval of the Site 5 biomooring. It will be retrieved on Cruise M4.

Methods

Settling plates are arranged in three experimental treatments: an uncaged treatment (U), a caged treatment (C), and a partially caged control treatment (P). The acronyms U, C, and P refer to experimental treatments, which are used to measure ecological processes. The uncaged (U) settling plate measures net recruitment with biotic and abiotic interactions. This includes gross larval settlement, recruitment, growth, and community development (S) and predation and disturbance (D):

$$U = S + D$$

The caged (C) settling plate is the experimental treatment to exclude predators. A common problem with enclosures is that water flow (W) at the settling plate surface is changed:

$$C = S + W$$

Therefore, we must add a cage-control treatment to subtract effects due to the enclosure. The control is a partial cage (P) that would have the same effects on water flow, but would allow predators access to the experimental treatment. Thus, the control treatment includes net recruitment (S + D) in addition to water flow interactions (W):

$$P = S + D + W$$

The effects on rates of recruitment by ecological process; predation (D), water flow (W), and net recruitment (S) are calculated by mathematical combinations of the experimental treatments:

$$W = P - U$$

$$D = P - C$$

$$S = U + C - P$$

The three experimental treatments (U = uncaged, C = caged, and P = partially caged control) are attached to one another forming a "Y"-shaped triad (Fig. 11.1A). Each treatment consists of four settling plates, or replicates, that have been attached to the triad (Fig. 11.1B). Three of the replicate settling plates are hard surfaces made of ceramic tiles and the other is a soft surface made of outdoor carpet. Each biomooring consists of an anchor, six triads, and a float (Fig. 11.2). A common pitfall in these types of experiments is pseudoreplication, where the treatment levels (U, C, and P) are not replicated. To avoid pseudoreplication, there are three replicate triads at two different depths on each mooring: 2 m and 13 m from the bottom. The replicate treatments have been placed on the wire so that there is no vertical bias in sampling. Each triad contains 12 settling plate replicates (3 experimental treatment replicates × 4 plate replicates). Altogether, each depth treatment consists of 36 samples (3 treatments × 3 replicate treatments × 4 sub-

treatment replicates). Therefore, the original biomoorings consisted of 72 samples (2 depths × 36 samples).

During the first scheduled retrieval cruise, the acoustic soundings failed to release the biomoorings. During an ROV inspection in October 1997, it was discovered that the shackles had parted and the floats of the biomoorings had released, causing the remaining triads to fall onto the bottom. Only one biomooring, consisting of three triads, was retrieved at this time. Therefore, there are 36 samples at the same depth (0 m above bottom). The results from this first biomooring of the temporal study are presented below.

The program was redesigned and approved in November 1997. The second deployment of four biomoorings occurred in January 1998. These were constructed with improved shackles and reinforced with nylon line to prevent further loss of any data. These biomoorings were deployed following the original design of two depths at 2 m and 13 m from the bottom. With these results, we will have available comparisons of three different depths (0 m, 2 m, and 13 m) instead of the original plan for two depths. The second retrieval of biomoorings occurred in August 1998. This included three from the temporal study and two from the spatial experiment (Table 11.1). One biomooring from the spatial experiment was not retrieved due to turbidity at Site 5.

Upon retrieval, the exact location of the biomooring is recorded, settling plates are removed from the triads, and tiles are placed in a separate container with 2% formalin for preservation.

Settling plates are scored for abundance as percent cover by species to the lowest taxonomic level possible. Comparing organisms on the settling plates with organisms found in the ROV transects ensures taxonomic validation. A transparent scoring card with 400 cells is placed on the plate. Presence of a species in any part of a cell counts for the entire cell. The size of non-colonial organisms is also measured. Diversity is calculated by the Shannon (H') diversity index and the exponential transformation ($_e{}^{H'}$), which indicates the total number of dominant species (Hill 1973).

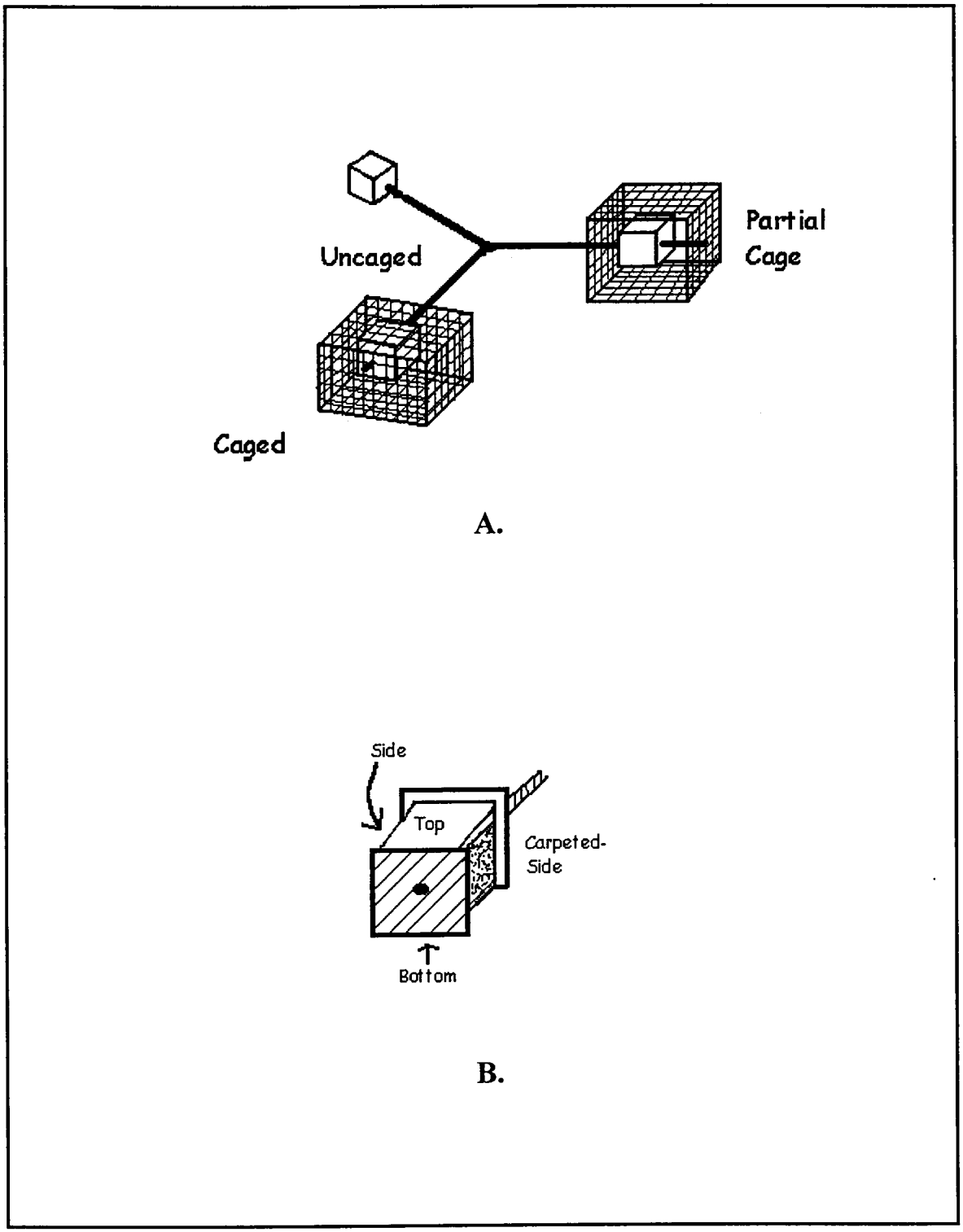

Fig. 11.1. Experimental settling plate treatments. A. Triad with each of the three treatments. B. Detail of the uncaged treatment showing four settling surfaces: three hard and one soft.

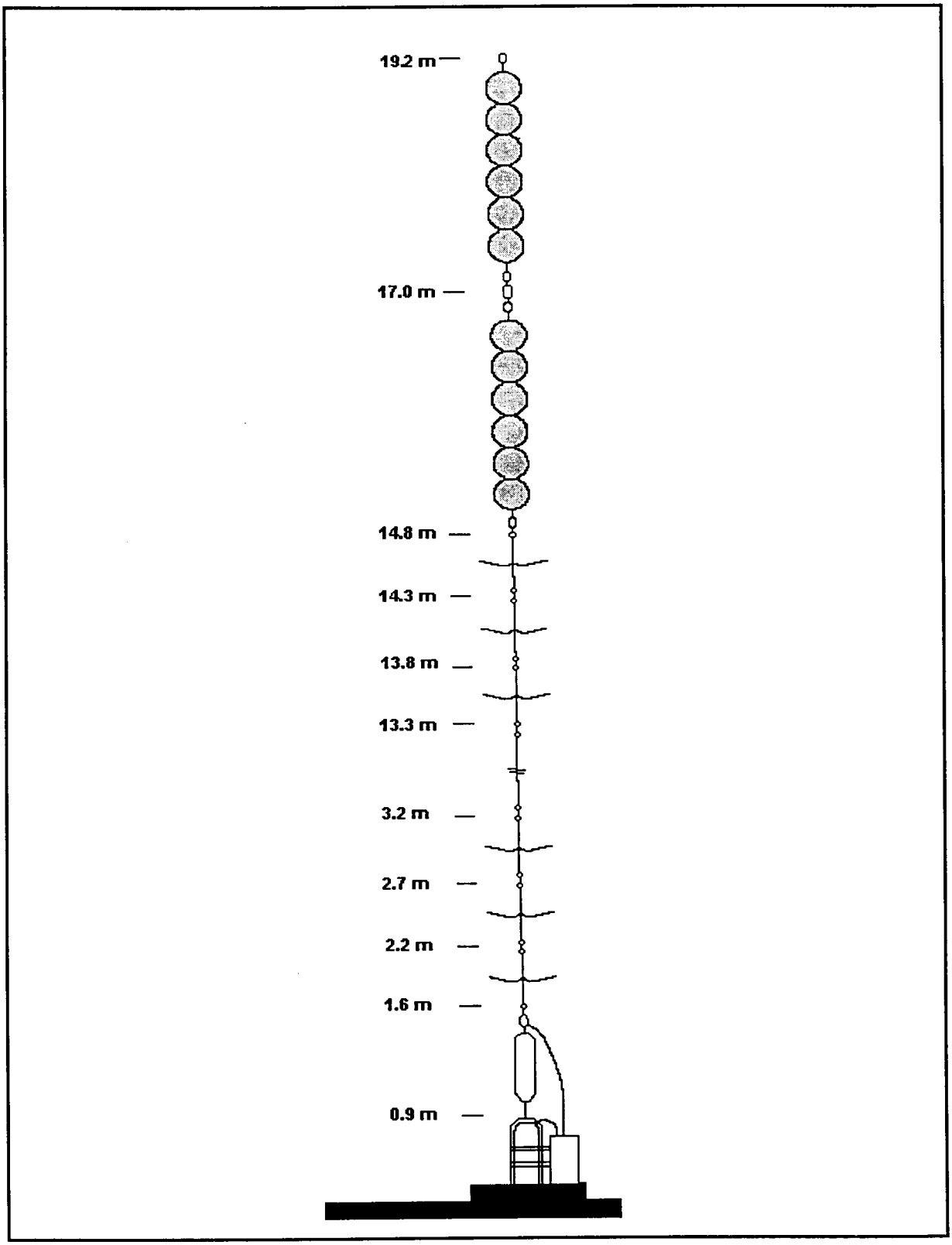

Fig. 11.2. Biomooring with three replicate triads at two distances from the bottom.

Results

The first time-series biomoorings were deployed in May 1997, and a single biomooring from Site 4 was retrieved in October 1997. The biomass of organisms was small, diversity was low, and total coverage of organic matter was extensive. The organic matter was primarily due to bryozoan colonies that comprised an average of 94% of total coverage on the settlement plates (Fig. 11.3). While the sample size is too small to calculate statistical significance, it is worth noting that both total coverage and bryozoan colony coverage were less in the caged (C) treatments than in the uncaged (U) treatments. Total polychaete coverage, however, was greater in the caged (C) treatments.

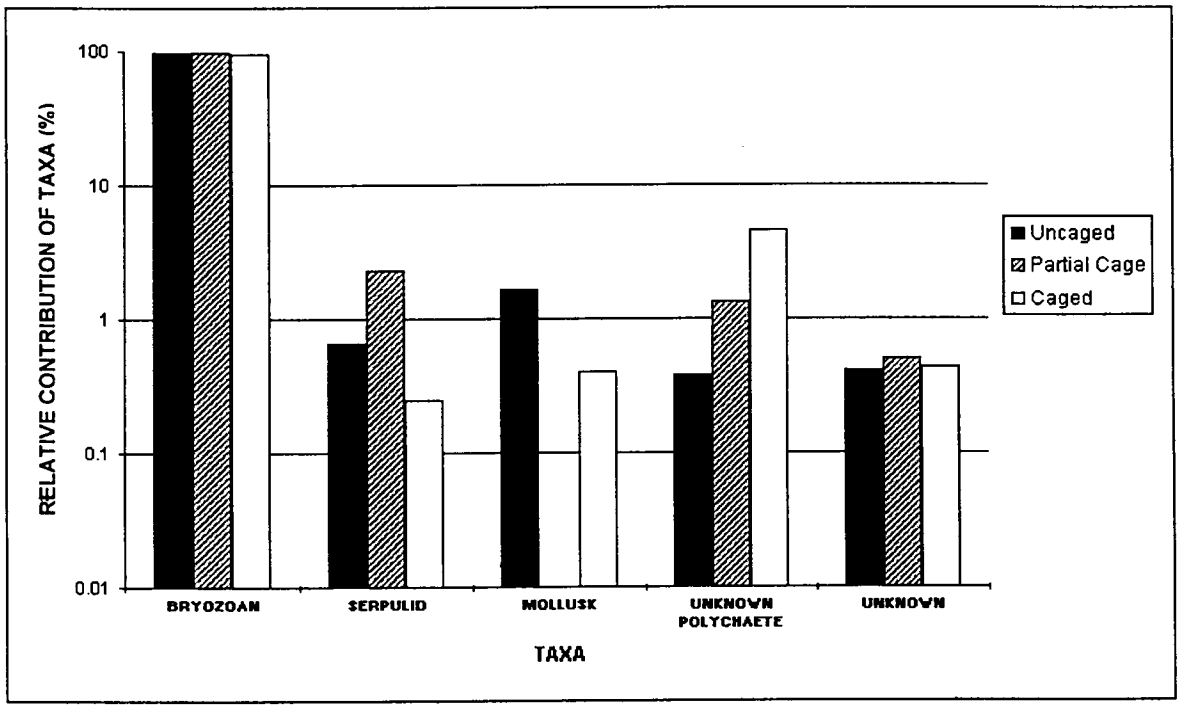

Fig. 11.3. Relative contribution of taxa to total coverage of organic matter.

Table 11.2. Rates of recruitment relative to treatments and ecological processes.

Treatment/Process	Recruitment Rate (cm^2/0.5 yr)		
	Bryozoa	Serpulidae	Unknown polychaeta
Treatment (measured)			
Uncaged (U)	363	2.5	1.5
Caged (C)	342	1	15
Partially Caged (P)	369	9	5
Process (calculated)			
Water Flow (W = P - U)	6	6.5	3.5
Predation/Competition (D = P - C)	27	8	-10
Gross Recruitment (S = U + C - P)	336	-5.5	11.5

Discussion

Total coverage on settlement plates was high. Coverage was comprised almost entirely of small, filamentous bryozoan colonies. We interpret this as an early succession community.

Generally, low diversity, opportunistic (or *r*-selected) species, high growth rates, and small animals (Odum 1969; Rhoads et al. 1978) characterize early succession. In contrast, late succession communities are characterized by high diversity, specialized slow-growing (or *k*-selected), and large species (Odum 1969; Rhoads et al. 1978). Community succession on deep sea hard bottoms will be slow compared to coastal areas (Levin and Smith 1984). In the pinnacle habitat, settlement rates of larvae are expected to decrease with depth and distance from shore (DePalma 1972). Gross recruitment rates (S) of organisms other than bryozoans in the pinnacle habitat were extremely low (Table 11.2). We also found low numbers of polychaetes and other larger organisms (Fig. 11.3).

Several differences were noted between treatments. Polychaetes, other than serpulids, increased in the caged treatments. These polychaetes were larger than the serpulid worms discovered. The polychaetes large size may make them more vulnerable to predation, explaining the negative predation recruitment rates (D) (Table 11.2). In contrast, serpulid worms were not affected negatively by predation. The negative value

for other polychaetes was most likely due to predation pressure, as space for colonization was not limited by competition from all polychaetes or the other organisms that settled on the plates.

None of the organisms appeared to be affected by small-scale turbulence produced by the caging material because all had positive recruitment rates relative to water flow (W) (Table 11.2). This is surprising because small-scale turbulence has been shown to have an impact on vertical and horizontal distributions of organisms in deep-water environments (Mullineaux 1989).

At this point, all conclusions are preliminary due to low sample sizes and difficulty in identification of some of the polychaete and mollusk species. Initial analyses, however, have indicated some interesting trends that may prove to represent generalities in the future.

Literature Cited

Baker, E.T. and J.W. Lavelle. 1984. The effect of particle size on the light attenuation coefficient of natural suspensions. J. Geophys. Res. 89:8197-8203.

Barham, E.G. and I.E. Davies. 1968. Gorgonians and water motion studies in Gulf of California. Underwater Naturalist 5(3):24-28.

Bartz, R., H. Pak, and J.R.V. Zaneveld. 1978. A transmissometer for profiling and moored observations in water. Proc. Soc. Photo-Opt. Instr. Engineers, Ocean Optics V, 160:102-108.

Boehm, P.D. and A.G. Requejo. 1986. Overview of the recent sediment hydrocarbon geochemistry of Atlantic and Gulf Coast over continental shelf environments. Est. Coast. Shelf. Sci. 23:29-58.

Boesch, D.F. and N.N. Rabalais. 1987. Long-Term Environmental Effects of Offshore Oil and Gas Development. Elsevier Applied Science Publishers Ltd., England. 708 pp.

Bohnsack, J.A. 1976. An investigation of a photographic method for sampling hard-bottom benthic communities. M.S. Thesis, University of Miami. 188 pp.

Bohnsack, J.A. 1979. Photographic quantitative sampling of hard-bottom communities. Bull. Mar. Sci. 29(2):242-252.

Boland, G.S., B.J. Gallaway, J.S. Baker, and G.S. Lewbel. 1983. Ecological effects of energy development on reef fish of the Flower Garden banks. Final Report to National Marine Fisheries Service, Galveston Laboratory by LGL Ecological Research Associates. 466 pp.

Boothe, P.N. and W.D. James. 1985. Neutron activation analysis of barium in marine sediments from the north central Gulf of Mexico. J. Trace and Microprobe Techniques 3:377-399.

Boothe, P.N. and B.J. Presley. 1987. The effects of exploratory petroleum drilling in the northwest Gulf of Mexico on trace metal concentrations in near rig sediments and organisms. Environ. Geol. Water Sci. 9:173-182.

Brassell, S.C., G. Eglinton, J.R. Maxwell, and R.P. Philip. 1978. Natural background of alkanes in the aquatic environment, pp. 69-86. In: O. Huntzinger, L.H. van Lelyveld, and B.C.J. Zoetman (eds.). Aquatic Pollutants, Transformations and Biological Effects, Oxford, Pergamon Press.

Bright, T.J. and L.H. Pequegnat (eds). 1974. Biota of the West Flower Garden Bank. Gulf Publishing Company, Houston, TX. 435 pp.

Brooks, J.M. (ed.). 1991. Mississippi-Alabama Continental Shelf Ecosystem Study: Data Summary and Synthesis, Volume I: Executive Summary, Volume II: Technical Narrative, Volume III: Appendices, Part 1 (Appendices A-D), Volume III: Part 2, (Appendix E), OCS Study MMS 91-0062 (I), 91-0063 (II), 91-0064 (III). U.S. Department of the Interior. Minerals Mgmt. Service, Gulf of Mexico OCS Regional Office, New Orleans,LA., 43 pp.(I), 862 pp.(II), 1,001 pp. (III-1), and 1,001 pp. (III-2).

Brooks, J.M., M.C. Kennicutt II, T.L. Wade, A.D. Hart, G.J. Denoux, and T.J. McDonald. 1990. Hydrocarbon distributions around a shallow water multiwell platform. Environmental Science and Technology 24:1,079-1,085.

Carpenter, J. 1965. The accuracy of the Winkler Method for dissolved oxygen analysis. Limnol. Oceanogr. 14:135-140.

Cashman, C.W. 1973. Contributions to the ichthyofauna of the West Flower Garden reefs and other reef sites in the Gulf of Mexico and western Caribbean. Ph.D. Dissertation, Texas A&M Univ., College Station, TX. 247 pp.

Chow, T.J. and C.B. Snyder. 1981. Barium in marine environment: a potential indicator of drilling contamination, pp. 691-722. In: Proceedings on Research on Environmental Fate and Effects of Drilling Fluids and Cuttings Symposia. Lake Buena Vista, Florida, 21-23 January 1980.

Connell, J.H. 1961a. The influence of interspecific competition and other factors on the distribution of the barnacle *Chthamalus stellatus.* Ecology 42:710-723.

Connell, J.H. 1961b. Effects of competition, predation by *Thais lapillus* and other factors on natural populations of the barnacle *Balanus balanoides.* Ecol. Monogr. 31:61-104.

Connell, J.H. and R.O. Slayter. 1977. Mechanisms of succession in natural communities and their role in community stability and organization. Am. Nat. 111: 1119-1144.

Continental Shelf Associates, Inc. 1983. Environmental Monitoring Program for Exploratory Well No. 3, Lease OCS-G 3316, Block A-384, High Island Area, South Extension near the West Flower Garden Bank. Draft Final Report to Union Oil Company. Tequesta, FL. 2 Vol.

Continental Shelf Associates, Inc. 1985a. Live-bottom survey of drillsite locations in Destin Dome Area Block 617. Report to Chevron U.S.A., Inc. 40 pp. + app.

Continental Shelf Associates, Inc. 1985b. Environmental monitoring program for Platform "A", lease OCS-G 2759, High Island Area, South Extension, East Addition, Block A-389 near the East Flower Garden Bank. Final Report to Mobil Producing Texas and New Mexico, Inc., Houston, TX. 3 Vol.

Continental Shelf Associates, Inc. 1987a. Southwest Florida Shelf Regional Biological Communities Survey, Year 3 Final Report. A report for the U.S. Department of the Interior, Minerals Management Service. Contract No. 14-12-0001-29036. Three volumes.

Continental Shelf Associates, Inc. 1987b. Live bottom survey for Destin Dome Area Lease Block 57. A final report prepared for Conoco, Inc.

Continental Shelf Associates, Inc. 1989. Fate and effects of drilling fluid and cutting discharges in shallow nearshore waters. Prepared for the American Petroleum Institute. 129 pp.

Continental Shelf Associates, Inc. 1992. Mississippi-Alabama Shelf Pinnacle Trend Habitat Mapping Study. OCS Study MMS 92-0026. U.S. Department of the Interior, Minerals Management Service, Gulf of Mexico OCS Regional Office, New Orleans, LA. 75 pp. + app.

Continental Shelf Associates and Texas A&M University, Geochemical and Environmental Research Group. 1998. Northeastern Gulf of Mexico Coastal and Marine Ecosystem Program, Mississippi/Alabama Shelf; First Annual Interim Report. U.S. Department of the Interior, U.S. Geological Survey, Biological Resources Division, USGS/BRD/CR-1997-0008 and Minerals Management Service, Gulf of Mexico OCS Region, New Orleans, LA, OCS Study MMS 97-0037. 133 pp. + app.

Dai, C.F. and M.C. Lin. 1993. The effects of flow on feeding of three gorgonians from southern Taiwan. Journal of Experimental Marine Biology and Ecology 173:57-69.

Darnell, R. 1991. Summary and Synthesis, pp 15-1 to 15-144. In: Brooks J.M. (ed.), Mississippi-Alabama Continental shelf ecosystem study: Data Summary and Synthesis. Vol. II: Technical Narrative. OCS Study MMS 91-0063. U.S. Dept. Interior, Minerals Management Service, OCS Regional Office, New Orleans, LA. 862 pp.

Davis, K.S. 1992. High-resolution seismic stratigraphy of the Mississippi-Alabama outer shelf and upper continental slope, M. S. Thesis, Texas A&M University, College Station, TX. 107 pp.

Dayton, P.H. 1971. Competition, disturbance, and community organization: the provision and subsequent utilization of space in a rocky intertidal community. Ecology 41:351-389.

Dennis, G.D. and T.J. Bright. 1988a. Reef fish assemblages on hard banks in the northwestern Gulf of Mexico. Bull. Mar. Sci. 43(2):

Dennis, G.D. and T.J. Bright. 1988b. New records of fishes in the northern Gulf of Mexico, with notes on some rare species. N.E. Gulf Sci. 10(1):1-18.

DePalma, J.R. 1972. Fearless fouling forecasting, pp. 865-879. In: *Proceedings of the Third International Congress on Marine Corrosion and Biofouling*. National Bureau of Standards, Washington, DC.

Environmental Science and Engineering, Inc., LGL Ecological Research Associates, Inc., and Continental Shelf Associates, Inc. 1987. Southwest Florida Shelf Ecosystems Study Data Synthesis. A report for the U.S. Department of the Interior, Minerals Management Service, Gulf of Mexico OCS Region, New Orleans, LA. Contract No. 14-12-0001-30276. Two volumes.

Folk, R.L. 1974. Petrology of sedimentary rocks. Hemphill Publishing Co., Austin, TX. 184 pp.

Gardner, W.D. and I.D. Walsh. 1990. The role of aggregates in horizontal and vertical flux across a continental margin. Deep-Sea Res. 37:401-412.

Gardner, W.D., M.J. Richardson, K.R. Hinga, and P.E. Biscaye. 1983. Resuspension measured with sediment traps in a high-energy environment. Earth Planet. Sci. Lett. 66:262-278.

Gardner, W.D., P.E. Biscaye, J.R.V. Zaneveld, and M.J. Richardson. 1985. Calibration and comparison of the LDGO nephelometer and the OSU transmissometer on the Nova Scotian Rise. Mar. Geol. 66:323-344.

Gardner, W.D., S.P. Chung, M.J. Richardson, and I.D. Walsh. 1995. The oceanic-mixed layer pump. Deep-Sea Res. pt. II 42:757-776.

Genin, A., P.K. Dayton, P.F. Lonsdale, and F.N. Spiess. 1986. Corals on seamount peaks provide evidence of current acceleration over deep-sea topography. Nature 322:59-61.

Gilmore, R.G., C.J. Donahoe, and D.W. Cooke. 1987. Fishes of the Indian River Lagoon and adjacent waters, Florida. Harbor Branch Foundation Tech. Rep. 41: 68 pp.

Gittings, S.R., G.S. Boland, K.P. Deslarzes, D.K. Hagman and B.S. Holland (ed.). 1992a. Long-term monitoring at the East and West Flower Garden Banks. U.S. Department of the Interior, Minerals Management Service, Gulf of Mexico OCS Region, New Orleans, LA, OCS Study MMS 92-0006. 206 pp.

Gittings, S.R., T.J. Bright, W.W. Schroeder, W.W. Sager, J.S. Laswell, and R. Rezak. 1992b. Invertebrate assemblages and ecological controls on topographic features in the northeast Gulf of Mexico. Bull. Mar. Sci. 50(3):435-455.

Gordon, H.R., R.C. Smith, and J.R.V. Zaneveld. 1984. Introduction to ocean optics, SPIE Ocean Optics 489:2-41.

Grigg, R.W. 1972. Orientation and growth form of sea fans. Limnology and Oceanography 17(2):185-192.

Hardin, D.D., J. Toal, T. Parr, P. Wilde, and K. Dorsey. 1994. Spatial variation in hard-bottom epifauna in the Santa Maria Basin: The importance of physical factors. Marine Environmental Research 37(2):165–193.

Heezen, B.C. and C.D. Hollister. 1971. The face of the deep. Oxford University Press, New York, NY. 659 pp.

Helmuth, B. and K. Sebens. 1993. The influence of colony morphology and orientation to flow on particle capture by the scleractinian coral *Agaricia agaricites* (Linnaeus). Journal of Experimental Marine Biology and Ecology 165:251-278.

Hill, M.O. 1973. Diversity and evenness: a unifying notation and its consequences. Ecology 54:427-432.

Houghton, J.P., D.L. Beyer, and E.D. Thielk. 1981. Effects of oil well drilling fluids on several important Alaskan marine organisms, pp. 1,017-1,043. In: Proceedings on Research on Environmental Fate and Effects of Drilling Fluids and Cuttings Symposia. Lake Buena Vista, Florida, 21-23 January 1980.

Hyland, J., D. Hardin, D. Coats, R. Green, M. Steinhauer, and J. Neff.. 1994. Impacts of offshore oil and gas development on the benthic environment of the Santa Maria Basin. Marine Environmental Research 37:195–229.

Jackson,D.A., K.M. Somers, and H.H. Harvey. 1989. Similarity coefficients: measures of co-occurrence and association or simply measures of occurrence? American Naturalist 133: 436-453.

Jerlov, N.G. 1976. Marine Optics, Elsevier Applied Science Publishers Ltd., New York.

Johnson, H.P. and M. Helferty. 1990. The geological interpretation of side-scan sonar. Rev. of Geophys. 28:357-380.

Kelly, F.J. 1991. Physical oceanography/water mass characterization, pp. 10-1 - 10-151. In: Mississippi-Alabama Shelf Ecosystem Study: Data Summaries and Synthesis. Volume II: Technical Narrative. U.S. Department of the Interior, Minerals Management Service, Gulf of Mexico OCS Regional Office, New Orleans, LA. OCS Study MMS 91-0063.

Kendall, J.J. 1990. Detection of effects at long-term production sites, pp. 23-28. In: R.S. Carney (ed). Northern Gulf of Mexico Environmental Studies Planning Workshop. Proceeding of a workshop held in New Orleans, Louisiana, 15-17 August 1989. Prepared by Geo-Marine, Inc. OCS Study MMS 90-0018. U.S. Dept. of the Interior, Minerals Management Service, New Orleans, LA. 156 pp.

Kennicutt, M.C., II (ed.). 1995. Gulf of Mexico Offshore Operations Monitoring Experiment, Phase I: Sublethal Responses to Contaminant Exposure. Final Report. OCS Study MMS 95-0000. U.S. Department of the Interior, Minerals Management Service, Gulf of Mexico OCS Region, New Orleans, Louisiana. 739 pp.

Kennicutt, M.C. II and P. Comet. 1992. Resolution of sediment hydrocarbon sources: Multiparameter approaches, pp. 308-337. In: J.K. Whelan and J.W. Farrington (eds.), Organic productivity, accumulation, and preservation in recent and ancient sediments. Columbia University Press.

Kennicutt, M.C. II, P.N. Boothe, T.L. Wade, S.T. Sweet, R. Rezak, F.J. Kelly, J.M. Brooks, B.J. Presley, and D.A. Wiesenburg. 1996. Geochemical Patterns in Sediments Near Offshore Production Platforms. Can. J. Fish. Aquat. Sci. 53:2254-2566.

Kindinger, J. L. 1988. Seismic stratigraphy of the Mississippi-Alabama shelf and upper continental slope. Mar. Geol. 83:79-94.

Kindinger, J.L. 1989. Depositional history of the Lagniappe Delta. Northern Gulf of Mexico. Geo-Mar. Lett. 9:59-66.

Lake Buena Vista Symposium. 1981. Research on Environmental Fate and Effects of Drilling Fluids and Cuttings. Volumes 1 and 2. January 21-24, 1980, Lake Buena Vista, Florida. 1,122 pp.

Laswell, J.S., W.W. Sager, W.W. Schroeder, K.S. Davis, and R. Rezak. 1992. High-resolution geophysical mapping of the Mississippi-Alabama outer continental shelf, pp. 155-192. In: R. Geyer, ed., Geophysical Exploration at Sea. CRC Press, Boca Raton, FL.

Lauenstein, G.G., A.Y. Cantillow, and S.S. Dolvin. 1993. Benthic surveillance and mussel watch projects analytical protocols 1984-1992. NOAA Technical Memorandum NPS ORCA. NOAA, Silver Spring, MD. pp. III-151 to III-185.

Leversee, G.J. 1976. Flow and feeding in fan-shaped colonies of the gorgonian coral, *Leptogorgia*. Biological Bulletin 151:344-356.

Levin, L.A. and C.R. Smith. 1984. Response of background fauna to disturbance and enrichment in the deep sea: a sediment tray experiment. Deep Sea Res. 31:1277-1285.

Ludwick, J.C. and W.R. Walton. 1957. Shelf-edge, calcareous prominences in the northeastern Gulf of Mexico. Amer. Assoc. Petrol. Geol. Bull. 41(9):2054-2101.

MacDonald, I.R., F.J. Kelly, N.L. Guinasso, Jr., and W.W. Schroeder. 1996. Deep Ocean Sea Fans (Gorgonacea: *Callogorgia* sp.) Choose their Location and Orientation to Optimize for Persistent Flow. EOS, Trans. AGU 76:O95.

MacLeod, W.D., D.W. Brown, A.J. Friedman, D.G. Burrows, O. Maynes, R.W. Pearce, C.A. Wigren, and R.G. Bogar. 1985. Standard Analytical Procedures of the NOAA National Analytical Facility 1985-1986. Extractable Toxic Organic Compounds, 2 ed., NOAA Technical Memo NMFSS R/NWC-92, U.S. Dept. of Commerce, NOAA/NMFS. Washington, DC.

Marine Resources Research Institute. 1984. South Atlantic OCS Area Living Marine Resources Study, Phase III. A report for the U.S. Department of the Interior, Minerals Management Service, Washington, DC. Contract No. 14-12-0001-29185.

Messing, C.G., A.C. Neumann, and J.C. Lang. 1990. Biozonation of deep-water lithoherms and associated hardgrounds in the northeastern Straits of Florida. Palaios 5:15.

Middleditch, B.S. 1981. Environmental Effects of Offshore Production. The Buccaneer Gas and Oil Field Study. Plenum Press, New York. 446 pp.

Miller, G.C. and W.J. Richards. 1980. Reef fish habitat, faunal assemblages, and factors determining distributions in the South Atlantic Bight. Proc. Gulf. Carib. Fish. Inst., 32nd Annual Meeting, pp. 114-130.

Mitchum, R.M., Jr. and P. R. Vail. 1977. Seismic stratigraphy and global changes of sea level, part 7: seismic stratigraphic interpretation procedure. In C. E. Payton, ed., Seismic Stratigraphy - Applications to Hydrocarbon Exploration, Memoir 26. Amer. Assoc. Petrol. Geol., Tulsa, OK, pp. 135-143.

Moody, J.A., B. Butman, and M.H. Bothner. 1986. Estimates of near-bottom suspended-matter concentration during storms. Cont. Shelf Res. 7:609-628.

Morel, A. 1974. Optical properties of pure water and pure sea water, In: Optical Aspects of Oceanography, N. Jerlov and E. Steeman Nielsen (eds.), Academic Press, New York, pp. 1-24.

Mullineaux, L.S. 1989. Vertical distributions of the epifauna on manganese nodules: implications for settlement and feeding. Limnol. Oceanogr. 34:1247-1262.

National Research Council. 1992. Assessment of the U.S. Outer Continental Shelf Environmental Studies Program. Volume II: Ecology. National Academy Press, Washington, DC. 152 pp.

Odum, E.P. 1969. The strategy of ecosystem development. Science 164:262-270.

Pak H., D.A. Kiefer and J.C. Kitchen. 1988. Meridional variations in the concentration of chlorophyll and microparticles in the North Pacific Ocean. Deep-Sea Res. 35:1151-1171.

Parker, R.O. and S.W. Ross. 1986. Observing reef fishes from submersibles off North Carolina. N.E. Gulf Sci. 8(1):31-50.

Pequegnat, W.E. 1964. The epifauna of a California siltstone reef. Ecology 45:272-283.

Phillips, N.W., D.A. Gettleson, and K.D. Spring. 1990. Benthic biological studies of the southwest Florida shelf. Am. Zool. 30:65-75.

Philp, R.P. 1985. Fossil Fuel Biomarkers: Application and Spectra. Methods in geochemistry and geophysics. Elsevier, NY. 294 pp.

Rezak, R., T.J. Bright, and D.W. McGrail. 1985. Reefs and Banks of the Northern Gulf of Mexico: Their Geological, Biological, and Physical Dynamics. John Wiley and Sons, New York. 259 pp.

Rhoads, D.C., P.L. McCall, and J.Y. Yingst. 1978. Disturbance and production on the estuarine seafloor. Am. Sci. 66:577-586.

Rohlf, F.J. 1997. NTSYS/PC, Version 2.0. Numerical taxonomy and multivariate analysis system. Exeter Publishing, Setauket, New York.

Rowe, G.T. and R.J. Menzies. 1968. Orientation in two bathy, benthic decapods, *Munida valida* Smith and *Parapagurus pilosimanus* Smith. Limnol. Oceanogr. 13(3):549-552.

Rubinstein, N.I., R. Rigby, and C.N. D'Asaro. 1981. Acute and sublethal effects of whole used drilling fluids on representative estuarine organism, pp. 828-846. In: Proceedings on Research on Environmental Fate and Effects of Drilling Fluids and Cuttings Symposia. Lake Buena Vista, Florida, 21-23 January 1980.

Sager, W.W., W.W. Schroeder, J.S. Laswell, K.S. Davis, R. Rezak, and S.R. Gittings. 1992. Topographic features of the Mississippi-Alabama outer continental shelf and their implications for sea level fluctuations during the Late Pleistocene-Holocene transgression, Geo-Mar.Lett. 12:41-48.

Schroeder, W.W., M.R. Dardeau, J.J Dindo, P. Fleisher, K.L. Heck, Jr., and A.W. Shultz. 1989a. Geophysical and biological aspects of hardbottom environments on the L'MAFLA shelf, northern Gulf of Mexico, pp. 17-21. In: Proceeding Oceans '88 Conference.

Schroeder, W.W., A.W. Shultz, and J.J. Dindo. 1989b. Inner-shelf hardbottom areas northeastern Gulf of Mexico. Trans. Gulf Coast Assoc. Geol. Soc. 38:535-541.

Science Applications International Corporation. 1995. Monitoring Assessment of Long-Term Changes in Biological Communities in the Santa Maria Basin: Phase III. Final Report. OCS Study MMS 95-0049. U.S. Department of the Interior, Minerals Management Service, Pacific OCS Region, Los Angeles, CA.

Shipp, R.L. and T.S. Hopkins. 1978. Physical and biological observations of the northern rim of the De Soto Canyon made from a research submersible. Northeast Gulf Sci. 2(2):113-121.

Smith, G.B. 1976. The ecology and distribution of the eastern Gulf of Mexico reef fishes. Fl. Dept. Nat. Res. Mar Res. Pub. 19:1-78.

Smith, G.B., H.M. Austin, S.A. Bortone, R.W. Hastings, and L.H. Ogren. 1975. Fishes of the Florida Middle Ground with comments on ecology and zoogeography. Fl. Dept. Nat. Res. Mar. Res. Pub. 9:1-14.

Sneath, P.H.A. and R.R. Sokal. 1973. Numerical taxonomy. W.H. Freeman and Co., San Francisco.

Sonnier, F., H.D. Hoese, and J. Teerling. 1976. Observations on the offshore reef and platform fish fauna of Louisiana. Copeia (1):105-111.

Southwest Research Institute. 1978. Ecological Investigations of Petroleum Production Platforms in the Central Gulf of Mexico. Report Prepared for the U.S. Department of Commerce.

Spinrad R.W., J.R.V. Zaneveld, and J. C. Kitchen. 1983. A study of the optical characteristics of the suspended particles in the benthic boundary layer of the Scotian Rise. J. Geophys. Res. 88:7641-7645.

Steinhauer, M. and E. Imamura (eds.). 1990. California OCS Phase II Monitoring Program: Year Three Annual Report. Volume I. OCS Study MMS 90-0055. U.S. Department of the Interior, Minerals Management Service, Pacific OCS Region, Los Angeles, CA.

Sutherland, J.P. 1974. Multiple stable points in natural communities. Am. Nat. 108:859-873.

Sydow, J. and H.H. Roberts. 1994. Stratigraphic Framework of a late Pleistocene shelf-edge delta, Northeast Gulf of Mexico. Amer. Assoc. Petrol. Geol. Bull., 78, 1276-1312.

Tornberg, L.D., E.D. Thielk, R.E. Nakatani, R.C. Miller, and S.O. Hillman. 1981. Toxicity of drilling fluids to marine organisms in the Beaufort Sea, Alaskapp, pp. 997-1,016. In: Proceedings on Research on Environmental Fate and Effects of Drilling Fluids and Cuttings Symposia. Lake Buena Vista, Florida, 21-23 January 1980.

U.S. Environmental Protection Agency. 1989. Preparing perfect project plans. EPA/600/9-89/087. Risk Reduction Engineering Laboratory. Cincinnati, OH. 61 pp.

U.S. Environmental Protection Agency. 1991. Methods for the determination of metals in environmental samples, pp. 227-239. EPA/600/4-91/010. Office of Research and Development. Washington, DC.

Velimirov, B. 1983. Orientation in the sea fan *Eunicella cavolinii* related to water movement. Helgolander wiss. Meeresunter 24:163-173.

Wade, T.L., E.L. Atlas, J.M. Brooks, M.C. Kennicutt II, R.G. Fox, J. Sericano, B. Garcia-Romero, and D. DeFreitas. 1988. NOAA Gulf of Mexico Status and Trends Program: Trace Organic Contaminant Distribution in Sediments and Oysters. Estuaries 11:171-179.

Wainwright, S.A. and J.R. Dillon. 1969. On the orientation of sea fans (Genus *Gorgonia*). Biological Bulletin 130-139.

Walsh, I.D. 1990. Project CATSTIX: Camera, Transmissometer, and Sediment Trap Integration Experiment. Ph. D. Dissertation, Texas A&M University, College Station, TX.

Walsh, I.D. and W.D. Gardner. 1992. A comparison of aggregate profiles with sediment trap fluxes. Deep-Sea Res. 39:1817-1834.

Walsh, I., K. Fischer, D. Murray, and J. Dymond. 1988. Evidence for resuspension of rebound particles from near-bottom sediment traps. Deep-Sea Res. 35:59-70.

Walsh, I.D., S.P. Chung, M.J. Richardson, and W.D. Gardner. 1995. The Diel Cycle in the integrated particle load in the equatorial Pacific: a comparison with primary production. Deep-Sea Res. pt. II 42:465-478.

Wessel, P., and W.H.F. Smith. 1995. New version of the Generic Mapping Tools released. EOS, Trans. AGU 76:329.

Woodward-Clyde Consultants. 1979. Eastern Gulf of Mexico marine habitat mapping study. Report to U.S. Department of the Interior, Bureau of Land Management, OCS Office, New Orleans, LA. Contract No. AA551-CT8-22.

Zhang, Y. 1997. Sedimentation and resuspension across the central Lousiana inner shelf. Ph.D. Dissertation, Texas A&M University, College Station, Texas. 171 pp.

U.S. Department of the Interior
U.S. Geological Survey
Biological Resources Division

As the Nation's principal conservation agency, the Department of the Interior has responsibility for most of our nationally owned public lands and natural resources. This responsibility includes fostering the sound use of our lands and water resources; protecting our fish, wildlife, and biological diversity; preserving the environmental and cultural values of our national parks and historical places; and providing for enjoyment of life through outdoor recreation. The Department assesses our energy and mineral resources and works to ensure that their development is in the best interests of all our people by encouraging stewardship and citizen participation in their care. The Department also has a major responsibility for American Indian reservation communities.